UNIVERSITY OF LONDON THESIS

Degree PhD Year 2007 Name of Author GRIFFITHS, Karen

The role of the kinetochore-associated Dam1 complex during fission yeast mitosis

Karen Griffiths

Submitted towards the degree of Doctor of Philosophy

University of London

University College London
Department of Biology
London, WC1E 6BT.

ProQuest LLC
789 East Eisenhower Parkway
P.O. Box 1346
Ann Arbor, MI 48106-1346

I declare that the work in this thesis is my own work

Acknowledgements

I would like to acknowledge the many people who supported and encouraged me in the completion of this work and thesis. I would like to thank my supervisor Takashi Toda and Cancer Research UK for giving me the opportunity to do this thesis. I would like to thank all the members of the Cell Regulation lab for their critique and discussion and technical help over the last 4 years. I would especially like to thank Yasmine Mamnun for always motivating and encouraging me in my work. I am extremely grateful to her for helping me stay focused even when things were tough. I would like to thank Nathalie Spielewoy for reading and correcting my thesis and encouraging me to think about science in a critical manner. I would also like to extend a special thanks to the other PhD students in the lab Amy Unsworth and Chii-shyang Fong for listening to my ideas over many lunches and tea breaks and never growing tired of my talkative nature. I am very grateful for their friendship and support over the last few years. I would like to acknowledge all the members of the other yeast labs for their support especially Rafael Carazo-Salas for teaching me how to use the Delta-vision microscope and Frank Uhlmann for his critical discussions of my work.

Finally I would like to thank all my family and friends for their encouragement over the last few years. I would especially like to thank my husband Stuart for all his love, support and patience during my PhD, when he was also contending with his own thesis. I cannot imagine that I could have come through the PhD successfully had we not taken the journey together.

Abstract

Bipolar attachment of the kinetochore to the spindle is crucial for sister chromatid separation during mitosis. The kinetochore, a specialised proteinaceous structure formed on centromeres is required for tethering the spindle. It consists of many sub complexes including core platform proteins and outer proteins. In budding yeast the Dam1/DASH complex is essential, constituting 10 components and plays a vital role in chromosome segregation. All 10 homologues of the Dam1 complex have been identified in the fission yeast, an organism that contains a more complex centromere structure. This thesis describes the study of the fission yeast Dam1 complex and its role during mitosis in ensuring proper chromosome segregation.

In this thesis we describe the localisation of this complex to the kinetochore and its dependence on both microtubules and functional Mis6 complex. We show that Dam1 complex genes are not essential but deletion shows monopolar chromosome segregation defects and spindle collapse indicative of an importance for proper microtubule dynamics and chromosome bi-orientation. We show that despite being non-essential, deletion mutants are synthetic lethal when combined with deletion of the kinesins Klp5/6, which play a role in promoting chromosome biorientation. To understand this further, we isolated a dam1 temperature-sensitive mutant in a klp5 null background, termed dam1-A8. This is a 'gain of function' mutant that shows resistance to the spindle drug TBZ unlike dam1 deletion, which is sensitive. We have shown in the double dam1-A8klp5 mutant massive chromosome mis-segregation, congression defects and monopolar attachment of the kinetochore to one SPB. Indeed dam1-A8 alone shows sister chromatid congression defects, thus indicating that the Dam1 complex despite its non-essentiality is required in concert with the mitotic kinesins Klp5/6 to promote proper bipolar attachment and spindle microtubule dynamics and either loss or gain of function dam1 mutants leads to defects in chromosome bi-orientation.

Table of Contents

Table of Figures

Table of Tables

Chapter 1

1 Introduction

The accurate separation of the genome during the cell cycle is crucial to maintaining cellular integrity. Loss of fidelity in this process can give rise to genomic instability, with the resulting aneuploidy a common hallmark of cancer in somatic cells and leading to genetic disease in gametes. The mechanisms of chromosome segregation are highly conserved from yeast to man, with this tightly regulated process involving interplay between spindle microtubules and the centromeric region of chromosomes. The kinetochore is a specialised proteinaceous structure that assembles on the centromeric DNA and attaches and tethers spindle microtubules to the centromeric region of chromosomes in metaphase. The kinetochores of each sister chromatid must become attached in a bipolar manner to ensure high fidelity separation of the sisters to opposite poles in anaphase.

The mechanism underlying the attachment of microtubules to the kinetochore involves a myriad of proteins, including molecules that tightly control microtubule dynamics such as kinesins, MAPs and other motor proteins, kinetochore components that provide a structural platform and docking site for the microtubules, kinases and other molecules which post-translationally modify microtubule and kinetochore regulators, and components of the spindle assembly checkpoint which prevent anaphase onset until each kinetochore is attached in a bipolar manner. This thesis presents a study of an outer kinetochore complex, the Dam1/DASH complex, in the fission yeast, and highlights the important role this complex plays in regulating the types of spindle microtubule attachments at the kinetochore, ensuring bi-orientation of sister chromatids and thus the accurate segregation of chromosomes during mitosis. In this first chapter we will introduce many of the mechanisms and molecules fundamental to kinetochore and microtubule function that facilitate proper chromosome segregation, not only in the fission yeast but also in higher organisms.

1.1 Fission yeast

The fission yeast *Schizosaccharomyces pombe* is a rod shaped unicellular organism that divides by medial fission. It belongs to the class of archaeascomycetes. It has a doubling time of between 2-4 hours and wild-type haploid fission yeast grows to a uniform size of 12-15μm at division with a width of 3-4μm. It has a relatively small genome of 14.2 Mb divided into three chromosomes of sizes 6, 4.7 and 3.5 Mb respectively and containing approximately 4900 genes (Moreno et al., 1991; Wood et al., 2002). The fission yeast is a predominantly haploid organism, but can exist as a diploid through the conjugation of haploids to form diploids and reductive meiosis to generate haploids. Haploid cells conjugate to form diploids only under conditions of nitrogen starvation (Fantes and Beggs, 2000). Haploid fission yeast cells have two mating types, h^+ and h^-. Homothallic (h^{90}) cells can switch mating types and mate their h^+ and h^- cells (Forsburg, 1994). The newly formed diploids that result from conjugation, immediately sporulate to form haploid spores and thus the default for this organism is the haploid state.

1.1.1 Fission yeast cell-cycle

Fission yeast is mostly a G2 organism with a very short G1 phase that occurs shortly after mitosis, with cells entering S phase before cytokinesis has even been completed. Cells decide at Start/G1 whether to commit to a mitotic cell cycle or to undergo meiotic cell division, depending on nutrient availability and environmental conditions. Upon commitment to the mitotic cell cycle cells enter at G1. In G1 phase cells grow in size and prepare for DNA synthesis. In S phase cells replicate their genome and then enter into a gap-phase G2 where they determine if the conditions are appropriate for mitotic division. In M phase spindle microtubules become attached to the kinetochores of sister chromatids in a bipolar manner and are segregated to opposite poles. Cells then undergo cytokinesis before re-entering the subsequent G1 phase (Figure 1.1). Cell cycle regulators monitor the cellular and environmental state and thus temporally order the fission yeast cell cycle progression by controlling the transition from one phase to the next. The fission yeast cells contain a number of checkpoint surveillance mechanisms that monitor DNA replication, DNA damage and spindle assembly and attachment to kinetochores during mitosis. These checkpoints can stall the progression of the cell cycle until errors are corrected and conditions, which activated the checkpoint cascades, are satisfied (Hartwell and Weinert, 1989).

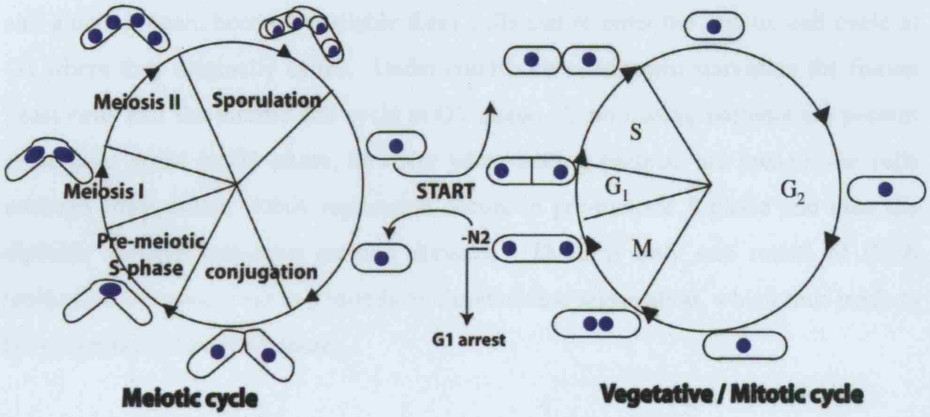

Figure 1.1: Meiotic and Mitotic cell cycle stages in the fission yeast *S. pombe*.

Fission yeast cells undergo four stages of the cell cycle in a similar manner to higher organisms, G1, G2, S and M phase. Fission yeast cells decide at Start/G1 phase whether to undergo meiotic or mitotic cell division according to environmental conditions. When starved of nitrogen cells either remain in G1 gap phase or if a mating partner is present enter a reductive meiotic cell division cycle, which consists of one round of S phase DNA replication and two rounds of chromosome segregation to generate haploid spores. Cells that commit to a mitotic cell division enter the cell cycle at G1 and prepare for DNA synthesis in S phase. Cells then proceed through S phase and enter G2 another gap phase, which prepares the cells for mitosis. In M phase the chromosomes are segregated to opposite poles and cytokinesis ensues. The cells then enter a subsequent G1 phase. In the absence of glucose cells exit the mitotic cell division cycle at G2 phase and enter a stationary G0 gap phase where growth does not occur. If glucose again becomes available the cells re-enter the mitotic cell cycle at G2.

Under conditions of low glucose cells exit the mitotic cell cycle at G2 and enter a gap stationary phase of no growth termed G0. If favourable environmental conditions, and glucose, again become available these cells can re-enter the mitotic cell cycle at G2 where they originally exited. Under conditions of nitrogen starvation the fission yeast cells exit the mitotic cell cycle at G1 phase. If no mating partners are present these cells arrest in G1 phase, however when mating partners are present the cells undergo conjugation. DNA replication occurs in pre-meiotic S phase and then the diploids undergo reductive meiotic division. There is only one round of DNA replication in meiosis but two rounds of chromosome segregation, which thus leads to the generation of haploid spores.

After the replication of DNA the zygotes undergo meiotic prophase whereby the nucleus elongates, telomeres cluster at the SPB and the telomere-led nucleus oscillates between both ends of the cell in what is known as horsetail movement. This movement facilitates the proper pairing of homologous chromosomes required for chiasmata formation and homologous recombination. Meiosis I involves the segregation of homologous chromosomes in a mono-polar manner. Cohesion at the centromere between sister chromatids is maintained at anaphase I until sister chromatid separation during meiosis II. These two rounds of chromosome segregation result in the formation of four haploid spores, which germinate to form four haploid cells, which can enter the mitotic cell cycle at Start/G1 (Figure 1.1) (Forsburg, 1994).

1.1.2 Fission yeast-model organism

The fission yeast is a genetically facile organism. Genetic manipulations such as gene tagging and gene deletions can be easily carried out and mutant alleles of various genes can be readily isolated and characterised. The fission yeast can be easily manipulated using different stress, nutrient conditions and mutant backgrounds that it therefore makes it a powerful tool to study various cellular processes. Indeed many of the genes for various cell cycle processes within the fission yeast are the same as those found in higher organisms and as such the fission yeast is an excellent model system to study how cell cycle related processes are regulated.

1.2 Cytoskeleton

The cytoskeleton is a cellular scaffolding which functions to maintain cell shape and polarity, provide mechanical strength, intracellular protein and organelle transport, cell migration and chromosome segregation. The cytoskeleton is made up of intermediate filaments, actin filaments and microtubules (Alberts et al., 1994). There are several types of intermediate filaments, all are composed of long monomers of their characteristic protein, and are approximately 10nm in diameter. Keratin filaments are found in epithelial cells and give rise to hair and nails. Nuclear lamins form a network that provides stabilisation and support for the inner membrane of the nuclear envelope. Neurofilaments function in strengthening the long axons of neurons and vimentins provide mechanical strength to muscles. Actin filaments known as F-actin are approximately 7nm in diameter and are composed of globular actin protein subunits termed G-actin. Actin is the most abundant protein in the cell and is one of the most highly conserved proteins amongst various organisms. Actin filaments like microtubules are polar in nature with a fast growing plus end and a slow growing minus end. Actin filaments are involved in many diverse functions including muscular contraction, cell growth, cell movement and cytokinesis (Alberts et al., 1994). The Actin filaments are further regulated by interactions with proteins which co-ordinate their polymerisation and depolymerisation and function in various cellular processes. The fission yeast cytoskeleton consists only of microtubules, actin cables and actin filaments.

1.2.1 Microtubules

Microtubules are linear polymers of a globular protein called tubulin. They serve as structural components within the cell and like actin are implicated in a variety of intracellular processes. Microtubules function in determining cell shape and polarity, the intracellular transport of organelles and proteins, cell locomotion and in the separation of sister chromatids during mitosis.

Microtubules can consist of α, β, γ, δ, and ε tubulin subunits. The α and β subunits exist as a heterodimer and form microtubule filaments that grow from an anchoring structure composed of γ tubulin by GTP hydrolysis. The γ tubulin subunit is found at microtubule organising centres (MTOCS) (Pickett-Heaps, 1969), where it interacts with other non-tubulin proteins to form the γ tubulin ring complex. This complex acts as a scaffold to initiate the nucleation of α and β tubulin protofilaments to form a

microtubule filament. The recently identified ε and δ tubulin subunits also play a role in the formation of MTOCs for microtubule nucleation. Human δ tubulin localises to the centriolar structures and partially co-localises with γ tubulin (Chang and Stearns, 2000; Inclan and Nogales, 2001). Human ε tubulin localises in a cell cycle dependent manner to the centrosome where it associates with only the old centrosome (Chang and Stearns, 2000; Inclan and Nogales, 2001).

1.2.2 MTOCs

In vertebrates the microtubule organising centres are called centrosomes. Centrosomes are cylindrical structures composed of two perpendicular centrioles, which are rich in ε tubulin, and are surrounded by pericentriolar material (PCM). Each centriole consists of nine triplets of microtubules. The PCM material contains proteins that function to nucleate and anchor microtubule filaments such as the γ tubulin complex, ninein and pericentrin. During interphase the centrosome is associated with the nuclear membrane. In S phase the centrosome duplicates and during mitotic prophase these migrate to opposite poles of the cell (Alberts et al., 1994). Following nuclear envelope breakdown the centrosomally nucleated spindle microtubules can interact with the chromatids to facilitate chromosome segregation. There are reports however that shows that the centrosome is not absolutely required for spindle formation in mitosis. Laser ablation of the centrosome in vertebrate cells can yield cells that form functional and morphologically normal mitotic spindles, and mutation of the *sas4*$^{+}$ gene in the fruitfly, which is required for centriole duplication, generates normally developed adult fruitflies albeit lacking centrosomes (Khodjakov et al., 2000; Megraw et al., 2001). It appears that in vertebrate cells microtubule nucleation can occur simply in the presence of chromatin, microtubules and motor proteins. However centrosomes are required for astral and interphase microtubule formation, cytokinesis, S phase entry and neuronal development highlighting the importance of this organelle for the overall survival of multicellular organisms.

Yeast cells contain several MTOCs including interphase MTOC (iMTOC), equatorial MTOC (eMTOC) and spindle pole bodies (SPBs) (Snyder, 1994). The iMTOC is a site of nucleation of interphase cytoplasmic microtubules (Becker and Cassimeris, 2005; Janson et al., 2005). These microtubules are nucleated in an independent manner from the SPB and require the binding of the γ tubulin complex to microtubules in the cytoplasm to initiate the nucleation. The eMTOC is involved in

the assembly of the post-anaphase array following chromosome segregation and this occurs in the centre of the cell at the site where cytokinesis will occur. The spindle pole body is analogous to the metazoan centrosome. The SPB functions to nucleate the mitotic spindle and astral microtubules during mitosis. The budding yeast SPB is quite distinct from the centrosomes of higher vertebrates, as it consists of a laminar body (Knop et al., 1999). In interphase the fission yeast SPB lies adjacent to the nuclear envelope in the cytoplasm, following the formation of a half bridge structure a duplicate laminar body structure forms around G1/S, although the exact timing of SPB duplication is still controversial (Ding et al., 1997; Uzawa et al., 2004). SPB maturation occurs in G2 and following invagination of the nuclear envelope the duplicated SPBs are incorporated into the nuclear envelope fenestra. As the cells enter mitosis the SPBs separate and the spindle microtubules are nucleated from the innermost layer of the SPB structure to form a bipolar spindle. Astral microtubules are nucleated in mid-late mitosis to regulate spindle length (Ding et al., 1997; Jaspersen and Winey, 2004; Uzawa et al., 2004). Despite the distinctions between vertebrate centrosomes and the yeast spindle pole bodies both MTOCs play conserved and important roles in the nucleation and organisation of microtubules within the cell.

1.2.3 Microtubule growth and shrinkage overview

Microtubules are nucleated from a starting structure composed of the γ tubulin ring complex, which acts as a scaffold for the polymerisation of α and β tubulin dimers to begin polymerisation to form a microtubule filament. Each microtubule filament is composed of ~ 13 protofilaments, which form a cylindrical microtubule structure of approximately 24-25nm in diameter. The microtubules are polar in nature with an anchoring minus end capped by the γ tubulin complex and a growing or shrinking plus end. Microtubule growth occurs through the addition of α and β tubulin heterodimers, bound to GTP, to the microtubule plus end. GTP that is bound to α-tubulin is stable, however, the GTP bound to β-tubulin is shortly hydrolysed to GDP. When GTP bound α and β-tubulin is incorporated at the plus end this stability facilitates the incorporation of further GTP bound tubulin heterodimers inducing microtubule growth. As tubulin heterodimers are added onto the plus end of microtubules only when in the GTP state there is usually a GTP cap protecting the plus end of microtubules from disassembly. The β-tubulin subunits undergo hydrolysis of GTP-GDP, when this hydrolysis catches up to the plus end tip of the

microtubule the β-tubulin at the tip hydrolyses its GTP-GDP and undergoes a conformational change which prevents GTP-tubulin heterodimers from adding onto the plus end and the filament undergoes rapid depolymerisation and shrinking. This switch from growth to shrinkage is known as a 'catastrophe'. Following this a microtubule may again undergo growth and polymerisation. This switch from depolymerisation and shrinkage to polymerisation and growth is called 'rescue'. Alternation between microtubule polymerisation and depolymerisation occurs continuously in what is termed 'dynamic instability' (Mitchison et al., 1986; Mitchison and Kirschner, 1984). This 'dynamic instability' is crucial to promote the function of microtubules both in cellular transport, the search and capture for attachment to chromosomes in mitosis, and for cellular locomotion. Assembled microtubule filaments are further regulated through various post-translational modifications such as acetylation and detyrosination to modify those filaments that have not recently been polymerised.

1.2.4 Microtubule regulators

Many proteins also function to regulate the dynamics of microtubules within the cell. Microtubule associated proteins (MAPs) interact with the microtubules to promote a diverse range of functions within the cell. Most MAPs have microtubule stabilizing properties, however some have been shown to play roles in microtubule disassembly, cross-linking microtubules, regulating microtubule growth towards specific locations and facilitating interactions of microtubules with other proteins or structures (Alberts et al., 1994). MAPs were initially identified biochemic ally from the isolation of bovine brain microtubules. Perhaps one of the most famous MAPs is the Tau protein. This protein has been linked to the neurological disorder, Alzheimer's disease. Tau binds to the outer surface of the microtubule protofilament and stabilises and bundles microtubules within neuronal cells (Cairns et al., 2004). The TOG family is another family of MAPs that are required for microtubule stabilisation and accurate chromosome segregation. One of the best studied is XMAP215 from *X. laevis*.

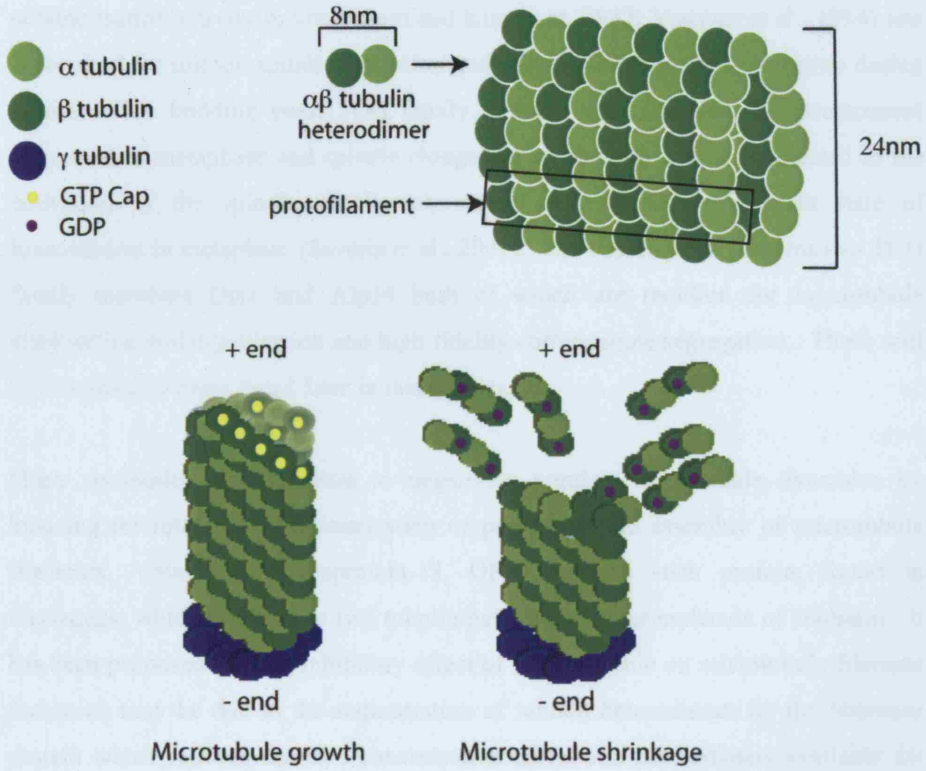

Figure 1.2 Schematic showing microtubule dynamics

Microtubule filaments are approximately 24-25 nm in diameter. The α/β heterodimer is 8nm in diameter. Each microtubule filament is composed of 13 protofilaments of tubulin arranged in a cylindrical tubular structure. The addition of αβ heterodimers to the plus end of the microtubule promotes microtubule polymerisation. These heterodimers must be bound to GTP to enable assembly at the plus end of the microtubule. When a filament contains GTP tubulin heterodimers at its plus end this promotes the addition of more heterodimers and microtubule growth ensues. Shortly after addition the β-tubulin subunit undergoes hydrolysis of its GTP to a GDP bound form. When this hydrolysis reaches the plus end of the microtubule the resultant conformational change in the β-tubulin subunit induces rapid depolymerisation and shrinkage of the microtubule filament.

XMAP215 has been shown biochemically to induce microtubule stabilisation and polymerisation activity in vitro (Gard and Kirschner, 1987; Vasquez et al., 1994) and is required for mitotic spindle formation and proper chromosome segregation during mitosis. The budding yeast TOG family member Stu2 functions in chromosome alignment in metaphase and spindle elongation in anaphase and is implicated in the activation of the spindle checkpoint, which monitors the attachment state of kinetochores in metaphase (Severin et al., 2001). The fission yeast contains two TOG family members Dis1 and Alp14 both of which are required for microtubule stabilisation and organisation and high fidelity chromosome segregation. These will be discussed in more detail later in this chapter.

Many molecules also function to negatively regulate microtubule dynamics by inducing microtubule depolymerisation or preventing the assembly of microtubule filaments. Stathmin (Oncoprotein-18, OP18) is one such protein, found in metazoans, which can bind to two tubulin heterodimers per molecule of stathmin. It has been proposed that the inhibitory effect of this molecule on microtubule filament formation may be due to the sequestration of tubulin heterodimers by the Stathmin protein which reduces the free concentration of tubulin heterodimers available for polymerisation, or that Stathmin may play a more direct role in inducing catastrophe at microtubule tips (Belmont and Mitchison, 1996; Cassimeris, 2002).

Kinesins are a class of microtubule based motor proteins that function in many diverse aspects of cellular function. Members of this family function in tasks in which force generation is required such as protein and organelle transport, regulation of microtubule dynamics and chromosome segregation. Conventional kinesin was the first member of the super-family identified and consists of two 120kDa heavy chains and two 64kDa light chains which make up a rod-like structure composed of two globular heads, a stalk and a fan-like end (Hirokawa and Takemura, 2004). The heavy chains in the globular head contain motor domains, coiled-coil domains and a stalk, which are required for microtubule binding and ATPase activity. Chromokinesins are a subgroup of kinesin motor proteins that function in mitosis to regulate chromosome condensation, chromosome alignment on the metaphase plate, chromosome segregation and cytokinesis. They belong to two families kinesin-4 and kinesin -10 and members include Kif4A and Kif4B (Kinesin-4 family) and KID (Kinesin-10 family). KID is a *C. elegans* plus end directed motor that demonstrates microtubule and DNA binding properties. It plays an important role in controlling the movement of chromosomes along the spindle in prometaphase and metaphase and

the alignment of the chromosomes to the metaphase plate (Tokai-Nishizumi et al., 2005). CENP-E is a member of the kinesin-7 family that is involved in the interaction of the spindle microtubules with the kinetochore. It localises to the kinetochore corona throughout the cell cycle and is also involved in the functioning of the spindle assembly checkpoint, and in the alignment of chromosomes to the metaphase plate (Cooke et al., 1997; McEwen et al., 2001; Schaar et al., 1997; Wood et al., 1997). Kinesin-5 (BimC) family members are structurally quite distinct from other kinesin super-family members. They have four motor domains with a 'dumbbell' like structure containing two motor domains at each end joined by a rod to form a bipolar homo-tetramer structure. This bipolar structure contributes to the function of this family of proteins in cross-linking microtubule filaments to form a bipolar spindle. Eg-5 is a vertebrate member of this family, which plays a crucial role in the cross-linking, and sliding of microtubules to form a proper bipolar spindle in mitosis (Cooke et al., 1997).

The kinesin-13 (KinI) family does not possess motor activity but surprisingly possesses microtubule depolymerising activity. The motor domain is found in the middle of the protein rather than in the N or C termini as in other kinesin families. This family functions to promote catastrophe and dynamic instability in microtubule filaments (Desai et al., 1999). There are three mitotic kinesin-13 members in human cells Kif2a, Kif2b (Klp10A-*Drosophila melanogaster*) and Kif2c/MCAK (Klp59C-*Drosophila melanogaster*). The *D. melanogaster* kinesin-13 proteins Klp10A and Klp59C demonstrate a 'division of labour' to regulate microtubule depolymerisation during mitosis. Klp59C (MCAK) induces microtubule depolymerisation at the kinetochore attached plus-end in a 'pac-man' like manner, whereby kineotchores induce the disassembly of spindle microtubules allowing the movement of sister chromatids towards the pole by depolymerising the spindle as it goes. The kinesin-13 member Klp10A (Kif2a, Kif2b) functions to induce depolymerisation of the mitotic spindle and to drive anaphase sister chromatid movement in a distinctive manner. Klp10A depolymerises microtubules at the centrosome associated minus end to allow anaphase segregation of chromosomes via 'poleward flux' (Rogers et al., 2004). Furthermore both of these kinesin-13 members have been shown to form ring like and spiral structures around microtubules in a similar manner to the budding yeast Dam1/DASH complex which may allow these molecules to remain associated with the ends of microtubules during depolymerisation (Tan et al., 2006). MCAK (Mitotic centromere associated kinesin) is a potent vertebrate microtubule destabiliser that can target either microtubule end, in a non-motile manner, through a 'diffusion and

capture' mechanism to allow rapid end binding of the microtubule (Helenius et al., 2006). MCAK induces catastrophe in stable microtubules through removal of the GTP cap from the plus end of microtubule filaments promoting rapid microtubule depolymerisation and disassembly in a motor and ATP hydrolysis dependent manner (Desai et al., 1999). MCAK and its homologues have been shown to oppose the microtubule stabilising properties of the TOG family (Holmfeldt et al., 2004; Tournebize et al., 2000). MCAK is found both in the cytoplasm and on centromeres throughout the cell cycle but its centromere association is enriched following mitotic entry, where it has been implicated in playing an important role alongside Aurora B in promoting proper kinetochore-microtubule interactions and error correction (Maney et al., 1998). The *X. laevis* XKCM1 (MCAK homologue) is also required for regulation of microtubule dynamics and accurate chromosome segregation (Desai et al., 1999; Severin et al., 2001). Disruption of XKCM1 activity in mitotic *X. laevis* egg extracts results in abnormally long asters and microtubules which lack dynamic instability, demonstrate a fourfold reduction in the catastrophe rate and are incapable of bipolar spindle formation (Walczak et al., 1996).

There are no kinesin-13 family members in yeast, they do possess however kinesin-8 family members which are thought to function in microtubule depolymerisation instead of kinesin-13 members in these organisms. Kinesin-8 proteins are quite similar to kinesin-13 members and disruption of their function yields longer interphase and mitotic microtubules, resistance to spindle drugs, mis-positioning of the mitotic spindle and disruption of correct spindle-kinetochore interactions (Cottingham and Hoyt, 1997; DeZwaan et al., 1997; Garcia et al., 2002a; Garcia et al., 2002b; Goshima et al., 2005; Rischitor et al., 2004). The budding yeast kinesin-8 member Kip3 depolymerises microtubules from the plus end in a length dependent manner. Kip3 possesses motor activity and uses ATP hydrolysis to move in a directed manner towards the plus end of the microtubule (Gupta et al., 2006; Varga et al., 2006). The *Drosophila melanogaster* kinesin-8 member Klp67A also serves to regulate microtubule dynamics by functioning as a microtubule destabiliser. Depletion of Klp67A by RNAi (RNA interference) causes the appearance of longer mitotic spindles, whereas overexpression of this protein leads to shorter mitotic spindles (Goshima et al., 2005). The fission yeast kinesin-8 family members Klp5 and Klp6 have been also implicated in microtubule depolymerisation, spindle length control, chromosome congression during metaphase and accurate chromosome segregation. These proteins will be discussed in further detail later in this chapter (Garcia et al., 2002a; Garcia et al., 2002b; West et al., 2002; West et al., 2001).

1.2.5 Fission yeast microtubules

Most organisms contain several α and β tubulin isoforms which can differentially regulate the localisation and functions of microtubule filaments. The fission yeast is no exception to this with two α-tubulin encoding genes *atb2*$^+$ and *nda2*$^+$and one β-tubulin encoding gene *nda3*$^+$ (Adachi et al., 1986; Hiraoka Y, 1984; Toda et al., 1984; Yanagida, 1987). The α-tubulin gene *nda2*$^+$ is essential for viability, however *atb2*$^+$ is not absolutely required for cell viability indicating some subtle differences between both α-tubulin isoforms. It seems however that these two genes are partially redundant as overexpression of *atb2*$^+$ can rescue the lethality of *nda2* mutants.

In the fission yeast interphase cytoplasmic microtubules are nucleated from iMTOCs or SPBs to form 3-6 microtubule arrays that grow along the length of the fission yeast cell and function to maintain the cell shape and polarity. These cytoplasmic microtubules are arranged with the plus ends facing the cell tips and with minus ends overlapping near the centre of the cell (Sawin and Tran, 2006; Tran et al., 2001). The interphase microtubule arrays disappear as cells proceed into mitosis (Figure 1.3).

Upon entry into mitosis the duplicated invaginated SPBs separate and the mitotic spindle is nucleated from the nuclear side of the SPB. This mitotic spindle is composed of a number of different types of microtubule filaments; including pole-to-pole microtubules, kinetochore-to-pole microtubules and astral microtubules. Pole-to-kinetochore microtubules are anchored at their minus ends to the SPB with their plus ends protruding towards the chromosomes to facilitate kinetochore capture and chromosome segregation during anaphase. The pole-to-pole microtubules extend from one pole to the other with a region of overlap at the centre of the cell. During mitosis the cytoplasmic side of the SPB nucleates astral microtubules, however the exact timing or function of these astral microtubules remains controversial. Previous published reports argue that these cytoplasmic astral microtubules are nucleated prior to anaphase, that they play a crucial role in aligning the metaphase spindle in a perpendicular manner to the cell axis and in the 'spindle orientation checkpoint' (SOC) (Gachet et al., 2001; Gachet et al., 2004; Oliferenko and Balasubramanian, 2002; Rajagopalan et al., 2004; Tournier et al., 2004). More recent work suggests these cytoplasmic astrai microtubules are nucleated after the metaphase-anaphase transition and therefore have no function in a mitotic checkpoint. It is also postulated that what were presumed to be prometaphase-metaphase astral microtubules might be in fact intranuclear microtubules that are nucleated from the nuclear side of the SPB

(Sawin and Tran, 2006; Zimmerman et al., 2004). It is therefore controversial when exactly these cytoplasmic astral microtubules are nucleated and indeed what their function if any is in mitosis.

The kinetochore-to-pole microtubules are nucleated from opposite poles, grow and interact with the kinetochores of sister chromatids. Bipolar attachments are formed so that a kinetochore of one chromatid is attached to one pole and the kinetochore of the sister is attached to the opposite pole. There are approximately 3 pole-to-kinetochore microtubules attached to each kinetochore in the fission yeast. Following this bipolar attachment tension is generated and anaphase onset can occur (Figure 1.3). Anaphase A involves the depolymerisation of the spindle microtubules, to facilitate the pulling of the sister chromatids towards the opposite poles. In anaphase B the pole-to-pole microtubules are elongated pushing the separated chromosomes and SPBs to opposite ends of the cell. At the end of mitosis the post anaphase array (PAA) is nucleated from the eMTOC in the centre of the cell where cell division will occur. A cytokinetic actomyosin ring then forms at this division site to facilitate cytokinesis (Sawin and Tran, 2006) (Figure 1.3).

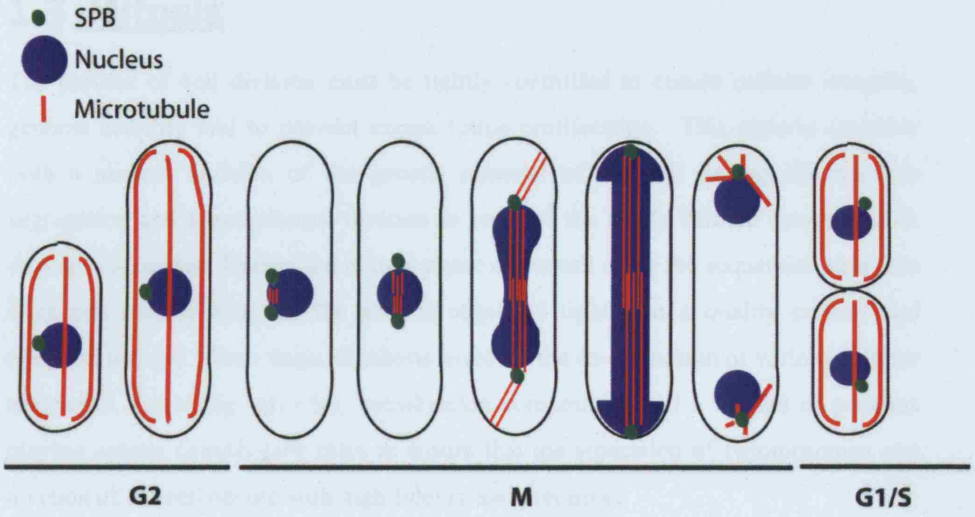

Figure 1.3: Microtubule structure throughout the fission yeast cell cycle

Cytoplasmic interphase microtubule bundles grow along the cell axis and function to maintain cell shape and polarity. The invaginated and duplicated SPBs separate in mitosis and form a bipolar mitotic spindle. The pole-to-kinetochore microtubules nucleated from the nuclear side of the SPB grow with their plus ends towards the equator of the cell and capture the chromosomes aligned at the metaphase plate. Anaphase A onset induces depolymerisation and disassembly of the spindle to pull the separated chromosomes towards the opposite poles. Astral microtubules may play a role in facilitating this process. During Anaphase B the pole-to-pole microtubules are elongated and push the SPBs and newly separated chromosomes apart to the cell ends. A post anaphase array is formed at the site of cell division and a cytokinetic actomyosin ring is deposited at this site. Red represents microtubules, blue represents DNA, and green represents the SPB.

1.3 Mitosis

The process of cell division must be tightly controlled to ensure cellular integrity, genome stability and to prevent excess tissue proliferation. This process involves both a nuclear division of the genetic material of the cell during chromosome segregation and a cytoplasmic division to separate the newly formed daughter cells during cytokinesis. During the mitotic phase of the cell cycle the sequential transition from one mitotic stage to the next is regulated tightly in a quality control and temporal manner. Each stage of mitosis involves the co-ordination of various cellular organelles, signalling cascades, cytoskeleton components and a myriad of proteins playing unique contributory roles to ensure that the separation of chromosomes and division of the cell occurs with high fidelity and precision.

1.3.1 Mitotic stages-overview

The mitotic phase of the cell cycle can be subdivided into various different mitotic stages, prophase, prometaphase, metaphase, anaphase and telophase followed by cytokinesis (Alberts et al., 1994). During prophase the chromosomes condense into well-defined sister chromatids and the cytoplasmic microtubule arrays breakdown and are disassembled. The separating centrosomes begin nucleating the mitotic spindle outside of the nucleus. At the start of prometaphase nuclear envelope breakdown (NEBD) occurs in metazoan cells and the spindle microtubules now enter the nucleus (Alberts et al., 1994). The kinetochore structures on the centromeres of sister chromatids mature and are ready to facilitate the attachment of the chromosomes to the spindle microtubules. The kinetochore microtubules search and capture the kinetochores and tension is generated which aligns the chromosomes along the equator of the cell. During metaphase all of the chromosomes are congressed to the equator of the cell, which is known as the 'metaphase plate', and the attachment state of each kinetochore is monitored. At this stage kinetochores must be attached in a bipolar manner, with the kinetochore of one sister chromatid attached to one pole and the other sister attached to the opposite pole, and sufficient tension generated.

A checkpoint-signalling cascade detects the attachment state of the kinetochores and delivers a 'wait' signal in the event of incorrect or improper attachment. This delays anaphase onset until all sister chromatids can be attached in a proper bipolar manner

and are correctly oriented (Hardwick et al., 2000; Hardwick et al., 1999; Wang and Burke, 1995; Waters et al., 1998). A cohesive complex, known as cohesin, holds the sister chromatids together. At anaphase onset this complex is cleaved allowing the separation of sister chromatids that can be then pulled pole-ward (Uhlmann, 2004; Uhlmann et al., 1999). During anaphase A the kinetochore microtubules are depolymerised to facilitate the movement of the chromosomes to the poles. Anaphase B involves the elongation of polar microtubules, which pushes the spindles poles apart and further separates the segregated chromosomes to opposite ends of the cell (Alberts et al., 1994; Barton and Goldstein, 1996). Telophase then follows which in mammalian cells involves the reformation of the nuclear envelope around each group of daughter chromosomes, the disappearance of the kinetochore microtubules, decondensation of the chromatin and the re-appearance of the nucleoli (Alberts et al., 1994). The newly formed daughter cells then undergo cytokinesis. In animal cells the plasma membrane around the cell centre is drawn inwards to form a cleavage furrow. This cleavage furrow continues to constrict until only a thin bridge of cytoplasm remains between the two new daughter cells. Eventually this bridge narrows and breaks and the cells are completely separated (Alberts et al., 1994).

Within the fission yeast cell cycle mitosis is also classified into the same distinct phases, prophase, prometaphase, metaphase, anaphase, telophase and cytokinesis. Unlike mammalian cells and other organisms the fission yeast nuclear envelope does not break down during mitosis and the fission yeast undergoes a 'closed mitosis' with mitotic spindle nucleation and chromosome segregation occurring completely within the nucleus (Egel et al., 1980). Prometaphase, metaphase and anaphase proceed in a similar manner as in mammalian cells with condensation of the chromosomes, breakdown of the cytoplasmic microtubule arrays, attachment of the pole-to-kinetochore microtubules to kinetochores, chromosome congression to the metaphase plate, segregation of the chromosomes during anaphase and pole-to-pole spindle elongation during anaphase B. During telophase a post anaphase array of microtubules is formed and septum formation occurs which allows separation of the fission yeast cells during cytokinesis.

Fission yeast mitosis can also be classified according to mitotic spindle dynamics. The pole-to-kinetochore microtubules cannot be visualised by fluorescence microscopy during fission yeast mitosis and only the pole-to-pole microtubules are apparent. Mitosis can therefore be classified according to the dynamics of these pole-to-pole microtubules as three distinct phases; phase I, phase II and phase III. In phase

I (prophase) mitotic spindle nucleation is initiated with spindle length corresponding to 0-2.5μm. In phase II (prometaphase-anaphase A) the spindle length remains constant at ~ 2.5μm. In phase III spindle elongation occurs (anaphase B) with the spindle length increasing to 12-15μm (Nabeshima et al., 1998). Mutations that affect kinetochore components, tubulin structure or dynamics and the regulation of mitotic timing can show delay in the duration of some of these phases.

1.3.2 Kinetochore attachment & tension overview

During mitosis the kinetochores of sister chromatids must become correctly and stably attached in a bipolar manner. Kinetochore microtubules 'search and capture' the kinetochores during prometaphase, but this is thought to be a stochastic process and often leads to the formation of incorrect and mal-oriented kinetochores. These incorrectly attached kinetochores must be 'turned-over' and repaired to allow bipolar attachments to form, tension to be generated and proper kinetochore bi-orientation to occur. Kinetochores that are stably attached in a bipolar configuration with the kinetochores of both sister chromatids attached to opposite spindle poles are known as amphitelic attachments (Figure 1.4). When this amphitelic state is achieved not only are the kinetochores attached to both poles but also tension, which is required to satisfy the spindle assembly checkpoint, is generated (Stern and Murray, 2001). This tension occurs due to the balance in opposing forces with the pole-ward force caused by depolymerisation of the attached kinetochore microtubules pulling against the sister chromatids, which are held together by cohesin (He et al., 2000; Tanaka et al., 2000). This tension is important to not only enable the sensing of correct attachment states but also in stabilising the microtubule attachments to the kinetochore.

Defects in microtubule-kinetochore attachment can be of several different configurations. If only one of the kinetochores on a pair of sister chromatids is attached and the other is unattached this is known as monotelic attachment (Figure 1.4). In this case the unattached kinetochore will activate the spindle assembly checkpoint-signalling cascade to induce a mitotic delay until an amphitelic configuration can be established (Hardwick, 2005; Zhou et al., 2002). Another type of mono-polar configuration exists whereby both sister kinetochores can become attached to the same pole, and is known as syntelic attachment (Figure 1.4). Syntelically attached kinetochores can satisfy the attachment criteria of the spindle assembly checkpoint, but sufficient tension is not generated by this configuration,

thus allowing the tension sensing components of the checkpoint to signal and induce an anaphase delay and activate an Aurora B dependent repair pathway (Dewar et al., 2004; Lampson et al., 2004; Pinsky and Biggins, 2005). Merotelic attachments occur when a single kinetochore is attached to both spindle poles by one or more microtubules (Figure 1.4). It has been shown that merotelic attachments occur frequently in tissue-cultured cells with approximately 30% of prometaphase Ptk1 cells showing one or more merotelically oriented kinetochores (Cimini et al., 2003). Despite the fact that evidence suggests that these attachments appear not to be detected by the spindle assembly checkpoint (Cimini et al., 2001) these defects do appear to be 'turned over' and repaired in an Aurora B and MCAK dependent manner (Cimini et al., 2003; Cimini et al., 2006; Knowlton et al., 2006). We will discuss the correction of mal-oriented kinetochore attachments in more detail later in this chapter.

It was reported that astral microtubules play an important role in the orientation of the spindle and the generation of tension at the kinetochore-microtubule interface. Fission yeast cells that lack 'astral' microtubules in metaphase were unable to orient the mitotic spindle along the length of the cell and it was thus concluded that 'astral' microtubules orient the position of pole-to-kinetochore microtubules in a perpendicular manner to the cell axis (Gachet et al., 2004; Oliferenko and Balasubramanian, 2002). More recently it has been demonstrated that these microtubules are not 'astral' in nature and are actually intranuclear microtubules, however it is likely that instead of contacting the cell cortex to orient the mitotic spindle as earlier proposed they are in fact contacting the nuclear envelope and in this manner facilitating the orientation of the spindle and the generation of kinetochore tension (Zimmerman et al., 2004).

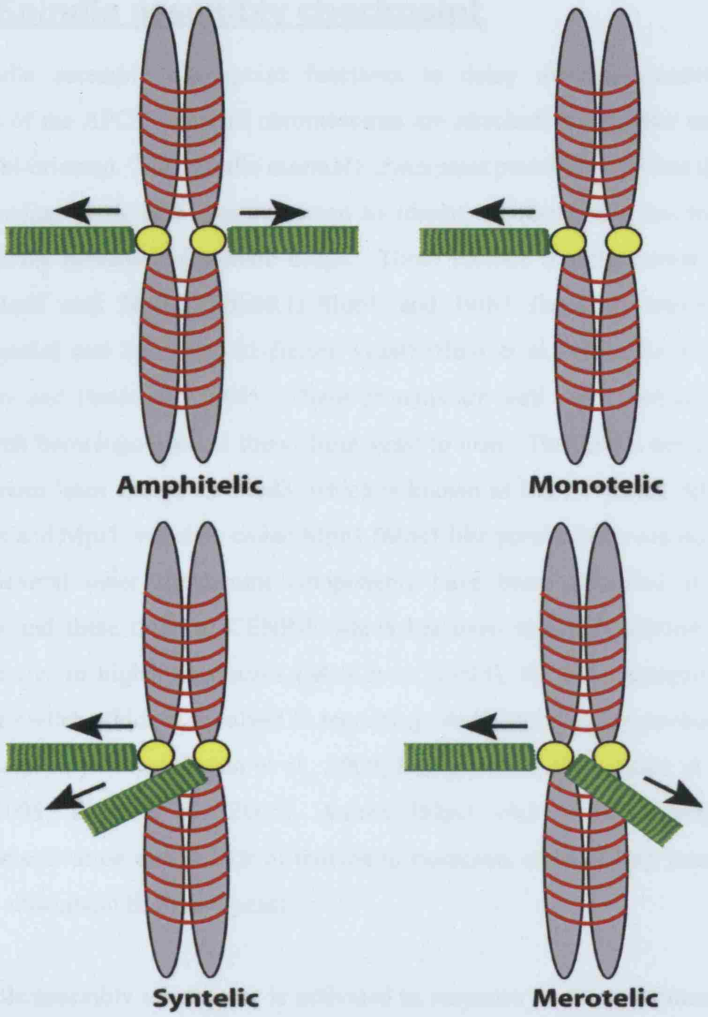

Figure 1.4: Kinetochore attachment configurations

Kinetochores that are correctly attached in a bipolar manner with both sister chromatids attached to opposite spindle poles are known as amphitelic attachments. If one of the kinetochores on a pair of sister chromatids is unattached this is known as monotelic attachment and leads to activation of the spindle assembly checkpoint. Syntelic attachments occur when both sister chromatids are attached to the same pole and causes activation of a tension-sensing arm of the checkpoint and induction of repair pathways. Merotelic kinetochores occur when kinetochores become attached to both spindle poles. These are not sensed by the checkpoint but are efficiently 'turned over' in an Aurora B dependent manner. Arrows represent direction of microtubule pulling force.

1.3.3 Spindle assembly checkpoint

The spindle assembly checkpoint functions to delay anaphase onset through inhibition of the APC/C until all chromosomes are attached in a bipolar manner and correctly bi-oriented. The spindle assembly checkpoint proteins were first discovered in the budding yeast in a genetic screen to identify mutants that fail to arrest in mitosis in the presence of spindle drugs. These include (mitotic arrest deficient) Mad1, Mad2 and Mad3 (hBubR1) Bub1 and Bub3 (budding uninhibited by benzimidazole) and Mps1 (Mph1-fission yeast) (Hoyt et al., 1991; Li and Murray, 1991; May and Hardwick, 2006). These proteins are well conserved across many species with homologues of all found from yeast to man. The names are maintained across species lines except for Mad3, which is known as BubR1 (Bub1 related 1) in metazoans and Mps1, which is called Mph1 (Mps1 like pombe homologue) in fission yeast. Several other checkpoint components have been identified in different organisms and these include; CENP-E which has been shown to stimulate BubR1 kinase activity in higher organisms (Mao et al., 2003), the RZZ complex of Rod, Zw10 and Zwilch which is involved in recruiting Mad1-Mad2 to kinetochores and in their subsequent removal (Basto et al., 2000; Buffin et al., 2005; Chan et al., 2000; Karess, 2005; Kops et al., 2005), Aurora B/Ipl1/Ark1 which is required for checkpoint activation due to lack of tension in mammals and budding yeast and due to lack of attachment in fission yeast.

The spindle assembly checkpoint is activated in response to chromosomes that lack attachment. Removal of unattached kinetochores either through the establishment of amphitelic orientation or through laser ablation results in silencing of the spindle assembly checkpoint and anaphase entry (Rieder et al., 1995). The checkpoint can also be activated when tension is lacking, such as is found in syntelic configurations or upon treatment with spindle poisons or chemicals (Kapoor et al., 2000; May and Hardwick, 2006; Skoufias et al., 2001). Mad1 and Mad2 localise to unattached kinetochores but do not localise to kinetochores that lack only tension (Waters et al., 1998), whereas Bub1 and BubR1/Mad3 can localise to both unattached and/or tensionless kinetochores (Skoufias et al., 2001) (Figure 1.5).

The spindle assembly checkpoint induces a mitotic delay through inhibition of the Anaphase promoting complex APC/C. The APC/C functions as an E3 ubiquitin ligase enzyme that ubiquitylates many cell cycle regulators and targets them for

degradation by the 26S proteasome. During metaphase the Cohesin complex holds the sister chromatids together. The Scc1 subunit of this complex is cleaved at the metaphase-anaphase transition by a protease called Separase, which facilitates the separation of sister chromatids during anaphase A (Ciosk et al., 1998; Klein et al., 1999; Uhlmann et al., 1999; Uhlmann et al., 2000). Securin is an inhibitory chaperone that prevents premature activation of Separase prior to anaphase onset (Hornig et al., 2002,; Salah and Nasmyth, 2000; Yanagida, 2000) and is a key anaphase substrate for the APC/C. Destruction of Securin releases Seperase and allows it to cleave Cohesin (Figure 1.5). The APC/C also targets Cyclin B for destruction during anaphase, which facilitates mitotic exit through the abolition of CDK activity (Shirayama et al., 1999). The APC/C is regulated by the presence of accessory proteins Cdh1 or Cdc20, which interact with specific substrates and target them to the APC/C for ubiquitylation (Peters, 2002). Cdc20 (Slp1-fission yeast) is the mitotic accessory regulator of the APC/C and is the target of the spindle assembly checkpoint. Several checkpoint proteins form a complex (MCC) that binds to Cdc20, rendering the APC/C inactive and inducing a mitotic delay (Kim et al., 1998)(Figure 1.5).

When kinetochores are unattached or lacking in tension the spindle assembly checkpoint components localise to the kinetochore where a 'wait anaphase' signal is generated and amplified. Mad1 and Bub1 can stably associate with unattached kinetochores where it is thought they act as a scaffold or platform for recruitment of the other checkpoint signalling molecules Mad2 and Mad3/BubR1 (Howell et al., 2004; Shah et al., 2004). There is a pool of Mad2 that always remains stably associated with Mad1 at the kinetochore whereas a second population of Mad2 and cdc20 cycles on and off the kinetochore in a dynamic fashion (Howell et al., 2004; Shah et al., 2004; Vink et al., 2006). Structural studies have revealed that Mad2 can exist as two different conformers. When free in solution Mad2 is in an open confirmation called O-Mad2, this Mad2 conformer can bind to Mad1or Cdc20 and undergoes a conformational change to form closed Mad2, C-Mad2.(De Antoni et al., 2005). The Mad1/C-Mad2 complex is very stable and acts as a template at the kinetochore for the recruitment of O-Mad2 and facilitates the binding of O-Mad2 to Cdc20, to form a Cdc20/C-Mad2 complex. This C-Mad2/Cdc20 complex displays potent inhibition of the APC/C *in vitro*, however *in vivo,* the formation of a complex consisting of Mad2, Mad3/BubR1, Bub3 and Cdc20 known as the mitotic checkpoint complex (MCC) is required for inhibition of the APC/C (Figure 1.5).

Once kinetochores have become properly attached and bi-oriented the spindle assembly checkpoint must be switched off to allow anaphase to proceed and cells to exit mitosis. Several molecules have been implicated in playing an important role in checkpoint silencing at the metaphase-anaphase transition. The motor protein Dynein has been shown to play an important role in the transport of Mad1, Mad2 and BubR1 away from the kinetochore along microtubules, which could serve to prevent the formation of further inhibitory MCC complexes, or in the generation of the 'wait anaphase' signal (Howell et al., 2001). CENP-E has been implicated in spindle assembly checkpoint silencing due to its ability to regulate BubR1 kinase activity. It has been shown that the binding of microtubules to CENP-E downregulates the BubR1 kinase activity and switches off the checkpoint (Mao et al., 2003). The checkpoint inhibitory protein $p31^{comet}$ (CMT2) possess the ability to selectively bind to Mad2 that is bound to Cdc20 (Mapelli et al., 2006; Xia et al., 2004). Furthermore *in vitro* studies demonstrate that purified $p31^{comet}$ enhances the activity of the APC/C and that $p31^{comet}$ plays a role in silencing the spindle assembly checkpoint. Recently a new report highlighted an important discovery in furthering our understanding of how the spindle assembly checkpoint is silenced. It now seems that Cdc20 is multi-ubiquitinated in an UbcH10 dependent manner, which causes disruption of the MCC complex through dissociation of Mad2 and BubR1. This ubiquitination and dissociation of checkpoint proteins are enhanced by the presence of both UbcH10 and $p31^{comet}$ (Reddy et al., 2007). This process can be reversed through the action of a de-ubiquitinating enzyme USP44, which can stabilise the MCC complex through de-ubiquitination of Cdc20 both *in vitro* and *in vivo* (Reddy et al., 2007; Stegmeier et al., 2007). This suggests that the metaphase-anaphase transition is regulated by a dynamic balance in ubiquitination by the APC/C and de-ubiquitination by USP44.

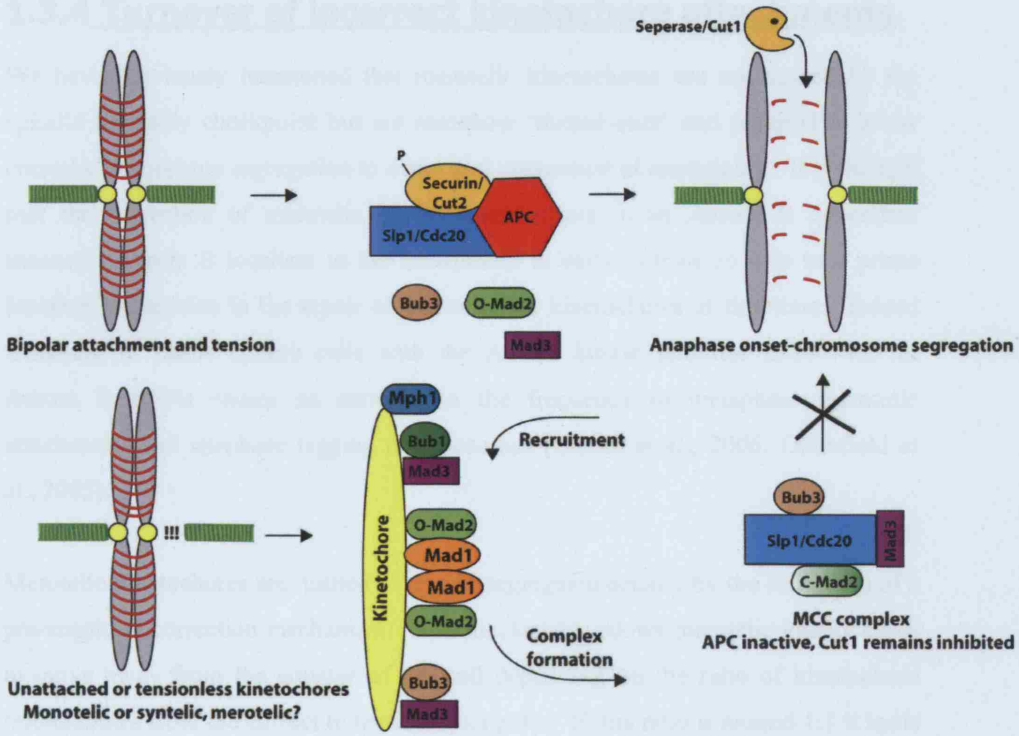

Figure 1.5: Activation mechanism of the spindle assembly checkpoint

During metaphase the kinetochores must become attached in a bipolar amphitelic manner and sufficient tension generated. When correct attachments are generated anaphase onset begins by APC/C mediated ubiquitylation of Securin/Cut2, which is an inhibitory chaperone for the thiol protease Separase. Degradation of Securin causes the release of Seperase and the cleavage of the Cohesin complex that holds sister chromatids together, allowing chromosomes segregation to occur. In conditions where kinetochores are unattached or lacking in tension the spindle assembly checkpoint cascade is activated. This process involves the recruitment of checkpoint proteins to the kinetochore. It is believed that Mad2 is recruited to the kinetochore through Mad1, Mad3 recruited through binding Bub1 and Bub3 through binding Mad3. The binding of Mad2, Bub3 and Mad3/BubR1 to the APC/C accessory protein Cdc20 then forms the MCC complex. This inhibits Cdc20 to prevent APC/C activation and induce a mitotic delay. O-Mad2 represents the open conformation of the Mad2 protein. C-Mad2 represents the closed conformation of the protein.

1.3.4 Turnover of incorrect kinetochore attachments

We have previously mentioned that merotelic kinetochores are not sensed by the spindle assembly checkpoint but are somehow 'turned over' and repaired to allow correct chromosome segregation to occur and prevention of aneuploidy. It is thought that the correction of merotelic kinetochores occurs in an Aurora B dependent manner. Aurora B localises to the centromere in early mitosis so it is in a prime location to function in the repair of mal-oriented kinetochores at this time. Indeed treatment of tissue culture cells with the Aurora kinase inhibitor ZM447439 or Aurora B RNAi causes an increase in the frequency of metaphase merotelic attachments and anaphase lagging chromosomes (Cimini et al., 2006; Ditchfield et al., 2003).

Merotelic kinetochores are 'turned over' and segregated equally by the activation of a pre-anaphase correction mechanism. This mechanism allows merotelic kinetochores to move away from the equator of the cell depending on the ratio of kinetochore microtubules from the correct to the incorrect pole. If this ratio is around 1:1 it leads to the failure in the 'turn over' of these merotelic kinetochores and anaphase lagging chromosomes result, however, if there is a higher ratio favouring the correct pole then poleward movement will occur with correct segregation of the sister chromatids in anaphase (Cimini et al., 2004). This mechanism has been shown to allow the correct segregation of merotelic kinetochores in tissue culture cells, with 16% of Ptk1 metaphase cells displaying one or more merotelic kinetochores but only ~1% of these produce anaphase-lagging chromosomes (Cimini et al., 2004).

Aurora B functions in the pre-anaphase 'turnover' of merotelic kinetochores that have a microtubule ratio of 1:1 by reducing the number of microtubules that are attached to the incorrect pole through microtubule detachment and depolymerisation. Evidence for this includes that kinetochore microtubules become much more stable when Aurora B is inhibited and also in anapahase when Aurora B relocalises from the centromere/kinetochore to the spindle midzone (Cimini et al., 2006). It is thought that the detachment of incorrect microtubule attachments occurs through the regulation of the depolymerising kinesin MCAK by Aurora B. Both Aurora B and active MCAK are enriched at merotelic kinetochore sites (Knowlton et al., 2006) and a previously published report shows that the prevention of centromeric localisation of MCAK increases the frequency of anaphase lagging chromosomes (Kline-Smith et

al., 2004). It would therefore seem that one of the roles of Aurora B in the 'turnover' of merotelic kinetochores in mammalian cells is through the regulation of the depolymerisation activity of MCAK. It seems likely that other downstream modulators exist which must be modified by Aurora B to function not only in sensing merotelic attachments and in detachment of the incorrect microtubules, but also in the re-attachment of correctly oriented microtubules.

In the budding yeast the Aurora B ortholog, Ipl1, is found in a complex with Bir1 (Survivin) and Sli15 (INCENP) which has been shown to be required for anaphase spindle elongation, cytokinesis and in early mitosis in the generation of correctly bi-oriented kinetochores (Biggins and Murray, 2001; Dewar et al., 2004; Tanaka et al., 2002). Furthermore Ipl1 has been shown to be required for spindle assembly checkpoint activation in response to a lack of tension (Biggins and Murray, 2001). When the function of Ipl1 is lost the 'turnover' of syntelically-attached kinetochores does not occur and mono-polar segregation defects occur (Dewar et al., 2004; Tanaka et al., 2002). Ipl1 must therefore function in the 'turnover' of these mal-oriented kinetochores through the detachment of incorrect microtubule configurations and the re-attachment of correct microtubules.

A key downstream target for Ipl1 in the 'turnover' of syntelic kinetochores in the budding yeast is the Dam1/DASH complex. Ipl1 has been shown to phosphorylate Dam1 at various sites *in vitro* (Cheeseman et al., 2002a; Courtwright and He, 2002; Kang et al., 2001). Indeed phospho deficient *dam1* mutants (S-A) phenocopy *ipl1* mutants with respect to persistent mono-polar attachments (Cheeseman et al., 2002a). Moreover phospho mimic *dam1* mutants (S-D) show a lagging chromosome phenotype indicative of unattached kinetochores (Cheeseman et al., 2002a). It seems that the phosphorylation of Dam1 by the Ipl1 kinase is required to detach incorrectly oriented kinetochore configurations and allow subsequent re-attachment of correct configurations. It has been demonstrated that the Dam1/DASH complex, which is bound to microtubules, can interact with Ndc80 on the outer kinetochore through the Dam1 subunit. Phosphorylation of Dam1 by the Ipl1 kinase is thought to disrupt this binding with Ndc80 and thus abrogate the kinetochore-microtubule interaction. Indeed phospho mimic *dam1* mutants show not only disrupted binding to Ndc80 but also reduced binding to the centromere region by chromatin Immunoprecipitation (ChIP) analysis (Cheeseman et al., 2002a; Shang et al., 2003).

More recently it has been demonstrated that Ipl1 functions in the activation of the spindle assembly checkpoint in response to a lack of tension by creating unattached kinetochores and that this seems to be through the Ipl1 regulated phosphorylation of Dam1 (Pinsky et al., 2006). Therefore in order to correctly repair tension defects in this system they must first be converted into attachment defects through Ipl1 kinase activation. The fission yeast Aurora B orthologue is thought to be required for both attachment and the generation of correct tension at the kinetochore, however the exact nature of its role in correct kinetochore-microtubule interactions is still to be elucidated (Petersen and Hagan, 2003).

1.4 Centromere

During mitosis the chromosomes become attached to the spindle microtubules at a special site known as the centromere. Centromeres were first described as far back as the 1880's as primary constrictions visible on condensed chromosomes and which corresponded to the site of attachment of the spindle microtubules (Fleming, 1882). The centromere directs the assembly of a multi-proteinaceous complex called the kinetochore, which facilitates the attachment of spindle filaments to enable sister chromatid separation.

1.4.1 Centromere sequence

Centromeres form on a specific site on each chromosome; therefore it was logical to assume that a specific DNA sequence would specify the assembly of centromeric chromatin and the site of kinetochore formation. However, while this appears to be the case for the simple 'point' centromere within the budding yeast *S. cerevisiae,* there is no apparent conservation of centromere sequence in other eukaryotes. While there are no obvious centromere determinant DNA sequences in these organisms, the centromeres do possess quite distinct features from the remainder of the chromosomal chromatin structure. The centromeres in these organisms contain tandem sequence repeats, which are specifically found only at the centromere region. Furthermore, centromeric chromatin contains a unique Histone H3 variant protein called CENP-A (fission yeast-Cnp1, budding yeast-Cse4) that is packaged in the nucleosomes to form a distinct centromeric chromatin structure.

1.4.1.1 Budding yeast centromere

The budding yeast centromere was the first to be cloned and sequenced (Clarke and Carbon, 1980). A 125-bp sequence was found to be necessary and sufficient for the formation of the centromere/kinetochore region (Cottarel et al., 1989; Gaudet and Fitzgerald-Hayes, 1989). The centromeric regions of the budding yeast chromosomes are divided into three distinct domains, CDEI, CDEII and CDEIII (Fitzgerald-Hayes et al., 1982). CDEI and CDEIII are palindromic and bind in a sequence specific manner to centromeric proteins complexes that constitute the inner kinetochore (McAinsh et al., 2003). CDEII is an AT rich sequence that can vary in length and is thought to wrap around the nucleosome, through interaction with the Histone H3 variant proteins Cse4 (Clarke and Carbon, 1980; Keith and Fitzgerald-Hayes, 2000). Cse4 can also interact with the CDEI sequence region. It is postulated that this binding of CSE4 to CDEI and CDEII forms a scaffold structure to facilitate the assembly of the kinetochore protein complexes (Cheeseman et al., 2002b; McAinsh et al., 2003).

The CDEI region also binds to the Cbf1 protein, which is a non-essential helix-loop-helix protein that shows some homology to the human CENP-B protein. While not an essential protein; Cbf1 does function to provide high-fidelity chromosome segregation, as in the absence of this protein the rate of chromosome loss is elevated (Cai and Davis, 1990; Stoyan et al., 2001). The CBF3 complex binds to the CDEIII region of the centromere. This complex is composed of 4 essential proteins, Ndc10, Ctf13, Cep3 and Skp1. The DNA binding activity of the CBF3 complex is through the zinc finger motif of the Cep3 protein (Espelin et al., 1997). The CBF3 complex acts as a scaffold or platform for the recruitment of all the other kinetochore proteins; indeed CBF3 is also required for the centromere binding of Cse4 and is a primary requirement and determinant of kinetochore localisation and assembly in the budding yeast (McAinsh et al., 2003; Measday et al., 2002). More recently Cse4 was shown to be also required for the recruitment of central and outer kinetochore components and therefore functions also as a determinant of kinetochore assembly along with CBF3 in the budding yeast (Collins et al., 2005; Westermann et al., 2007).

1.4.1.2 Fission yeast centromere

The fission yeast centromere spans approximately 40-100 kb in length and is composed of distinct and separate domains. All of the three fission yeast centromeres have the same fundamental structure, with a central core (*cnt*) of non-repetitive DNA that is flanked by inverted tandem repeats, the innermost repeats (*imr*) and the outermost repeats (*otr*) (Pidoux and Allshire, 2004; Wood et al., 2002). The *cnt* region is approximately 4-7kb in length that together with the *imr* forms a central domain that acts as the site of kinetochore assembly. The *otr* region forms a heterochromatic outer domain, which is involved in transcriptional silencing (Carroll and Straight, 2006; Pidoux and Allshire, 2004). The fission yeast centromere is therefore a good model to study centromere structure and formation in that it resembles centromeres of higher organisms.

The central core region has a unique chromatin structure, which forms a smear pattern following micrococcal nuclease digestion, whereas other chromosomal regions yield a typical nucleosomal ladder pattern (Polizzi and Clarke, 1991). This unique structure does not correlate with the centromeric sequence, as the introduction of fission yeast central core sequences into the budding yeast does not yield this smear pattern (Polizzi and Clarke, 1991). It is thought that epigenetic regulation may play a role in this central core chromatin structure (Pidoux and Allshire, 2004). The fission yeast, like other organisms, contains a Histone H3 variant protein, Cnp1, which is incorporated into the nucleosomes in the central core region. Several kinetochore proteins are required for the assembly of Cnp1 into the central core nucleosomes, including Mis15-18 and Mis6 (Hayashi et al., 2004; Takahashi et al., 2000).

The *otr* outer repeat region is maintained in a heterochromatic state. The histones H3 and H4 in the nucleosomes of the *otr* region are hypo-acetylated on the lysine residues in their N-termini, K14 (Histone 3) and K9 (Histone 4) respectively (Ekwall et al., 1997). In addition to this, lysine 9 of Histone H3 is methylated in these *otr* heterochromatic regions in a Clr4 dependent manner (Pidoux and Allshire, 2004; Rea et al., 2000). This creates a binding pocket for the chromodomain protein Swi6. Mutants in *swi6* or *clr4* show an alleviation of centromeric silencing, chromosome loss with a predominantly lagging chromosome phenotype and hypersensitivity to microtubule drugs (Allshire et al., 1995; Ekwall et al., 1996; Ekwall and Ruusala, 1994). Furthermore Swi6 has been implicated in the enrichment and retention of the

cohesin complex to the centromere, indicating the importance of heterochromatin for accurate sister-chromosome segregation and not just transcriptional silencing (Bernard et al., 2001; Nonaka et al., 2002).

As we have already stated the two domains in the fission yeast centromere are quite distinct, indeed when viewed by a light microscope the two domains can be seen as quite distinct cytological domains. It seems that these domains are prevented from spreading into each other. It is thought that the presence of tRNA genes within the inner repeat sequences forms a barrier between the two domains to keep them distinct and partitioned (Kuhn et al., 1991; Takahashi et al., 1991). The presence of inverted repeat symmetry within the *imr* and *otr* regions has generated speculation as to the higher order structure of the centromere and the function of the heterochromatic domain. It has been postulated that the two sides of the centromere interact to form a 'loop' like structure, which could project the central core region outwards to facilitate proper kinetochore assembly and a microtubule interaction site (Clarke et al., 1993; Pidoux and Allshire, 2004; Takahashi et al., 1992).

1.4.1.3 Metazoan centromere

The centromeres in metazoans are more complicated than the centromeres in yeast. The centromeres of human chromosomes contain large arrays of alpha satellite DNA that can span up to 4Mb (Carroll and Straight, 2006). The α-satellite DNA consists of 171 bp repeats called α-I satellite DNA. This α-I satellite DNA is flanked each side by divergent repetitive sequences and retrotransposons, called α-II satellite DNA. The external edge of human centromeric DNA is rich in LINE-1 elements (long interspersed element 1) (Schueler et al., 2001). The centromere usually forms on the α-I satellite DNA, however there are reports of centromere formation within regions devoid of α-satellite DNA. These 'neo-centromeres' tend to form on AT rich regions, which contain LINE-1 elements, this suggests that while α-satellite DNA is not required for centromere formation some higher-order structure and possibly other factors may be required.

The histone H3 variant CENP-A is incorporated into the nucleosomes of metazoan centromeric chromatin. The recruitment and incorporation of human hCENP-A relies on the same pathway as in the fission yeast, with both spMis16 homologues hRbAp46 and hRbAp48 required (Hayashi et al., 2004). CENP-A incorporation at

the centromere is essential for accurate chromosome segregation to occur (Howman et al., 2000; Vos et al., 2006). Furthermore CENP-A is required for the recruitment of CENP-C, CENP-H and CENP-I (Howman et al., 2000; Vos et al., 2006). Regions of pericentric heterochromatin flank the CENP-A containing regions. These heterochromatin regions contain tri-methylated Histone H3 lysine 9 and are hypo-acetylated on histone H3 and H4. This tri-methylation creates a binding site for the heterochromatin protein HP1, which silences the region and recruits and maintains cohesin at the centromere (Nonaka et al., 2002). The central core, CENP-A containing region, contains several epigenetic markers, including histone H3 dimethylated lysine 4. This modification is usually found on euchromatin, however the central core region is transcriptionally silent and does not contain any other euchromatic modifications. This di-methylated H3-K4 is found on the internal face of metaphase chromosomes, where cohesion is established, whereas CENP-A occurs on the external face of the chromosomes where the kinetochore is assembled (Sullivan and Karpen, 2004), thus allowing the formation of a higher-order structure which may facilitate a kinetochore-microtubule interface.

1.5 Kinetochore

The kinetochore is a specialised large multi-proteinaceous structure, which assembles onto centromeric DNA. A stable kinetochore structure is fundamental to ensure accurate and high fidelity chromosome segregation. Kinetochores function as the attachment sites for the spindle microtubules to anchor to the chromosomes to facilitate sister-chromatid separation during mitosis. Kinetochores are also required as a platform for the recruitment and signalling of spindle assembly checkpoint proteins and for the generation of pole-ward forces that separate the chromosomes during anaphase. The kinetochore consists of myriads of various proteins, which are arranged into various sub-complexes. In the budding yeast more than 65 different kinetochore proteins have been identified (De Wulf et al., 2003; Westermann et al., 2007). Fewer proteins have been identified in metazoan kinetochores, however what is clear is that the overall structure of the kinetochore, while not identical, is conserved amongst diverse organisms.

1.5.1 Budding yeast architecture

Budding yeast kinetochores are intrinsically different to kinetochores of other organisms with respect to their properties. The kinetochores are attached to only one spindle microtubule emanating from the pole (Figure 1.6). Furthermore these kinetochores are attached to microtubules throughout the cell cycle, and are only briefly disassembled in S-phase to allow passage through the replication machinery (Westermann et al., 2007; Winey et al., 1995). The proteins in the budding yeast kinetochore are classed into 3 different groups depending on their position in the centromere/kinetochore structure, (A) inner kinetochore proteins that are DNA binding and associate with the centromere, (B) central kinetochore proteins that act as linkers, and (C) microtubule binding proteins including MAPs, motor proteins and kinesins (McAinsh et al., 2003; Westermann et al., 2007). As discussed in the previous section the inner kinetochore proteins are those that associate closely with the centromeric DNA, including the Histone H3 variant Cse4, Cbf1 and the CBF3 complex. Mif2 is a protein that exists in the interface between these inner kinetochore proteins and the central linker kinetochore proteins. It has been shown by TAP-purification to associate with both Cse4 and the linker Mtw1 complex (Westermann et al., 2003). Mif2 is the budding yeast homologue of the vertebrate CENP-C protein. Indeed in vertebrates there is a close association between the Histone H3 variant protein CENP-A and CENP-C, reminiscent of the Cse4-Mif2 interaction (Cleveland et al., 2003; Westermann et al., 2007) (Figure 1.6).

The inner core kinetochore proteins connect the DNA binding proteins to the microtubule binding side of the kinetochore. These proteins also function to transduce the force generated by microtubule instability and tension into centromere oscillations (Westermann et al., 2007). The Mtw1 complex was originally identified as Mis12 in the fission yeast and Mtw1 in the budding yeast (De Wulf et al., 2003; Takahashi et al., 1994). This complex contains at least 4 essential proteins, Mtw1, Nnf1, Nsl1 and Dsn1 and is also known as the MIND (Mtw1 including Nnf1, Nsl1 and Dsn1) complex (De Wulf et al., 2003; Westermann et al., 2003) (Figure 1.6).

The Mtw1 complex associates very closely with Cse4, Mif2 and the Ndc80 complexes (Pinsky et al., 2003), and is highly conserved amongst higher organisms. Mutations in Mtw1, *mtw1-1*, result in a loss of tension at the kinetochore and spindle assembly checkpoint activation in an Ipl1 dependent manner (Pinsky et al., 2003). The Mtw1 complex has been proposed to form a rod-like structure of 30-35nm in

length with branched ends both sides, which can facilitate its function as a kinetochore linker complex (Westermann et al., 2007). The Spc105 complex consists of at least two proteins, Spc105 and YDR535c. Spc105 was first identified in preparations of Spindle pole bodies (Wigge et al., 1998). Mutants of Spc105 show defects in chromosome segregation (Nekrasov et al., 2003) and its homologues in the fission yeast Spc7 and in *C. elegans* KNL-1 have also been implicated in ensuring kinetochore-microtubule attachment and proper chromosome segregation (Cheeseman et al., 2006; Cheeseman et al., 2004; Kerres et al., 2004).

The Ctf19 complex, also called the COMA complex, consists of at least 4 proteins, Ctf19, Okp1, Mcm21 and Ame1 (Cheeseman et al., 2002a; De Wulf et al., 2003). Both *OKP1* and *AME1* are essential but the other two are disposable for cell growth. The Ctf19 complex is thought to form a super-complex with the Ctf3 complex. Indeed Ctf3 has been shown to interact closely with Mcm21 and Mcm16 (Measday et al., 2002), and Chl4 and Iml3 of the Ctf3 complex localise to the kinetochore in a Ctf19 dependent manner (Pot et al., 2003). The exact function of this complex at the kinetochore remains elusive but it is thought to play a role in kinetochore assembly as well as functioning as a linker complex (Westermann et al., 2007)(Figure 1.6).

The Ndc80 complex contains 4 essential subunits, Ndc80, Nuf2, Spc24 and Spc25. This complex is highly conserved from yeast to higher organisms. Ndc80 and Nuf2 have been implicated in many organisms in functioning to ensure accurate chromosome segregation (DeLuca et al., 2002; Hori et al., 2003; McAinsh et al., 2003; Westermann et al., 2007; Wigge and Kilmartin, 2001). In the budding yeast the proteins were originally identified by mass spectrometry of spindle pole body preparations (Wigge et al., 1998). The Ndc80 complex is required for the localisation of outer kinetochore components such as the Dam1/DASH complex, Kip1, Stu2 and Cin8 (Cheeseman et al., 2001b; He et al., 2001; Tytell and Sorger, 2006), and also for spindle assembly checkpoint function (Gillett et al., 2004). All 4 of the complex proteins possess coiled coil domains and globular head domains, with the head domains in the N-termini of Ndc80 and Nuf2 and in the C-termini of Spc24 and Spc25 (Westermann et al., 2007). Electron microscopy of negatively stained samples has determined that the Ndc80 complex exists as a 570Å rod, with two globular domains at either end. The rod is formed by the tail-to-tail interaction of the coiled-coil domains of the four proteins and the molecule is oriented so that the Spc24/Spc25 globular head is facing the inner kinetochore and the Ndc80/Nuf2 head faces the microtubule interaction site of the kinetochore (Ciferri et al., 2005; Wei et

al., 2005). The Ndc80 and Nuf2 head has been shown to possess the ability to bind directly to microtubules and as such functions not only to facilitate the assembly of other outer kinetochore subunits but in directly attaching the spindle microtubule to the kinetochore (Cheeseman et al., 2006; DeLuca et al., 2006; Wei et al., 2007) (Figure 1.6).

The Dam1/DASH complex is an outer kinetochore complex that consists of 10 essential proteins. It has been shown to bind microtubules *in vitro* and can also bind the Ndc80 complex. This complex functions to establish proper bipolar attachment and bi-oriented chromosomes through Ipl1/Aurora B (Asbury et al., 2006; Cheeseman et al., 2002a; Cheeseman et al., 2001a; Janke et al., 2002; Kang et al., 2001; Miranda et al., 2005; Westermann et al., 2005; Westermann et al., 2006). We shall discuss this complex, which is the focal point of this thesis in the fission yeast, in more detail later in this chapter (Figure 1.6).

The third class of kinetochore proteins includes MAPs, kinesins and motor proteins. Kar3 is a kinesin-14 family member that has been shown to co-purify with the Cbf3 complex and localise to centromeric DNA by chromatin immunoprecipitation experiments (Hyman et al., 1992; Middleton and Carbon, 1994). In the budding yeast the spindle microtubules are initially captured by the kinetochores in a lateral manner (Dewar et al., 2004; Tanaka et al., 2005). Kar3 then promotes pole-ward movement of the chromosomes to promote end-on-attachment of the spindle to the kinetochore (Tanaka et al., 2005; Westermann et al., 2007). Cin8 belongs to the BimC family of motor proteins and is localised to the kinetochore where it functions with Kip1 in proper spindle assembly and in the metaphase clustering of budding yeast kinetochores into a bi-lobed configuration (Tytell and Sorger, 2006). Bik1 and Bim1 are + TIPS, plus end microtubule binding proteins that can localise to the outer kinetochore and are thought to function in kinetochore capturing of the microtubule plus end and also play a role in the regulation of microtubule dynamics (He et al., 2001). Kip3 is a member of the kinesin-8 family of kinesins and localises at the outer kinetochore of the budding yeast where it has been implicated in microtubule destabilisation and the pole-ward movement of kinetochores during Anaphase A (Tytell and Sorger, 2006). Stu2 is a TOG family member that has been shown to localise to the kinetochore as well as plus ends of microtubules and the mitotic spindle Stu2 has been shown to possess microtubule depolymerising activity *in vitro*, however *in vivo* it functions as a microtubule stabiliser (Al-Bassam et al., 2006; van Breugel et al., 2003). Stu2 associates with α/β tubulin hetero-dimers and facilitates

the stabilisation of kinetochore- microtubule plus ends, however once bi-orientation has been established Stu2 promotes depolymerisation of the attached kinetochore-microtubule (Al-Bassam et al., 2006; Westermann et al., 2007). These molecules function in concert with the kinetochore molecules to facilitate the attachment of a spindle microtubule to the budding yeast kinetochore and promote proper bi-orientation and pole-ward movement required for accurate chromosome segregation.

1.5.2 Metazoan kinetochore structure

The metazoan kinetochore is composed of distinct layers arranged in a trilaminar plate structure with an inner plate consisting of chromatin and DNA binding proteins, an outer plate with approximately 20 microtubule binding sites for spindle attachments and the outermost fibrous corona, which is a dynamic network of proteins usually only visualised in the absence of microtubules (Ris and Witt, 1981) (Figure 1.7). The inner plate contains the Histone H3 variant protein CENP-A, which is required for kinetochore assembly and accurate chromosome segregation (Howman et al., 2000). Purification of CENP-A nucleosomes has led to the identification and classification of a novel complex termed the CENP-A-NAC (CENP-A nucleosome associated complex), which represents proteins that associate with CENP-A in the centromere proximal region. These include CENP-C, CENP-H, CENP-M, CENP-N, CENP-T and CENP-U(50) (Foltz et al., 2006).

CENP-B is the only protein that has been demonstrated to localise independently of CENP-A to the kinetochore. This protein binds specific DNA sequences in the α-satellite repeat region of the centromere known as a 17bp CENP-B box (Ohzeki et al., 2002). The function of this protein however, remains elusive, as it is non-essential in mammals with CENP-$B^{-/-}$ null mice showing normal kinetochore assembly and function.

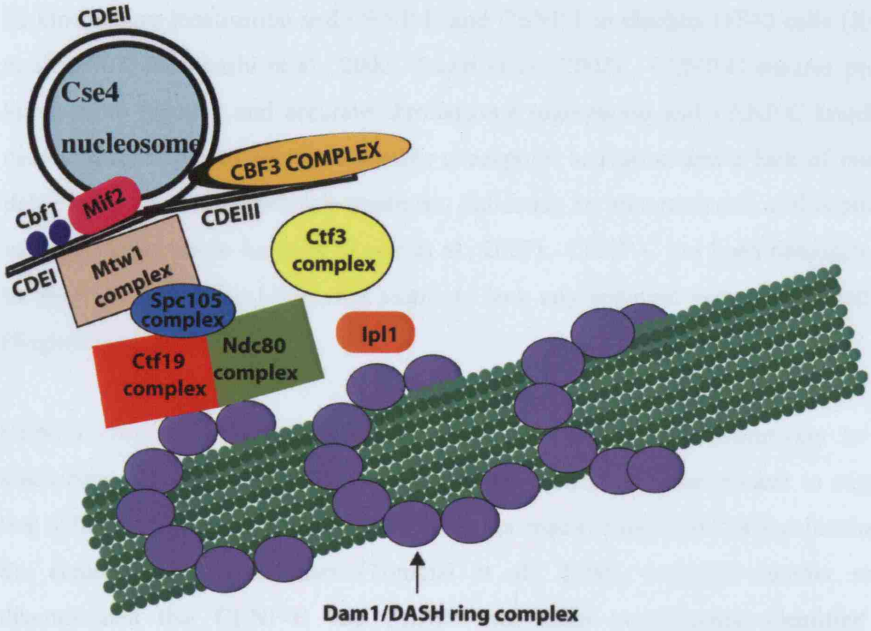

Figure 1.6: Schematic of budding yeast kinetochore structure and components

CENP-C (budding yeast-Mif2) is dependent on CENP-A in all organisms tested for its kinetochore localisation and CENP-H and CENP-I in chicken DT40 cells (Kwon et al., 2007; Nishihashi et al., 2002; Trazzi et al., 2002). CENP-C ensures proper kinetochore function and accurate chromosome segregation and CENP-C knockout cells display impaired spindle assembly checkpoint activation and a lack of mitotic delay in response to nocodazole treatment, indicating an important role of this protein in proper kinetochore function (Kwon et al., 2007). CENP-C has been demonstrated to bind to centromeric DNA, but seems to lack any apparent sequence specificity (Sugimoto et al., 1994).

CENP-I (fission yeast-Mis6, budding yeast Ctf3) localises constitutively to the kinetochore in DT40 cells (Okada et al., 2006). There is some evident to suggest that unlike the fission yeast Mis6, CENP-I is not required for CENP-A localisation to the centromere in vertebrates (Tomkiel et al., 1994), however another study demonstrated that CENP-H and CENP-I and other components, identified by purification with CENP-I in both DT40 and human cells, are required for the incorporation of newly synthesized CENP-A into centromeric nucleosomes (Okada et al., 2006). The newly identified CENP-I/ CENP-H interacting proteins include members of the CENP-A-NAC, CENP-M, and CENP-U and other proteins termed CENP-K, CENP-L, CENP-O, CENP-P, CENP-Q and CENP-R. These proteins are all required for proper kinetochore function and faithful chromosome segregation (Okada et al., 2006).

The outer kinetochore plate and the fibrous corona consist of many proteins that have been implicated in microtubule-kinetochore interaction and in spindle assembly checkpoint signalling. The Mis12 complex (budding yeast Mtw1) localises to the metazoan kinetochore throughout the cell cycle. Depletion of hMis12 causes mitotic delay through activation of the spindle assembly checkpoint, unaligned metaphase chromosomes, abnormally elongated metaphase spindles and lagging anaphase chromosomes (Goshima et al., 2003). The hMis12 complex has been shown to be required for the recruitment of the CENP-I/CENP-H complex but has no effect on CENP-A incorporation into the centromere (Goshima et al., 2003). Furthermore disruption of hMis12 function causes a reduction in the kinetochore levels of Ndc80/Hec1, CENP-E and the checkpoint protein Bub1 (Kline et al., 2006).

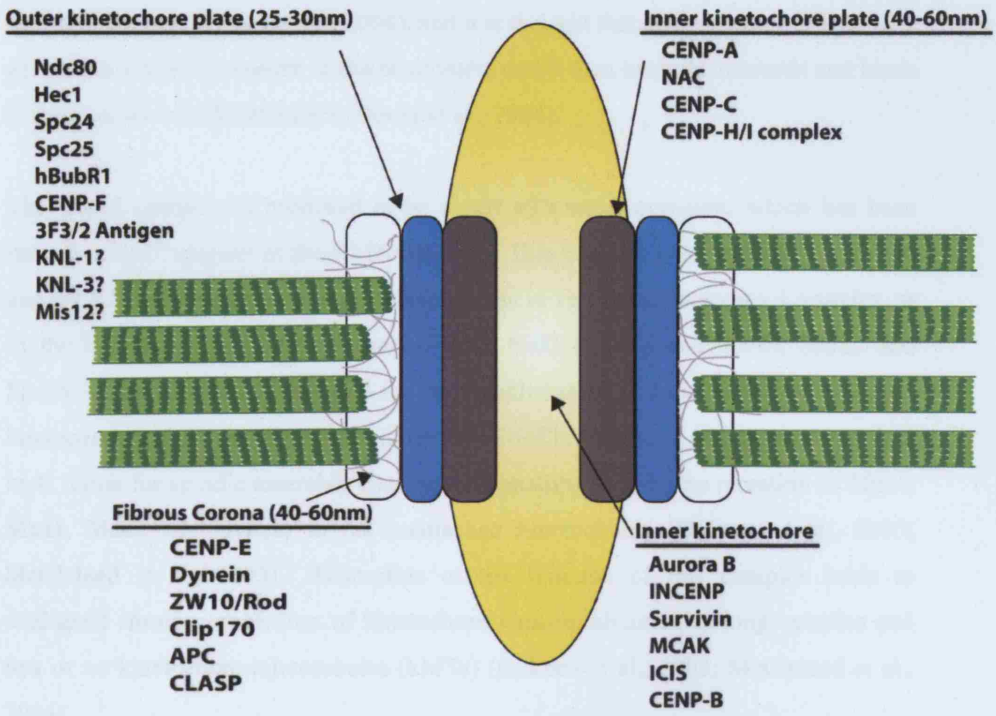

Figure 1.7: Schematic of metazoan trilaminar kinetochore structure and components

The hMis12 complex has been found to interact with the heterochromatin modulator HP1 and Zwint-1 (Obuse et al., 2004), and it is thought that centromere localised HP1 anchors this Mis12 complex to the centromere and it then extends outwards and binds Zwint-1 in the core kinetochore (Obuse et al., 2004).

The Mis12 complex is proposed to be a part of a super-complex, which has been described in *C. elegans* as the KMN network. This network also contains the Ndc80 and the KNL-1 complexes. The Ndc80 complex in vertebrates contains 4 proteins, as in the budding yeast, Ndc80 (human-Hec1), Nuf2 (*C.elegans*-Him10), Spc25 and Spc25. This complex is required for the establishment of kinetochore-microtubule interactions and for the generation of tension (McCleland et al., 2004). It is required in *X. laevis* for spindle assembly checkpoint signalling and for the retention of Mps1, Mad1, Mad2 and Dynein to the unattached kinetochores (DeLuca et al., 2003; McCleland et al., 2003). Disruption of the function of this complex leads to unaligned chromosomes, loss of kinetochore tension, abnormally long spindles and few or no kinetochore microtubules (kMTs) (DeLuca et al., 2002; McCleland et al., 2004).

The Ndc80 complex has been shown to possess direct microtubule binding activity *in vitro*. It can co-sediment with stabilised microtubules and demonstrates *in vitro* microtubule bundling activity (Cheeseman et al., 2006). The Ndc80/Nuf2 head exhibits the microtubule binding activity of the complex with regulation of this binding controlled by Aurora B kinase. Phosphorylation of Ndc80 *in vitro* reduces the affinity of the complex for microtubules; perhaps highlighting the important role phospho-regulation of kinetochore components by Aurora B kinase plays in 'turnover' of microtubule attachments in higher organisms as in the budding yeast. The Ndc80 complex seems to be dependent on Knl-3 and Knl-1 for its kinetochore localisation in *C. elegans*. Furthermore KNL-1 also demonstrates microtubule binding and microtubule bundling activity *in vitro*, however this activity is synergised by the presence of all three subcomplexes of the KMN network, Mis12, Ndc80 and KNL-1/3 (Cheeseman et al., 2006). KNL-1 and KNL-3 were first identified in an RNAi screen in *C. elegans* to identify genes required for chromosome segregation (Desai et al., 2003). Depletion of either of these proteins results in a 'kinetochore-null' phenotype with failure in chromosome congression, an absence of chromosome segregation in anaphase and premature separation of the spindle poles (Desai et al., 2003). KNL-3 and KNL-1 function downstream of CENP-A and CENP-C and are thought to provide a platform for the assembly of the kinetochore-microtubule

interface. KNL-3 is required for the stability of the Mis12 complex and KNL-1 is required for the kinetochore localisation of the NDC80 complex highlighting the interdependency that exists between various KMN network members (Cheeseman et al., 2006; Desai et al., 2003).

CENP-E localises only in mitosis to the fibrous corona on the metazoan kinetochore (Yen et al., 1991). This kinesin like protein plays a role in aligning chromosomes during metaphase, with cells lacking CENP-E showing congression defects and also mono-oriented chromosomes indicative of a failure in the establishment of correctly bi-oriented sister chromatids (Chan et al., 1998; Schaar et al., 1997; Weaver et al., 2003; Wood et al., 1997). CENP-E interacts with BubR1 at kinetochores and activates its kinase activity in the absence of microtubules *in vitro* (Mao et al., 2003; Weaver et al., 2003). It is therefore proposed to act as a mechano-sensor to monitor the state of attachment and tension at the kinetochore and relay this to the spindle assembly checkpoint through BubR1. CENP-F associates with metazoan kinetochores following nuclear envelop breakdown. This molecule plays an important role in chromosome alignment and perhaps checkpoint signalling. Depletion of CENP-F by RNAi results in a dramatic reduction in the localisation of the checkpoint proteins Mad2, Bub1, Mps1 and BubR1 to the kinetochore (Feng et al., 2006). However, another report suggests that CENP-F is dispensable for checkpoint signalling with CENP-F depleted cells showing a mitotic delay and reduced tension between the kinetochores and with decreased stability of kinetochore-microtubules (kMTs) (Bomont et al., 2005). CENP-F has been shown to possess two microtubule-binding domains at each end of the molecule with the C-terminus microtubule-binding domain stimulating microtubule polymerisation *in vitro* (Feng et al., 2006).

The RZZ complex associates with the fibrous corona of metazoan kinetochores. This complex consists of 3 proteins, Rod (Rough Deal), ZW10 (Zeste-white 10) and Zwilch. These proteins were originally identified in *D. melanogaster* but are conserved amongst higher organisms (Karess and Glover, 1989; Scaerou et al., 1999; Starr et al., 1997; Williams et al., 1992). Null mutations show chromosome segregation defects with lagging chromosomes, chromosome non-disjunction, anaphase bridges and cells fail to arrest in mitosis even in the presence of spindle damage (Karess, 2005). This complex associates with the kinetochore following mitotic entry but its kinetochore localisation is dramatically reduced following microtubule attachment, with re-distribution to kinetochore-microtubules towards the

poles (Scaerou et al., 2001; Williams et al., 1992). This process is termed 'kinetochore-shedding' and is a dynein-dynactin dependent process. Indeed Dynein-Dynactin are implicated in the removal of several outer kinetochore components from the kinetochore following bipolar attachment (Howell et al., 2001). The RZZ complex is required for the recruitment of Dynein to the kinetochore to facilitate this 'kinetochore-shedding' (Starr et al., 1998). Dynein levels are high on unattached kinetochores where this molecule has been implicated in the removal of Mad1-Mad2 from the kinetochore following microtubule attachment to facilitate inactivation of the spindle assembly checkpoint (Howell et al., 2001). Apart from its role in Dynein recruitment, and thus checkpoint inactivation, the RZZ complex also is involved in the recruitment of Mad1-Mad2 to unattached kinetochores. Depletion of RZZ or perturbation of the function of this complex prevents Mad1-Mad2 recruitment to unattached kinetochores (Buffin et al., 2005; Kops et al., 2005). These proteins have no as yet known homologues in yeast. This is thought to reflect the differences between the simpler kinetochores in yeast and the increased complexity in the kinetochore structure and spindle assembly checkpoint mechanisms in metazoan cells.

1.5.3 Fission yeast kinetochore structure

Fission yeast is an excellent model for the study of kinetochore structure and kinetochore function during mitosis. Fission yeast possesses centromeres that span from 35-100 kb and the assembled kinetochores are of a more complex nature than in 'point-kinetochore' containing yeasts. The fission yeast kinetochores can bind to more than one microtubule and thus reflect a level of organisation more reminiscent of the kinetochores in higher organisms. The kinetochores in fission yeast, unlike budding yeast, can become attached in a merotelic fashion. This provides an excellent study system to understand the cellular mechanisms that function to resolve these merotelic attachments, as merotelic attachments are regularly seen in human tissue cultures cells (Cimini et al., 2001).

In the fission yeast the inner kinetochore proteins are those capable of binding to centromeric DNA. The fission yeast is no different to other eukaryotic organisms and contains a Histone H3 variant protein in its centromeric nucleosomal structures, called Cnp1 (Takahashi et al., 2000). This protein is required for centromeric chromatin structure and to ensure accurate chromosome segregation during mitosis

(Takahashi et al., 2000). The fission yeast contains three proteins that are homologous to the metazoan centromere binding protein CENP-B; Abp1, Cbh1 and Cbh2 (Irelan et al., 2001; Lee et al., 1997; Murakami et al., 1996). These genes are not essential but deletion of Abp1 and either Cbh1 or Cbh2 results in severe chromosome mis-segregation, sensitivity to spindle drugs and de-silencing at centromere regions (Irelan et al., 2001). It is thought that these proteins act as nucleation factors for Swi6 association to the centromeric and the sub-sequent establishment of heterochromatin (Pidoux and Allshire, 2004).

The Mis6/Sim4 complex is a large kinetochore complex consisting of Mis6, Sim4, Mal2, Mis15, Mis17 and Fta1-7 (Sim4 & Mal2 associating proteins) (Liu et al., 2005). Mis6 was first identified in a screen for mini-chromosome loss mutants (Takahashi et al., 1994). Mis6 is an essential protein that localises constitutively to the kinetochore and was found to associate with the central core region by chromatin immunoprecipitation experiments (Saitoh et al., 1997). Perturbation of Mis6 function results in unequal chromosome segregation and elongated metaphase spindles. Furthermore *mis6* mutants alter the structure of centromeric chromatin, with the typical centromeric 'smear' pattern following micrococcal nuclease (MNase) digestion abolished to a 'ladder-like' pattern in *mis6* mutants (Goshima et al., 1999; Saitoh et al., 1997; Takahashi et al., 1994). Mis6 and other members of the Mis6 complex, along with two upstream proteins Mis16 and Mis18, have been implicated in Cnp1 loading to the centromeric nucleosome, with mis6-302 cells defective in the incorporation of newly synthesized Cnp1 into the centromere (Takahashi et al., 2000). Mis6 has also been implicated in the functioning of the spindle assembly checkpoint in the fission yeast. It has been shown to physically interact with Mad2 under conditions of checkpoint activation; furthermore there is no localisation of Mad2 or activation of the spindle assembly checkpoint in mis6 mutants, despite obvious chromosome segregation defects (Saitoh et al., 2005; Takahashi et al., 1994). Sim4 is another essential member of this complex, and associates with the central core region of the centromere in a Mis6 dependent manner (Pidoux et al., 2003). Sim4 is also involved in the loading of Cnp1 to the fission yeast centromere and for the maintenance of the unique chromatin structure and 'smear' pattern following MNase digestion.

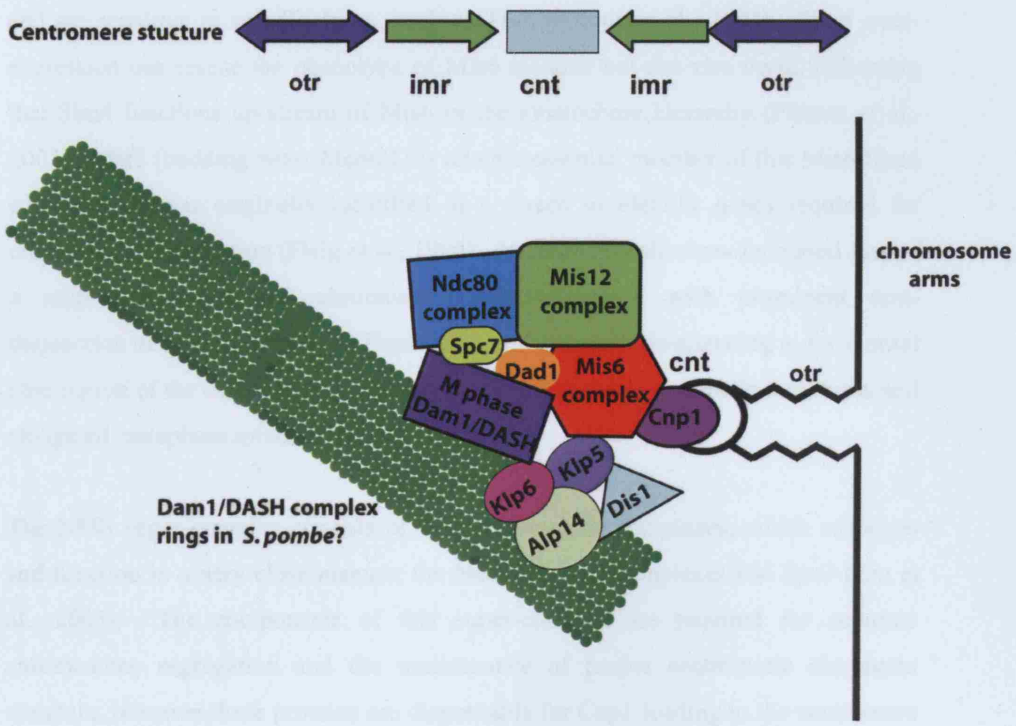

Figure 1.8: Schematic representation of fission yeast kinetochore structure

Sim4 mutants display chromosome segregation defects with lagging chromosomes and are sensitive to spindle drugs, such as TBZ (Pidoux et al., 2003). Sim4 over-expression can rescue the phenotype of Mis6 mutants but not vice versa, indicating that Sim4 functions up-stream of Mis6 in the kinetochore hierarchy (Pidoux et al., 2003). Mal2 (budding yeast-Mcm21) is another essential member of this Mis6/Sim4 complex. It was originally identified in a screen to identify genes required for chromosome segregation (Fleig et al., 1996). Mutants of mal2 show increased loss of a mini-chromosome and chromosome mis-segregation with prominent non-disjunction of sister chromatids. These mal2 mutants show de-silencing at the central core region of the centromere and aberration in centromeric chromatin structures and elongated metaphase spindles (Jin et al., 2002).

The NMS super-complex consists of three kinetochore complexes, which associate and function in a very close manner; the Ndc80, Mis12 complexes and Spc7 (Liu et al., 2005). The components of this super-complex are required for accurate chromosome segregation and the maintenance of proper centromeric chromatin structure, however these proteins are dispensable for Cnp1 loading to the centromere (Kerres et al., 2006). The Ndc80/Nuf2 complex in the fission yeast contains Ndc80, Nuf2, Spc24 and Spc25 as in other organisms. Nuf2 was the first identified member of this sub-complex in the fission yeast (Nabetani et al., 2001). Disruption of Nuf2 yielded cells that showed an elongated mitotic spindle without chromosome segregation and a failure to activate the spindle assembly checkpoint. Temperature sensitive *nuf2* strains show allelic differences in the type and penetrance of mitotic defects at the restrictive temperature, with some alleles arresting in metaphase with a short spindle and condensed chromosomes indicating the activation of the spindle assembly checkpoint (Nabetani et al., 2001). Biochemical purification of Nuf2-TAP allowed the identification of the fission yeast Ndc80, Spc24 and Spc25 homologues and revealed that the Ndc80 complex forms part of a much larger NMS complex with Spc7 and the Mis12 complexes (Liu et al., 2005).

The Mis12 complex consists of Mis12, Mis13, Mis14, and Nnf1. Mis12 was first identified in the same genetic screen as Mis6 for mutants that show elevated levels of mini-chromosome loss (Takahashi et al., 1994). Mis12 is an essential protein that localises constitutively to the kinetochore (Goshima et al., 1999). Mutants of mis12 show unequal chromosome segregation with a failure to activate the spindle assembly checkpoint and elongated metaphase spindles indicative of a failure in microtubule attachments and tension (Goshima et al., 1999; Takahashi et al., 1994). Furthermore

Mis12, and all other Mis12 complex members, are required for proper centromeric chromatin structure (Goshima et al., 1999; Kerres et al., 2006). Spc7 (budding yeast-Spc105, metazoan-KNL-1) was first identified as a binding partner of the plus end protein Mal3 (fission yeast-EB1) (Kerres et al., 2004). Spc7 is essential and localises to the central core region of the kinetochore but unlike other proteins hat associate with the central core it does not seem to be involved in the maintenance of centromeric silencing (Kerres et al., 2007). Mutants of Spc7 show severe chromosome mis-segregation, spindle assembly checkpoint activation and defects in mitotic spindle formation. Indeed Spc7 is required for the kinetochore localisation of the Mis12 complex members Mis12 and Mis14 (Kerres et al., 2007).

Mal3 (fission yeast-EB1) localises to the plus end of growing microtubules (Beinhauer et al., 1997) and interacts with the NMS kinetochore component Spc7 during mitosis where it plays a role in ensuring accurate chromosome segregation (Asakawa and Toda, 2006; Asakawa et al., 2005; Kerres et al., 2004). Mal3 is not essential but mutants show an accumulation of mono-oriented sister chromatids indicating the importance of this molecule for the 'turnover' of mono-polar attached microtubule-kinetochore interactions. It is thought that Mal3 regulates microtubule dynamics to facilitate detachment and re-attachment of spindle microtubules to the kinetochore and enable 'turnover' of mal-oriented kinetochores (Asakawa and Toda, 2006). Recently it has been demonstrated that Mal3 stabilises microtubule through binding to the microtubule lattice seam and perhaps in this way regulates mitotic spindle dynamics and thus chromosome segregation (Sandblad et al., 2006).

Alp14 and Dis1 are the fission yeast members of the TOG family of microtubule stabilisers. Fission yeast is the only organism to possess two TOG family members and both genes are required for accurate chromosome segregation during mitosis. Alp14 or Dis1 deletion mutants, *Δalp14* and *Δdis1*, or point mutants are conditional mutants, with *alp14* mutants lethal at high temperatures and *dis1* mutants lethal in the cold (Garcia et al., 2001; Nabeshima et al., 1995; Nabeshima et al., 1998; Nakaseko et al., 1996; Ohkura et al., 1988). Deletion or loss of function of one of the TOG proteins is compensated by the presence of the other, however deletion of both results in lethality at any temperature (Garcia et al., 2001; Nakaseko et al., 2001). Disruption of Alp14 function causes cells to become bent and branched through the perturbation of cytoplasmic interphase microtubule arrays. During mitosis Alp14 localises to the periphery of the centromere/kinetochore region. Mutants of *alp14* show weak and short mitotic spindles and activation of the spindle assembly

checkpoint, however this checkpoint cannot be maintained implicating Alp14 as a component of the spindle assembly checkpoint mechanism (Garcia et al., 2001). Furthermore the recruitment of Mad2 to the kinetochores in Alp14 mutant cells indicates that the kinetochores are unattached in these mutants and highlights the important role Alp14 plays in the microtubule-kinetochore interaction (Garcia et al., 2001; Nakaseko et al., 2001).

Dis1 was first identified in a cytological screen for mutants that show cold sensitivity (Ohkura et al., 1988). A group of mutants termed '*dis*' (defect in sister chromatid dis-joining) were identified due to their cold sensitive non-disjunction phenotype, of which Dis1 was found to be a non-essential member. Dis1has been shown to localise to the mitotic kinetochore and to the pole-to-pole microtubule lattice in anaphase, analysis of centromeric association by ChIP analysis demonstrates that Dis1 localizes to the central core region (Nakaseko et al., 2001; Ohkura et al., 2001). Deletion of *dis1*$^{+}$ is compensated by the presence of Alp14, but the cells display cold-sensitivity and a typical '*dis*' phenotype with defects in pole-to-kinetochore microtubule formation (Nabeshima et al., 1995). Dis1 is phosphorylated in a Cdc2 dependent manner and this phosphorylation is required for the regulation of Dis1 localisation to the mitotic kinetochore and to the pole-to-pole lattice in anaphase, and is thus required for the regulation of kinetochore microtubule structure and accurate chromosome segregation (Aoki et al., 2006).

Budding yeast	Fission yeast	Metazoan
CBF3 Complex		
Ndc10		
Ctf13		
Cep3		
Skp1		
Cse4	Cnp1	CENP-A
Mif2	Cnp3	CENP-C
Cbf1	Abp1	CENP-B
	Cbn1	
	Cbn2	
Ctf19 complex		
Okp1		
Mcm21	Mal2	hMcm21
Ame1		
Mtw1 Complex	Mis12	hMis12
Nnf1	Nnf1	hNnf1
Nsl1	Mis14	hNsl1
Dsn1	Mis13	hDsn1
Ndc80 complex	Ndc80 complex	Hec1
Nuf2	Nuf2	hNuf2
Spc24	Spc24	hSpc24
Spc25	Spc25	hSpc25
Ctf3 Complex	Mis6	CENP-I
Mcm16	Sim4	hSim4
Mcm22		
Iml3	Mis15	
Chl4	Mis17	hChl4
Nkp-1	Fta1-7?	
Nkp-2	Fta1-7?	
	Fta3	CENP-H
Spc105	Spc7	hKNL-1
Ydr532		
Dam1 Complex	Dam1	
Dad1	Dad1	
Dad2	Dad2/Hos2	
Dad3	Dad3	
Dad4	Dad4	
Duo1	Duo1	
Ask1	Ask1	
Spc19	Spc19	
Spc34	Spc34	
Dad5/Hsk3	Dad5/Hsk3/Hos3	

Figure 1.9: Table of kinetochore components in budding yeast, fission yeast and metazoans

1.6 The Dam1/DASH kinetochore complex

The Dam1/DASH complex was first identified in the budding yeast as a complex implicated in the interaction of kinetochores and spindle microtubules and the establishment of bi-oriented kinetochores during metaphase and for the integrity of anaphase mitotic spindles (Cheeseman et al., 2001b; Jones et al., 1999; Jones et al., 2001; Westermann et al., 2005; Westermann et al., 2006). This complex consists of 10 essential proteins, Ask1, Duo1, Dam1, Dad1-4, Hsk3, Spc34 and Spc19. The first component identified was Duo1 (Death Upon Overproduction) which was identified in a screen for genes that when overexpressed cause a morphological arrest and death phenotype (Hofmann et al., 1998). Indeed overexpression of Duo1 caused cells to arrest at the large budded stage with short spindle microtubules. A temperature sensitive allele was generated; *duo1-2* which when incubated at the restrictive temperature caused a mitotic arrest with short spindles between 1-2μm long. Removal of the spindle assembly checkpoint by deletion of checkpoint signalling molecules enables these *duo1-2* cells to bypass the mitotic arrest but microtubule morphology defects become apparent, with broken, bent and splayed anaphase microtubules and obvious chromosome segregation defects (Cheeseman et al., 2001b; Hofmann et al., 1998).

Dam1 (Duo1 and Mps1 interacting factor), was identified in a two-hybrid screen for Duo1 interacting factors and also independently in a screen to identify mutants that enhanced defects in *mps1* mutants (Hofmann et al., 1998; Jones et al., 1999). The *dam1-1* allele identified arrests at the restrictive temperature with large budded cells and spindles that have begun anaphase elongation but show a bent, broken and splayed phenotype and with mis-segregation of chromosomes (Jones et al., 1999). This mutant shows sensitivity to microtubule depolymerising drugs such as benomyl and exhibits a range of genetic interactions with other mitotic regulators, such as synthetic lethality with *Δcin8* or *Δkar3* cells and exacerbation of *stu1* mutants (Cheeseman et al., 2001a; Jones et al., 1999). Furthermore this mutant is synthetically lethal with various kinetochore mutants and with mutants of the chromosomal passenger complex, *sli15-1* and *ipl1-2* indicating an important role for this protein in kinetochore function (Cheeseman et al., 2001a).

Other Dam1/DASH temperature sensitive mutants show similar types of mitotic microtubule and chromosome segregation defects. The temperature sensitive strain *dad1-1* also shows spindle assembly checkpoint mediated mitotic arrest with short

spindles at the restrictive temperature. Extended incubation at this temperature results in the Dam1/DASH mutant phenotype of broken, bent and splayed anaphase elongated spindles and this mutant demonstrates synthetic lethality with other Dam1/DASH mutants and exacerbates *Δbim1* and *stu1-5* cells (Enquist-Newman et al., 2001). Similarly *spc34-3* cells and *ask1-2* cells arrest at the conditional temperature with large budded cells and short spindles and prolonged incubation at the restrictive temperature causes the appearance of the 'broken' spindle phenotype (Janke et al., 2002; Li et al., 2002).

Duo1 was shown by immunoflourescence and immunoelectron microscopy to localise to intranuclear spindles and to the SPB (Hofmann et al., 1998). However, it was realised that Duo1and Dam1 localise not to the SPB but the kinetochore, as visualised by chromosome spreads where they co-localised with Ndc10, and Dam1 was found by chromatin immunoprecipitation experiments to associate with centromeric DNA (Cheeseman et al., 2001b; Jones et al., 2001). Subsequently the remaining Dam1/DASH members were identified biochemically and shown to localise to kinetochores and spindle microtubules by chromosome spreads, fluorescence microscopy and chromatin immunoprecipitation (ChIP) experiments (Cheeseman et al., 2001a; He et al., 2001; Janke et al., 2002; Li et al., 2002). The association of the Dam1/DASH complex is dependent on a functional kinetochore platform with the association of Dam1-GFP by ChIP abolished in *ndc10-1* cells and both Spc34-GFP and Dad2-GFP failing to localise in *ndc80-1* cells (Janke et al., 2002; Jones et al., 2001).

Localisation of the Dam1/DASH complex to the kinetochore has also been shown to be dependent on spindle microtubules. (Li et al., 2002) The centromere binding of Ask1 by ChIP is significantly reduced in G2 cells in the presence of nocodazole, a known spindle poison which results in depolymerisation of the spindle microtubules (Li et al., 2002). This loss of localisation is reversible. If the nocodazole is removed and spindle microtubules are allowed to form the centromere association of Ask1 by ChIP is restored (Li et al., 2002). These experiments also highlighted that the kinetochore association of Ask1 is most sensitive to spindle disruption by nocodazole during S-phase. This period of S-phase is the time when the kinetochores are re-assembled after DNA replication and microtubule attachments are re-established. It would seem therefore that binding of microtubules to the kinetochores in S-phase of *S. cerevisiae* results in re-deposition of the Dam1/DASH complex at the kinetochore where it can then play a crucial role in facilitating kinetochore-spindle bi-orientation.

Recently the Dam1/DASH complex has been shown to form closed rings on microtubules in the budding yeast (Asbury et al., 2006; Miranda et al., 2005; Westermann et al., 2005; Westermann et al., 2006). Co-expression and purification of all ten subunits of the *S. cerevisiae* Dam1/DASH complex shows this to be a 210kDa heterodecamer with a stoichiometry of one copy of each subunit, which has the ability to oligomerize and form rings and/or paired helices that can encircle microtubules (Miranda et al., 2005; Westermann et al., 2005). The C-termini of α and β tubulin are required for Dam1/DASH ring formation with subtilisn digestion of microtubules resulting in no ring formation (Westermann et al., 2005). It appears that the budding yeast Dam1/DASH ring complex preferentially binds to GTP tubulin and that the C terminus region of Dam1 is required for this microtubule binding, but is dispensable for complex formation (Westermann et al., 2005). This complex thus appears to bind and encircle microtubules, facilitating an attachment of the microtubule to the kinetochore and playing an important role in bi-orientation.

The addition of the Dam1/DASH complex to microtubules *in vitro* induces microtubule polymerisation, microtubule bundling and stabilisation against dilution-induced disassembly (Westermann et al., 2005). It has been shown that the Dam1/DASH ring complex exhibits lateral mobility on microtubules and has the ability to track along with depolymerising microtubules without detaching from the microtubule lattice (Westermann et al., 2005; Westermann et al., 2006). This complex can harness the energy from depolymerising microtubules to generate force for movement and can couple cargo movement to the depolymerising microtubules (Asbury et al., 2006). This leads to an attractive model whereby this complex may form part of the proposed kinetochore sleeve that has been suggested to allow kinetochores to remain attached to depolymerising microtubule plus ends in anaphase and indeed may contribute directly to microtubule driven kinetochore movement.

Dam1/DASH mutants display a mono-polar segregation phenotype that is observed when a centromere pair is tagged with a GFP flourophore and their respective separation monitored by fluorescence microscopy. The temperature sensitive mutant *dam1-1* displayed a mono-polar segregation defect following incubation at the restrictive temperature (Cheeseman et al., 2001b; Jones et al., 2001). Furthermore *spc34-3* cells are also unable to correctly bi-orient their kinetochores displaying mono-polar segregation defects with sister chromatids almost always associated with the mother SPB (Janke et al., 2002). These mono-polar segregation defects

phenocopy mutants of the Aurora B kinase protein Ipl1 which have been shown to typically display mono-polar defects with attachments to the old spindle pole (Tanaka et al., 2002). This result along with the synthetic lethality between *ipl1* and *sli15* and Dam1/DASH mutants highlights the overlap that the Dam1/DASH complex and the Aurora B passenger complex must play in ensuring properly oriented kinetochore-microtubule interactions.

The budding yeast passenger complex members Ipl1 and Sli15 have been shown to associate with both Dam1 and Duo1 by two-hybrid analysis and to co-purify with GST-Dam1 *in vivo* (Kang et al., 2001). Ipl1 can phosphorylate Dam1 *in vitro* and the slowly migrating multiple Dam1 isoforms are dramatically reduced in both *ipl1-2* and *sli15-3* cells or in the presence of λ phosphatase, suggesting that Ipl1 phosphorylates Dam1 *in vivo* on multiple sites (Kang et al., 2001). Mass spec analyses confirmed the identification of at least four different *in vivo* Ipl1 phosphorylation sites on the Dam1 protein, one Ipl1 phosphorylation site on the Spc34 Dam1/DASH subunit and at least 1 *in vivo* phosphorylation site on the Ask1 protein (Cheeseman et al., 2002a). Mutation of individual Dam1 phosphorylation sites to alanine (S-A) had no effect on growth, however mutation of all four Dam1 phosphorylatable serines to alanine resulted in lethality, suggesting a crucial role for phospho-regulation in Dam1 function. The double or triple Dam1 S-A mutants were synthetically sick or lethal with the *ipl1-2* mutant and *spc34 T-A* mutant. Furthermore these double or triple *dam1 S-A* mutants, or the *spc34 T-A* mutant, displayed severe chromosome segregation defects with more than 90% of the DNA segregated to a single pole in anaphase cells (Cheeseman et al., 2002a). These S-A mutants pheno-copy the temperature sensitive *ipl1-2* and *ipl1-321* mutants highlighting that the Dam1/DASH complex acts as a crucial downstream target for the Ipl1 kinase during mitosis.

Mutation of all four Dam1 phosphorylation sites to aspartate to mimic constitutive phosphorylation resulted in poor growth showing that the phospho-state of the Dam1/DASH complex must be tightly regulated. Careful examination of the *dam1 S-D* mutants by immunoflourescence showed the presence of lagging chromosomes in the middle of the spindle, indicating an inability to form proper kinetochore-microtubule attachments. It should be noted that the budding yeast has only one microtubule attachment site per kinetochore so that lagging chromosomes in this organism indicate a failure in attachment rather than merotelic configurations as in other systems. It was previously demonstrated that Dam1 associates to the centromere by ChIP in an Ndc10 dependent manner (Enquist-Newman et al., 2001).

This centromeric association is dramatically reduced in the *dam1 S-D* mutants corroborating the idea that constitutive phosphorylation of Dam1 causes the kinetochores to be unable to generate proper kinetochore-microtubule attachments (Cheeseman et al., 2002a).

A genome-wide two-hybrid screen using Dam1 as bait identified many kinetochore proteins that can interact with the Dam1/DASH subunit. Alongside this, binding assays for Dam1 were carried out and from a combination of both techniques Dam1 was shown to interact with Ndc80 of the Ndc80 complex, Ndc10, Ctf13 and Cep3 of the CBF3 complex, Cse4, and Ctf19, Okp1, Mcm22, Mcm17 and Mcm16 as well as other Dam1/DASH members, spindle assembly checkpoint proteins and the mitotic regulators Bim1 and Stu2 (Shang et al., 2003). To ascertain if the phosphorylation state of Dam1 alters the interactions of Dam1 with other proteins a genome-wide two-hybrid screen was carried out using quadruple *dam1 S-A* and *dam1 S-D* mutants. The *dam1 S-A* mutant showed the same range and strength of interactions with other Dam1/DASH subunits, however the *dam1 S-D* mutant displayed a reduction in the strength of interaction with Spc34 and Dad2 compared to wild-type, indicating that the interactions within the Dam1/DASH complex are largely unchanged, despite changes in the phosphorylation state of Dam1, but there are some alterations in the affinity of binding with Dad2 and Spc34 (Shang et al., 2003). In vitro binding assays revealed that the wild-type Dam1 protein showed a 5.5 times greater binding to Ndc80 than the *dam1 S-D* mutant, but the *dam1 S-A* mutant showed the same affinity as the wild-type Dam1 (Shang et al., 2003). Moreover mutants of the Glc7 protein phosphatase, which antagonizes Ipl1 kinase activity, are synthetically lethal with the *dam1 S-D* mutants indicating that waves of phosphorylation and de-phosphorylation are important in the regulation of Dam1/DASH function. These results have led to the development of a 'turnover' model whereby mal-oriented mono-polar attachments at budding yeast kinetochores are sensed by the Ipl1 kinase, which phosphorylates the Dam1/DASH complex members Dam1 and/or Spc34 and the Ndc80 protein to allow the detachment of incorrect microtubule structures and to facilitate the attachment of correctly oriented microtubules.

Ask1 is phosphorylated in a cell cycle regulated manner with the slowest migrating isoform of Ask1 detected in mitosis (Li et al., 2003). This phosphorylation is dependent on the budding yeast cyclin dependent kinase, Cdc28 (Li et al., 2003). Examination of the Ask1 protein sequence has led to the identification of 2 putative CDK sites, S216 and S250, and mutation of these sites to alanine abolishes the Cdc28

dependent phosphorylation of Ask1 demonstrating that these may be the *in vivo* Cdc28 target sites. This phosphorylation is thought to act to regulate Ask1 in a positive manner, as a double or triple mutant between *ask1 S-A* and *ask1-3* causes synthetic growth defects (Li et al., 2003).

There is also evidence to suggest Dam1 is phosphorylated by an alternative kinase to the Ipl1/Aurora B kinase. Mps1 has been shown to phosphorylate Dam1 *in vitro* on six different residues; S13, S49, S217, S218, S221 and S232 (Shimogawa et al., 2006). A mutant Dam1 allele, *dam1-765*, in which the residue S221 is mutated to S221F was isolated in a synthetic lethality screen with the SPB mutant *spc110-226*. This *spc110-226* allele weakens the SPB structure at the restrictive temperature so that when tension is established in metaphase following bi-orientation of kinetochores the SPBs become delaminated (Yoder et al., 2005), combining this *spc110-226* mutant with the *dam1-765* mutant must increase the stress on the SPB, possible through additional spindle or tension defects which would cause SPB delamination even at the permissive temperature and synthetic lethality (Shimogawa et al., 2006). The *dam1-765* mutant shows normal growth and no chromosome segregation defects, however careful analysis of kinetochore and sister chromatid kinetics revealed shorter mitotic spindles and the kinetochores are clustered closer to the SPBs in these cells compared to wild-type cells. Mutation of another Mps1 phosphorylation site S218 to S218A resulted in a reproduction of this same kinetochore clustering phenotype as seen in *dam1-765* cells and synthetic lethality with the *spc110-226* mutant (Shimogawa et al., 2006). In the *dam1-765* or *dam1-S218A* cells the kinetochore position is not coincident with the microtubule plus ends, as marked by measurement of the distribution of Bik1-GFP fluorescence peaks and Nuf2-Cherry. Therefore in these mutant cells it appears that the kinetochores are not attached to the plus end of microtubules in an 'end-on' manner and must be laterally attached to the mitotic spindle. It is known that in budding yeast the kinetochores are first attached in a lateral manner and subsequent 'end-on' attachment and bi-orientation are established in a Dam1/DASH complex dependent manner. It is proposed that lateral attachments are converted to bipolar attachments by the Dam1/DASH complex and subsequently Mps1 dependent phosphorylation of Dam1 facilitates a switch to a stable 'end-on' attachment (Shimogawa et al., 2006).

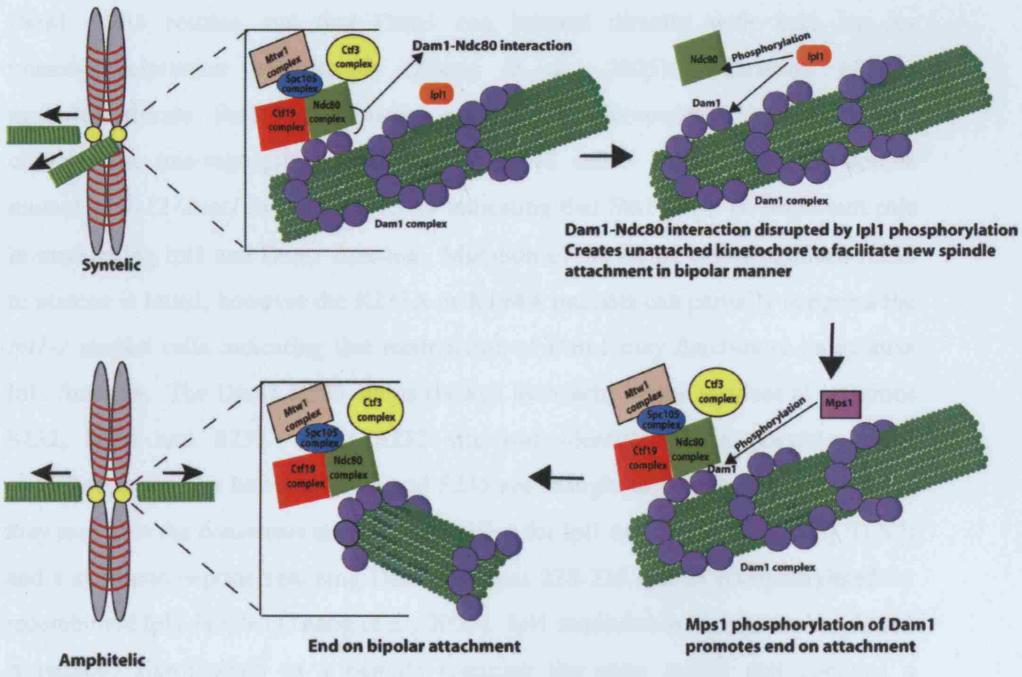

Figure 1.10: Model for Ipl1 and Mps1 phospho-regulation of attachment and bi-orientation of kinetochores in the budding yeast

The Dam1 protein is post-translationally modified in another manner other than phosphorylation. The Set1 methyltransferase can methylate Dam1 *in vivo* at the Dam1 K233 residue and that Dam1 can interact directly with Set1 by co-immunoprecipitation experiments (Zhang et al., 2005). Deletion of the methyltransferase Set1 can partially suppress the temperature sensitivity and chromosome mis-segregation phenotype of *ipl1-2* cells. Furthermore the double mutant *glc7-127Δset1* is synthetic lethal indicating that Set1 plays an important role in modulating Ipl1 and Dam1 function. Mutation of the Dam1 lysine residues K233 to alanine is lethal, however the K233A or K194A mutants can partially suppress the *ipl1-2* mutant cells indicating that methylation of Dam1 may function to antagonise Ipl1 function. The Dam1 K233 site is flanked by nearby serine residues at positions S232, S234 and S235. This S232 site was identified as a possible Mps1 phosphorylation site however S324 and S235 are thought to be possible Ipl1 sites as they resemble the consensus sequence identified for Ipl1 targets ([R/K] X [TS] [ILV]) and a synthetic peptide spanning Dam1 residues 228-239 can be phosphorylated by recombinant Ipl1 *in vitro* (Zhang et al., 2005). Ipl1 mediated *in vitro* phosphorylation is reduced significantly in a peptide spanning the same region that contains a dimethyl-lysine at position K233, corroborating the idea that the methylation of Dam1 may act antagonistically to Ipl1 mediated phosphorylation of Dam1. Mutation of S232 or S234 to alanine rescued the lethality of the *K233A* mutation suggesting that the severe effect of loss of methylation can be rescued by a reduction in phosphorylation of Dam1 at these sites highlighting the importance of this region to regulate Dam1 function through post-translational modifications.

It would seem that the Dam1/DASH complex within the budding yeast is subjected to multiple levels of regulation at the protein level to ensure the attachment of correctly configured spindle microtubules to the kinetochores and the facilitation of bi-oriented sister chromatids, which enables a high-fidelity chromosome segregation process during mitosis.

1.6.1 Overview of this thesis

In this thesis we study the Dam1/DASH complex within the fission yeast. The fission yeast is an attractive model for kinetochore biology. It contains a more complex centromere/kinetochore structure (Pidoux and Allshire, 2004), and each kinetochore is bound by between 2-4 spindle microtubules allowing for the study of

more complex attachment configurations. We wished to study the Dam1/DASH complex in this more complex kinetochore system to elucidate if this complex was firstly conserved and whether it played a similarly vital role in microtubule-kinetochore interactions, bi-orientation, spindle integrity and chromosome segregation in the fission yeast, as in the budding yeast, and thus by inference in organisms with more complex kinetochore structures and mechanisms.

We first aimed to identify the fission yeast homologues of the Dam1/DASH complex and we present a discussion of residues and motifs shown to be important for the Dam1/DASH complex function in the budding yeast and their conservation in *S. pombe*. We then examine the localisation of the Dam1/DASH complex and make the surprising discovery that all the Dam1/DASH subunits examined, except Dad1, show localisation to the kinetochore only in mitosis. Dad1 shows constitutive localisation to the kinetochore throughout the cell cycle. We ascertain that Dad1's association to the kinetochore is dependent on a functional Mis6/Sim4 complex, but not on Mis12, Nuf2 or Cnp1. We demonstrate that the mitosis specific Dam1/DASH subunits may show some dependency on microtubules for their localisation to the kinetochore by examining Dam1-GFP localisation in the β-tubulin mutants *nda3-1828* and *nda3-311* and after cold shock treatment.

In chapter 4 we address whether the Dam1/DASH complex is essential in the fission yeast by carrying out gene replacement of several complex members. We demonstrate that the Dam1/DASH complex genes are dispensable for viability in the fission yeast but play an important role in the accurate segregation of chromosomes. We carry out some examination of the deletion phenotype of Dam1/DASH null mutants and show that these strains are sensitive to the presence of spindle drugs such as TBZ and show a range of genetic interactions with mutants of other kinetochore and/or microtubule regulators. We will show that the spindle assembly checkpoint is activated in our Dam1/DASH deletion strains and that chromosome segregation defects occur in the absence of Dam1/DASH subunits. Furthermore we will carry out detailed live analysis of the patterns of chromosome segregation defects and spindle collapse seen in *Δdam1* cells and confirm that the Dam1/DASH complex in the fission yeast is required to resolve mono-polar segregation defects and for spindle integrity during mitosis in a similar manner to its budding yeast counterparts.

In chapter 5 we will examine the reasons for the synthetic lethality between Dam1/DASH and Klp5/6 double deletion mutants. We identified a temperature

sensitive *dam1* mutant in a *Δklp5* background, termed *dam1-A8Δklp5* and characterise the mitotic defects associated with this mutant following incubation at the restrictive temperature. The double mutant shows activation of the spindle assembly checkpoint even at the permissive temperature and massive mis-segregation of chromosome at the restrictive temperature. Live analysis of the double mutants demonstrates an inability to resolve mono-polar segregation defects, however the *dam1-A8* mutation does not behave as a 'loss of function' mutant like *Δdam1*, as it is resistant to TBZ. We will demonstrate that the single *dam1-A8* mutant shows cells with congression defects, although there is little mis-segregation of chromosomes. Furthermore we will show that the temperature sensitivity of this double mutant can be rescued by the addition of the microtubule depolymerising agent TBZ, which suggests that the extreme rigidity of the microtubule attachments and lack of microtubule dynamics at the kinetochore is the main reason for the failure in the resolution of mal-oriented kinetochore configurations in this mutant. We will conclude that the non-essential Dam1/DASH complex works in concert with the Klp5 and Klp6 to facilitate end-on attached and bi-oriented kinetochores in the fission yeast.

Chapter 2

2 Identification of the Dam1/DASH complex in the Fission yeast

Introduction

In the budding yeast the Dam1/DASH complex plays an important role in ensuring accurate chromosome segregation. A fundamental question is whether this complex is conserved in other fungal species containing more complex centromere/kinetochore systems. We are interested in identifying orthologues of this complex within the fission yeast, *schizosaccharomyces pombe* to examine if it also plays an essential role in kinetochore-microtubule regulation in this organism during mitosis. In this chapter we show the identification of the fission yeast orthologues of the Dam1/DASH complex through a bioinformatics approach and discuss the lack of conservation of residues shown to be important to the function of this complex in the budding yeast.

2.1 Identification of the Dam1/DASH complex

To identify orthologues of this complex in the fission yeast we searched through several sequence databases. Using the *S. pombe* protein database containing the sequenced *Schizosaccharomyces pombe* genome we initially identified six of the ten subunits of the Dam1/DASH complex within the fission yeast-Dam1, Duo1, Dad1, Dad2 (which is called Hos2 in fission yeast), Ask1 and Spc34. By analysing the *S. pombe* DNA sequence database we identified Spc19 and Dad4 orthologues. Concurrently I Sanchez-Perez & J Millar identified these subunits and the remaining complex members (J. Millar personal communication) as Dad3 and Hsk3 (S. *pombe* Hos3) (Table 2.1). We then carried out an alignment of the fission yeast Dam1/DASH orthologues against their counterparts in *S. cerevisiae.* The fission yeast Dam1/DASH complex shows low but significant sequence similarity to its budding yeast counerpart. We searched for conservation within the fission yeast

Dam1/DASH complex components of known important residues, motifs and phosphorylation sites from the budding yeast Dam1/DASH sequences.

2.2 Alignment of Dam1

The Dam1 protein in the fission yeast *Schizosaccharomyces pombe* is much smaller than *Saccharomyces cerevisiae* Dam1 at 155 amino acids and 343 amino acids respectively. Alignment of the proteins between both organisms shows 29% identity. The most conserved region within the *S. pombe* Dam1 is in the N terminus with some homologous regions also present in the middle of the protein (Figure 2.1). Sequence analysis of the *S. cerevisiae* Dam1 proteins shows the presence of a coiled-coil motif between residues 123-161 and a leucine zipper region between residues 63-98 (Figure 2.1).

It has been shown in the budding yeast that Dam1 interacts with the other Dam1/DASH complex members (Cheeseman et al., 2001a; Hofmann et al., 1998), to both the kinetochore passenger complex containing Ipl1, Sli15 and Bir1 and the Ndc80 kinetochore complex and can bind directly to microtubules (Cheeseman et al., 2001a). It has been speculated that the coiled-coil domain, a known protein-protein interaction motif, perhaps plays a role in the proteins various interactions both at the kinetochore and with microtubules and microtubule modifiers (Jones et al., 1999). It is interesting to note then that the fission yeast Dam1 does not contain a coiled coil domain and there appears to be no detectable motifs or domains within the fission yeast Dam1, perhaps therefore there is another mechanism of regulating the *S. pombe* Dam1 protein interactions (Figure 2.1).

In the budding yeast Dam1 protein several residues have been identified as playing an important role in the protein's function and regulation. We analysed whether any of these motifs or residues were conserved in the fission yeast Dam1 to give us further insight into possible functions of the *S. pombe* protein (Figure 2.1, Figure 2.2). The budding yeast temperature sensitive *dam1-1* allele, which results in a 'broken spindle' phenotype (Jones et al., 1999; Jones et al., 2001), contains a single point mutation C111Y. This cysteine is conserved in the fission yeast protein and is also highly conserved amongst many other fungal species (Figure 2.1 Figure 2.2 Table 2.2).

Gene Name	*S. pombe* ORF annotation	*S. cerevisiae* ORF annotation
Dam1	SPAC589.08c	YGR113W
Duo1	SPBC32F12.08c	YGL061C
Dad1	SPAC16A10.05c	YDR016C
Dad2/Hos2	Hos2/SPAC1805.07c	YKR083C
Ask1	SPBC27.02c	YKL052C
Spc34	SPAC8C9.17c	YKR037C
Spc19	SPCC1223.15C	YDR201W
Dad4	SPBC3B9.22c	YDR320C-A
Dad3	SPAC14C4.16c	YBR233W-a
Hsk3/Dad5/Hos3	Hos3/SPCC417.02	YPL116W

Table 2.1:Table of orthologues of Dam1/DASH complex in Fission yeast

(A)

(B)

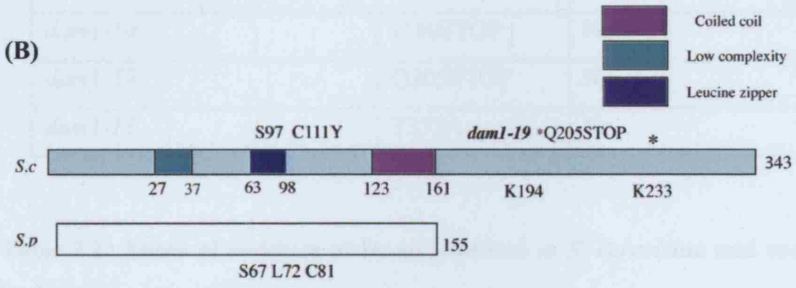

Figure 2.1: Fission yeast Dam1 alignment and comparison with *S. cerevisiae* Dam1

(A). Residues of conservation between proteins from both species are marked with grey asterisks, the regions of homology are marked with dots. The coiled coil region within the *S. cerevisiae* sequence is underlined in black, the leucine zipper region is underlined in red and *S. cerevisiae* identified phospho-serines are highlighted by a black box. The conserved cysteine residues in both proteins are highlighted by the presence of a black asterisk (Jones et al., 1999; Jones et al., 2001) and the lysine residue implicated in methylation in *S. cerevisiae* is highlighted by the presence of a black arrowhead (Zhang et al., 2005). **(B)** Schematic comparison of the *S. pombe* and *S. cerevisiae* Dam1 protein.

S. cerevisiae allele	Mutation	Conserved in *S. pombe*?
dam1-1/dam1-10	C111Y/C111R	Yes-C81
dam1-5	T58I	No
dam1-5/dam1-11	L98P	No-F68
dam1-5/dam1-10/dam1-11	N139S	No-D100
dam1-5/dam1-9	T332A	No
dam1-9	S97F	Yes-S67
dam1-9	K170E*	No
dam1-9	S328P*	No
dam1-10	L102S	Yes-L72
dam1-10	T249I	No
dam1-10	N302D	No
dam1-10	I336STOP	No
dam1-19	Q205STOP	No
dam1-11	T332A	No

Table 2.2: Table of residues of Dam1 mutated in *S. cerevisiae* and conservation in *S. pombe*.

dam1-1 (Cheeseman et al., 2001a; Jones et al., 1999; Jones et al., 2001)
dam1-5, dam1-9, dam1-10, dam1-11, dam1-19 (Cheeseman et al., 2001a)
Asterisk denotes numbering from published literature is incorrect. K170E is actually K171E, S328P is actually S327P.

Analysis of the phylogram (Figure 2.2) generated by the alignment shows that the *S. pombe* Dam1 protein sequence is not particularly close to its *S.cerevisiae* counterpart and is closer in sequence to several of the other fungi which reflects the divergence seen between both budding and fission yeast by phylogenetic analysis (Figure 2.2).

It has been shown in *S. cerevisiae* that Dam1 is phosphorylated by the Aurora B kinase homologue Ipl1 (Cheeseman et al., 2001a; Kang et al., 2001). Analyses by mass spec on Dam1 protein identified four *in vivo* phosphorylation sites (Cheeseman et al., 2002). Mutational analyses of these sites suggest the critical importance of phospho-regulation of Dam1 for its association to the centromere kinetochore region. The sites identified by mass spec as *in vivo* phosphorylation sites for *S. cerevisiae* Dam1 are S20, S257, S265 and S292 and are highlighted in Figure 2.1 and Figure 2.2. It is interesting to note that none of these sites are conserved as phosphorylation sites within the *S. pombe* Dam1 sequence (Figure 2.2). Within the other fungi the serine20 residue is also not conserved instead a threonine residue is present with high conservation of this region amongst the other fungi (Figure 2.2). S265 is conserved in some of the fungal species listed here. Sequence analysis shows the presence of a consensus Aurora B site ({RK}×{TS}{ILV}) (Cheeseman et al., 2002) at T105-KATL and a consensus Polo kinase site (E/D-X-S/T) at S143 –DTS, suggesting there are putative phosphorylation sites present on *S. pombe* Dam1 (Figure 2.2). However this is purely speculative as at present there is no biochemical evidence that *S. pombe* Dam1 is phosphorylated. (X. He personal communication)

In 2005 a paper by Zhang et al. demonstrated the methylation of the *S. cerevisiae* Dam1 at K233 by the methyltransferase Set1 *in vivo* (Zhang et al., 2005). This group speculates that perhaps methylation of this residue is critical for regulation of phosphorylation at nearby serines and thus some higher form of regulation of the role of the Dam1/DASH complex in chromosome segregation. However it is worth noting that in *S. pombe* neither the lysine residues K233 or K194 nor the nearby serines are conserved, and also do not appear to be well conserved in the fungal species aligned in Figure 2.2.

It appears that many of the individual residues deemed to be crucial for the function of Dam1 in the budding yeast are not highly conserved, suggesting that the essentiality of this complex in other organisms may not be conserved and functionally it may behave differently in organisms with a more complex kinetochore/centromere system.

(A)

```
CLUSTAL W (1.83) multiple sequence alignment


G.zeae          MSMTPKDAAKRPNSRSRTS-RPTTPLRPSSRSS--------FRDSARSARH-HDAPFP-- 48
N.crassa        MPDSQTPAPQRSTSRPRTPNRPTTPLRPSSRSS--------LRESARESIHGSSASFP-- 50
A.fumigatus     ---MEP-ALARSSSRPRPSSRPTTPLRPSSRSS--------IREAHGYGTSISNAGYTQ- 47
A.oryzae        ---MDPTAFSRSSSRPRPSSRPTTPLRPSSRSS--------LREAHGYGGSISNAGYTQ- 48
A.nidulans      ---MDA--ASRSSSRSRAVSRPTTPLRPGSRSS--------VREAHGYDRKISRVPYTQ- 46
Y.lipolytica    ------------------MQRPTTPLRRSNSRQ--------SDHEEHYPIVESVLDMA-- 32
S.pombe         ----------------------MEKYQKATQNP--------LENVDNVKIESENAIPSN- 29
S.cerevisiae    ---MSEDKAKLGTTRSATEYRLSIGSAPTSRRSSMGESSSLMKFADQEGLTSSVGEYNEN 57
K.lactis        ----------------------MSQRP-------------------------------- 5

                                                                        *
G.zeae          --LNAFEPAFAELSDAMADLETNMMHFQLMHESLARFSESFASFLYGLNMNAFCVDFPEG 106
N.crassa        --LNAFEPAFAELADAMADLEANMMHFQLMHESLARFSEDFASFLYGLNMNAFCVDFPEG 108
A.fumigatus     PAINALEPQFAELADSMADLEANFMHLQLMHESLTRFSESFASFLYGLNMNAFCVDFPEA 107
A.oryzae        PAINALEPQFAELADSMADLEANFMHLQLMHESLTRFSESFASFLYGLNMNAFCVDFPEA 108
A.nidulans      PAINALEPQFADLADRMAELEANFDKLQLMHESLTRFSESFASFLYGLNMNAFCVDFPEA 106
Y.lipolytica    -----IGEQMAELADGMSALDRNLKDLQVIHTNLNNFNESFSTLIYGLQMNAWCAEFHNG 87
S.pombe         --LQAFTKSLAVLDDNVSEFRKRMNHLSATKQILDNFNESFSSFLYGLQINAFCVDYENA 87
S.cerevisiae    TIQQLLLPKIRELSDSIITLDSNFTRLNFIHESLADLNESLGSLLYGIMSNSWCVEFSQA 117
K.lactis        ----------------MVTLDGNMTHMNFIHESIADLNEALSALLYGLMCNSWCVDFPNI 49
                              :  :  .:  :.  :  :  :.* :.:::**:  *::*.:: :

G.zeae          P--VPESFRRDRTR-------------------------------------------QEQ--- 121
N.crassa        P--LTESFKRMKEKEVREAAAGG---------------------------GGQGQNNM 137
A.fumigatus     P--IADSFRRAKQAEAQKEAEAEEVRRANDAEA----TFIILLARFPQSPLPSHQFLLEE 161
A.oryzae        P--IPESFKRAKQAEAQKGIN-----------------------------------VTLHLME 134
A.nidulans      E--EEESAK-GNEADMTFMTS-------------------------------DTTFIEH 131
Y.lipolytica    P--RSCDFARRKEVEEMEERAR---------------------------------RAQMQA 113
S.pombe         P--LSESFLLQAKKDQFK-------------------------------------ATLMTR 109
S.cerevisiae    PHDIQDDLIAIKQLKSLEDEKNNLVMELSNMERGIKRKKDEQGENDLAKASQNKQFNQPL 177
K.lactis        SHDTPHELKLIQRLEELKQERQALQAKLKPKELTKG-----------------SILPLSR 92

G.zeae          ------------PAVTPSKSEADAEMTFMTTDGSFVENPPT----TTKTSKFTTPEPPK- 164
N.crassa        ETGVMGTGTGMMATVKQEREGFDGETTFMTTDTSFVDNPTSNISGPTPRKPLVAPKTPAP 197
A.fumigatus     LLGGLQRASRHAVAIQREGLIGLGPAHCLEVEVFGLIRPNG---------RGTAIPDQPE 212
A.oryzae        LYG---TNTLQEAEVEQTRQANEGETTFMTTDTTFVENPS------------STTPPKPV 179
A.nidulans      PPS-----TVSTKQVPKPGTSR-GRDCGNFKGADGALKSS------------RAIKTPFG 173
Y.lipolytica    ERDRMAMQQIQETPTRLPSEPSDGDVTYMRNDNSFIIQPPS------SYQSQLPSRIPQS 167
S.pombe         TGHSISDPPYDGGVISHDPNFATADETFATNDTSFIERPET----------YSASR---- 155
S.cerevisiae    FPSSQVRKYRSYDNRDKRKPSKIGNNLQVENEEDYEDDTSSEASFVLNPTNIGMSKSSQG 237
K.lactis        QPLSRGSQMLYRDENVPGSTASSNVNIDINDDEDNTAASFVSNPTTFKPQMISSVGASTD 152

G.zeae          RQSRLPAAPG--RGTTAR--GR----STRGVGRG---RPSGLARARGRGVR--------- 204
N.crassa        RQSRVPAPSGTTRGTSGRGVGRGVTPSSRTTSRGAITRSTSNGRVGGKGLR--------- 248
A.fumigatus     RYKYLLPLNTSSKGGVPL---------SVGDPGPVPYRSERRTLRRQRSL---------- 253
A.oryzae        RKTPTSSRGTTRGSSTRG---------RYTTRG--TSRARPSALPRGRGLR--------- 219
A.nidulans      RRATLDDFGLSHHGAL------------------------------------------- 189
Y.lipolytica    SRASRIRPPNSLRPPRGRGLYLRGGSRGVTGGRGSYTGVRGSGRPASEGTTRRWL----- 222
S.pombe         ---------------------------------------------------------- 
S.cerevisiae    HVTKTTRLNNNTNSKLRRKSILHTIRNSIASGADLPIENDNVVNLGDLHPNNRISLGSGA 297
K.lactis        FMGKQTVGSASSKLRRRSILHQIRNNAAIGTIPNTLTGITPGERKRSLAVSAKRIPILAG 212

G.zeae          ---------------------------------------------
N.crassa        ---------------------------------------------
A.fumigatus     ---------------------------------------------
A.oryzae        ---------------------------------------------
A.nidulans      ---------------------------------------------
Y.lipolytica    ---------------------------------------------
S.pombe         ---------------------------------------------
S.cerevisiae    ARVVNGPVTKNRNSMFSGRAERKPTESRHSVAKKTEKKINTRPPFR 343
K.lactis        SSTTAGSASSANRESTNTEPALPNRVVRTRQRTYNPKNLASRPPFR 258
```

(B)

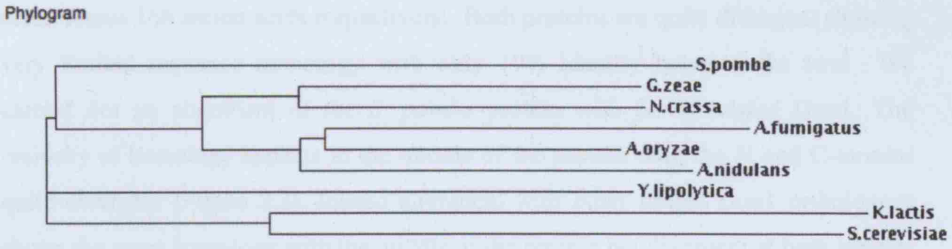

(C)

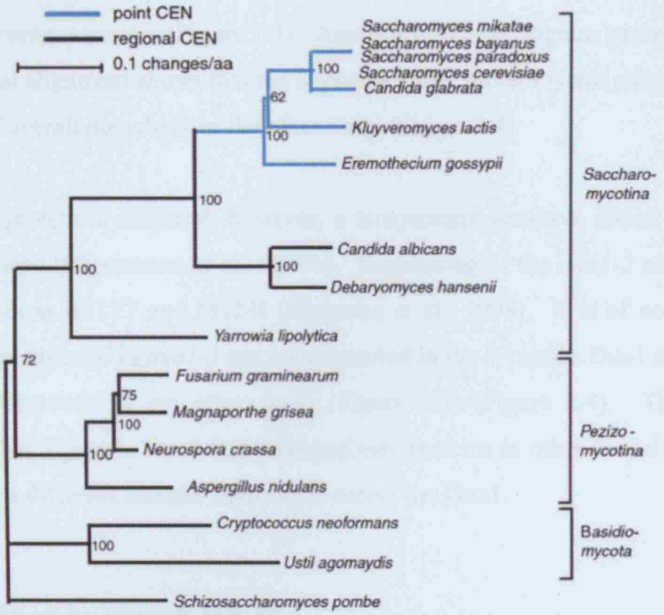

Figure 2.2: Alignment of Fission yeast Dam1 sequence with Dam1 orthologues from other fungi.

(A) Conserved residues are marked with an asterisk and regions of similarity are marked with dots. The highly conserved cysteine residue is marked with a black asterisk. Serine residues that are phosphorylated in *S. cerevisiae* Dam1 are underlined in black and lysine residues critical to *S. cerevisiae* Dam1 regulation are underlined in blue. **(B)** Phylogram of Dam1 sequence divergence drawn up from the result in (A). **(C)** Phylogram of fungi divergence taken from Meraldi *et al.* 2006.

2.2.1 Alignment of Duo1

The Duo1 protein in *S. cerevisiae* is larger than its *S. pombe* counterpart, 247 amino acids versus 166 amino acids respectively. Both proteins are quite divergent showing very limited sequence homology with only 19% identity between the two. We carried out an alignment of the *S. pombe* protein with *S. cerevisiae* Duo1. The majority of homology appears in the middle of the protein with the N and C-termini quite divergent (Figure 2.3). Indeed alignment with other fungal Duo1 orthologues shows the same homology with the middle of the protein but divergent at both termini (Figure 2.4). Interestingly sequence analysis reveals the presence of a candidate coiled-coil motif from residues 76-127 in the *S. pombe* Duo1, but this is not present in its *S. cerevisiae* partner (Figure 2.3). Analysis of the phylogram garnered from the multi-fungal alignment shows that the *S. pombe* Duo1 protein is not particularly close in terms of overall homology to the other fungi (Figure 2.4).

The Duo1 protein is essential, however, a temperature sensitive allele, *duo1-2*, has been generated (Cheeseman et al., 2001b). Sequencing of the *duo1-2* allele revealed point mutations A117T and M124I (Hofmann et al., 1998). It is of note that these two residues mutated in *duo1-2* are not conserved in the *S. pombe* Duo1 sequence and not well conserved in the other fungi (Figure 2.3) (Figure 2.4). Thus one can speculate that *S. pombe* Duo1 and perhaps Duo1 proteins in other fungal species may function in a different manner from the *S. cerevisiae* Duo1.

2.2.2 Alignment of Dad1

The *S. cerevisiae* and *S. pombe* Dad1 proteins are similar in size, 94 amino acids and 85 amino acids respectively. Sequence analysis of the Dad1 protein between the two organisms shows again low sequence homology with 31% identity (Figure 2.5). The *S. cerevisiae* Dad1 protein is essential but mutagenesis resulted in the creation of temperature sensitive allele *dad1-1* (Enquist-Newman et al., 2001). This mutant contains two point mutations responsible for the temperature dependent phenotype, L69R and D71N (Enquist-Newman et al., 2001). In the *S. pombe* Dad1 protein neither of these residues are conserved and are instead replaced by 69F and 71N (Figure 2.5). It appears from alignment with other fungal species that again neither the leucine nor the aspartate present in *S. cerevisiae* are conserved and the other fungi show conservation of the residues seen in the *S. pombe* sequence, i.e. 69F and 71N (Figure 2.6).

(A)

```
CLUSTAL W (1.83) multiple sequence alignment

S.pombe          ----------------------------------------MTSELQQELQILRSFN--- 16
S.cerevisiae     MSEQSQLDDSTIDKLIPQIFNEMRSNLNNTTNKFPKSTGGGASDNISANSNSIRSFNSIT 60
                                                         :.:::. : : :****

S.pombe          -YTIEKLTDGLSASKEKIKSFETSINN--------------SNRLIQLWSSVLSQTEHT 60
S.cerevisiae     TQSLLKESESLDKITAMIKNVTAALKNNLPVYVNQVHEVCKSTNSILDSWINIHSQAGYI 120
                   :: * ::.*.  .  **.. ::::*                :* ::: * .: **: :

S.pombe          QNLILNSDWKGLSFD---NEELERLQHQKMLQIQAEEQRKIELQQEQERLEQERRQKEEA 117
S.cerevisiae     HKLMSDQTYLKLINDRLHNENVNTNDEDGSTLHNVIALKKKEILDLRQKLENRKGEKDAA 180
                 ::*: :. :  *  *   **:::  :.:      :.   :* *: : :::**:.: :*: *

S.pombe          IALQKQQQQRLLRSKDPKVRPAR--------RAASSYVPS--RPSHVPKVFIHECAFSG- 166
S.cerevisiae     PAKPPNQGLNPRYGVQSGRRPVPSAGISNNGRVRKTHVPASKRPSGIPRVTNRWTKPTAS 240
                  *   :*  .   . :.  **.         *. .::**:  *** :*:*  :    :.

S.pombe          -------
S.cerevisiae     SSRKMFR 247
```

(B)

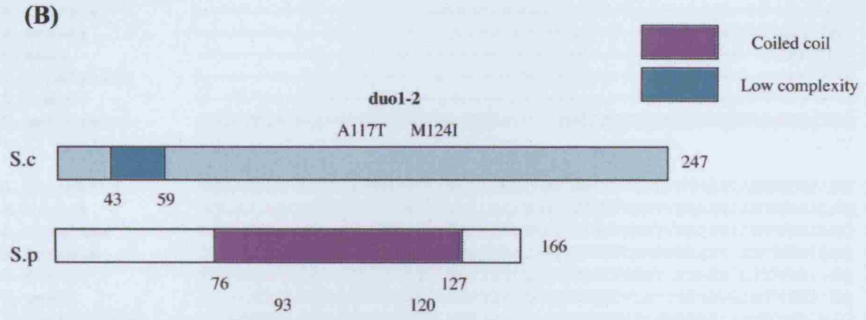

Figure 2.3: Alignment of Duo1 sequences from *S. cerevesiae* and *S. pombe* and schematic representation of proteins.

(A) Regions of homology are marked with dots and conserved residues are marked with an asterisk. The coiled coil residues in *S. pombe* Duo1 are overlined in black. The residues mutated in the *duo1-2* allele from *S. cerevisiae* are underlined in red (Hofmann et al., 1998). **(B)** A schematic representation showing the Duo1 protein structure comparison between both yeasts.

(A)

```
CLUSTAL W (1.83) multiple sequence alignment

A.fumigatus       ----------------MAVHSTAEEMDRLQFSDDDSDDLWNSP-----SKRRSNKPTH 37
A.oryzae          ----------------MTFRSTAEEMERLQLSDEDTDDLWDSP-----SKRGTRKVNR 37
A.nidulans        ----------------MAPYSTAEEMDRLQLSDSDSDELWDSP-----SKRGKKKLNQ 37
A.terreus         ------------------------------------------------------------
N.crassa          ----------------------MSDDRMEISDEEGSSLFASPTHPPTSRAHPPSQAQ 35
G.zeae            ----------------------MADDTTEYTE---SNIWQSP-----SQEDGPPTSR 27
Y.lipolytica      ---------------------MSVRDSLLGLKESMETPLAQDP--------------- 22
S.pombe           ------------------------------------------------------------
C.neoformans      MDSPLLPTLSRSNYSVDEDNNGDASLSLADLSIASDGPDGLSPLPPPRQLAQHSQSQIKS 60

A.fumigatus       HTVPEER-----------STTPETRPS------------------------------- 53
A.oryzae          TPVKEE------------STTPPPISS------------------------------- 52
A.nidulans        AAVKQE------------NSPPPADTD------------------------------- 52
A.terreus         -----------------MPTRSST---------------------------------- 7
N.crassa          QQQQKTPVASSAAAAAAAASTSKDPSTNQS----------------------------- 65
G.zeae            PRTPKTP-----------KTPKTPTQE------------------------------- 43
Y.lipolytica      ------------------------------------------------------------
S.pombe           ------------------------------------------------------------
C.neoformans      LYAQESGHIGAIGGAGTESSATLGSTSTRENIPPTAISNDIQGDTGTIFMGKPRFSLFAP 120

A.fumigatus       ------------------------------------------------HDEGTLFD 61
A.oryzae          ------------------------------------------------HDGETLFD 60
A.nidulans        ------------------------------------------------RDEETLFD 60
A.terreus         ------------------------------------------------------------
N.crassa          ------------------------------------------------SGSRSFGIDNT 76
G.zeae            ----------------------------------------------RPEPLD-- 49
Y.lipolytica      ------------------------------------------------------------
S.pombe           ------------------------------------------------------------
C.neoformans      SRQAYEDDDRQSVMEEEGDKRTSAIEGRDDVTISNEDYEREEDGEEEDEERVRPHEHSRQ 180

A.fumigatus       RQEAREAALQHELQTVRNINQVIEGLLSSLDRAKGNMDTVARTVDSASTLLNTWTRILSQ 121
A.oryzae          RQEAREAALRNELQTVRNINQVIESLLSSLDRAKGNMDTVSRTVDSASTLLNTWTRILSQ 120
A.nidulans        RQEAREAALRNELRIVRNVNQVIEGLLGSLDKAKGNMETVSRTVNSASTLLNTWTRILSQ 120
A.terreus         QQEARESALRNELQSVRNINQVIESLLTSLDHAKGNMDNVSRTVDSASTLLNTWTRILSQ 67
N.crassa          TIESREAALQRELEGVRKINQVIEGVIGTLERAKGNMGTVNRTIHSASHLLTTWTRILSQ 136
G.zeae            ----REAALRKELEGVRNINESLEGVISTLERAGGNMNTVLSTVNNASVLLNTWTRILSQ 105
Y.lipolytica      --REREDQLQKELRQLQELNLVIENTREAVRAATLHVETVQANVNSSHLLADKWNTIMAQ 80
S.pombe           ----MTSELQQELQILRSFNYTIEKLTDGLSASKEKIKSFETSINNSNRLIQLWSSVLSQ 56
C.neoformans      RDSDGEKKLRESLYELRKFNEVFEGFIGSLEGVKGHNERLAERVQQTSLLLDEYTAILGQ 240
                        *:..*  ::..*  :*     :     :   .   :..:  *   :. ::.*

A.fumigatus       TEHNQRLILNTNWQGALQDIADMEN----------EELLRQQAAERRERELQQQREAAAR 171
A.oryzae          TEHNQRLILNPNWQGAVQDVADLEN----------EERLKQQAAERRERELQEQREAAAR 170
A.nidulans        TEHNQRVILNPSWQGASQDMADLEN----------EELLRQQAAERRERELQQQREAAAR 170
A.terreus         TEHNQRLILNPNWQGAVQDVADMEN----------EELLKQQAAERRERELQQQREVAAR 117
N.crassa          TEHNQRLLLNPSWKGATADLLEIEA----------EALERQREAERKAAEAERKREEARR 186
G.zeae            TEHNQRLLLDPGWKGATEDMAEQEA----------EAIQKQQAAERKAAEEEERREQLRQ 155
Y.lipolytica      TSHTYSLLNDSTWHGRMAEQEQHEQRMRE------LELQHQREEEDRLQREAQMAEQAQI 134
S.pombe           TEHTQNLILNSDWKGLSFDNEELER-LQH------QKMLQIQAEEQRKIELQQEQERLEQ 109
C.neoformans      AEHTQRLLLNPRWTGSSDDAAAIAAEEQARAAAAAKALEEAQAAAEAARAEEQARKSAE 300
                  :.*.  :: :. * *   :                    . :       .  .  .

A.fumigatus       KAEEEEKKRAMAGSSRGTRGTTT------RGRIVRTTGLGRTPS-VSHSGTSSSTSR--- 221
A.oryzae          RAAEEEKRRTQA-AARGTRGR-----------VRSSGLGRTPS-VSYSRTNPSATRTT- 215
A.nidulans        KAEEDERKRAQSTSTRGTRIVS-------RGRVIRS-GIGRSPS-VSHSKTSTSGTRTTS 221
A.terreus         RAEEQERKRALVAGTRGTRGTT-------RGRVVRSTGLGRTPS-VSYSGTSGS-SRTTT 168
N.crassa          KAEEEAERRRLAVASSGLGSSRGRPRSRSVGVASSRYGIGVTRSSVTGTRGGRSGSGVGS 246
G.zeae            RREEEEERRRLAASAPARG-TRG-----------------TRG-VRGTTRAR------- 188
Y.lipolytica      QAKQEEEKRERQERMKRRLYRGG---------------------------------- 157
S.pombe           ERRQKEEAIALQKQQQQRLLRSK-----------------DPK----------------- 135
C.neoformans      RERAQSELRTRGGGTRGRGTVRGSGLARGSKLARGGSGLARGESGLARGGSGLARGGSGL 360
```

```
A.fumigatus     IAANRGDIMNFAPYQDESPEVERALSPPLGDANRFKSPILGSPRGSPPIPSAQSGSLPSP 281
A.oryzae        STATRGSTTTTTRRPDESPEVERAMSPALGDANRVKSPIIRSPVGSPPVPGLASNALPSP 275
A.nidulans      KTSGTNPSTTTTRR------------------------------PVSGIAR------ 242
A.terreus       STATRGSSTTTTRR------------------------------PVSGIAR------ 189
N.crassa        LVGTGRTGTGTAGAAAGRVGMTT-----------RSGLAYRPAGATGTSGIPSV----- 289
G.zeae          --GTTRAGSSTASSTS----------------------------RTSSIPS------ 209
Y.lipolytica    --SVRGGGIR---------------------------------------------- 165
S.pombe         VRPARRAASSYVPS------------------------------RPSHVPK------ 156
C.neoformans    TRGRGVGTSVTKPSVAP---------------------PRPESATASSAARRGGST 395

A.fumigatus     THFAGANPIHGGGQANQGYGRDVEALIPEQIVHLIFSWSSFLSWLLFICDLGLIGFLSMR 341
A.oryzae        SHFAGSGQPGATGFGNSGYGGDVES-------------------------GRWNMG 306
A.nidulans      ----GPGVTRGRGRQ------------------------------------------ 253
A.terreus       ----GSGATRGRGRT------------------------------------------ 200
N.crassa        -RGGRGGTTTTRGARGGSTT-----------------------------TTRGARG 315
G.zeae          ----RGTSNIGRGFG-----------------------------------ARRARG 226
Y.lipolytica    ----RGGVRRG---------------------------------------------- 172
S.pombe         ------VFIHECAFSG------------------------------------------ 166
C.neoformans    GTTGKYSHVKSSGYGPRQT-------------------------------------- 414

A.fumigatus     AYRDGESSLWIMTVDFCADRSLVDTLDHFEVPIFGRLANSFVDNE 386
A.oryzae        AF---DTSLPIH---------------------------------- 315
A.nidulans      ---------------------------------------------
A.terreus       ---------------------------------------------
N.crassa        GTTRGGSAR------------------------------------ 324
G.zeae          T------------------------------------------- 227
Y.lipolytica    ---------------------------------------------
S.pombe         ---------------------------------------------
C.neoformans    ---------------------------------------------
```

(B)

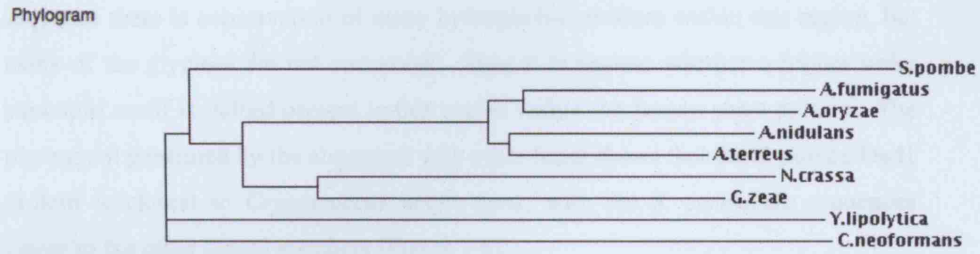

Figure 2.4: Alignment of Fission yeast Duo1 protein sequence with Duo1 protein sequences from other organisms.

(A) Sequence alignment of *S. pombe* Duo1 protein with sequences of orthologues from other fungi. Regions of homology are marked with dots and conserved residues are marked with an asterisk. **(B)** Phylogram based on sequence alignment in (A) showing conservation and divergence of the Duo1 protein sequences within those fungi listed.

Through the application of PASA-PCR (preferential amplification of the shortest amplicon using PCR) and using the yeast two-hybrid system in *S. cerevisiae* the Dad1 interaction domain within Spc34 has been mapped (Ikeuchi et al., 2003; Kawarasaki et al., 2002). From this analysis Dad1 appears to interact with Spc34 from region M1-D47 of the N terminus of Spc34 and also at the C-terminus 89 residues T207-E295 (Ikeuchi et al., 2003). This C terminus region also overlaps with the Spc19 mapped region and incorporates the entire coiled-coil motif of the Spc34 protein. As discussed later in this chapter Spc19 in *S. cerevisiae* appears to have three coiled-coil motifs for trimeric coiled-coil interactions. This suggests that Spc19 Dad1 and the C terminus of Spc34 may form a trimeric coiled-coil structure (Ikeuchi et al., 2003). From sequence analysis there is no obvious coiled-coil domain within the Dad1 protein, however it has been pointed out by Ikeuchi et al, 2003 that the Dad1 protein contains periodical hydrophobic residues interspersed with glycine residues and containing a linker region from V27-P81 in the middle of the Dad1 sequence suggesting an important motif for interaction with Spc19 and Spc34 (Ikeuchi et al., 2003). It is interesting therefore that the point mutations from the *dad1-1* allele L69R and D71N could potentially disrupt this motif, if indeed one exists. In the *S. pombe* sequence there is conservation of many hydrophobic residues within this region, but many of the glycines are not conserved. Thus it is unclear whether a higher order structural motif is indeed present in this region within the fission yeast protein. The phylogram generated by the alignment with other fungi shows that the *S. pombe* Dad1 protein is closest to *Cryptococcus neoformans*, with the *S. cerevisiae* sequences closer to the other fungal members (Figure 2.6).

2.2.3 Alignment of Dad2

The fission yeast Dad2 was originally termed Hos2. Mutants of *hos2* were identified because of their inability to grow and proliferate under high osmolarity conditions (Aoyama et al., 2000). Both the budding and fission yeast Dad2 proteins are quite small, 94 amino acids and 133 amino acids respectively. Sequence alignment of both proteins shows low homology with 26% identity (Figure 2.7). Alignment with other fungi shows homology in the middle of the proteins with high divergence in the C terminus (Figure 2.8). The *S. cerevisiae* Dad2 protein contains a coiled coil domain from residues 103-116 (Figure 2.7). This is not conserved in its *S. pombe* orthologue. Analysis of the phylogram created by alignment of the Dad2 sequence with the listed

(A)

```
CLUSTAL W (1.83) multiple sequence alignment

S.pombe          MDITENIQNEQNKDFDDIDFERRRRLLTLQISKSMNEVVNLMSALNKNLESINGVGKEFE 60
S.cerevisiae     MMASTSNDEEKLISTTDKYFIEQRNIVLQEINETMNSILNGLNGLNISLESSIAVGREFQ 60
                 *  : . ::*:  .  *  * .:*.::  :*.::**.::* :..** .***  .**:**:

S.pombe          NVASLWKEFQNSVLQKKDREMLD-AP-------- 85
S.cerevisiae     SVSDLWKTLYDGLESLSDEAPIDEQPTLSQSKTK 94
                 .*:.*** : :.: . .*.  :*  *
```

(B)

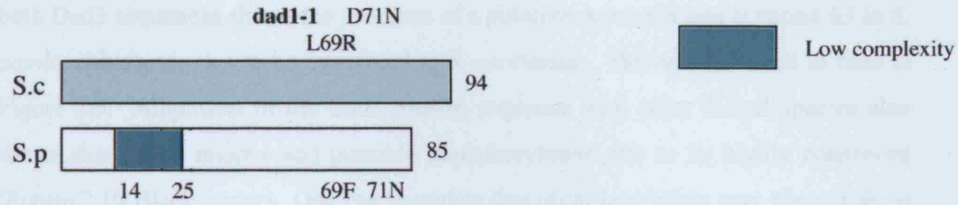

Figure 2.5: Alignment of *S. pombe* Dad1 with *S. cerevisiae* Dad1 protein and schematic of protein structure.

(A) Regions of homology are marked with dots and conserved residues are marked with an asterisk. The residues mutated in the *dad1-1 S. cerevisiae* mutant are underlined in black. **(B)** Schematic of the Dad1 protein structure for both yeasts.

fungi reveals that the *S. pombe* Dad2 sequence is closest to *Candida albicans* (Figure 2.8).

2.2.4 Alignment of Dad3

Both the *S. pombe* and *S. cerevisiae* Dad3 proteins are similarly small in size at 86 and 94 amino acids respectively. Protein sequence alignment shows again low but significant homology with 28% identity between the two (Figure 2.9). The *S. cerevisiae* Dad3 protein is predicted to contain a coiled-coil region between amino acids 16-36, underlined in black in Figure 2.9, however it is interesting to note that this motif is lacking in the fission yeast protein (Figure 2.9). Sequence analysis of both Dad3 sequences shows the presence of a putative Aurora B site at serine 63 in *S. pombe*, which appears to be conserved in *S. cerevisiae.* This site is boxed in blue in Figure 2.9. Alignment of the Dad3 protein sequence with other fungal species also shows this serine residue and possible phosphorylation site to be highly conserved (Figure 2.10 Black arrow). One can speculate that phosphorylation may play a role in regulating this protein's interaction with the Dam1/DASH complex and or microtubules and kinetochore proteins. Analysis of the phylogram created from the multi sequence alignment reveals that within this list of orthologues *S. pombe* Dad3 is closest to the *Cryptococcus neoformans* homologue and quite divergent from its *S. cerevisiae* counterpart (Figure 2.10).

2.2.5 Alignment of Dad4

The *S. pombe* and *S cerevisiae* Dad4 proteins are very small, both 72 amino acids respectively. Sequence alignment of Dad4 in *S. pombe* and *S. cerevisiae* shows high homology with 52% identity between the two yeast proteins (Figure 2.11). The *S. cerevisiae* Dad4 protein contains a putative coiled-coil motif between amino acids 20-47, underlined in black in Figure 2.11. This motif is not conserved in the fission yeast sequence. There also does not appear to be any putative consensus phosphorylation sites present in the *S. pombe* sequence. Alignment of the Dad4 protein with orthologues from other organisms shows that the high sequence homology is conserved (Figure 2.11). Analysis of the phylogram created from the multi-sequence alignment shows that amongst the orthologues listed the Dad4 *S. pombe* protein is closest in homology to its homologue in *Giberella zeae* (Figure 2.11).

(A)

```
CLUSTAL W (1.83) multiple sequence alignment

G.zeae          --MASHSRS-ASAMGG-HDKTYFEQQREALLGEIAMSFEHVLANINKLNRSLEAVTAVGN 56
N.crassa        --MASQNFLGASITGGTREKTYFEQQREALIGEIANSFEHVLANINKLNRSLEAVITVGN 58
A.terreus       --MSVTPGP-KSRSGT---PTVFEQQREELVREIAVGMEQVLQNINRLNRNLESIISVGN 54
A.oryzae        --MSMTPGS-KSRSST---PTVFEQQREELVREIAVGMEQVLQNINRLNRNLESIVAVGN 54
K.lactis        -----MTEEVQQLSTG---DKYFIEQRSLILQEINESMDAILNQLNGLNITLENSIAVGK 52
S.cerevisiae    MMASTSNDEEKLISTT---DKYFIEQRNIVLQEINETMNSILNGLNGLNISLESSIAVGR 57
S.pombe         --MDITENIQNEQNKD-FDDIDFERRRRLLTLQISKSMNEVVNLMSALNKNLESINGVGK 57
C.neoformans    MSLSRPSNVYDALAPS---ESFFEREKARLIEEISTNFEELMGNMNTLNRTLEQVYGVGR 57
Y.lipolytica    --MSRVSMFPTEDKRS-----YFERQRDQYIKNISASMEDVLNNLNALNRSLEHTVGLSQ 53
                                    * ..:     :*   :: ::  :. ** .**    :..

G.zeae          EFSSVEALWSQFENVMGKDE-------KAEGEAGQADQ-----------------TERH 91
N.crassa        EFSSVEALWSQFENVMAKDETQGQQQQQQQGQQQQAEQGTATARQEHGQRRGQEGRQEED 118
A.terreus       EFSSVEALWSQFENFMGRSE------EEDPAVGGKAKE-----------------SPQA 90
A.oryzae        EFSSVEALWSQFENFMGRPE------EEK-AESGVKKE-----------------ELHE 89
K.lactis        EFENVSQIWKLFYNGLESEEQ-------NMETVGVADS-----------------EHIT 87
S.cerevisiae    EFQSVSDLWKTLYDGLESLS----------DEAPIDEQ-----------------PTLS 89
S.pombe         EFENVASLWKEFQNSVLQKK----------DREMLDAP--------------------- 85
C.neoformans    EFTTVASLWGRFNTLIKEQQ----------TELATSADVG----------------VPGTG 92
Y.lipolytica    KSEELAEMWSHEYNTVNEDL--------VKTEDG----------------------DIEV 83
                :   :  :*  :   :

G.zeae          DETMEG---ETTVKHEDA-- 106
N.crassa        DTKMEVDEEDSKIKMERPS- 137
A.terreus       DDAGDQHEHEL--------- 101
A.oryzae        DHT-ELHEQELADERSELDG 108
K.lactis        EDVNPEGK------------ 95
S.cerevisiae    QSKTK--------------- 94
S.pombe         -------------------
C.neoformans    GANFAASASTAASR------ 106
Y.lipolytica    DTTKE--------------- 88
```

(B)

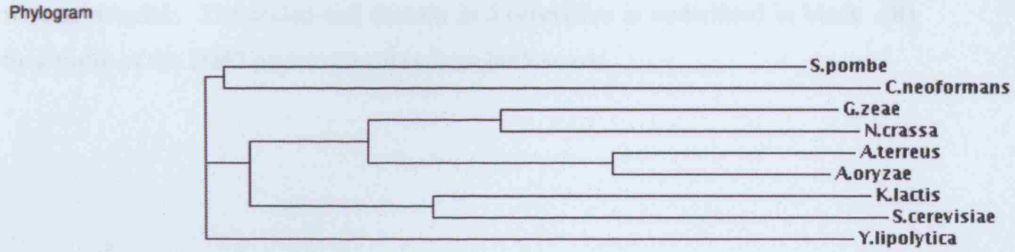

Figure 2.6: Alignment of *S. pombe* Dad1 sequence with Dad1 sequences from other fungi.

(A) Regions of homology are marked with dots and conserved residues are marked with an asterisk. The region containing 69F and 71N is underlined in black. **(B)** Phylogram derived from the alignment in (A) above.

(A)

```
CLUSTAL W (1.83) multiple sequence alignment

S.pombe          --MLQARIEEKQKEYELICKLRDSSNDMVQQIETLAAKLETLTDGSEAVATVLNNWPSIF 58
S.cerevisiae     MDSIDEQIAIKRKELQSLQKITSLTDGLKIQLTELNEQIKEMGMNADSVAQLMNNWDSII 60
                    :: :*  *:** : : *: . ::.:  *:  *  ::: :  .:::** ::*** **:

S.pombe          ESIQIAS----QHSGALVRIPP----------------STSNTNASATEQGDVEEV--- 94
S.cerevisiae     NNISQASLGLLQYAEGDYEIGPWKDSKKKESEQSNETGLEAQENDKNDEDNDEDEDLVPL 120
                 :.*. **    *:: .  .* *                 .:.:.: .  ::.: *::

S.pombe          ------------
S.cerevisiae     PETMVRIRVDGNE 133
```

(B)

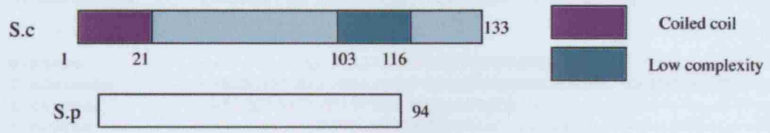

Figure 2.7: Alignment of *S. pombe* Dad2 protein with Dad2 in *S. cerevisiae*

(A) Regions of homology are marked with dots and conserved residues are marked with an asterisk. The coiled-coil domain in *S.cerevisiae* is underlined in black **(B)** Schematic of the Dad2 protein structure from both yeasts.

(A)

```
CLUSTAL W (1.83) multiple sequence alignment

S.pombe          ----------------------------------MLQARIEEKQKEYELICKLRDSSND 25
C.albicans       -----------------------------MSKTNTAIYQKIAEKRANLERFREFKELTDD 31
A.terreus        MAYSSRPTSMLG-ASSSSGLRQP-NLSGIPPQQSSALAARIAAKKTELENLKQLRDMSAT 58
A.oryzae         -------------MSSSSFRQPSTHHAAPQQQLSALAARIASKKAELDNLKQLREMSGA 46
A.nidulans       MAYASRPTSIFPPGPSTASLRQT--NSAISQQQSSALAARIASKKAELDNLIQLRDMSND 58
N.crassa         -------MSAFPARGFS-------SMGASTTGQSPALVARVNEKKAELENLKELRDLSAA 46
G.zeae           -------MS-YPTRSLSSHMRAP-SASASSSGQSPALIARIEEKKAELENLKELRELSAA 51
Y.lipolytica     ---------MVRPRVSLAPNRLN--------HAGSELDEKIAAKKRELQQLVQLRQYSSD 43
C.neoformans     ----------------------MSRPSIEMNLPPSLLNFYQKQQEYAGLQALREASAD 36
                                                .. *: :   : ::: :

S.pombe          MVQQIETLAAKLETLTDGSEAVATVLNNWPSIFESIQIAS-------------------- 65
C.albicans       LVLQLESIGDKLETMNGGTASVALILANWKSVVQSISLASLALMK--------------- 76
A.terreus        LAMQMQALETKIGTLKDGTEAVACVLANWDNVLRAISMASTKAAA---------IQGPEG 109
A.oryzae         LAMQMQVLEEKIGTLKDGTEAVACVLANWDNVLRSISMASSKPPP---------CSLP-- 95
A.nidulans       LAGQMQALQAKLETLKDGTEAVACVLANWDNVLRAITMASNYPSSESLRIFLTDVYEPHS 118
N.crassa         MATQMEALAQKLATLSDGTEAIALVLSNWHNVLRAINMASAKLPKPSAGV--QEPSEEEL 104
G.zeae           VATQMEALE--------------------------------------------------- 60
Y.lipolytica     LADELEGLVQHVSCLAEETDVVAEVMGNWAAVIRAINLASTALAR--------------- 88
C.neoformans     LVARAEKLAEMSNIMADGGEAIGGVLRNWPHVFSILSLFTAQMEKASG------------ 84
                 :. . : :

S.pombe          ----------QHSGALVRIPPSTSNTNASATEQGDVEEV--------------------- 94
C.albicans       --ESNDNNKEAFPEPLVRVRVGQSNEENQDEEEADEEEGVRDSEEVEESTE--------- 125
A.terreus        -HTAEQSQAPLMPATLVRIPAEDRKKTDDS----------------------------- 138
A.oryzae         ------MLALLRSVLLVAIADPLVP----------------------------------- 114
A.nidulans       PEFDALRTTRLVSDLLPCVRTSDSPETSSEHHMLDARLVLSGPFVSGRPWRFGIMFPDIS 178
N.crassa         PQTLVRIPTEHAPALQAHAEG---AAEEE------------------------------- 130
G.zeae           --------TEHAPALQAQAEAAEAAAEEQQS----------------------------- 83
Y.lipolytica     -YTEEDYREPVLPEQLIRVPLEDEQEE--------------------------------- 114
C.neoformans     DHSRQEDEDEEPLPCLVRLAYGGETASVESSAPTTTTASDKTKQ---------------- 128

S.pombe          ------------------------------------------------------
C.albicans       ------------------------------------------------------
A.terreus        ------------------------------------------------------
A.oryzae         ------------------------------------------------------
A.nidulans       MDVYEGLRYLAFKIGRKQNNMQILIIAVSSCLLEQDPCAWFKVEPARDKSELGM 232
N.crassa         ------------------------------------------------------
G.zeae           ------------------------------------------------------
Y.lipolytica     ------------------------------------------------------
C.neoformans     ------------------------------------------------------
```

(B)

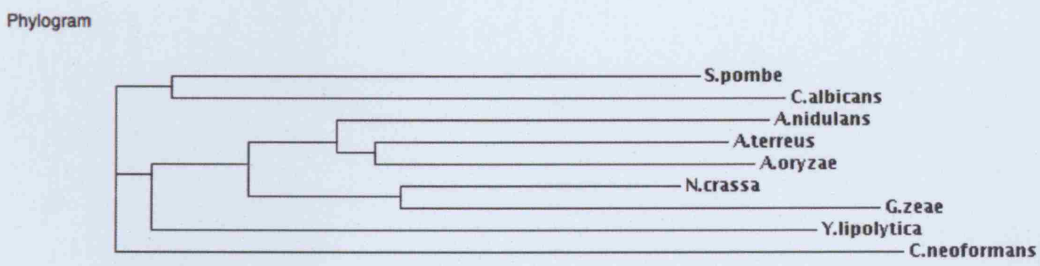

Figure 2.8: Alignment of Dad2 from *S. pombe* with other fungal orthologues.

(A) Regions of homology are marked with dots and conserved residues are marked with an asterisk. **(B)** Phylogram generated from the alignment in (A).

(A)

Alignment

```
S.pombe         MSLEEKRALQNQILAEYANLASNLETLVKVLQDMVYNPS----------NNILDSLRD 48
S.cerevisiae    MEHN-LSPLQQEVLDKYKQLSLDLKALDETIKELNYSQHRQQHSQQETVSPDEILQEMRD 59
                *. :   .**:::* :* :*: :*::* :.:::: *.              ::**:.:**

S.pombe         LEKEVGLVYTLYKASVWAILADLENNQEGKSGMFQDES 86
S.cerevisiae    IEVKIGLVGTLLKGSVYSLILQRKQEQESLGSNSK--- 94
                :* ::*** ** *.**:::: : :::**. ..  :
```

(B)

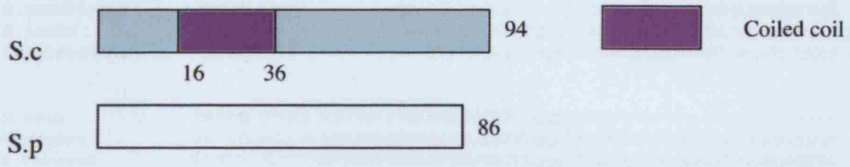

Figure 2.9: Alignment and schematic representation of *S. pombe* Dad3 protein with its *S. cerevisiae* homologue.

(A) Regions of homology are marked with dots and conserved residues are marked with an asterisk. The coiled coil motif of *S. cerevisiae* is underlined in black and the putative Aurora B phosphorylation site is boxed in blue. **(B)** Schematic representation of the Dad3 protein structure from the two organisms.

(A)

```
CLUSTAL W (1.83) multiple sequence alignment

G.zeae          ------------------------------------------------------------
N.crassa        ------------------------------------------------------------
A.terreus       MCVIVATQSDGYTDPNNANTFQPNHNNHQTPRPLLSSTLHTPTTLTTFANPPSRTASTHT 60
A.oryzae        ------------------------------------------------------------
A.nidulans      ----------------------------------------------------MSETTPIPS 9
S.cerevisiae    ------------------------------------------------------------
S.pombe         ------------------------------------------------------------
C.neoformans    ------------------------------------------------------------

G.zeae          -MDQTQAGG-----------LLD-PPELTPLEQEVLDEYERLADNMNKLATILEHLASN 46
N.crassa        -MEQQQQSNP----------LLNSPPELTPTEQDVLDEYERLAENMKKLASVLDTLASQ 48
A.terreus       LMDHDPTTPPPARESSSENPLLRASNPLVSDLEQEVLDEYSRLLGNVNKLSQKLADLSGD 120
A.oryzae        -MSTPMSDGSPAQES--ENPLLRASNPMVSDLEQEVLDEYSRLLGNVNKLSEKLADLSGD 57
A.nidulans      RSTTPPIEPPLDTVSSTENAFLRPSHPLVSDLEQEVLDEYARLLGNVNKLSAKLAELADS 69
S.cerevisiae    -MEHNLSPLQ---------QEVLDKYKQLS-LDLKALDETIKELNYSQHRQQHSQQETVS 49
S.pombe         ----------------------MSLEEKRALQNQILAEYANLASNLETLVKVLQDMVYN 37
C.neoformans    -MSINTVNP----------YADNSQLSQLEQELLWEFAKLSDKVKRAASLAKLTAES 46
                                          : . * *  .    :          .

G.zeae          PSSEILDGLRELERKTSLAFTLLKASVYSIVLQQEIDWG---------------------- 85
N.crassa        PSVAILDGLRELERKTSLVFTLMKASVYSIVLQQEIDWGGPAAGENGGGG-GGGGGGDGP 107
A.terreus       PSSLTLDGLRVLERKTATVCTLLKASVYSIVLQQQIFNESEEQQQQQHQQ-QQDQEQQEG 179
A.oryzae        PSSLTLDGLRLLERKTATVCTLLKASVYSIVLQQQIFNENEEQQQMEQQQSDQMQYHDQG 117
A.nidulans      PTTITLDGLRQLERKTATVYTLLKASVYSILLQEQIVNEGEWQQQQQQQD-EGQEYATGT 128
S.cerevisiae    PDE-ILQEMRDIEVKIGLVGTLLKGSVYSLILQRKQEQESLGSNSK-------------- 94
S.pombe         PSNNILDSLRDLEKEVGLVYTLYKASVWAILADLENNQEGKSGMFQDES----------- 86
C.neoformans    PNESLLAELRTLEKRMGLVLTLVKASVWAVIVDSQAAEEARQQQSAESAP----EISYNE 102
                *    *  :* :* . . . ** * .** :::: : :

G.zeae          -----DGSMAQ---------------------- 91
N.crassa        GGAGSDGVGEQP--------------------- 119
A.terreus       MDYPDQGV-MDEG-------DVSFTGRFA---- 200
A.oryzae        YDYQDEDM-SFEGRCGLWVYPFCFIVGFGTGLI 149
A.nidulans      MNAGEEGIYMGEG-------DMSYQQY------ 148
S.cerevisiae    ---------------------------------
S.pombe         ---------------------------------
C.neoformans    TRSWDDSIMR---------------------- 112
```

(B)

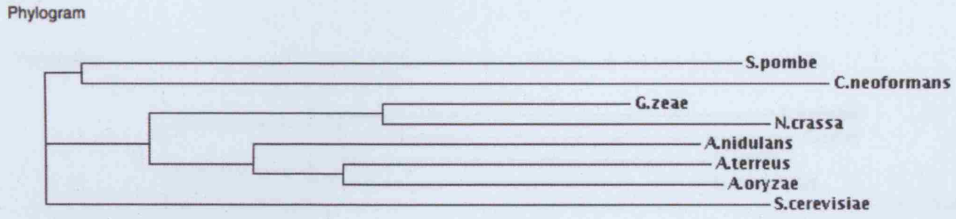

Figure 2.10: Alignment of many fungal Dad3 orthologues with *S. pombe* Dad3 protein sequence.

(A) Regions of homology are marked with dots and conserved residues are marked with an asterisk. The conserved serine residue of a putative phosphorylation site is underlined in black. **(B)** Phylogram derived from the sequence analysis in (A) above.

(A)

Alignment

```
S.pombe         MNNPMEEQQSALLGRIISNVEKLNESITRLNHSLQLINMSNMNVELASQMWANYARNVKF 60
S.cerevisiae    MENPHEQVQANILSRIIGNVKRLNESVAILNQELVTINNRNKNLEIMGAICDNYHSSVQF 60
                *:** *: *: :*.***.**::****:: **:.*  **  * *:*: . :  **  .*:*

S.pombe         HLEETHTLKDPI 72
S.cerevisiae    NLEATNNKKPPL 72
                :** *:. * *:
```

(B)

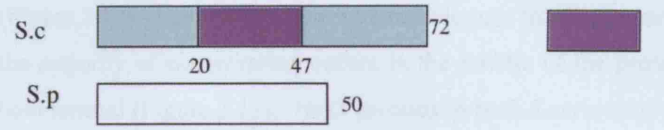

(C)

CLUSTAL W (1.83) multiple sequence alignment

```
S.pombe         MNNPMEEQQSALLGRIISNVEKLNESITRLNHSLQLINMSNMNVELASQMWANYARNVKF 60
G.zeae          MESPHEHQQNLLLSRIITNVEKLNEAVMVMNKSLQDINIQNMNVELVAQMFKNYQSNVLF 60
K.lactis        MENPYEKVQSNILARIIGNVERLNQSVVILNQELRRVNTKNKNLELMSQMCENYRESVDF 60
S.cerevisiae    MENPHEQVQANILSRIIGNVKRLNESVAILNQELVTINNRNKNLEIMGAICDNYHSSVQF 60
Y.lipolytica    MENPHEKDQSDALARIISGVSKLNSSIARVNEIQEEVYSRNLNLSVVSEIMQNYQASVDY 60
                *:.* *. *   *.*** .*.:**.::  :*.    :   * *:.: . :  **  .* :

S.pombe         HLEETHTLKDPI---- 72
G.zeae          HLEATDNLKPPS---- 72
K.lactis        QLQATSKKQDPL---- 72
S.cerevisiae    NLEATNNKKPPL---- 72
Y.lipolytica    YLRESGAMKEPFKNDD 76
                 *. :   : *
```

(D)

Phylogram

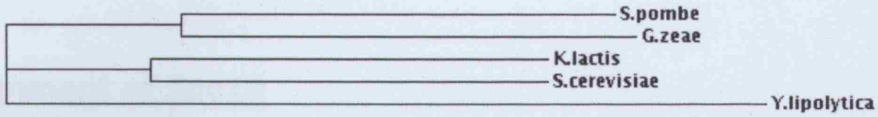

Figure 2.11: Alignment of *S. pombe* Dad4 with *S. cerevisiae* and other fungal Dad4 orthologues.

(A) Regions of homology are marked with dots and conserved residues are marked with an asterisk. The coiled-coil motif from *S. cerevisiae* is underlined in black. **(B)** Schematic representation of the *S. pombe* and *S. cerevisiae* Dad4 protein structures. **(C)** Multi-sequence alignment of the *S. pombe* Dad4 protein with other orthologues. **(D)** Phylogram derived from the multi-alignment in (C) above.

2.2.6 Alignment of Hsk3 (Dad5/Hos3)

The *S. pombe* Hsk3 homologue was first termed Hos3. Mutants of *hos3* were identified in the same screen that identified *hos2* because of their inability to grow and proliferate under high osmolarity conditions (Aoyama et al., 2000). Sequence analysis shows that Hos3 in *S. pombe* is the Hsk3 Dam1/DASH complex homologue. Alignment with *S. cerevisiae* Hsk3 protein shows low homology with 31% identity (Figure 2.12). Upon alignment with orthologues from other organisms it appears that the majority of conservation occurs in the middle of the protein, with divergence at both termini (Figure 2.12). Hsk3 proteins in both *S.cerevisiae* and *S. pombe* are quite small, 69 and 94 amino acids respectively. The budding yeast Hsk3 protein contains a coiled-coil motif between amino acids 2-36, underlined in black in Figure 2.12. The *S. pombe* Hsk3 sequence also contains a coiled coil domain within this region, between residues 27-47 (Figure 2.12). Perhaps this coiled-coil domain facilitates interaction with the rest of the Dam1/DASH complex members and/or the kinetochore. The fission yeast Hsk3 sequence contains a putative Aurora B phosphorylation site at threonine 5-RSTI, which does not appear to be conserved in the *S. cerevisiae* sequence, whereas some of the other organisms show a serine at this residue (Figure 2.12). The *S. pombe* sequence also contains two putative CDK sites at serines 16 and 18 but these do not seem to be conserved in the other orthologues. It should be pointed out that there is no evidence as of yet that this protein is phosphorylated. Analysis of the phylogram shows that the Hsk3 sequence from *S. pombe* appears to be closest in homology to *Neurospora crassa* and *Giberella zeae.*

2.2.7 Alignment of Spc19

The Spc19 proteins in *S. pombe* and *S. cerevisiae* are 152 and 165 amino acids respectively. Alignment of *S. pombe* and *S. cerevisiae* Spc19 proteins shows low sequence homology with 29% identity (Figure 2.13). Sequence alignment with other fungal orthologues show that the homology is strongest in the middle of the protein with divergence in the N and C termini (Figure 2.14). The *S. cerevisiae* Spc19 protein has two predicted coiled-coil motifs from the yeast database between amino acids 74-94 and 135-165, but it has been reported in the literature that it contains three coiled-coil regions for trimeric coils (Ikeuchi et al., 2003).

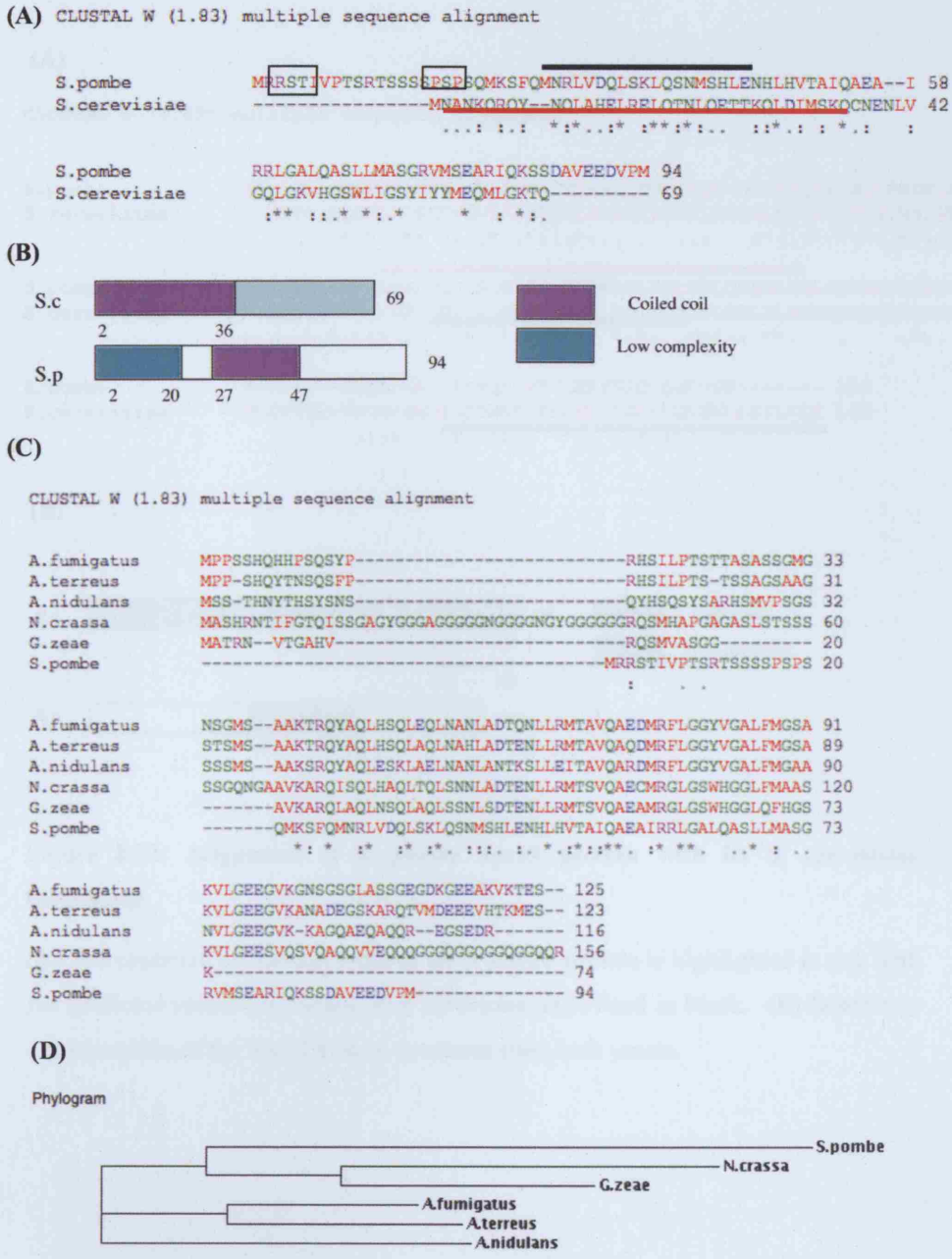

Figure 2.12: Alignment of *S. pombe* Hsk3 with orthologues from other fungi.

(A) Regions of homology are marked with dots and conserved residues are marked with an asterisk. The coiled-coil motifs from *S. cerevisiae* and *S. pombe* are underlined in black and red. A putative Aurora B site is marked by a blue box and putative CDK sites are marked with black box. **(B)** Schematic representation of the *S. pombe* and *S. cerevisiae* Hsk3 protein structures. **(C)** Multi-sequence alignment of *S. pombe* Hsk3 protein with other orthologues. **(D)** Phylogram derived from the multi-alignment in (C) above.

(A)

```
CLUSTAL W (1.83) multiple sequence alignment

S.pombe          MSYLDGLQQCVDSLQISIGTLSSSIDTLESGIHDFPRIK-HILKVQRHFNLISEDELSAR 59
S.cerevisiae     --MTDALEQSVLALEGTVSVLKDSVESLKCANEPSTNLASTMLQTKRVFRLVPEYDVERS 58
                    *.*:*.*  :*:  ::..*..*:::*:.. .   ..:    :*:.:* *.*:.* ::.

S.pombe          QAKFEEIVKPILSKAFQRLEDSISSLQRQEDSLKTKYELQEARLDMLKNRPATSAFSVTT 119
S.cerevisiae     KLDLIEEVEPLVRTLGDKLRKSMGRMQRELDTLQQTYELNDLRLKKNISMDDDDALNSPD 118
                 : .: * *:*:: .  ::*..*:. :**: *:*: .***:: **.    .    .*:. .

S.pombe          E-------SSEQLKAIIAKRQKLVYTLERYTLQLQQKRGH------- 152
S.cerevisiae     MGQEYEGRDADDVVMMASSTNEELEELKKLKEKKKQLENKLEILKQK 165
                        .::::  : :. :: :  *:: . : :* ..:
```

(B)

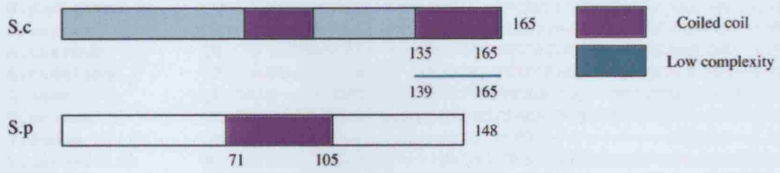

Figure 2.13: Alignment of *S. pombe* Spc19 protein with its *S. cerevsisiae* homologue.

(A) The predicted coiled-coil motif in the *S. pombe* protein is highlighted in red, with the predicted coiled-coil motifs of *S. cerevisiae* underlined in black. **(B)** Schematic representation of the Spc19 protein structures from both yeasts.

(A)

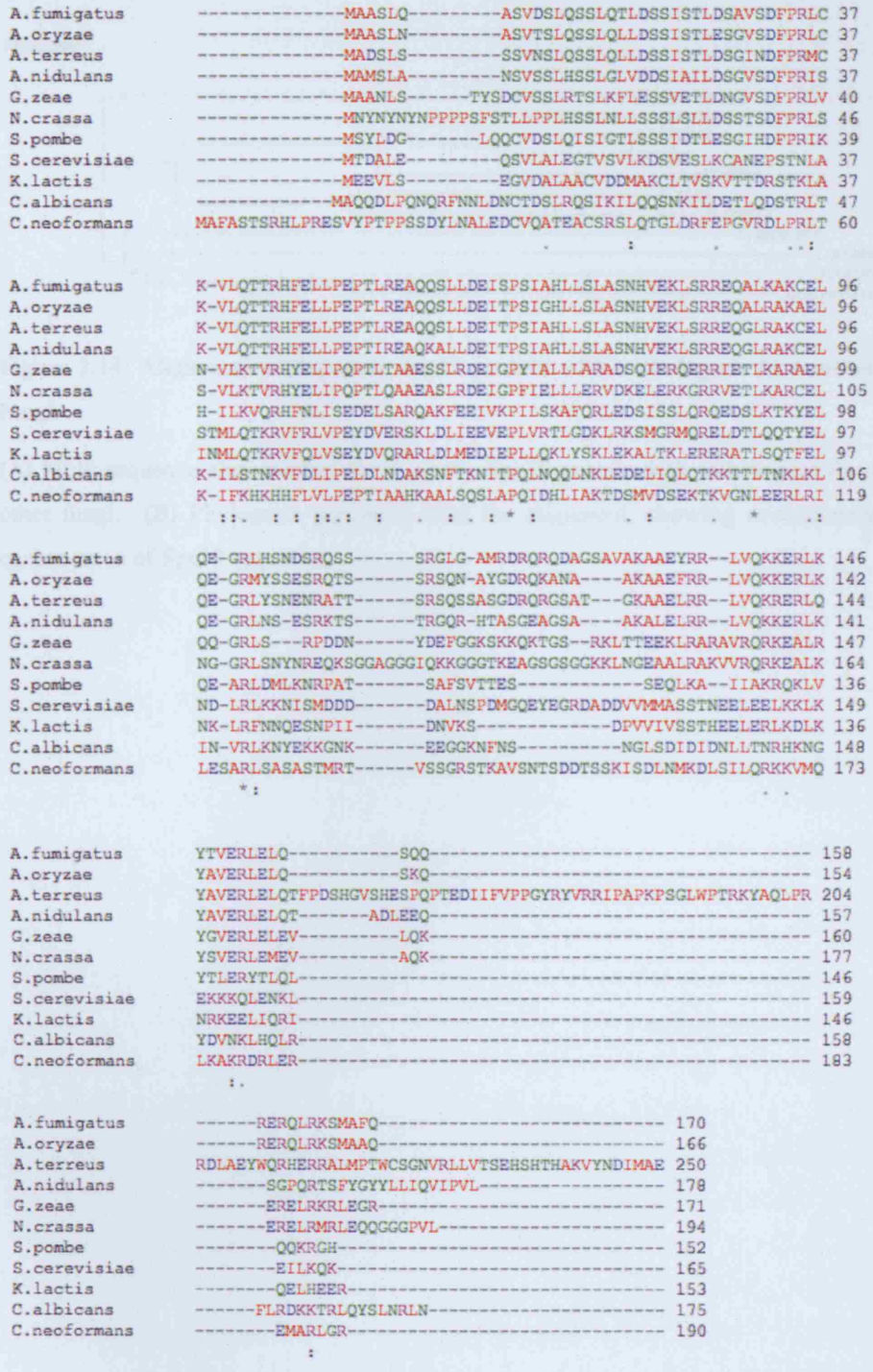
A.fumigatus
A.oryzae
A.terreus
A.nidulans
G.zeae
N.crassa
S.pombe
S.cerevisiae
K.lactis
C.albicans
C.neoformans

(B)

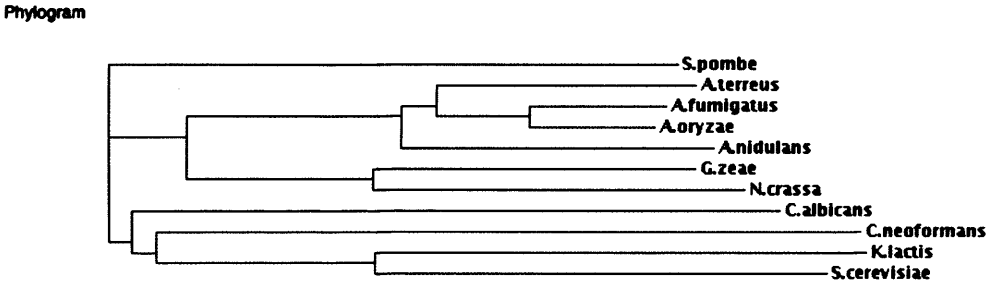

Figure 2.14: Alignment of *S. pombe* Spc19 protein with orthologues from other fungi.

(A) Multi sequence alignment of the *S. pombe* Spc19 protein with orthologues from other fungi. **(B)** Phylogram generated from the alignment, showing evolutionary conservation of Spc19 sequence.

There is evidence within *S. cerevisiae* that the Spc19 protein interacts with Spc34 (Ikeuchi et al., 2003; Kawarasaki et al., 2002). Through the application of PASA-PCR (preferential amplification of the shortest amplicon using PCR) using the yeast two- hybrid system the interaction of Spc19 to Spc34 was mapped to a region of the C-terminus S154-Q194 within the Spc34 protein (Ikeuchi et al., 2003; Kawarasaki et al., 2002). This region incorporates the entire coiled-coil motif of the Spc34 protein to which the Dad1 protein has also been mapped. This suggests that Spc19 Dad1 and the C terminus of Spc34 may form a trimeric coiled-coil structure (Ikeuchi et al., 2003). In the fission yeast *S. pombe* there is a single coiled coil motif from residue 71-105, perhaps implicating this motif as also playing a role in protein-protein interactions with the other Dam1/DASH subunits. There is no obvious consensus phosphorylation site detected in the *S. pombe* sequence. Analysis of the phylogram generated from the multi-sequence alignment in (Figure 2.14) shows that the *S. pombe* Spc19 protein is quite divergent from the other orthologues in the alignment.

2.2.8 Alignment of Spc34

The *S. pombe* Spc34 protein is much smaller than its *S. cerevisiae* homologue, 164 versus 294 amino acids respectively. From the yeast database the *S. cerevisiae* protein contains a predicted coiled-coil motif between residues 223-250, underlined in black in Figure 2.15. The *S. pombe* Spc34 protein contains two predicted coiled-coil motifs within its C-terminus, between residues 109-129 and 134-161 (Figure 2.15). However Ikeuchi et al. describe Spc34 in *S. cerevisiae* as possessing two coiled coils between residues 207-262 and 272-294. Through the application of PASA-PCR and yeast two-hybrid it has become apparent that many of the Dam1/DASH components bind to Spc34 in the budding yeast (Ikeuchi et al., 2003). It appears that Dam1 can interact with Spc34 at the N-terminus of the Spc34 protein (M1-D47) and may be facilitated by Dad1 acting as a linker bridge (Ikeuchi et al., 2003). Indeed as previously mentioned Dad1 can interact with Spc34 at region M1-D47 and also interact with Spc34 at the C-terminus 89 residues T207-E295, a region that overlaps with Spc19 binding (S154-Q194) (Ikeuchi et al., 2003). Domain binding mapping for Duo1 shows it interacts also with the N-terminus region of Spc34 M1-E59 (Ikeuchi et al., 2003). One could imagine then that the N-terminus and C terminus regions of the Spc34 proteins are probably well conserved to maintain these interactions in other organisms.

(A)

```
CLUSTAL W (1.83) multiple sequence alignment

                                    *           *
S.pombe             MSDLLN-YLQSIAATSEKLLEPENPNAARFTDAVLH--------THAITDLIRDTQKEE- 50
S.cerevisiae        MGESLDRCIDDINRAVDSMSTLYFKPPGIFHNAILQGASNKASIRKDITRLIKDCNHDEA 60
                    *.: *:  ::.*  : :.:       .. * :*:*:         : ** **:* :::*

S.pombe             ------------------------------------------------------------
S.cerevisiae        YLLFKVNPEKQSVSRRDGKEGVFDYVIKRDTDMKRNRRLGRPGEKPIIHVPKEVYLNKDR 120

                     *
S.pombe             ----------------------------------------LIAAEFKSLPKDWSERLA 68
S.cerevisiae        LDLNNKRRRTATTSGGGLNGFIFDTDLIGSSVISNSSSGTFKALSAVFKDDPQIQRLLYA 180
                                                            ::* **. *:      *

                                    *
S.pombe             SEN-------------------PADYVA-CIEELLDIYPMQGGREYLETLVEKYNLH 105
S.cerevisiae        LENGSVLMEEESNNQRRKTIFVEDFPTDLILKVMAEVTDLWPLTEFKQDYDQLYHNYEQL 240
                     **                 *:* :   : *: *::*:   ::  : * .:*:

S.pombe             MSGIENLENVLLEQKEQLQQLEKRQTDQVSARENILQRETSEIQRLEREIEKVKQLIQS 164
S.cerevisiae        SSKLRFIKKEVLLQDDRLKTMSQYHPSSSHDVAKIIRKEKDEIRRLEMEIANLQE---- 295
                     * :. ::: :* *.::*: :.: :...     :*:::*..**:*** ** ::::
```

(B)

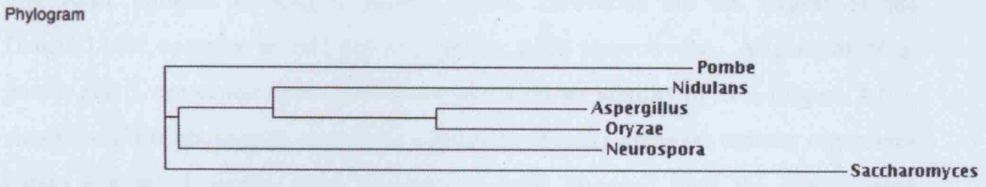

Figure 2.15: Alignment of *S. pombe* Spc34 protein with its homologue in *S. cerevisiae*.

(A) Regions of similarity are marked by dots and asterisks mark regions of conservation. The coiled-coil regions of *S. pombe* Spc34 are overlined in blue and the coiled-coil region within the *S. cerevisiae* protein is underlined in black. Aurora B (Ipl1) phosphorylation sites within the *S. cerevisiae* sequence are boxed in black. Point mutation sites from *S. cerevisiae spc34-5, spc34-6* and *spc34-7* mutants are indicated with an asterisk. **(B)** Schematic representative of the Spc34 protein structure in the two yeasts.

Alignment of Spc34 between *S. cerevisiae* and *S. pombe* shows a low sequence homology with 22% identity and indeed it does appear that the N and C termini are quite well conserved with the middle of the proteins showing high divergence (Figure 2.15). However alignment with orthologues from other fungi shows little homology, with both *S. pombe* and *S. cerevisiae* Spc34 proteins quite divergent from the other sequences in the phylogram analysis (Figure 2.16).

Spc34 is an essential gene but conditional mutants do exist that exhibit a bi-orientation defective phenotype when shifted to the restrictive temperature. The conditional lethal *spc34-5* allele contains an F30L mutation resulting in a change of amino acid from phenylalanine to leucine (Janke et al., 2002) (Figure 2.15). Interestingly this residue is conserved in the *S. pombe* sequence, however mutations present in the other mutant alleles *spc34-6* (S18D and K198E) and *spc34-7* (S18D and N124D), are not conserved in the fission yeast.

2.2.9 Alignment of Ask1

The Ask1 proteins in both *S. pombe* and *S. cerevisiae* are the largest of the Dam1/DASH complex at 307 and 292 amino acids respectively. Alignment of *S. pombe* and *S. cerevisiae* Ask1 protein sequences shows identity of 29% (Figure 2.17). Analysis of the phylogram created by alignment of Ask1 amongst various organisms shows that the *S. pombe* Ask1 sequence is quite diverged from the others listed (Figure 2.18). The *S. cerevisiae* Ask1 protein does not seem to contain any coiled-coil motif, however the *S. pombe* Ask1 protein contains a coiled-coil motif between residues 274-294, underlined in black in Figure 2.17. Studies in *S. cerevisiae* have shown that Ask1 is phosphorylated in a Cdc28 (CDK) dependent manner and de-phosphorylated upon anaphase entry (Higuchi and Uhlmann, 2005; Li et al., 2003). Two putative CDK phosphorylation sites are present within the Ask1 sequence at serine 216 and serine 250 (Li et al., 2003). Interestingly these possible CDK sites are conserved in the *S. pombe* Ask1 sequence and it has been shown that the *S. pombe* Ask1 protein is phosphorylated specifically during mitosis (Liu et al., 2005). There are several putative CDK sites present in the fission yeast Ask1 protein sequence and even a putative Polo site. It is tempting to speculate that this phosphorylation is mediated by Cdc2 kinase and plays a role in the mitotic function of Ask1 and perhaps de-phosphorylation of Ask1 in *S. pombe* is also required to silence microtubule dynamics in anaphase in a similar manner to the budding yeast.

2.3 Discussion

The Dam1/DASH complex exists as an essential ten-subunit complex in *S. cerevisiae*. It has been implicated in facilitating high fidelity chromosome segregation by ensuring the establishment of bi-oriented sister kinetochores and the maintenance of spindle integrity during anaphase. This complex also exists in the fission yeast *S. pombe* where it perhaps plays a similar role in mediating accurate chromosome segregation. BLAST searching revealed the presence of orthologues of the subunits of each of the Dam1/DASH complex members in various other fungal species but so far there is no strong bioinformatical or experimental evidence that this complex is conserved in vertebrates or other higher organisms.

In *S. pombe* Dam1 we showed the presence of putative Aurora B and Polo phosphorylation sites. As discussed earlier, phospho-regulation of Dam1 by Ipl1 in *S. cerevisiae* has been shown to be critical in turning over incorrectly attached kinetochores to facilitate bi-orientation (Cheeseman et al., 2002; Shang et al., 2003; Tanaka, 2002; Tanaka et al., 2002). One can imagine that such a regulatory system should exist in the fission yeast, which has the potential for merotelic as well as syntelic attachments. Although there is no biochemical evidence for modulation of the Dam1 protein in *S. pombe* it is tempting to speculate that there may be some form of regulation required. We also demonstrated that the critical lysine residues implicated in controlling the phospho state of Dam1 in *S. cerevisiae* are not conserved in the fission yeast. Hsk3 and Dad3 also show the presence of candidate Aurora B phosphorylation sites and Ask1 contains several possible CDK sites and a polo consensus site. Ask1 is the only subunit in *S. pombe* in which phosphorylation has been shown. It is tempting to speculate phospho-regulation of Dam1/DASH function in this organism occurs through Ask1.

The Dad1 subunit of the fission yeast complex does not appear to have a classical coiled-coil motif in either organism but as Ikeuchi et al discussed in their paper, there is a conserved region in many Dad1 orthologues of hydrophobic residues interspersed with glycines, perhaps indicating a possible function in protein protein interactions (Ikeuchi et al., 2003). Other proteins that may be implicated in protein-protein interactions in this complex in fission yeast Dam1/DASH complex are Ask1, Duo1, Spc19, Spc34 and Hsk3. These possess at least putative coiled-coil motifs that may enable the proteins to form an interactome with the other members of the complex, microtubules and other kinetochore subunits.

(A)

```
A.fumigatus       -MSLLENHLEQIQLSSNAIAELPFPQPRIFTNALLG--------PHDITALIRDTEAHER 51
A.oryzae          -MSLLDSHLEQILLSSNAIAELPFPPPRIFTNALLG--------PHDITALIRDTETHER 51
A.nidulans        -MSLLESHLEQIMLSSNAIAELPFPQPRIFTNALLG--------SHDITALIRDTEAHER 51
N.crassa          -MSLLLAHLEQISTSCESIDSLPFPPPKIFTNALLS--------NHDITSLIRDTEAHER 51
S.pombe           -MSDLLNYLQSIAATSEKLLEPENPNAARFTDAVLH--------THAITDLIRDTQKEEL 51
S.cerevisiae      MGESLDRCIDDINRAVDSMSTLYFKPPGIFHNAILQGASNKASIRKDITRLIKDCNHDEA 60
                    . *   ::.*  : : :       . * :*:*          : ** **:* : .*

A.fumigatus       -ALFQTDP----SAK----SQRRATRRGTMFQSEADGESMASRIYAVRNNR---NQSAVA 99
A.oryzae          -ALFQTDP----SVKAINASQRRSTRRGTVFPSETEGESMASRIYAARNSK---SQSAVA 103
A.nidulans        -ALFQSDP----TVK-------------------------------AMSWA---FQASLP 72
N.crassa          -ALFSVPPPPPKATTQAPDPPKPANRRQTIFNVAGGEVTTGPPAKSTRSSGPTRRNTAVA 110
S.pombe           -IAAEFKS-------------------------LPKDWSERLASENPAD--------- 74
S.cerevisiae      YLLFKVNP-------EKQSVSRRDGKEGVFDYVIKRDTDMKRNRRLGRPGEKPIIHVPKE 113
                     . .

A.fumigatus       RVLGSDMMDEIKRSAGTSARGTRNEVNIDVLLRGAEILCNVYPVAGAQEKIATLRYRHEL 159
A.oryzae          RVLGSDMMEEIKRSAGTSSRG-RGEVNVDVLLRGAEILCNVYPVSGAQEKIASLRYRHQL 162
A.nidulans        RFLTVALS---------------------------------PVAGAQDKIASLRYRNQV 98
N.crassa          AVLGGDLHAQITRRNPAGSGG--GELDIEVLLRGAEKLCTVYPLPGALERIPAQRRKNEQ 168
S.pombe           ----------------------------YVACIEELLDIYPMQGGREYLETLVEKYNL 104
S.cerevisiae      VYLNKDRLDLNNKRRRTATTSGGGLNGFIFDTDLIGSSVISNSSSGTFKALSAVFKDDPQ 173
                                                        . *  . : :

A.fumigatus       ISGSIAQLEDRVARNTAELEQMSQSYGEEYDDYDNPTTAT---LEVTDADIEREMEEIRE 216
A.oryzae          VTDSIVDLEDRVARNTAELEKMSHSYGGDYDDYESSGTLQPDVADLTDADIEQEMDEIRE 222
A.nidulans        ISESIAELEERVARNASELESMSHLHDDDYDELDNASSPSAGVLDVTDADIERELKEIRE 158
N.crassa          LMNTLAYYETRVAEQQEALDRLNLDRYAEEEEEEAGRESAAAADVMTEEDLRREEEEIRE 228
S.pombe           HMSGIENLENVLLEQKEQLQQLEKRQTDQVSAREN-------------ILQRETSEIQR 150
S.cerevisiae      IQRLLYALENGSVLMEEESNNQ-RRKTIFVEDFPTDLILKVMAEVTDLWPLTEFKQDYDQ 232
                     :  *         :          .                 : .  .:  .

A.fumigatus       LERRKRALEARVSGMERDLVNRQLYKQHLNVCAHATVKT---RFLGLAPSQPCQFWPSAL 273
A.oryzae          LEKMKRTLEARVSGMERDLGG---------------------LIG-------------- 246
A.nidulans        LERRKRNLEDRVNGMERDLGGLSHARDIRAVTTFSLPNKNAGKFVGSGKQRYCSYRANEE 218
N.crassa          LDRRRRELQARLRATERDLNG---------------------LMEF------------- 253
S.pombe           LEREIEKVKQLIQS---------------------------------------------- 164
S.cerevisiae      LYHNYEQLSSKLRFIKKEVLLQDDRLKTMSQYHPSSSHDVAKIIRKEKDEIRRLEMEIAN 292
                  * :  . :.  :

A.fumigatus       TQWA------------------------------------------ 277
A.oryzae          ---------------------------------------------
A.nidulans        PRINNRGTYIRSKWQRKSPFSGNSAGRGILVIVVATFESMLIAISAA 265
N.crassa          ---------------------------------------------
S.pombe           ---------------------------------------------
S.cerevisiae      LQE------------------------------------------- 295
```

(B)

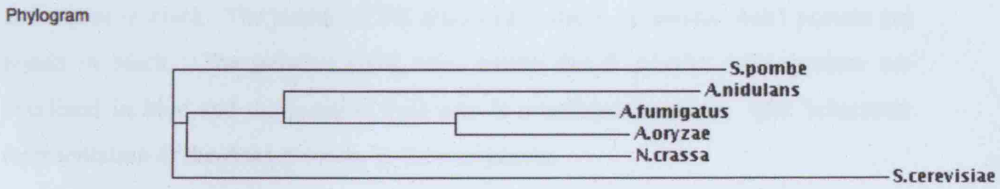

Figure 2.16: Alignment of *S. pombe* and *S. cerevisiae* Spc34 proteins with orthologues from other fungi.

(A) Regions of similarity are marked by dots and an asterisk marks regions of conservation. **(B)** Phylogram generated from the alignment above.

(A)

```
CLUSTAL W (1.83) multiple sequence alignment

S.pombe          ---MNNLEQLERLEQSITLALYEIDANFSKCHRTVTTKILPIVEKYAKNCNTIWDSSKFW 57
S.cerevisiae     MDSASKEETLEKLVQEITVNLQKIDSNLSFCFHKITQDIIPHVATYSEICERIMDSTEWL 60
                    .: * **:* *.**: * :**:*:* *.:.:* .*:* * .*:: *: * **:::

S.pombe          KQFFEASANVSLSG-VEEPV---PVESNPSD-QDVMSNSTEADLQLHTKNEHLEKRHSFV 112
S.cerevisiae     GTMFQETGLVNLQANAAAPVGNAPVKSLVSNNVGIFPTSAEEASRQSQTDNGPNEADSAV 120
                   :*: :. *.*.. .  **   **:*  *:  .::..*:*   :   .::  :: .* *

S.pombe          GKSDFPDAAVQGDNTKNEDFVQSTPKKMDVSLEDISLDDAALTPIPARMQTPLRKPENNP 172
S.cerevisiae     HVNRDVHSMFNNDSIDDFHTANITSTGQILKLPDSSDEDTGSEAVPSREQTDLTG----- 175
                   .   .: .:.*. .: . .: *..   :.* * * :*:.  .:*:* ** *

S.pombe          HTGRSALLHRVLDTNWQVQVTPREPKNLQSQEVMDIDSSPFVSPSPISMKMDMPSLNDRN 232
S.cerevisiae     -EGHGGADDEQDESTIQRQSRKRKISLLLQQ---QYGSSSSMVPSPI-----VPNKMRKQ 226
                  *:..  ..  ::. * *   *: . * .*   : .**. : ****      :*.   ::

S.pombe          SSHALSLFAEFEHESYDSINPSGMSPPKTIQFSPHTMGVGSSQQANERSLSLQRKLETLN 292
S.cerevisiae     LAHEEHINNDGDNDDENSNNIE-SSPLKQGHHHPK----GQADDNNEGPDEEESTKEVPK 281
                  :*   : : :::. :* * .  ** *  :. *:    *.::: ** . . : . *. :

S.pombe          DSNDSFVKEEDSWEL 307
S.cerevisiae     PGTIIHFSTNR---- 292
                  ..  ... :
```

(B)

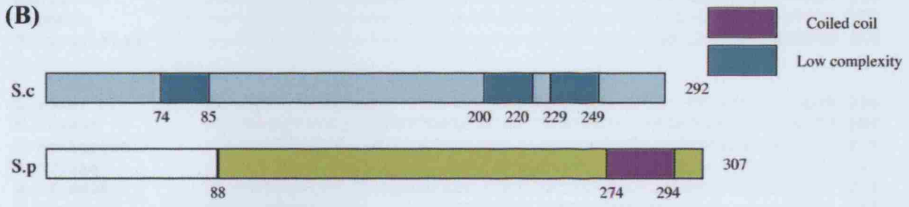

Figure 2.17: Alignment of *S. pombe* Ask1 protein with its homolog in *S. cerevisiae*.

(A) Regions of similarity are marked by dots and asterisks mark regions of conservation. The coiled-coil region within the *S. pombe* Ask1 sequence is underlined in black. The putative CDK sites within the *S. cerevisiae* Ask1 protein are boxed in black. The putative CDK sites within the *S. pombe* Ask1 protein are overlined in blue and the putative Polo site is overlined in green. **(B)** Schematic representation of the Ask1 proteins in the two yeasts.

(A)


G.zeae MSRQ-SVAAR-NLSLTEELERLEQSITLTLQEIDHNFSKSHRIVTTSILPLVEKYGDHSR 58
N.crassa MSVPGTSSTR-PLTLTEELEKLEQSITLTLQEIDSNFSRAHRIVTTNILPLP-------- 51
A.fumigatus MSRP-SSISQRPLTLTEELEKLEQSITLTLQEIDHNFSQAHRIVTTSILPLVEQYAEHSR 59
A.oryzae MSRP-SSMSQRPLTLTEELEKLEQSITLTLQEIDHNFSQAHRIVTTSILPLVEKYAEHSH 59
A.terreus MSRPTSAMPQRPLTLTEELEKLEQSITLTLQEIDHNFSQAHRIVTSSILPLVEQYAEHSR 60
S.pombe ----------MNNLEQLERLEQSITLALYEIDANFSKCHRTVTTKILPIVEKYAKNCN 48
S.cerevisiae ---------MDSASKEETLEKLVQEITVNLQKIDSNLSFCFHKITQDIIPHVATYSEICE 51
G.zeae AVWEASKFWKQFFEASANVSLSGYEELANDDES---ESVEESTAMREDISEDYTAQHN-- 113
N.crassa ---LASQFWKQFFEASANVSLSGYEELANGNETTVLNSNEESTSAHDQTTPAGTPHPQSA 108
A.fumigatus DVWESAKFWKQFFEASANVSLSGYEERPDE------DTTQDQTVTED--SADVTHSNLT- 110
A.oryzae DVWEGAKFWKQFFEASANVSLSGYEERPNE------DTLQEQSVTEDDSTADITPSNLT- 112
A.terreus DVWDGAKFWKQFFEASANVSLSGYEERPNEEGEG--DTSQEHTVTEDD-PSHITHSQLS- 116
S.pombe TIWDSSKFWKQFFEASANVSLSGVEEPVPVE-----SNPSDQDVMSNSTEADLQLHTKN- 102
S.cerevisiae RIMDSTEWLGTMFQETGLVNLQANAAAPVG-------NAPVKSLVSNNVGIFPTS----- 99
G.zeae --------EDVTTATGAEQSTFQA-----EDSMLDDA--ELSGSTPRPGKTKTR------ 152
N.crassa GRSHDITIDDESSATFNAQGQNQVRQRTTNDSVLTDTGDDLSGSTPRPPATKSIP----S 164
A.fumigatus -----------DTVSYETPSMERH--HHRADDLELTSLGVSSHSTPRAATNERPD-ADTT 156
A.oryzae -----------DTGTYETPSSEHLDINHRPDDLELT-LSLSSHSTPRPPVFDRPDDNDTT 160
A.terreus -----------ESASYETPSSARLDINHRADDLELTSLSLSSHSTPRAPPHMNPNTADDT 165
S.pombe -----------EHLEKRHSFVGKSDFPDAAVQGDNTKNEDFVQSTPKKMDVS-------- 143
S.cerevisiae ----------AEEASRQSQTDNGPNEADSAVHVNRDVHSMFNNDSIDDFHTANIT----- 144
G.zeae ---FSDMESPYEVMKR-EMEDEDDGHDNTTVLDG-------NEDSTILFAQHTARLPDMS 201
N.crassa RPQFANLDSPYEQLRRRELKAAAEASKTPGFGSGSGGDTMEDDDSELIFQQHTARLPDMS 224
A.fumigatus ITSAVSYTSPYETLKQEIHETDPPFDVDDSNLPSTPGRSPRLHDYAGN-SGETL-MSSSP 214
A.oryzae VTSSIARPSPYEALKREIEENDAPFEGEDDDLPTTPGRPFRPQGYSFN-PRDEL-MSSSP 218
A.terreus ISS-IAHPSPYDHGQRAES---PAYD--DDDLPTTPGRHSRPRGYSHENTSRTP-MSSSP 218
S.pombe ----------LEDISLDDAALTP-IPARM 161
S.cerevisiae ----------STGQILKLPDSSDEDTGSE 163
G.zeae MTPQGQRDHTMTGEQSAQ---PQKDPLLHRILDKNYRIQATPHK--PALRTSPLKSAQSK 256
N.crassa MTPHRAQNTPFGEQQQQRGGTANKDPILHRMPDRNYRVGATPHKGHQASGVSPIKWKVTE 284
A.fumigatus FVPPASHEQPSGAR--RNPHQKTSDPIMHRVLDKTYRVQATPLGKGYGTATSRSKFTVTP 272
A.oryzae FVPPVSHEKFSTSG--KSP----ADPVLHRLQDKTYRVQATPLGKDYG--AGRSKFTITP 270
A.terreus FIPPVSRDAPPSTAGTRHRAGSGSDPVLHRVLDKTYRVQATPLGKGHA--AGRSKFTVTP 276
S.pombe QTPLRKPENNPHTG---------RSALLHRVLDTNWQVQVTPRE---------- 196
S.cerevisiae AVPSREQTDLTGEG----------HGGADDEQDESTIQRQ---------- 193
G.zeae S----------AKKNVPTWNDSPGSSPEMAVPTLRSEAFMSPYKSNAR--QRLAAAT- 301
N.crassa KKPPLIDPKGKGKAREEKPLWQDSFMSSPEMEVPQLRSAAFMSPIRSAYRGNTRAAAAAY 344
A.fumigatus K----------ASTSKYAFDDSPISSPEPEAPQLHAEIFSSPLKATTPGTGRKRRPSG 320
A.oryzae K----------LSTSKHGYDDSPISSPEPEAPQLHAEIFSSPLK--TPGTNRKRRTSS 316
A.terreus K----------QSSSKYAADDSPLSSPEMEAPRLHAEIFSSPLK--TPGTNRKRRTSS 322
S.pombe ----------PKNLQSQEVMDIDSSPFVSPSPISMKMDMPSL 228
S.cerevisiae ----------SRKRKISLLLQQQYGSSSSMVPSPIVPNK 222
G.zeae ---QGPRTPGVSVQTPATARKTRDVFAADDS----------AKSKDKYELSWD 341
N.crassa AARSAPRTPGVSVQTPLAGRKTKDVFSANAANAHTNAGKTPIPKGTVEAKKRYLEEIDWE 404
A.fumigatus HLRITPK-PGMSVLTPAKNGGGKRSG----------WD 347
A.oryzae HLRATPK-PGISVLTPVKSGGTGRPV----------WD 343
A.terreus HLRATPK-PGTSVLTPAK--GSSRPV----------WD 347
S.pombe NDRNSSHALSLFAEFEHESYDSINPS---------- 254
S.cerevisiae MRKQLAHEEHINNDGDNDDENSNNIE---------- 248

```
G.zeae          SDDDDEDI-DLYAGMSPPKTIQFALPPSKLLQTPAREASQRIVGDILIDAGADPNS---- 396
N.crassa        SDSEQ----DPFGGMSPPKTIQFALPPSKLLQTPAREASKKIVENLLLTAGEMPEGE--- 457
A.fumigatus     SDEDFDDEEDENFGPSPPKTMQFHIPQSRLMKTPAKEASKRIVEDLLFTAGVNDTTDDII 407
A.oryzae        SD-DFD----------PPKTMQFHIPQSRLMKTPAKEASRRIVEDLLFTAGANDTTDDIA 392
A.terreus       SDDDFEDE-DETFGPSPPKTMQFHIPQSRLMKTPAKEASKRIVEHLLYTAGANDTTDDIQ 406
S.pombe         ------------GMSPPKTIQFSPHTMGVGSSQQANERSLSLQRKLETLND-------- 293
S.cerevisiae    --------------SSPLKQGHHHPKGQADDNNEGPDEEESTKEVPK------------ 281
                                .*  .  .        ..

G.zeae          SEYSPSMVKINEDILDDSF 415
N.crassa        SEFSPSVVKMNPDLMDETF 476
A.fumigatus     DEQSPSVIRRVERLEDETF 426
A.oryzae        AEQSPSIIQRVQRIEDETF 411
A.terreus       DEQSPSMVRRMERLEDDTF 425
S.pombe         --SNDSFVKEEDSWEL--- 307
S.cerevisiae    ---PGTIIHFSTNR----- 292
                    :.::
```

(B)

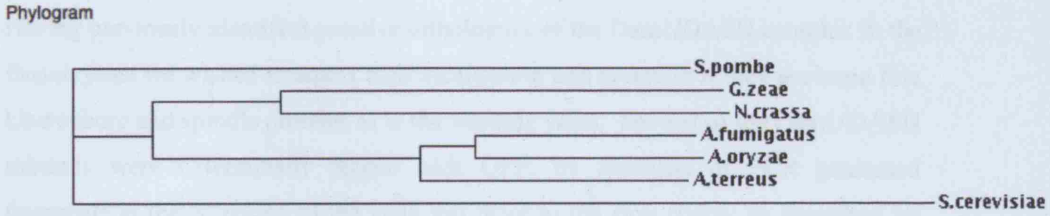

Figure 2.18: Alignment of Ask1 protein from *S. pombe* with orthologues from other organisms.

(A) Regions of similarity are denoted by dots and asterisks denote regions of conservation. **(B)** Phylogram generated from the alignment in (A)

Chapter 3

3 Localisation of the Dam1/DASH complex

Introduction

Having previously identified putative orthologues of the Dam1/DASH complex in the fission yeast we wished to assess their localisation and ascertain if they are bona fide kinetochore and spindle proteins as in the budding yeast. Several of the Dam1/DASH subunits were C-terminally tagged with GFP, by insertion of PCR generated fragments at the 3' region of the gene just prior to the stop codon: as described by Bahler *et al.* 1998 (Figure 3.1). Tagging these Dam1/DASH genes with GFP did not seem to affect the functionality of the proteins. The localisation of these GFP tagged proteins at various stages of the cell cycle was then examined. We demonstrate that several of the components bind to the kinetochore as cells enter mitosis. However the Dad1 component is constitutively localised to the kinetochore throughout the cell cycle. We show that this association of Dad1 with the kinetochore is dependent on a functional Mis6/Sim4 complex, but not on Mis12, Nuf2, or Cnp1. We also try to assess the microtubule dependency of the mitosis-specific Dam1/DASH components by examining localisation of Dam1 in the β-tubulin mutants *nda3-1828* and *nda3-311* and after cold shock treatment.

3.1 Kinetochore localisation of Dam1 complex

Analysis of the sub-cellular localisation of Ask1-GFP, Duo1-GFP and Dam1-GFP in fixed cells shows no signal detected in interphase cells; localisation of these subunits is only visualised as cells enter mitosis (Figure 3.2). In early mitotic cells localisation appears as one or two discrete dots possibly reflecting kinetochore or SPB localisation. As cells progress through metaphase multiple dots and/or weak spindle staining becomes apparent (Figure 3.2).

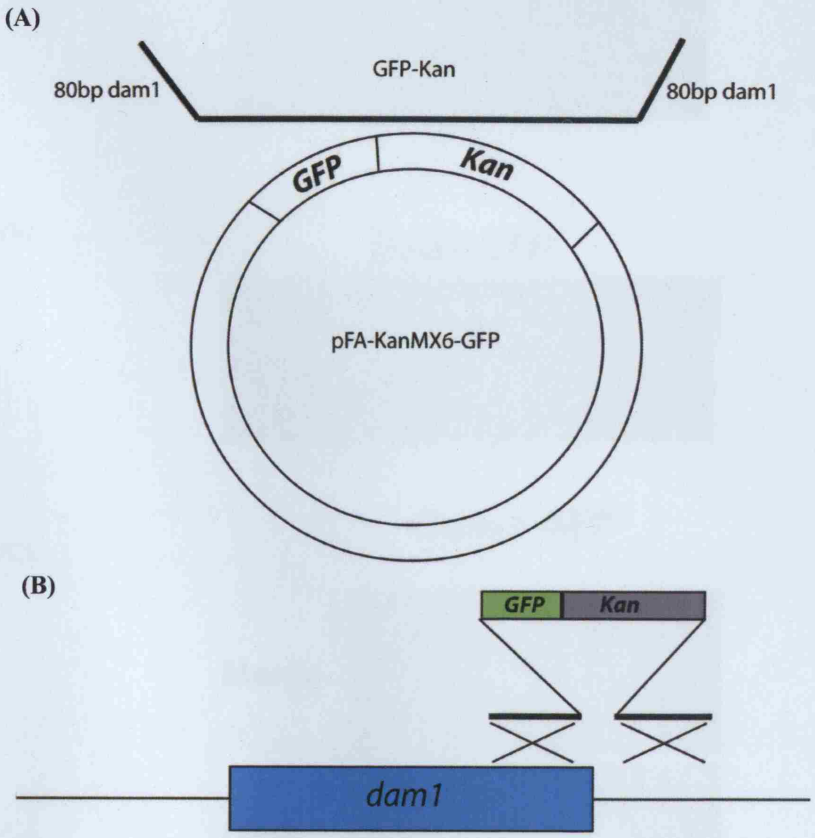

Figure 3.1: Schematic showing C-terminal GFP epitope tagging steps.

(A) The first step involves PCR from a plasmid containing the GFP-Kanamycin cassette pFa-KanMX6 (Bahler et al., 1998). The forward oligo for the PCR contains 80bp of the gene sequence just prior to the stop codon and 20bp from the cassette. The reverse oligo likewise contains an 80bp sequence downstream of the stop codon of the gene and 20bp from the GFP-kanamycin cassette. **(B)** The PCR product containing GFP-Kan is inserted at the 3' end of the gene just prior to the stop codon by homologous recombination.

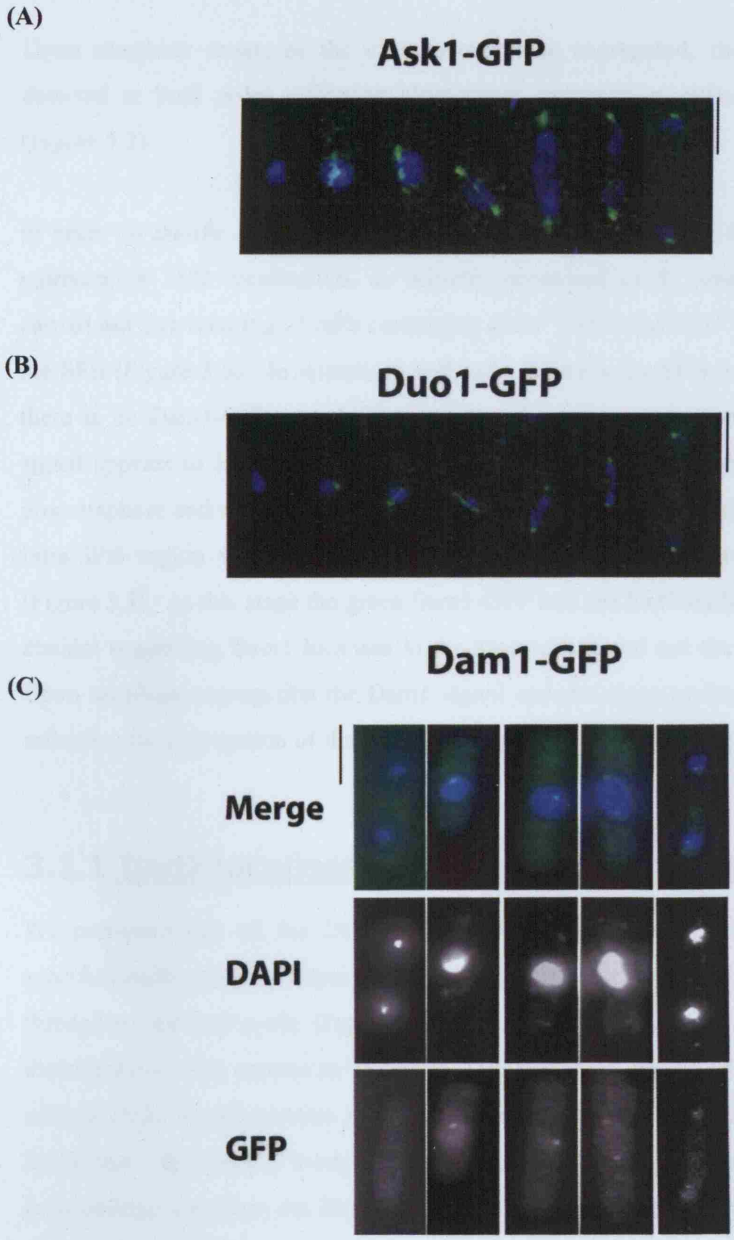

Figure 3.2: Localisation of Ask-GFP, Duo1-GFP and Dam1-GFP in fixed cells

Cells containing either *ask1*$^{+}$*-GFP* **(A)** *duo1*$^{+}$*-GFP* **(B)** or *dam1*$^{+}$*-GFP* **(C)** were fixed in 3% formaldehyde (See Materials & Methods). The cells were stained with DAPI mounting medium and viewed by fluorescence microscopy. **(A)** Ask1-GFP in green, DAPI stained DNA in blue. **(B)** Duo1-GFP in green, DAPI stained DNA in blue. **(C)** Dam1-GFP in green, DAPI stained in blue. The scale bars represent 10μm.

Upon anaphase onset, as the chromosomes are segregated, the GFP signals are detected at both poles reflecting kinetochore segregation and/or SPB localisation (Figure 3.2).

In order to clarify if the mitosis-specific GFP dots visualised in Figure 3.2 were representing SPB localisation, as initially presumed in *S. cerevisiae* studies, we carried out live imaging of cells containing *dam1*$^{+}$*-GFP* and *sad1*$^{+}$*-dsRed* to visualise the SPB (Figure 3.3). In interphase and early G2 cells the SPB is clearly visible but there is no Dam1-GFP signal (Figure 3.3). As cells enter mitosis the Dam1-GFP signal appears to localise close to the SPB. When SPB separation is visualised in prometaphase and metaphase cells Dam1-GFP localises between the two poles in the intra-SPB region where the kinetochores can be found clustered on the spindle (Figure 3.3). At this stage the green Dam1-GFP and red Sad1-dsRed signals are quite distinct suggesting Dam1 localises to the kinetochore and not the SPB (Figure 3.3). Upon anaphase segregation the Dam1 signal appears close to the Sad1 SPB signal, reflecting the segregation of the kinetochores to opposite poles (Figure 3.3).

3.1.1 Dad1 localises constitutively to the kinetochore

We presumed that all the Dam1/DASH subunits would show this same mitosis-specific localisation, but surprisingly Dad1-GFP appears to localise at the kinetochore throughout the cell cycle (Figure 3.4A). In interphase cells Dad1 localises as a discrete dot at what appears to be clustered kinetochores, and as cells proceed through mitosis Dad1 signal remains at the kinetochore and can be visualised by up to 6 kinetochore dots during metaphase (Figure 3.4B) (Sanchez-Perez et al., 2005). As cells undergo anaphase the Dad1-GFP signals are visualised at both poles reflecting segregation of the kinetochores to the poles (Figure 3.4).

To assess if this Dad1-GFP pattern reflects kinetochore localisation we carried out live imaging on cells containing *dad1-GFP*$^{+}$ and *nuf2-CFP*$^{+}$ to visualise the kinetochore (Nuf2, a known kinetochore protein, is a member of the Ndc80 complex). The Dad1 signal closely correlates with the Nuf2 signal throughout the cell cycle, showing tight co-localisation at the kinetochore (Figure 3.4B). We therefore conclude that Dad1 is a bona fide kinetochore component, and unlike the other Dam1/DASH subunits it shows constitutive localisation to the kinetochore throughout the cell cycle.

3.1.2: Dad1 acts as anchor for recruitment of mitosis-specific Dam1/DASH complex.

The constitutive localisation of Dad1 to the kinetochore suggests this protein may play an active role in recruiting the remaining Dam1/DASH complex subunits during mitotic maturation of the kinetochore. To address this possibility we assessed the localisation of Dam1-GFP in a Δ*dad1* strain. Unsurprisingly Dam1-GFP does not appear to localise to the kinetochore at any stage of the cell cycle in Δ*dad1* cells (Figure 3.3B). It also appears that several of the other mitosis-specific Dam1/DASH components, namely Ask1 and Dad2 cannot localise in *Δdad1* cells (Liu et al., 2005). Thus it appears that Dad1 acts as a platform for the recruitment of the mitosis-specific components of the Dam1/DASH complex during mitosis.

3.2 Dad1 localisation in kinetochore mutants

As we have demonstrated in the previous section Dad1 is constitutively localised to the kinetochore, where it acts as a platform for recruitment of the remaining Dam1/DASH complex during mitosis. It is clear that Dad1 itself must be anchored to the kinetochore by some other kinetochore protein, or proteins, to facilitate this Dam1/DASH recruitment role. We wished to elucidate which, if any, of the known kinetochore proteins are responsible for tethering Dad1 to the kinetochore. To address this we analysed Dad1-GFP localisation in various kinetochore temperature sensitive conditional mutants (Figure 3.5). The fission yeast kinetochore seems to be organized into discrete subcomplexes such as the Mis6/Sim4-Sim4 complex, the Mis12 complex and the Ndc80 complex (Liu et al., 2005; Pidoux and Allshire, 2004). Rather than test each individual member of these subcomplexes for Dad1 localisation to the kinetochore, we examined one or more mutants from each to ascertain if any of these subcomplexes are involved in tethering Dad1 at the kinetochore.

(A)

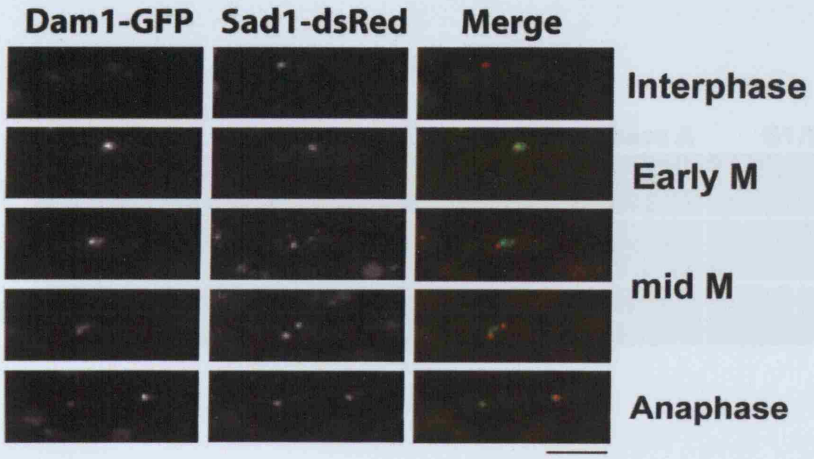

(B)

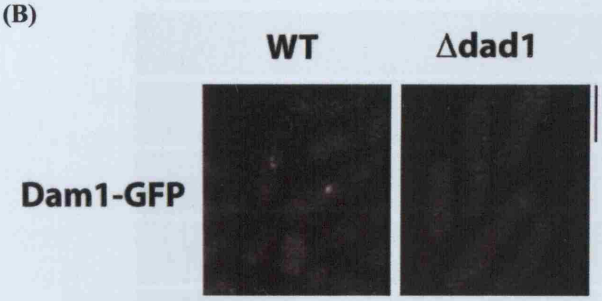

Figure 3.3: Dam1 does not localise to the SPB but localises to the kinetochore in a Dad1 dependent manner.

(A) Live imaging of cells containing *dam1*$^{+}$*-GFP* and *sad1*$^{+}$*-dsRed* fluorescence microscopy. Dam1-GFP in green: Sad1-dsRed in red. **(B)** Dam1-GFP localisation visualised in WT and Δ*dad1* fixed cells by fluorescence microscopy. (See Materials & Methods). Scale bars represent 10 μm.

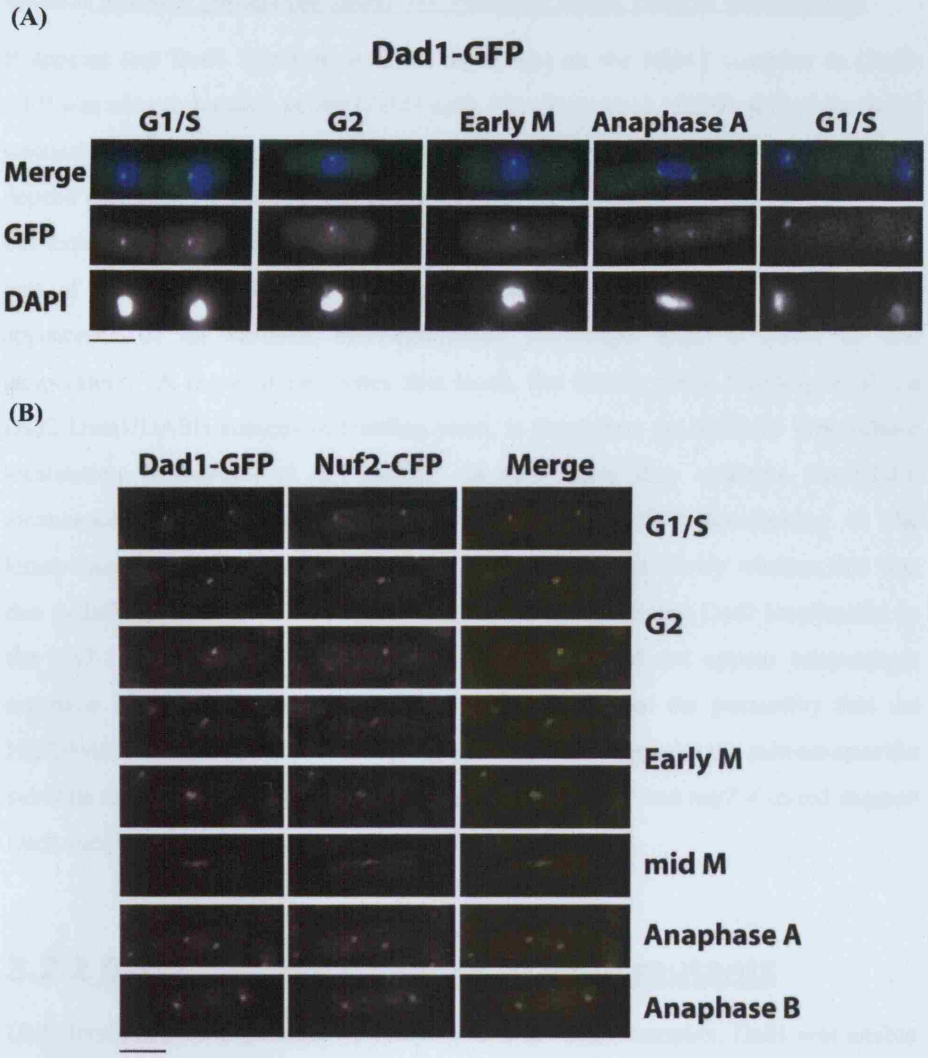

Figure 3.4: Dad1-GFP localises constitutively to the kinetochore .

(A) Localisation of Dad1-GFP visualised in fixed cells by fluorescence microscopy (See Materials & Methods). Dad1-GFP in green, DAPI stained DNA in blue. **(B)** Live cell imaging of cells containing *dad1-GFP* and *nuf2-CFP* by fluorescence microscopy. Dad1-GFP is green; Nuf2-CFP is red. The scale bars represent 10μm.

3.2.1 Dad1 localisation in Mis12 and Nuf2 mutants

It appears that Dad1 localisation is not dependent on the Mis12 complex as Dad1-GFP was able to localise in *mis12-537* cells (Goshima et al., 1999) shifted up to the restrictive temperature of 36° for 6 hours (Figure 3.5). Dad1 also does not appear to depend on Nuf2 and perhaps the Ndc80 complex for anchorage to the kinetochore. In our experiment using the *nuf2-4* allele (Nabetani et al., 2001) we could not see any loss of Dad1 localisation at the restrictive temperature (Figure 3.5), despite the appearance of an obvious mis-segregation phenotype after 6 hours at this temperature. A recent paper states that Hos2, the fission yeast homologue of the Dad2 Dam1/DASH subunit in budding yeast, is dependent on Nuf2 for kinetochore localisation (Kobayashi et al., 2007). In this paper they examine Hos2-GFP localisation in *nuf2-1* cells and show reduced Hos2-GFP localisation at the kinetochore at the restrictive temperature. We attempted to clarify whether this was due to differences in the alleles *nuf2-1* and *nuf2-4* by examining Dad1 localisation in the *nuf2-1* cells, but in our hands this *nuf2-1* allele did not appear temperature sensitive. (Data not shown) Therefore we cannot rule out the possibility that the Nuf2/Ndc80 complex does play a role in tethering Dad1or maybe the mitosis-specific subunits to the kinetochore, however the two alleles *nuf2-2* and *nuf2-4* tested suggest Dad1 localisation to be independent of Nuf2.

3.2.2 Dad1 localisation in Mis6/Sim4 mutants

Dad1 localisation is dependent on a functional Mis6/Sim4 complex. Dad1 was unable to localise at the restrictive temperature in both *mal2-1* and *mis6* -302 (Fleig et al., 1996; Saitoh et al., 1997) cells after shift up to the restrictive temperature. (Figure 3.5) Intriguingly Dad1 was still present in the Sim4 mutant *sim4-193* (Pidoux et al., 2003), despite the appearance of an obvious mis-segregation phenotype after 6 hours at the restrictive temperature. Sim4 is also a component of the Mis6/Sim4 complex but perhaps this particular allele is not compromised for Dad1 localisation activity or indeed maybe Mis6 and Mal2, but not Sim4, are the physical docking proteins for Dad1.

3.2.3 Cnp1 is not required for Dad1 localisation

It has previously been established that the Mis6 protein is required for loading of Cnp1, the fission yeast CENP-A homolog, to the kinetochore (Saitoh et al., 1997; Takahashi et al., 2000). We have identified Mis6 as a requirement for anchoring Dad1 to the kinetochore and thus for the recruitment of the whole Dam1/DASH complex during mitosis. We postulate that the failure of Dad1 to localise in *mis6-302* and *mal2-1* cells is due to this complex playing a direct tethering role for Dad1 and the incoming Dam1/DASH complex at the kinetochore. Another intriguing possibility however, is that Dad1 fails to localise due to the loss of Cnp1 at the kinetochore in *mis6-302* and possibly *mal2-1* cells. To address this possibility directly we analysed Dad1-GFP localisation in *cnp1-1* conditional mutant cells (Figure 3.5). If Dad1 is delocalised in Mis6/Sim4 complex mutants due to loss of Cnp1 from the kinetochore then Dad1 should similarly become delocalised at the restrictive temperature in *cnp1-1* cells. Dad1 signal, however, appears intact even after 6 hours at 36°C in *cnp1-1* cells (Figure 3.5). It seems that Dad1 localisation to the kinetochore is independent of Cnp1 and that Mis6 and Mal2 therefore play a more direct role in tethering this protein to the kinetochore throughout the cell cycle.

3.3 Dam1/DASH complex localisation is dependent upon microtubule integrity?

The budding yeast Dam1/DASH complex requires microtubules for its kinetochore localisation (Li et al., 2002). In the fission yeast it is thought that the kinetochores interact and attach to the microtubules only in mitosis. This is the time when the Dam1/DASH complex becomes fully loaded to the kinetochore in this organism (Figure 3.2, Figure 3.3). It therefore seems an attractive hypothesis to postulate that microtubules also play an important role in depositing the mitosis-specific Dam1/DASH subunits to the kinetochore in *S. pombe*. In order to assess this we analysed Dam1-GFP localisation in the β tubulin mutants *nda3-1828*, a temperature sensitive allele and *nda3-311*, a cold sensitive allele and after cold shock treatment of *nda3-311* cells (Funabiki et al., 1993; Hiraoka Y, 1984; Radcliffe et al., 1998; Umesono et al., 1983). We used Dad1-GFP as a control, as it is constitutively localised to the kinetochore and should not be affected by depolymerisation of microtubules either by cold shock or β tubulin mutation.

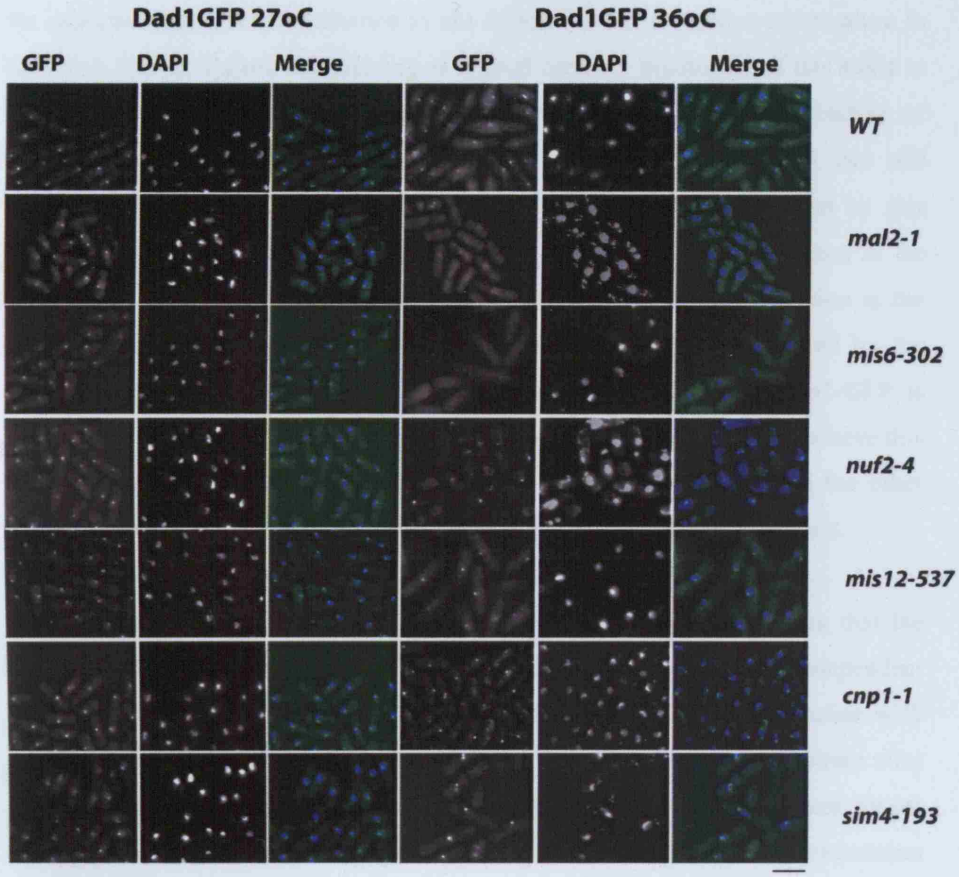

Figure 3.5: Analysis of Dad1 localisation in various kinetochore mutants.

Dad1-GFP signal analysed in WT and kinetochore mutant cells at permissive and restrictive temperature. Cells containing *dad1*$^{+}$*-GFP* were grown in rich medium at 27°C. Cultures were then split and incubated at 27°C or shifted for 6 hours to the restrictive temperature of 36°C. Cells were then fixed and stained with DAPI mounting medium and viewed by fluorescence microscopy (See Materials & Methods). Scale bar represents 10μm.

As expected Dad1-GFP localisation is not affected at the restrictive temperature in the *nda3-1828* ts mutant, thus serving as a good control. Incubation of this strain at the restrictive temperature leads to mitotic arrest and the depolymerisation of microtubules due to the β tubulin conditional mutation, however Dad1 can still localise to the kinetochore throughout the cell cycle and is unperturbed by this microtubule loss (Figure 3.6 a&b). Dam1-GFP localisation appears normal in the *nda3-1828* ts allele at the permissive temperature (Figure 3.6c). Incubation at the restrictive temperature for 4 hours induces a mitotic arrest, as evidenced by the presence of condensed DNA, and the kinetochore localisation of Dam1-GFP is abolished in favour of diffuse cytoplasmic localisation (Figure 3.6d). We believe this to be strong evidence of a microtubule role in deposition of Dam1 and the other mitosis-specific Dam1/DASH complex members to the kinetochore in mitosis.

There is however a differing result published by Liu *et al.* 2005, inferring that the Dam1/DASH complex is localised first to the SPB in a microtubule independent manner. In this paper they show Dam1-GFP and Ask1-GFP can co-localise with Ndc80-CFP to the kinetochores in over 80% of the cells in an *nda3-311* strain after shift down to 18°C for 10 hours (Liu et al., 2005). These kinetochores are almost always associated with an SPB with only a fraction of unattached kinetochores showing Dam1 or Ask1 binding (Liu et al., 2005). To assess if the localisation of Dam1 is truly intact in the cs allele *nda3*-311 we analysed Dam1-GFP localisation in this strain after shift down to the restrictive temperature for 8 hours (Figure 3.6e). We obtained the same result, whereby Dam1-GFP localisation appears intact in this strain. We hypothesized that this discrepancy in localisation between the two alleles, *nda3-1828* and *nda3-311*, may reflect the presence of residual microtubules that are nucleated near the SPB in the *nda3-311* strain. Therefore we decided to carry out ice-treatment in the *nda3-311* strain after 8hours at the restrictive temperature to fully depolymerise any remaining microtubules (Figure 3.6f). In this strain incubation on ice for 30 minutes followed by fixation in 3% formaldehyde on ice results in total loss of Dam1-GFP signal from the kinetochore and the appearance of a diffuse cytoplasmic and nuclear signal (Figure 3.6f). This clear delocalisation of Dam1-GFP under these conditions strongly suggests that the fission yeast Dam1/DASH complex requires microtubules for kinetochore localisation during mitosis.

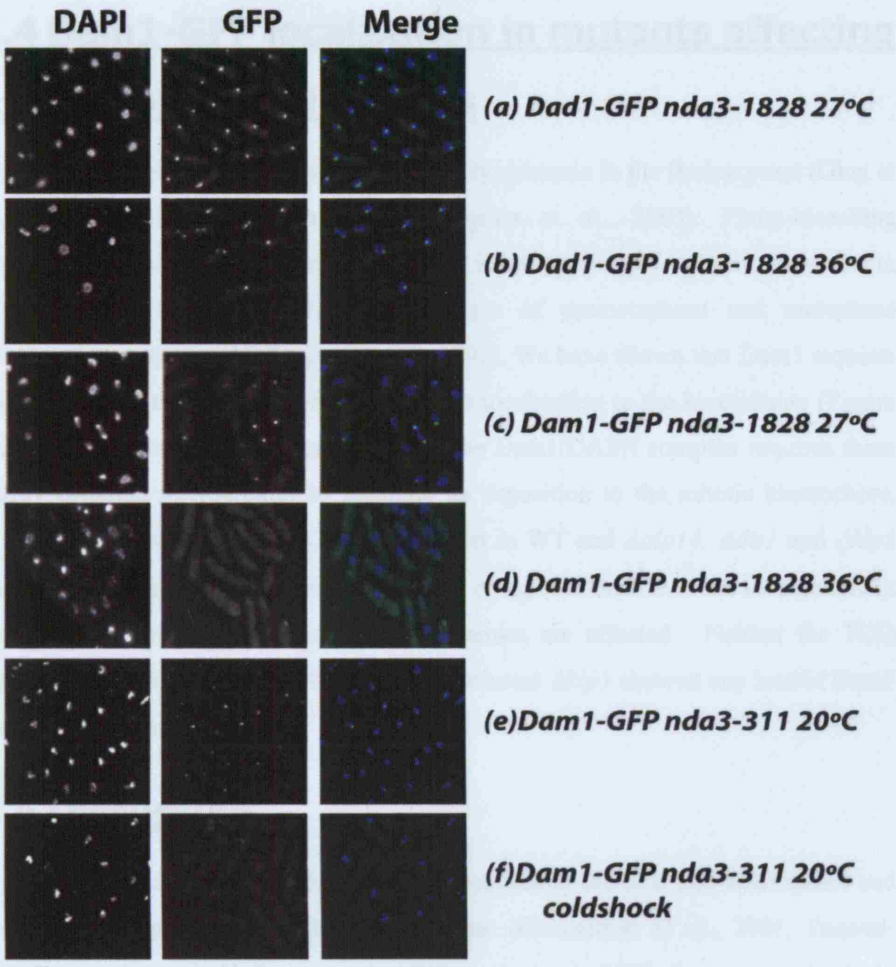

Figure 3.6: Dam1 is microtubule dependent for localisation to the kinetochore.

Cells containing Dad1-GFP or Dam1-GFP were grown in rich medium at 27°C prior to incubation at the restrictive temperature or cold shock treatment. The cells were fixed, stained with DAPI and visualised by fluorescence microscopy. GFP is visualised in green and DAPI in blue. **(a&b)** Dad1-GFP *nda3-1828* mutant cells visualised at 27°C, or after 4 hours incubations at 36°C. **(c)** Dam1-GFP visualised in the *nda3-1828* strain at 27°C. **(d)** Visualisation of Dam1-GFP in the *nda3-1828* strain after 4hours at 36°C. **(e)** The Dam1-GFP *nda3-311* strain is shifted down to 20°C for 8 hours prior to fixation and/or cold shock in (f). **(f)** Dam1-GFP *nda3-311* cells subjected to ice/cold shock treatment.. Scale bars represent 10μm.

3.4 Dam1-GFP localisation in mutants affecting microtubule dynamics

The microtubules in early mitosis are extremely dynamic in the fission yeast (Ding et al., 1993; Mallavarapu et al., 1999; Sagolla et al., 2003). Photo-bleaching experiments have demonstrated that there is a more rapid tubulin turnover in microtubules during the early mitotic stages of prometaphase and metaphase compared to anaphase (Mallavarapu et al., 1999). We have shown that Dam1 requires microtubules at this early mitotic stage for its localisation to the kinetochore (Figure 3.6). We therefore next addressed whether the Dam1/DASH complex requires these highly dynamic microtubules to facilitate its deposition to the mitotic kinetochore. We therefore analysed Dam1-GFP localisation in WT and *Δalp14*, *Δdis1* and *Δklp5* backgrounds to ascertain whether Dam1-GFP could still localise to the kinetochore in these mutant strains when microtubule dynamics are affected. Neither the TOG mutants *Δalp14* and *Δdis1* nor the kinesin-13 mutant *Δklp5* showed any loss of Dam1 localisation (Figure 3.7).

3.5 Discussion

In *S. cerevisiae* the Dam1/DASH complex localises to the SPB and kinetochore and decorates the spindle microtubules in mitosis (Cheeseman et al., 2001; Enquist-Newman et al., 2001; Hofmann et al., 1998; Janke et al., 2002; Jones et al., 1999; Li et al., 2002). As mentioned in the introduction to this chapter the Dam1/DASH complex members have been shown to associate to the centromere region by ChIP and to co-localise to the kinetochore along with Ndc10 throughout the cell cycle (Cheeseman et al., 2001; Jones et al., 2001). Within the fission yeast *S. pombe* the microtubules and kinetochores only interact and attach in mitosis, therefore one would expect in this organism that the Dam1/DASH complex would localise to the kinetochore specifically during the mitotic phase to facilitate the microtubule-kinetochore attachments. We C-terminally tagged various Dam1/DASH subunits with GFP and monitored their sub-cellular localisation at various stages of the cell cycle. As we expected Dam1 and other complex members did show a kinetochore localisation only as cells entered into mitosis (Figure 3.2, Figure 3.3). Surprisingly however Dad1, one of the subunits of the Dam1/DASH complex exhibited kinetochore localisation throughout the whole cell cycle (Figure 3.4).

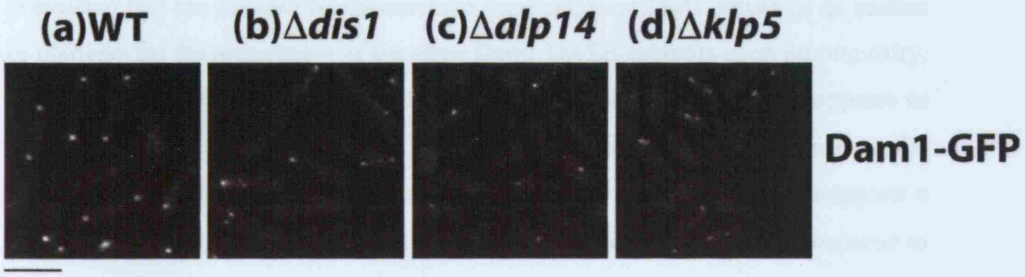

Figure 3.7: Dam1 localisation in mutants that perturb microtubule dynamics

Cells containing Dam1-GFP were grown in rich medium at 27°C, shifted to their respective restrictive temperatures prior to fixation and visualised by fluorescence microscopy. **(a)** WT Dam1-GFP cells at 27°C. **(b)** Δ*dis1* Dam1-GFP cells shifted down to 20°C for 8hrs. **(c)** Δ*alp14* Dam1-GFP cells shifted up to 36°C for 6hrs. **(d)** Δ*klp5* Dam1-GFP cells at 27°C. The scale bar represents 10μm.

This was an intriguing result and seemed to suggest that Dad1 may play an additional important role at the kinetochore perhaps in a structural or functional capacity that is independent of the remaining Dam1/DASH complex members. We postulated that the constitutive kinetochore localisation of Dad1 serves as an anchor or platform for the recruitment of the other Dam1/DASH subunits upon mitotic entry. Our observation that Dam1-GFP localisation is abolished in *Δdad1* cells appears to corroborate this hypothesis. Indeed Dad2 and Ask1 localisation also appears to be lost in *Δdad1* cells according to a recent paper by Liu *et al.* 2005. This suggests a difference in *S. pombe* Dam1/DASH localisation and possible function compared to their *S. cerevisiae* counterparts. The Dad1 protein acts as a dock for the incoming mitotic complex members and possibly other mitotic kinetochore or microtubule regulators to promote proper kinetochore function and to ensure high fidelity chromosome segregation.

In *S. cerevisiae* the Dam1/DASH complex requires an intact core kinetochore structure for localisation. As we have previously discussed the association of Dam1 to the centromere by ChIP is dramatically reduced in an *ndc10-1* background (Jones et al., 2001), and it has also been demonstrated that the localisation of Spc34-GFP and Dad2-GFP to the kinetochore is abolished in *ndc80-1* cells (Janke et al., 2002). This suggests that a core intact kinetochore platform consisting of the CBF3 and the Ndc80 complexes are required for Dam1/DASH localisation in *S. cerevisiae*. We have shown that similarly in the fission yeast a core kinetochore structure is required for Dad1 and thus Dam1/DASH kinetochore loading. We have demonstrated that the Mis6/Sim4 complex is required to anchor Dad1 to the kinetochore (Figure 3.5). Dad1-GFP localisation is abolished from the kinetochore after shift-up to the restrictive temperature in *mal2-1* and *mis6-302* cells. It is worth noting that an interaction between Dad1 and the Mis6/Sim4 complex has been proven by Liu *et al.* 2005. They performed TAP purification using Dad1-TAP and repeatedly could co-purify Dad1 with Mal2, Mis6 and Sim4 of the Mis6/Sim4 complex. In interphase cells only Dad1 forms a complex with the Mis6/Sim4 complex, however the other Dam1/DASH complex members can be co-purified with the Mis6/Sim4 complex during mitosis (Liu et al., 2005). This thus supports our delocalisation data and model that Dad1 is docked to the kinetochore through this core kinetochore Mis6/Sim4 complex. It appears however that Mis12, Nuf2 and Cnp1 are dispensable for this localisation, but we cannot rule out allele specificity, therefore there is a possibility that other mutant alleles of these kinetochore components could result in a loss of Dad1 localisation.

The *S. cerevisiae* Dam1/DASH complex can form closed rings on microtubules and has been shown *in vitro* to possess polymerising and bundling activity (Asbury et al., 2006; Miranda et al., 2005; Westermann et al., 2005; Westermann et al., 2006). It is also known that within the budding yeast this complex requires the mitotic spindle microtubules for loading to the kinetochore (Li et al., 2002). This leads to a tempting model whereby the Dam1/DASH ring complex forms around microtubules and can "surf" into the kinetochore upon the spindle microtubules where it then interacts with core kinetochore components such as the Ndc80 and/or CBF3 complex to enable the attachment of kinetochores to the spindle microtubules. Intriguingly it appears that this microtubule dependency may also occur within the fission yeast for loading of the mitosis-specific subunits to the kinetochore (Figure 3.6), and perturbation of microtubule dynamics appears to have no effect on Dam1/DASH localisation (Figure 3.7). Recently there was another report using cold-shock treatment suggesting that the fission yeast Dam1/DASH complex can bind to the kinetochore in the absence of microtubules (Kobayashi et al., 2007). However they admit that some very short microtubules may still exist in these cells even after ice treatment, which could account for residual Hos2-GFP localisation and therefore cannot rule out the possibility of microtubule dependency. While it is not easy to fully reconcile this result with our own ice-treatment data, we feel strongly that the Dam1/DASH complex requires microtubules for its kinetochore localisation during mitosis. We believe the mitosis-specific Dam1/DASH subunits can interact with microtubules, whether by a ring or some other structural entity, and "surf" in on the incoming microtubule towards the kinetochore. This complex can then anchor the spindle at the kinetochore through interaction with Dad1 and the Mis6/Sim4 complex, thus facilitating proper bipolar attachment and bi-orientation.

Chapter 4

4 Characterisation of Dam1/DASH deletion mutants

Introduction

We have now seen that the conserved Dam1/DASH complex within the fission yeast can localise to the kinetochore during mitosis. The next critical question is what is the function of this complexat the kinetochore during mitosis. To address this we deleted various Dam1/DASH genes and intriguingly found that this complex was not essential in the fission yeast. We will examine the phenotype of these Dam1/DASH deletion mutants to understand the role of this complex during mitosis in the fission yeast. In this chapter we address the deletion of various subunits of the Dam1/DASH complex and demonstrate that this complex, while not essential, plays an important role in ensuring high fidelity chromosome segregation. We show that deletion strains are slightly sensitive to the spindle drug TBZ and show activation of the spindle assembly checkpoint. We show a range of genetic interactions with other kinetochore mutants and mutants of microtubule regulators and assay whether Dad1 may play an additional role in the spindle assembly checkpoint. We demonstrate anaphase spindle defects in fixed Dam1/DASH deletion strains and show spindle collapse in live cells, indicating this complex plays a role in ensuring bipolar spindle and anaphase spindle integrity maintenance in a similar manner to its budding yeast counterparts.

4.1 Deletion of Dam1/DASH subunits in the fission yeast

In order to ascertain if the Dam1/DASH complex is essential within the fission yeast, the genes coding for the various subunits of this complex were deleted using a simple PCR based approach, involving the insertion of a kanamycin resistance gene (Kan^R)

into the gene locus within a diploid strain (Figure 4.1) (Bahler et al., 1998). It was found that deletion of Dam1/DASH complex members was not essential (Carried out by N. Koonrugsa & S. Dhut).

4.1.1 Growth of Dam1/DASH deletions

The Dam1/DASH complex is not essential in the fission yeast. In order to ascertain how deletion mutants of this complex behave we first examined the growth of logarithmically growing Δ*dam1*, Δ*ask1*, and Δ*dad1* cells in rich medium at both 27°C and 36°C and in the presence of a red dye Phloxin B to stain dead or dying cells. These strains did not appear to have difficulty growing in rich medium at either 27°C or 36°C when compared to WT growth kinetics (Figure 4.2A). We then carried out a tenfold serial dilution spot assay of Δ*dam1*, Δ*ask1* and Δ*spc34* to further analyse the growth of Dam1/DASH deletion mutants at 36°C and in the presence of the microtubule destabiliser Thiabendazole (TBZ). This drug is used regularly to assess the presence of mitotic defects. Mutants with mitotic defects may show either a sensitivity or resistance to the drug. We compared the growth on plates of these strains against other mutants of known mitotic regulators, Δ*mad2*, Δ*alp14*, and Δ*klp5*. Mad2 plays a role in the spindle assembly checkpoint; it localises to unattached kinetochores and can induce mitotic arrest until correct attachments are established (Gillett et al., 2004; He et al., 1997; Kim et al., 1998; Pangilinan and Spencer, 1996; Waters et al., 1998). Deletion of *mad2*$^+$ yields cells that are very mildly sensitive to microtubule depolymerisation induced by the addition of TBZ, as these cells cannot arrest to repair the spindle damage (He et al., 1997). Alp14 is a microtubule stabilising protein that belongs to the Dis1/TOG and deletion of the *alp14*$^+$ gene yields cells that are temperature sensitive and very sensitive to TBZ (Garcia et al., 2001). Klp5, a member of the kinesin-8 family, is a microtubule depolymeriser and deletion of the *klp5*$^+$ gene results in hyper stabilised microtubules, which causes cells to become resistant to drugs such as TBZ. Consistent with known results both Δ*mad2* and Δ*alp14* cells show modest sensitivity to TBZ in our spot assay, Δ*alp14* cells show little growth at 36°C and the Δ*klp5* cells appear resistant to TBZ (Figure 4.2B).

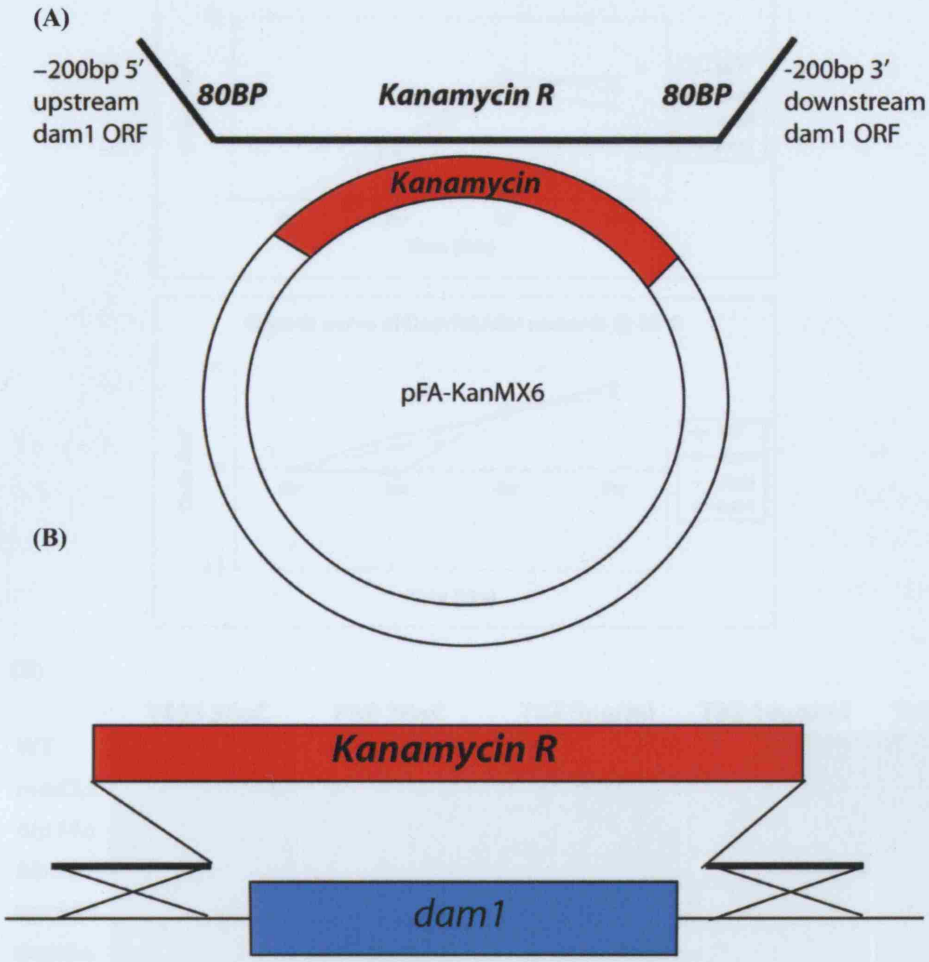

Figure 4.1: Schematic showing gene deletion steps.

(A) The first step of gene deletion involves PCR from a plasmid containing a Kanamycin cassette pFA-KanMX6 (Bahler et al., 1998). The forward oligo for the PCR contains 80bp of the gene sequence approx 200bp upstream of the ORF of gene to be deleted and 20bp from the cassette. The reverse oligo likewise contains 20bp from the cassette and an 80bp sequence approx 200 bp downstream of the ORF of the gene to be deleted. **(B)** The PCR product containing kanamycin is inserted into the gene locus by homologous recombination.

(A)

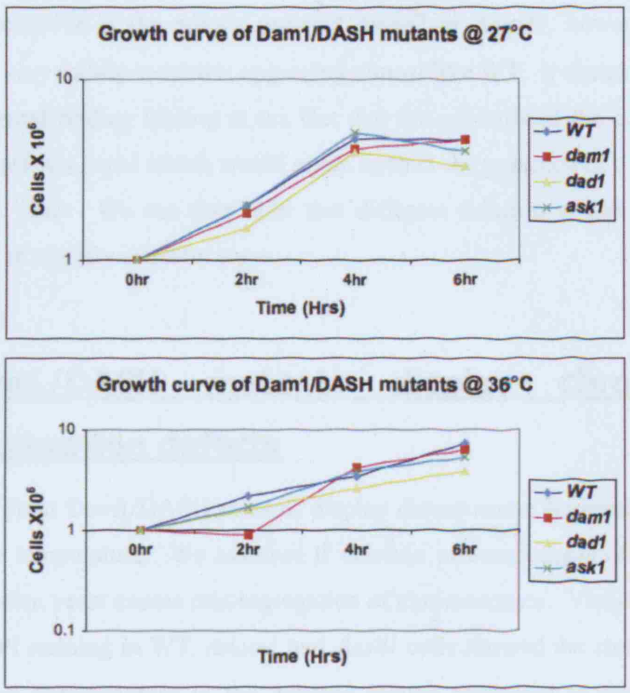

(B)

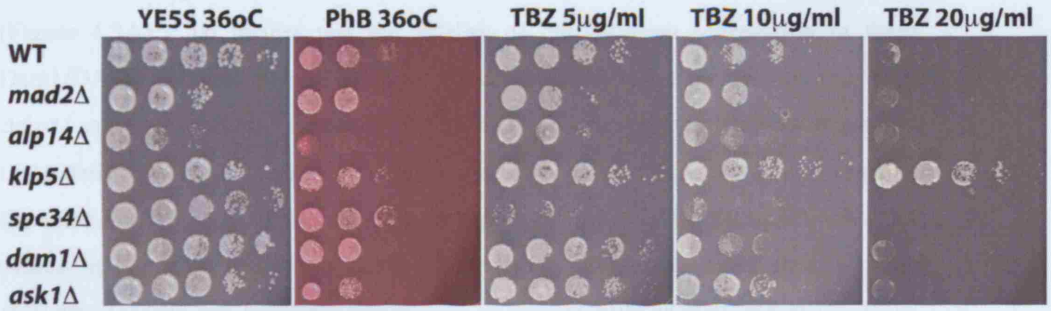

Figure 4.2: Analysis of growth rate of Dam1/DASH deletion mutants.

(A) WT, *dam1Δ, dad1Δ,* and *ask1Δ* cells were cultured in rich medium at 27°C to a log-phase concentration of $1x10^6$ cells/ml. The cultures were split and incubated at either 27°C or 36°C and the cell number was counted every 2 hours. The cell number was plotted against time **(B)** A tenfold serial dilution spot assay with the first spot containing $5x10^4$ cells, plated onto rich agar YE5S, YE5S & Phloxin B, YE5S & TBZ 5μg/ml, 10μg/ml, or 20μg/ml concentrations.

Deletion of the Dam1/DASH genes results in cells that show some sensitivity to TBZ, however this sensitivity is not equal amongst the different Dam1/DASH mutants tested. The Δ*spc34* cells appear strongly affected by the addition of TBZ, the Δ*dam1*

cells are as sensitive as the mitotic mutants *Δmad2* or *Δalp14,* however the *Δask1* strain is only very mildly sensitive, appearing almost like WT. It seems that this may be a fundamental finding hinting at the fact that the subunits of the complex in the fission yeast are not equal which would argue against the presence of a ring complex in the fission yeast. We can thus infer that different subunits within this complex may function in slightly different ways.

4.1.2 Dam1/DASH mutants display chromosome segregation defects

The budding yeast Dam1/DASH mutants display chromosome segregation defects at the restrictive temperature. We assessed if deletion of components of this complex within the fission yeast causes mis-segregation of chromosomes. Visualisation of the DNA by DAPI staining in WT, *Δdam1* and *Δask1* cells showed the clear presence of mis-segregated chromosomes in the deletion strains compared to wild-type. The variable DAPI signals that are evident indicate aberrant DNA separation in these cells (Figure 4.3A). To further test the fidelity of chromosome segregation in these Dam1/DASH deletion mutants we incorporated a linear minichromosome into WT, *Δdam1* and *Δask1* strains (Niwa et al., 1989). This nonessential minichromosome Ch16 derives from the centromeric region of chromosome 3 in *S. pombe* and contains the *ade6-m216* allele. This allele compensates for the *ade6-m210* allele, which is present endogenously in the genome of the WT, *Δdam1* and *Δask1* strains. This minichromosome can be stably maintained in normal cells as they undergo mitosis, however when chromosome segregation defects occur this minichromosome will be lost and these cells can be observed as red auxotrophs on adenine- medium. The Dam1/DASH deletion strains *Δdam1* and *Δask1* clearly show the presence of red and sectored colonies in this plate assay (Figure 4.3B&C). The percentage of plasmid loss was calculated by counting the number of red sectored cells, to be 0.3% for WT, 7.8% for *Δdam1* and 5.3% for *Δask1* (Figure 4.3B&C). The Dam1/DASH deletion cells therefore have obvious defects in chromosome segregation during mitosis.

(A)

(B)

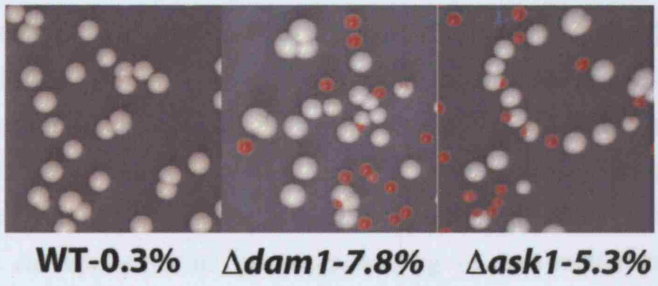

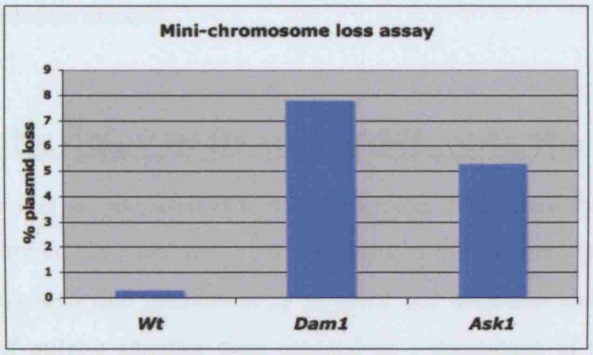

Figure 4.3: Dam1/DASH deletion mutants result in chromosome mis-segregation.

(A) WT, *Δdam1* and *Δask1* cells were shifted to 36°C for 4 hours, fixed and the DNA visualised by fluorescence microscopy. DAPI in red and Bright field in blue. The scale bar represents 10μm. **(B)** WT, *Δdam1* and *Δask1* strains containing a minichromosome were grown on selective medium to retain the mini-chromosome and then plated onto rich medium and incubated at 30°C for 4 days. Colonies that show sectored adenine auxotrophs indicate a loss of the mini-chromosome and are counted. **(C)** Graph of the percentage of plasmid loss from (B) N=1000.

4.2 Dam1/DASH mutants and the spindle assembly checkpoint

Mutants that give rise to spindle or attachment dysfunction in mitosis often cause a prolonged mitotic delay. Errors in microtubule attachment to the kinetochore, or disruption of spindle formation which leads to kinetochores becoming unattached, activates the spindle assembly checkpoint. This checkpoint causes a metaphase arrest by the activation of a signalling cascade that results in inhibition of the APC/C through binding of its activator protein Slp1/CDC20 (Chan and Yen, 2003; Chen et al., 1998; Fang, 2002; He et al., 1997; Millband and Hardwick, 2002). The checkpoint cascade involves localisation of the checkpoint proteins to the kinetochore and results in mitotic delay. We wished to investigate if there is a noticeable mitotic delay in our Dam1/DASH deletion mutants and whether this delay is dependent on the spindle checkpoint to aid our understanding of the mitotic phenotype of Dam1/DASH deletion mutants.

4.2.1 Mitotic delay in Dam1/DASH mutants.

To assess if there is an increased frequency of mitotic cells when the Dam1/DASH complex is perturbed we counted the mitotic index in WT, *Δdam1* and *Δdad1* cells. Cells were cultured in rich medium at 27°C, fixed and α-tubulin and DNA stained. The numbers of mitotic spindles were counted as a percentage of total cells. The stages of the spindles were assigned by subdividing the total number of spindles according to length, into short prometaphase /metaphase like spindles of <2μm in length, and longer anaphase like spindles of >2μm. The incidence of mitotic cells are slightly increased in both *Δdam1* and *Δdad1* strains, particularly cells possessing spindles of <2μm (Figure 4.4A). This infers that the increase in the mitotic index is probably due to accumulation of metaphase cells and is likely to be mediated by the spindle assembly checkpoint. To assess whether this delay is dependent on the spindle checkpoint we counted the mitotic index in *Δdad1* and *Δdam1* cells in which the spindle checkpoint components *mad2*$^+$ or *bub1*$^+$ have been deleted, which results in cells that cannot delay mitosis even in the presence of spindle damage or when kinetochore attachments have not been established (Rieder et al., 1994; Waters et al., 1998).

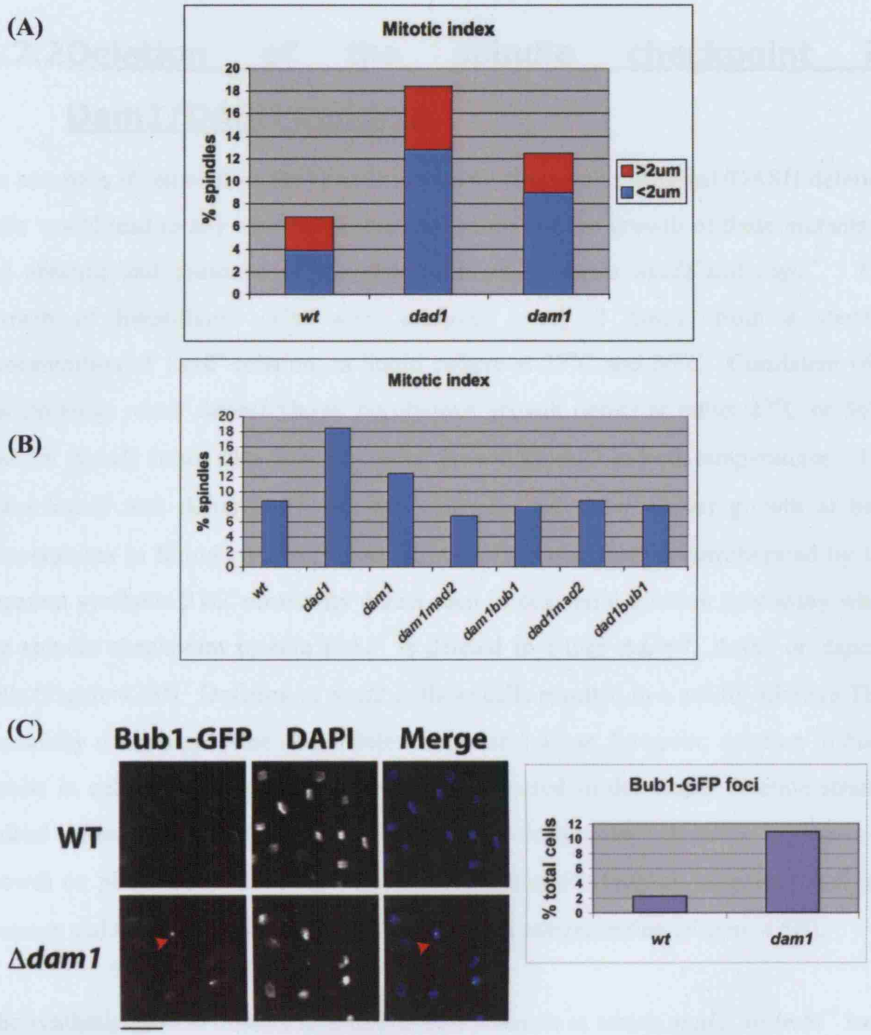

Figure 4.4: Spindle checkpoint induced mitotic delay in Dam1/DASH mutants.

(A&B) Graph showing the percentage of mitotic cells counted in WT, *Δdad1*, *Δdam1*, *Δdad1mad2*, *Δdad1bub1*, *Δdam1mad2* and *Δdam1bub1* cells. Cells were cultured at 27°C, fixed and immunoflourescence microscopy to visualise microtubules and DNA was carried out. N > 200 cells. **(C)** Quantification of frequency of Bub1-GFP in WT and *Δdam1* cells. Cells were cultured in rich medium at 27°C, fixed, stained with DAPI and viewed by fluorescence microscopy. The scale bar represent 10μm. Red Arrowhead highlights Bub1-GFP foci. N > 200 cells.

4.2.2 Deletion of the spindle checkpoint in Dam1/DASH mutants.

To ascertain if removal of the spindle assembly checkpoint in Dam1/DASH deletion cells would lead to any additive defects, we examined the growth of these mutants in the absence and presence of the checkpoint components *mad2*$^+$and *bub1*$^+$. The growth of logarithmic cells were analysed every 2 hours, from a starting concentration of 1x10^6 cells/ml, in liquid culture at 27°C and 36°C. Consistent with our previous result *Δdam1* shows no obvious growth defect at either 27°C or 36°C and the *Δmad2* strain also showed normal growth kinetics at both temperatures. The *Δdam1mad2* and *Δdam1bub1* mutants however, did show slower growth at both temperatures in liquid culture (Figure 4.5A). This was further corroborated by the apparent synthetic TBZ sensitivity defect seen in our serial dilution spot assay when the spindle checkpoint protein *bub1*$^+$ is deleted in either *Δdam1, Δask1* or *Δspc34* cells (Figure 4.5B). Deletion of *mad2* in these cells resulted in a mildly additive TBZ sensitivity compared to the single deletion mutants alone, however, deletion of *bub1* results in cells that are extremely sensitive compared to the single deletion strains. Indeed *Δdam1bub1, Δask1bub1* and *Δspc34bub1* cells show very little to almost no growth on plates containing TBZ at a concentration of 10μg/ml, whereas the single mutants and wild-type cells are not affected at this concentration (Figure 4.5B).

The synthetic growth defects in Dam1/DASH mutants in which *mad2*$^+$ or *bub1*$^+$ have been removed suggests that these cells require the spindle assembly checkpoint to delay mitotic progression, thus providing the cells sufficient time to correct any errors in mitosis. Therefore one can postulate that removal of the spindle assembly checkpoint in Dam1/DASH mutants should lead to an increase in the frequency of mis-segregated chromosomes. Indeed this appears to be the case, a result published by Sanchez Perez *et al.* 2005 shows that the frequency of aberrant mitoses is doubled in *Δdam1mad2* and *Δdam1bub1* compared to the single *Δdam1* mutant. It is plausible therefore that the spindle assembly checkpoint is required when Dam1/DASH function is compromised to give the cells sufficient time to correct errors in mitosis and thus enable a proportion of cells to undergo high fidelity chromosome segregation.

(A)

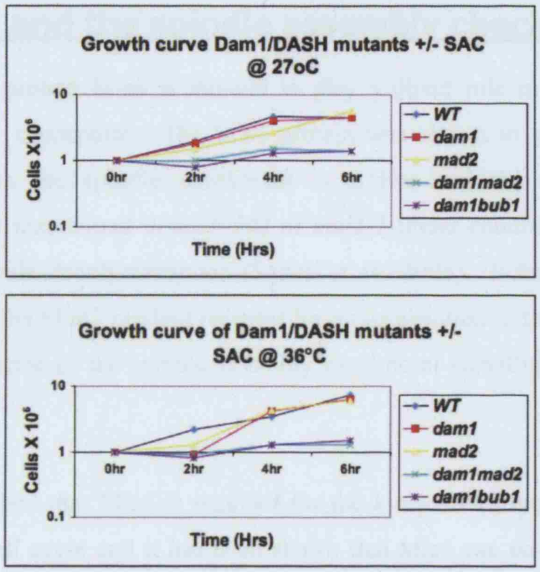

(B)

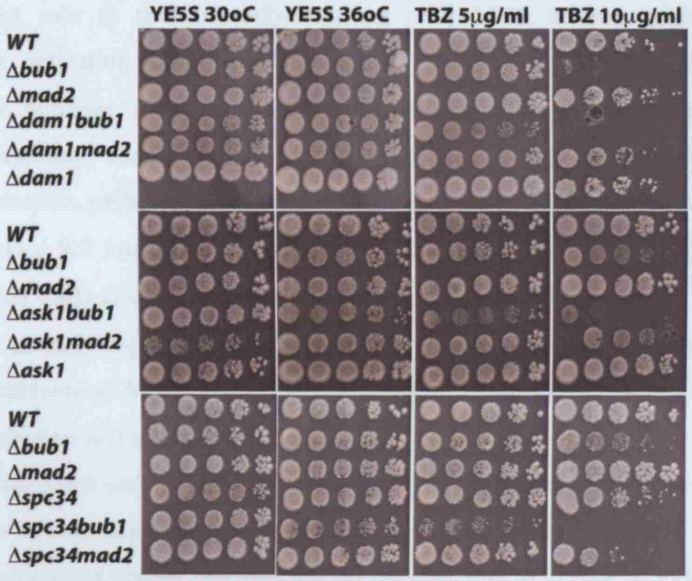

Figure 4.5: Synthetic growth defects when spindle checkpoint is removed.

(A) WT, *dam1Δ, mad2Δ, Δdam1bub1* and *dam1mad2Δ* cells were cultured in rich medium at 27°C to a concentration of $1x10^6$ cells/ml. Cultures were split, incubated at either 27°C or 36°C and the cell number counted every 2 hours and plotted against time **(B)** Serial dilution growth assay of Dam1/DASH, spindle checkpoint deletion mutants, and double mutants on YE5S plates at 30°C or 36°C and in the presence of TBZ 5μg/ml or 10μg/ml at 30°C.

4.2.3 Dad1 and the spindle assembly checkpoint

The kinetochore protein Mis6 is thought to play a direct role in activation of the spindle assembly checkpoint. The Mis6 protein was shown to physically interact with Mad2 when the spindle checkpoint is active, and the spindle assembly checkpoint is not maintained in *mis6-302* or *mal2-1* under conditions of CBZ drug induced microtubule depolymerisation (Saitoh et al., 2005). It has been postulated that Mis6 acts as the Mad2 binding receptor for its localisation to the kinetochore and subsequent activation of the spindle assembly checkpoint-signalling cascade (Saitoh et al., 2005).

We have established that Mis6 is required for the kinetochore localisation of Dad1 throughout the cell cycle and it has been shown that Mis6 can co-purify with Dad1 (Liu et al., 2005). We pondered whether Dad1 might have a Dam1/DASH complex independent role at the kinetochore along with Mis6 in maintaining spindle checkpoint activation. We have shown that *Δdad1* cells activate the spindle checkpoint, however, under certain conditions where prolonged maintenance of the spindle assembly checkpoint is required such as drug induced microtubule depolymerisation, perhaps *Δdad1* cells are unable to maintain this arrest. To address this we treated WT and *Δdad1* cells at 27°C with 11mM HU (Hydroxyurea) for four hours, which stalls DNA replication through inhibition of Ribonucleotide Reductase, leading to an early S-phase arrest. Then after washout, we re-suspended the cells in medium containing MBC/CBZ (Carbendazim) at 50μg/ml, causing microtubule depolymerisation and mitotic arrest. Cells were harvested every hour for five hours, stained with DAPI and calcoflour to visualise DNA and septa respectively, and the percentage of cells displaying hypercondensed or "cut" DNA (cells that form septa without undergoing proper chromosome segregation due to bypass of mitotic arrest) were calculated at each time point as a measure of the maintenance of mitotic arrest in these cells. If Dad1 plays a role in maintenance of the spindle assembly checkpoint under these conditions we would expect the *Δdad1* cells to show a peak of hypercondensed and "cut" cells earlier than the wild-type peak, however, our results show that the checkpoint arrest is maintained in *Δdad1* cells for as long as it is in wild-type cells. Furthermore the timing of septation was delayed in *Δdad1* cells, consistent with our previous data that the spindle assembly checkpoint is activated in Dam1/DASH deletion mutants (Figure 4.6). We can therefore conclude that Dad1 does not function with Mis6 in spindle assembly checkpoint maintenance.

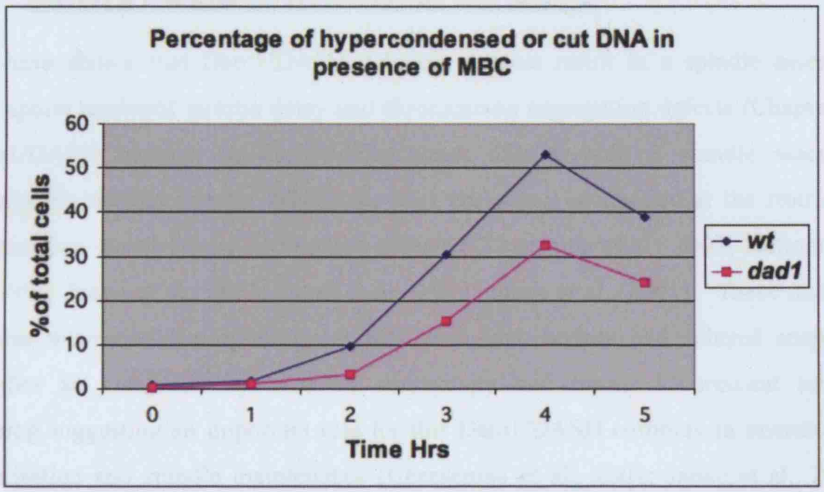

Figure 4.6: Dad1 does not play a role in spindle assembly checkpoint maintenance.

WT and *Δdad1* exponentially growing cells were cultured in rich medium at 27°C and arrested in S-phase by the addition of 11mM HU for 4 hours. Cells were filtered, washed and re-suspended in medium containing 50μg/ml MBC/CBZ to arrest the cells in M-phase. Cells were harvested every hour for 5 hours after MBC/CBZ addition, stained with DAPI and calcoflour to visualise DNA and septa and visualised by fluorescence microscopy. The percentage of cells displaying hypercondensed and "cut" DNA were counted at each time-point and plotted against time.

4.3 Non-disjunction phenotype of fixed Dam1/DASH mutants at 20°C

We have shown that Dam1/DASH deletion mutants result in a spindle assembly checkpoint mediated mitotic delay and chromosome segregation defects (Chapter 4). Dam1/DASH mutants in the budding yeast display both a spindle assembly checkpoint induced mitotic delay and, after prolonged incubation at the restrictive temperature, chromosome segregation defects (Cheeseman et al., 2001; Hofmann et al., 1998; Janke et al., 2002; Jones et al., 1999; Jones et al., 2001). These mutants possess microtubule morphology defects with bent, broken and splayed anaphase spindles as visualised by electron microscopy and immunoflourescent tubulin staining suggesting an important role for this Dam1/DASH complex in microtubule stabilisation and spindle maintenance (Cheeseman et al., 2001; Janke et al., 2002; Jones et al., 1999; Jones et al., 2001). We were interested in whether the Dam1/DASH complex in *S. pombe* also plays a role in microtubule stabilisation and spindle integrity maintenance during mitosis. We already possess some tantalising hints that this complex may have such a role in the fission yeast, with deletion of various components results in sensitivity to the spindle drug TBZ (Figure 4.2). We had not, however, carefully analysed the microtubule morphology in the Dam1/DASH deletion mutants. We therefore wished to focus on whether there were obvious spindle microtubule defects in these cells to thus uncover a role for this complex in the regulation of spindle integrity.

4.3.1 Dam1/DASH deletion results in broken spindles and chromosome mis-segregation at 20°C

To ascertain if the Dam1/DASH complex in fission yeast functions in maintaining mitotic spindle integrity, we first examined microtubule morphology and DNA segregation in asynchronous fixed *Δdam1* and *Δdad1* cells at both 20°C and 36°C. The cells were cultured in rich medium overnight and shifted to either 20°C for 8 hours or 36°C for 4 hours prior to fixation and immunoflourescent staining of microtubules and DNA. The mitotic index and frequency of mis-segregated

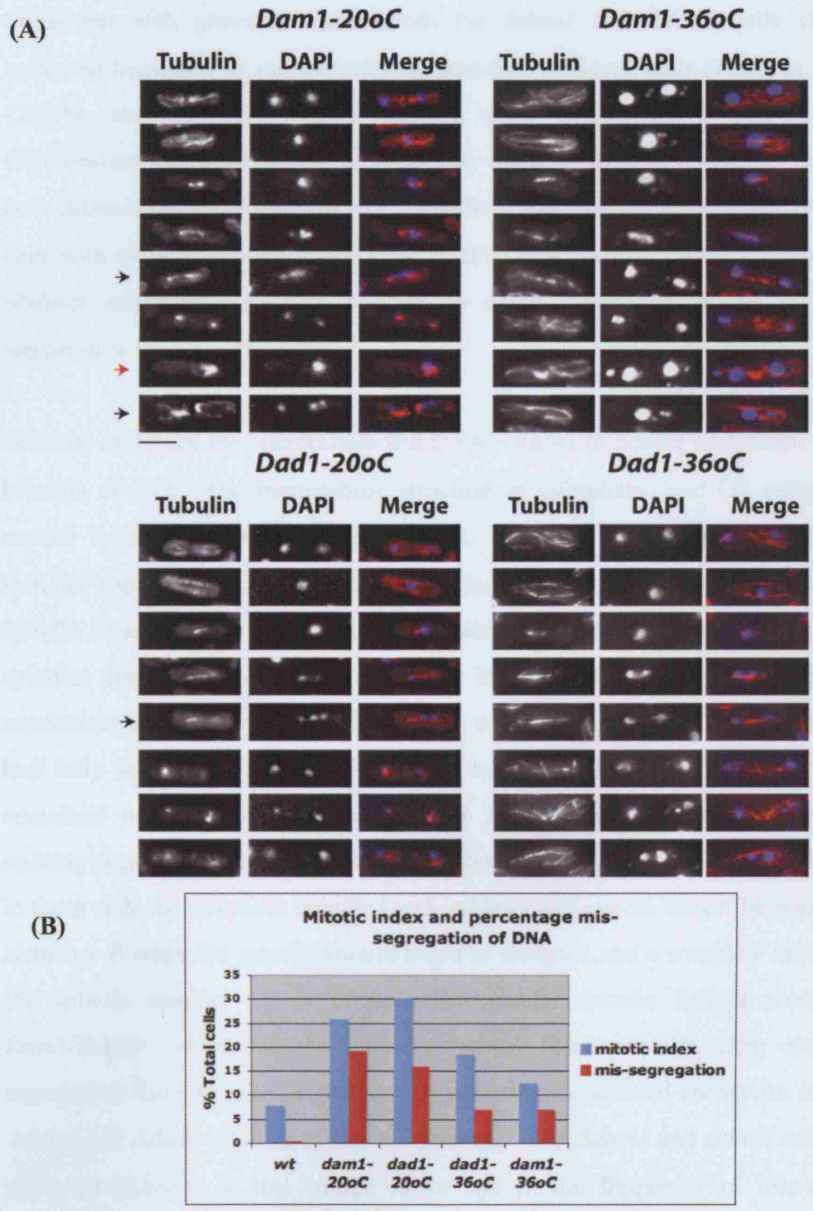

Figure 4.7: Non-disjunction phenotype of Dam1/DASH mutants at 20°C

(A) *Δdam1* and *Δdad1* cells were cultured in rich medium at 20°C for 8 hours, or 36°C for 4 hours, fixed and immunoflourescent microscopy of microtubules and DNA carried out. The scale bar represents 10 μm. The black arrowhead highlights lagging chromosomes. The red arrowhead represents mono-polar defects. **(B)** Graph of the mitotic mis-segregation indexes counted from cells in (A). WT is included as a control. N>200 cells.

chromosomes were counted for both strains at both 20°C and 36°C (Figure 4.7A&B). Consistent with previous results both the *Δdam1* and *Δdad1* cells showed an increased frequency of mitotic cells compared to wild-type cells (7.8%) at 36°C with 12.49% and 18.45% percent mitotic cells respectively (Figure 4.7A&B). Chromosome segregation defects were also apparent by DAPI staining the DNA in both *Δdam1* and *Δdad1* cells at 36°C, with both strains showing approximately 7% of cells with mis-segregated nuclear material (Figure 4.7A&B). However there were no obvious microtubule defects detected in either *Δdam1* or *Δdad1* cells at this temperature (Figure 4.7A&B)

We then examined the microtubule and DNA staining in *Δdam1* and *Δdad1* cells after 8 hours at 20°C. The microtubule structure in interphase, and G2 cells appeared normal in both *Δdam1* and *Δdad1* cells, however, the prometaphase/metaphase spindles appeared elongated in these cells and as cells proceeded into late mitosis the spindle structure no longer looked completely normal or intact with anaphase like spindles displaying weak tubulin staining in the middle of the spindle, giving the appearance that they were starting to break down (Figure 4.7A). Moreover cells that had fully segregated their DNA content to opposite poles of the cell no longer contained normal elongated anaphase B type spindles, instead distinct tubulin staining regions at one or both poles were detected (Figure 4.7A). This indicates that in these cells the anaphase spindle loses integrity and can no longer be maintained in anaphase B when the spindle should begin to elongate, and a complete breakdown of the spindle ensues. It is of note that similar spindle defects were seen in Dam1/DASH mutants in the budding yeast. There are also clear chromosome segregation defects and the presence of persistent condensed chromatin in both the *Δdam1* and *Δdad1* mutants at this temperature. The *Δdam1* and *Δdad1* cells at 20°C show an increase in the mitotic index and in the frequency of mis-segregated chromosomes that is much higher even than *Δdam1* and *Δdad1* cells at 36°C (Figure 4.7B). Indeed some cells show the entire DNA, as represented by DAPI staining, segregating completely to one side of the cell (Figure 4.7A Top). This broken spindle phenotype and presence of condensed and sometimes mono-segregated DNA suggests that these cells are displaying a non-disjunction "*dis*" phenotype at 20°C. Mutants that display a "*dis*" (defective in sister-chromatid disjoining) phenotype classically show hyper-condensed, un-separated sister-chromatids with activation of the spindle assembly checkpoint and elongation of the mitotic spindle despite high Cdc2 kinase activity and without chromosome segregation (Nabeshima et al., 1995;

Nabeshima et al., 1998; Ohkura et al., 1988). These elongated spindles may then proceed to collapse and break.

There are three genes that when deleted or mutated show the "*dis*" phenotype *dis1*$^+$, *dis2*$^+$ and *dis3*$^+$. The Dis1 protein is a member of the TOG family in fission yeast and is a kinetochore binding microtubule-associated protein. Dis2 encodes a type I protein phosphatase that has been implicated in mitotic exit and Dis3 is a large 110 kDa protein that contains an RNAse II (RNB) domain but is thought to function at the kinetochore and in the maintenance of heterochromatin silencing (Murakami et al., 2007). It is thought that the abnormal spindle elongation in these mutants occurs due to the disruption of force balance in these "*dis*" mutant cells (Nabeshima et al., 1998). The normal attachment of kinetochores to spindle microtubules may be defective in these mutants, and it is this interaction that restrains the metaphase spindle length in normal cells. The force created when the kinetochores are pulled towards the poles, which also pull the two poles towards each other, may offset other microtubule-based forces that work to push the opposite poles apart. In these mutants this force balance is disordered resulting in the abnormal elongation of prophase spindles despite the lack of sister-chromatid separation (Nabeshima et al., 1998). It is possible that in these Dam1/DASH deletion mutants this force balance is also disrupted resulting in the spindle breakage phenotype seen in these cells. We know that Dam1/DASH deletion mutants are synthetically lethal when Dis1 is deleted and that this complex and Dis1 must therefore play an essential overlapping role in the cell, perhaps this role is in proper bipolar spindle formation and the establishment of end on attachment to the kinetochores and subsequent bi-orientation of sister kinetochores.

4.3.2 Analysis of *cen2*-GFP sister-chromatid separation in fixed *Δdam1* cells.

To further characterise the defective mitotic chromosome segregation phenotype in Dam1/DASH deletion mutants at 20°C we constructed wild-type and *Δdam1* strains with centromere 2 tagged with GFP (*cen2*-GFP) in order to carefully visualise sister-chromatid separation in these cells. In this *cen2*-GFP system a LacO array is integrated approximately 5 kB from centromere two and is bound by a GFP-LacI fusion protein which is expressed from the *his7*$^+$ locus. We then examined the separation pattern of *cen2*-GFP in asynchronous fixed WT cells at 27°C and asynchronous fixed *Δdam1* cells at 20°C, 27°C or 36°C on the Zeiss Axioplan

(A)

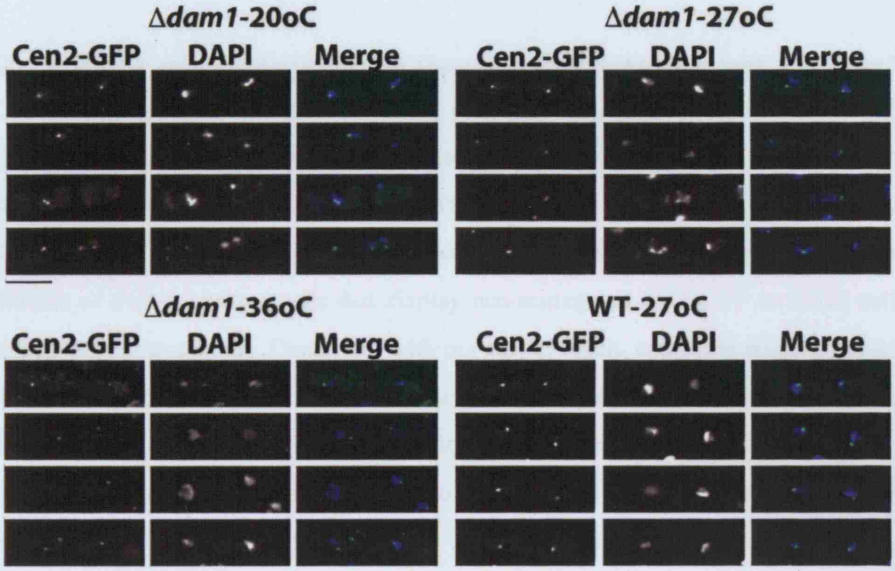

(B)

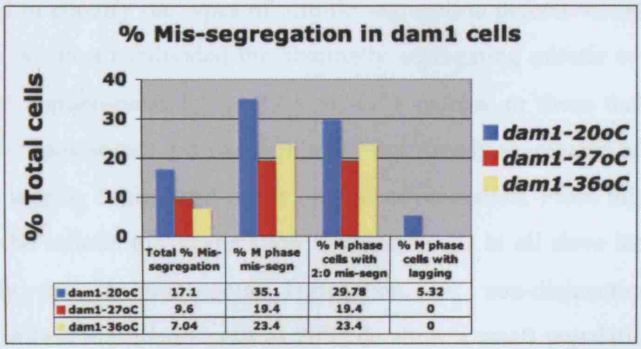

	Total % Mis-segregation	% M phase mis-segn	% M phase cells with 2:0 mis-segn	% M phase cells with lagging
dam1-20oC	17.1	35.1	29.78	5.32
dam1-27oC	9.6	19.4	19.4	0
dam1-36oC	7.04	23.4	23.4	0

Figure 4.8: Mono-polar segregation of sister-chromatids occurs in *Δdam1* cells

(A) WT and *Δdam1* cells containing *cen2*-GFP were cultured overnight in rich medium at 27°C. The *Δdam1* culture was split and incubated at either 27°C for 4 hours, 20°C for 8 hours or 36°C for 4 hours prior to formaldehyde fixation. The wild-type culture was fixed at 27°C. The cells were stained with DAPI and viewed by fluorescence microscopy. The scale bar represents 10 μm. **(B)** The percentage of total cells with mis-segregation and mitotic cells showing mis-segregation were counted and graphed for *Δdam1* cells at all three temperatures. The types of mitotic mis-segregation were further classified as mono-polar cells, i.e. cells with a 2:0 or 1:0 *cen2* separation pattern, or lagging cells and the frequencies of each graphed. N> 200 cells.

fluorescence microscope to determine whether deletion of *dam1*$^{+}$ results in a chromosome non-disjunction phenotype as in the "*dis*" mutants.

The wild-type cells displayed normal sister-chromatid separation with a 1:1 *cen2*-GFP segregation pattern at 27°C (Figure 4.8A). There is a population of mitotic cells in the *Δdam1* strain however, which do not undergo normal *cen2*-GFP separation. In these cells a mono-polar 1:0 or 2:0 *cen2*-GFP segregation pattern is evident at 20°C, 27°C or 36°C (Figure 4.8A). We quantified the total number of *Δdam1* cells and the number of mitotic *Δdam1* cells that display mis-segregated cen2-GFP or DAPI cells at all three temperatures. Consistent with our earlier result, analysing fixed α-tubulin stained *Δdam1* cells (Figure 4.7), we again saw a dramatic increase in the frequency of mis-segregation in both the total population of cells and mitotic cells when *Δdam1* cells are incubated at 20°C as compared to incubation at either 27°C or 36°C (Figure 4.8B).

We attempted to classify the types of mitotic segregation defects visualised in these *Δdam1* cells. We thus subdivided the aberrantly segregating mitotic cells into those that displayed a mono-polar 1:0 or 2:0 *cen2*-GFP pattern, or those that appeared to have lagging chromosomes, i.e. one *cen2*-GFP dot already segregated at the pole and one that was lagging behind and in the process of separation. From this analysis we can see that the mitotic mis-segregation in *Δdam1* cells at all three temperatures is predominantly due to mono-polar segregation, i.e. non-disjunction of sister-chromatids. Albeit the *Δdam1* cells at 20°C do show a small population of lagging chromosomes, which are never seen when incubated at either 27°C or 36°C.

We conclude from our analysis of cen2-GFP in fixed cells that deletion of Dam1 and most probably the other Dam1/DASH components results in mono-polar non-disjunction of sister-chromatids with a phenotype reminiscent of the "*dis*" mutants. We postulate that in a similar manner to "*dis*" mutants deletions of the Dam1/DASH complex are not able to maintain proper kinetochore-microtubule-pole interactions causing a force imbalance, which leads to premature spindle elongation and breakage and non-disjunction of sister-chromatids.

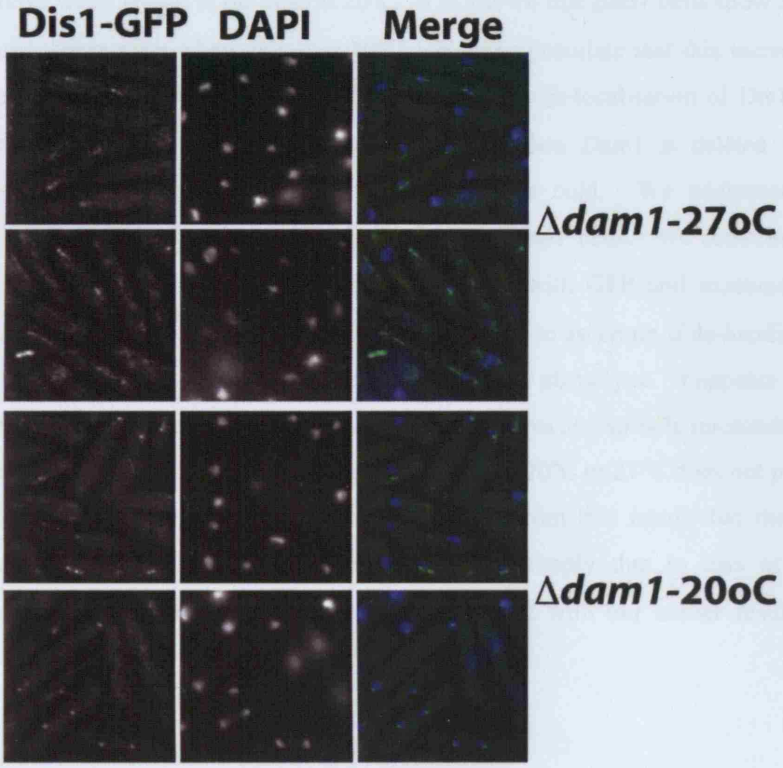

Figure 4.9: Dis1-GFP can still localise in *Δdam1* cells at 20°C or 27°C

Δdam1 cells containing Dis1-GFP were cultured in rich medium overnight. The cultures were split and incubated at either 27°C for 4 hours or 20°C for 8 hours. The cells were then fixed, stained with DAPI and visualised by fluorescence microscopy. The scale bar represents 10 μm.

4.3.3 Dis1-GFP localisation in *Δdam1* cells.

From our analysis it appears that *Δdam1* cells show an increased frequency of mitotic aberrations when grown in the cold at 20°C. It is known that *Δdis1* cells show a non-disjunction phenotype when grown at 20°C. We thus postulate that this increase in mitotic "*dis*" defects in *Δdam1* cells at 20°C is due to de-localisation of Dis1-GFP from the kinetochore and/or spindle microtubules when Dam1 is deleted which renders the cells more susceptible to growth in the cold. We addressed this possibility by examining Dis1-GFP localisation in *Δdam1* cells. We constructed a *Δdam1* strain in which Dis1 is C-terminally tagged with GFP and examined the localisation of Dis1 in this strain at both 20°C and 27°C to ascertain if de-localisation of Dis1 in these cells is the cause of the non-disjunction phenotype. It appears in our hands that Dis1-GFP can still localise to both kinetochores and spindle microtubules despite the deletion of *dam1*$^+$, and that growth at either 20°C or 27°C does not perturb this localisation (Figure 4.9). We would conclude from this result that the non-disjunction phenotype seen in *Δdam1* cells is not simply due to loss of Dis1 localisation in these cells. Moreover this is consistent with our earlier result that Dam1/DASH mutants are synthetically lethal with *Δdis1*.

4.4 Analysis of *Cen2*-GFP sister chromatid separation in live cells

We wished to more carefully examine the non-disjunction and spindle breakage phenotype in *Δdam1* cells to gain a further insight into the roles of this protein in spindle formation and kinetochore-microtubule interactions. We carried out live imaging of *cen2*-GFP and Sad1-dsRed (a constitutive SPB component) separation in both wild-type and in *Δdam1* mitotic cells using the Deltavision fluorescent inverted microscope. Images were taken at room temperature (approximately 20-22°C) using 8 Z-stacks (200nm steps) every 30 seconds for each channel, compressed into a projection for each time-point, deconvolved and the channels for each time-point were merged to produce a series of time-lapse images showing clearly the segregation pattern of the two sister-chromatids of chromosome 2. Filming (Timepoint 0:00) started at prometaphase/metaphase when the two Sad1-dsRed signals indicative of the two SPBs had separated and was continued until after the sister-chromatids had segregated and anaphase B spindle elongation was carried out. In the case of *Δdam1*

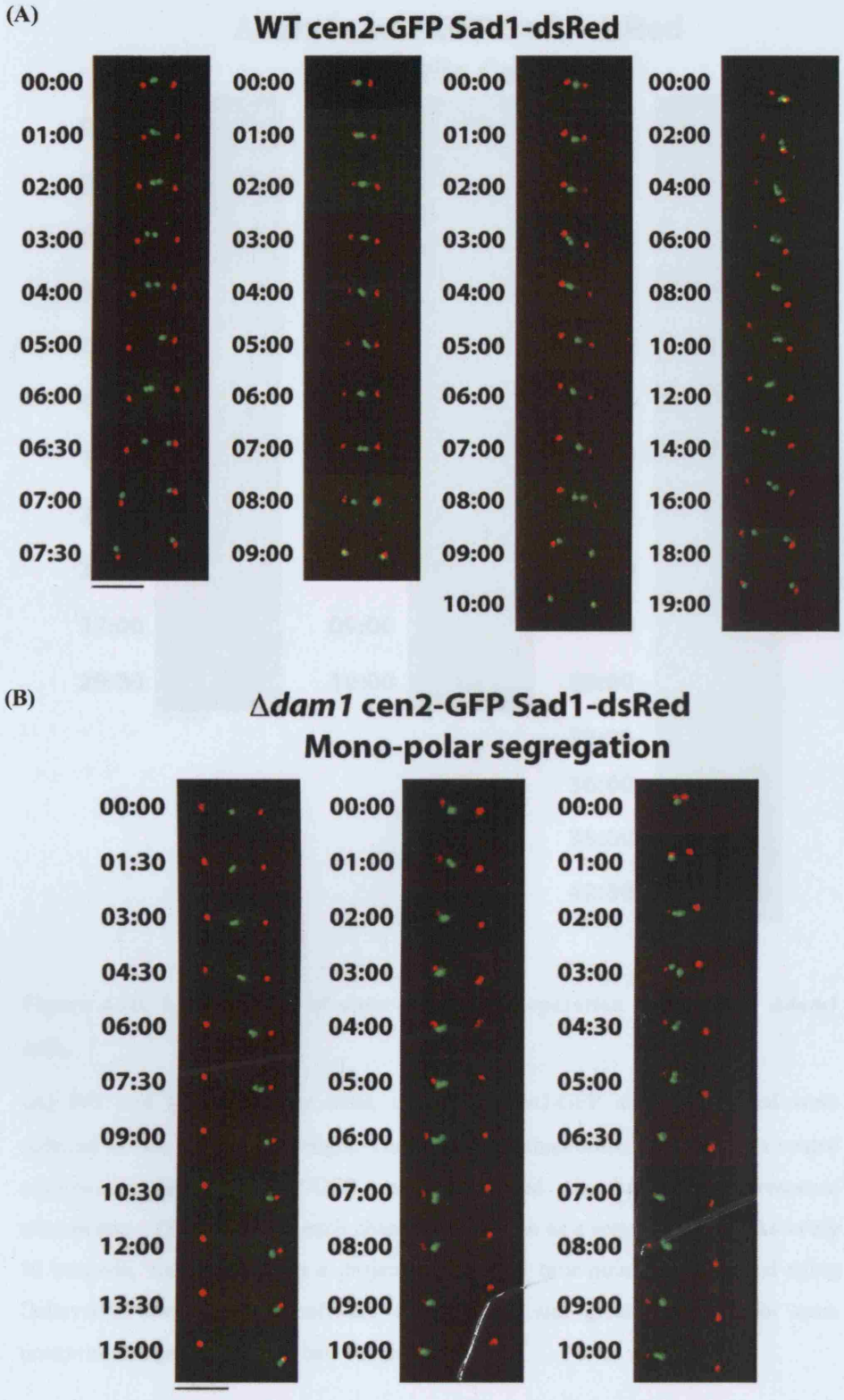
(A)
WT cen2-GFP Sad1-dsRed
00:00
01:00
02:00
03:00
04:00
05:00
06:00
06:30
07:00
07:30
00:00
01:00
02:00
03:00
04:00
05:00
06:00
07:00
08:00
09:00
00:00
01:00
02:00
03:00
04:00
05:00
06:00
07:00
08:00
09:00
10:00
00:00
02:00
04:00
06:00
08:00
10:00
12:00
14:00
16:00
18:00
19:00
(B)
Δdam1 cen2-GFP Sad1-dsRed
Mono-polar segregation
00:00
01:30
03:00
04:30
06:00
07:30
09:00
10:30
12:00
13:30
15:00
00:00
01:00
02:00
03:00
04:00
05:00
06:00
07:00
08:00
09:00
10:00
00:00
01:00
02:00
03:00
04:30
05:00
06:30
07:00
08:00
09:00
10:00

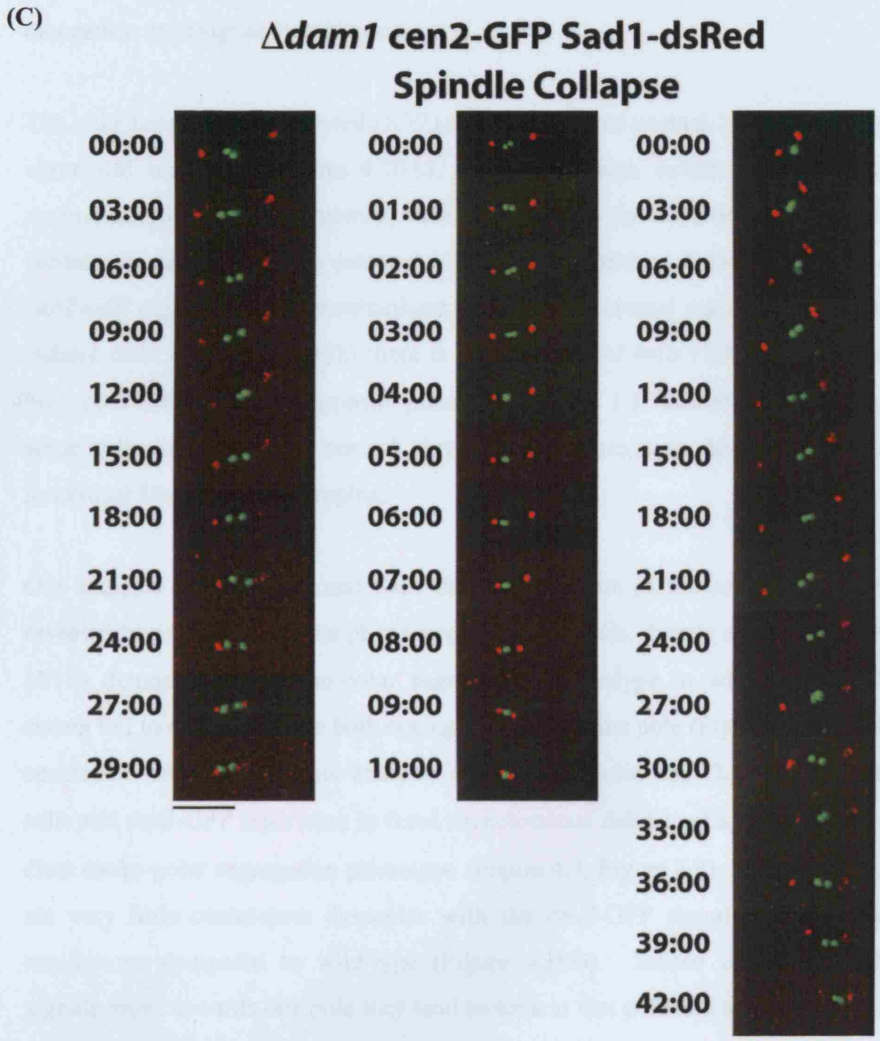

Figure 4.10: Live analysis of sister-chromatid separation in WT and *Δdam1* cells.

(A) WT and **(B&C)** *Δdam1* cells, containing *cen2*-GFP and Sad1-dsRed were cultured in rich medium overnight. The cells were immobilised onto a lectin coated microscopy dish and *cen2*-GFP and Sad1-dsRed visualised by fluorescence microscopy. The images for each channel were taken as a series of 8 Z-stacks every 30 seconds, compressed into a projection for each time-point, deconvolved using Deltavision deconvolution software and the red and green channels for each timepoint merged. The scale bars represent 10μm.

cells filming continued for approximately 30-60 minutes after anaphase B spindle elongation until signal bleaching occurred.

The wild-type cells as expected (N=7) all demonstrated normal 1:1 *cen2*-GFP sister-chromatid separation (Figure 4.10A), with no obvious defects or delay. Indeed normal sister-chromatid dynamics were visualised in the wild-type cells as obvious centromere oscillations was detected with some oscillations in the movements of the *cen2*-GFP signals across the metaphase plate prior to normal segregation. Within the *Δdam1* cells examined (N=18) there is a population of cells (10/18) that segregated both *cen2*-GFP sisters to opposite poles in a normal 1:1 fashion demonstrating that some cells can carry out normal chromosome segregation despite the lack of a functional Dam1/DASH complex.

Our analysis of *cen2*-GFP and Sad1-dsRed separation in the remaining eight cells revealed two distinct aberrant phenotypes in *Δdam1*cells. Firstly a population of cells (4/18) demonstrate a mono-polar segregation phenotype in which the *cen2*-GFP sisters fail to disjoin and are both segregated to the same pole (Figure 4.10B). This is consistent with our previous analysis of both α-tubulin and DAPI stained *Δdam1* cells and *cen2*-GFP separation in fixed asynchronous *Δdam1* cells, in which we saw a clear mono-polar segregation phenotype (Figure 4.7, Figure 4.8). In these cells there are very little centromere dynamics with the *cen2*-GFP signals showing reduced oscillations compared to wild-type (Figure 4.10B). Indeed once the *cen2*-GFP signals move towards one pole they tend to stick at that pole and no further *cen2*-GFP oscillations are detected, even if filming continues up to one hour past this point (Figure 4.10B, data not shown). Perhaps this lack of centromere oscillations and mono-polar segregation is demonstrative of the failure in these cells, in which the Dam1/DASH complex is non-functional, of proper bi-polar attachment of the kinetochores to the spindle and the subsequent establishment of tension and bi-orientation.

The second aberrant mitotic phenotype observed in these *Δdam1* cells is what we have termed a "spindle collapse" phenotype. In this population of *Δdam1* cells (4/18) the two SPBs are able to separate and mitotic onset can occur with the *cen2*-GFP sisters again showing little centromere oscillations compared to wild-type cells. In these cells instead of *cen2*-GFP segregation in a mono-polar fashion as in some *Δdam1* cells, or to opposite poles as in wild-type cells, there is no separation of the

cen2-GFP signals and theSad1-dsRed marked SPBs start to converge and come back closer together until there is a total spindle collapse (Figure 4.10C). One could postulate in the live *Δdam1* cells that there is a failure in the microtubule based forces that act to push the two poles apart resulting in a breakage or collapse of the pole-pole microtubules, which thus allows the two SPBs to converge and prevents the sister-chromatids from undergoing segregation. This defect probably stems again from disruption of the force balance, between the forces pulling the kinetochores towards the poles, which also pull the poles closer together, and the microtubule regulated forces, which push the poles apart. Albeit this disruption of force balance resulting in spindle collapse appears to be quite the opposite from that which causes the spindle elongation and breakage phenotype in *Δdam1* fixed cells, in that case it is probably rather due to a failure in kinetochore-microtubule interactions.

4.5 Genetic Interactions of the Dam1/DASH complex

In order to gain a further understanding of Dam1/DASH complex function we screened for mutants that are synthetically lethal in Dam1/DASH deletion backgrounds (Table 4.1).

4.5.1 Deletion mutants of Dam1/DASH complex require Klp5/6 and Dis1 to survive

We were unable to construct double deletions of *Δdam1, Δask1* or *Δdad1* with either *Δklp5, Δklp6 or Δdis1* by random spore analysis (Table 4.1). This indicates that double mutants between either *klp5/klp6* and Dam1/DASH deletions or double mutants between *dis1* and Dam1/DASH deletions results in a synthetic lethality. It is of note however that Dam1/DASH mutants while inviable in the absence of Dis1 are viable when Alp14 is deleted. The reasons behind this distinction between the two TOG members are at present unknown. It has been published from previous members of this lab that deletion of either *klp5* or *klp6* is synthetically lethal with *Δdis1* or *Δalp14* (Garcia et al., 2002). It would seem therefore there is a close functional link between Klp5/Klp6, Dis1, Alp14 and the Dam1/DASH complex. The Dam1/DASH complex and Klp5/Klp6 and/or Dis1 probably overlap in some essential mitotic function to ensure proper chromosome segregation. The requirement for *klp5*

	Δask1	*Δdam1*	*Δdad1*
Δklp5	SL	SL	SL
Δklp6	SL	SL	SL
Δmal3	ND	V	V
Δsgo2	ND	V	ND
Δalp14	V	V	V
Δdis1	SL	SL	SL
cnp1-1	V	V	SL
mis6-302	SL	SL	SL
mal2-1	SL	SL	SL
sim4-193	V	V	V
nuf2-2	V	V	V
nuf2-4	V	V	V
mis12-537	V	V	V
Δscd1	SL	SL	V

Table 4.1: Genetic interactions of various mitotic mutants with *Δdam1*, *Δask1* and *Δdad1*.

All interactions were tested at 27°C. V: viable; SL: synthetically lethal; ND: not determined.

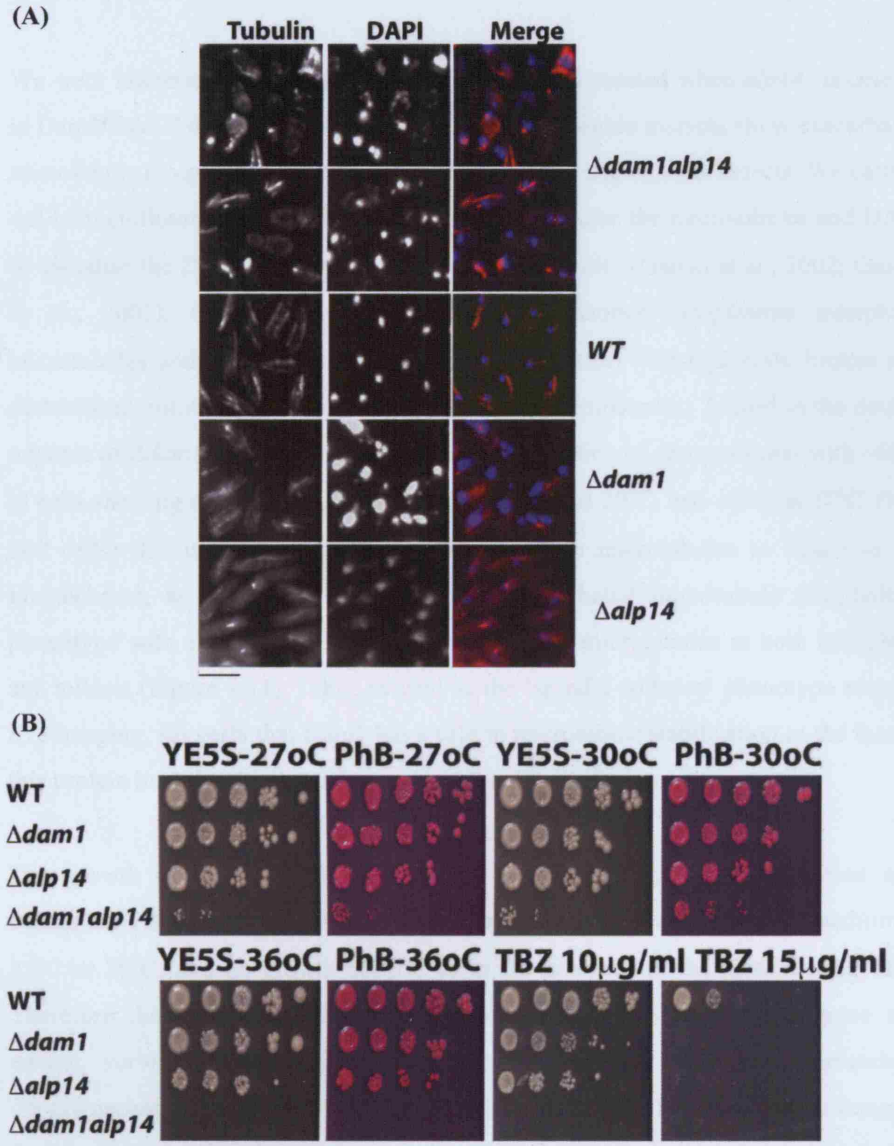

Figure 4.11: Severe segregation and morphology defects in *Δdam1alp14* cells

(A) WT, *Δdam1*, *Δalp14* and *Δdam1alp14* strains cultured in rich medium at 36°C. Cells were fixed and immunoflourescent staining of microtubules and DNA carried out. The scale bar represents 10 μm. **(B)** Tenfold serial dilution spot assay plated onto rich agar YE5S plates, YE5S & Phloxin B plates at 27°C or 36°C and YE5S plates containing TBZ 10μg/ml or 15μg/ml concentrations at 27°C.

and/or *klp6* when Dam1/DASH function is compromised will be the focus of study in the next chapter.

We were interested in examining the double mutants created when *alp14*$^{+}$ is deleted in Dam1/DASH deletion backgrounds, to see if the double mutants show exacerbated microtubule morphology defects and/or chromosome segregation defects. We carried out immunoflourescent staining of α-tubulin to visualise the microtubules and DAPI to visualise the DNA. Consistent with published results (Garcia et al., 2002; Garcia et al., 2001), the single *Δalp14* cells show shorter cytoplasmic interphase microtubules with weaker staining and less bundles than wild-type cells, broken and destabilised mitotic spindles and mis-segregated chromosomes. Indeed in the double mutants of *Δdam1alp14* there is massive mis-segregation of chromosomes with ~69% of cells showing aberrant DNA staining after 4hours at 20°C, and ~68% at 27°C, (N > 200 cells) this is probably due to a lack of stable microtubules to attach to the kinetochores, as these cells also show an exacerbated microtubule morphology phenotype with extremely disorganized and broken microtubules at both interphase and mitosis (Figure 4.11). This, as well as the 'spindle collapse' phenotype seen by live-imaging, suggests that Dam1 has a role in microtubule stabilisation as the loss of this protein in *Δalp14* cells leads to an increased loss of microtubule stability.

The growth of these double mutants on a serial dilution spot assay was also examined. These *Δdam1alp14* cells show very little growth on YE5S rich medium at 27°C or 30°C, and no growth at 36°C or in the presence of the spindle drug TBZ. Therefore these cells are defective even at normal permissive temperatures and cannot survive when shifted to higher temperatures or when microtubule depolymerisation is induced through the addition of TBZ. It is probable to imagine that the *Δdam1dis1* cells, which are synthetically lethal, do not survive due to similar defects in microtubule stabilisation and chromosome mis-segregation.

4.5.2 Mis6/Sim4 kinetochore mutants are synthetically lethal with Dam1/DASH mutants

We have previously shown Mis6 and Mal2 are required for Dad1 localisation to the kinetochore throughout the cell cycle (Sanchez-Perez et al., 2005). We wondered if deletion of Dad1 or the mitosis-specific Dam1/DASH components would exacerbate the phenotype of Mis6/Sim4 complex mutants *mis6-302* and *mal2-1*. We therefore

attempted to construct double mutants between deletions of the Dam1/DASH components *Δask1*, *Δdam1*, *Δdad1* and *mis6-302* and *mal2-1* mutants of the Mis6/Sim4 kinetochore complex.

s

We were unable to construct double mutants between *Δdad1*, *Δask1* or *Δdam1* and either *mis6-302* or *mal2-1* by random spore analysis (Table 4.1). This implies these double mutants are synthetically lethal and the Dam1/DASH complex is required for the survival of Mis6/Sim4 complex mutants even at the permissive temperature. It would appear that the Dam1/DASH complex works closely with the Mis6/Sim4 complex in performing some essential overlapping function. Interestingly we could construct double mutants between *Δdad1*, *Δdam1* or *Δask1* and *sim4-193* (Table 4.1). This result is consistent with our earlier localisation studies in which Dad1-GFP can still localise in a *sim4-193* mutant at the restrictive temperature. It seems this allele is less penetrative than the *mis6-302* or *mal2-1* alleles and does not fully disrupt Mis6/Sim4 complex function.

It is established that the Mis6/Sim4 complex plays an important role in the loading of Cnp1, the fission yeast CENP-A histone H3 variant to the centromere (Saitoh et al., 1997; Takahashi et al., 2000). We speculated that perhaps the overlapping function of the Mis6 and Dam1/DASH complexes is in loading of this histone variant Cnp1 to the centromere in fission yeast. To address this we examined whether Cnp1-GFP localisation is dependent on Dad1 and is abolished in *Δdad1* cells. However Cnp1-GFP localisation is completely intact when $dad1^{+}$ is deleted (Figure 4.12). The Dam1/DASH complex thus appears to have no major role in Cnp1 loading to the kinetochore and functionally overlaps with the Mis6/Sim4 complex in some other manner.

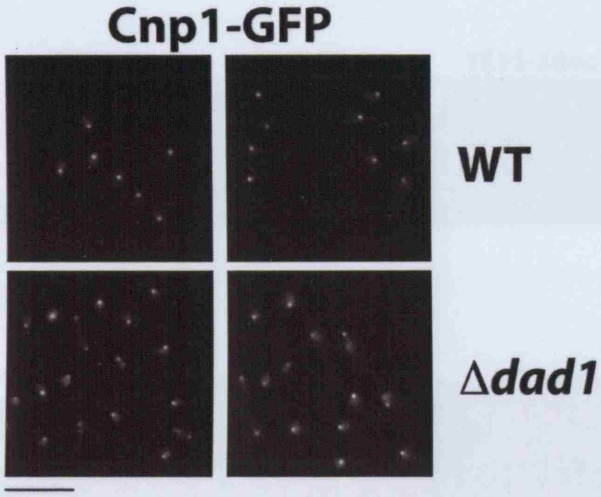

Figure 4.12: Cnp1 localisation is unperturbed in *Δdad1* cells.

WT and *Δdad1* cells containing Cnp1-GFP were cultured in rich medium at 27°C and fixed. The localisation of Cnp1-GFP was visualised by fluorescence microscopy. The scale bar represents 10μm.

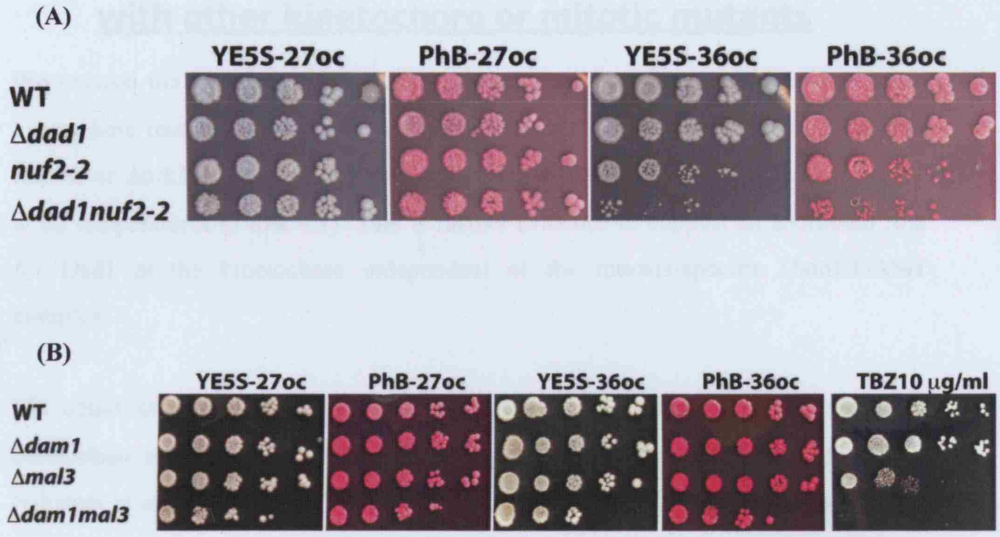

Figure 4.13: Synthetic growth defects of Dam1/DASH mutants combined with *nuf2-2* or *Δmal3* mutants.

Tenfold serial dilution spot assay plated onto rich agar YE5S plates, YE5S & Phloxin B plates at 27°C or 36°C and YE5S plates containing TBZ (Thiabendazole) 10μg/ml at 27°C. **(A)** WT, *Δdad1*, *nuf2-2*, and *Δdad1nuf2-2* cells spotted for 4 days at indicated temperatures. **(B)** WT, *Δdam1*, *Δmal3* and *Δdam1mal3* cells spotted for 4 days at indicated temperatures.

4.5.3 Genetic interactions of Dam1/DASH mutants with other kinetochore or mitotic mutants

We crossed the Dam1/DASH deletion mutants *Δask1*, *Δdam1* and *Δdad1* to other kinetochore mutants. The *cnp1-1* kinetochore mutant is viable in combination with *Δdam1* or *Δask1*, although intriguingly *cnp1-1* is synthetically lethal with only *Δdad1* at all temperatures (Table 4.1). This is further evidence to support an additional role for Dad1 at the kinetochore independent of the mitosis-specific Dam1/DASH complex.

We could construct double mutants between *Δdad1*, *Δdam1* or *Δask1* and the kinetochore mutants *mis12-537*, *nuf2-2* and *nuf2-4* (Table 4.1) (Goshima et al., 1999; Nabetani et al., 2001; Saitoh et al., 1997; Takahashi et al., 1994). We examined the growth of the double mutants *Δdad1nuf2-2* compared to the single *nuf2-2* or Dam1/DASH mutants (Figure 4.13A). The *nuf2-2* allele shows slight growth defects at the restrictive temperature of 36°C. This is aggravated by deletion of *Δdad1*, with little or no growth at the restrictive temperature in *Δdad1nuf2-2* cells (Figure 4.13A). It is easy to imagine that the exacerbated growth defect in the double mutant is due to an increased perturbation of kinetochore structure and/or microtubule attachments at the restrictive temperature in these cells.

We also examined the genetic interaction between the Dam1/DASH deletion mutants *Δdad1*, *Δdam1* and *Δask1* with a deletion of the fission yeast EB1 homologue *Δmal3*. Mal3 is a plus end microtubule binding protein that plays a vital role in cell polarity and cytoplasmic microtubule stability in interphase and mitotic spindle organisation and chromosome stability in mitosis (Asakawa and Toda, 2006; Beinhauer et al., 1997; Busch and Brunner, 2004; Chen et al., 2000; Kerres et al., 2004; Sandblad et al., 2006). The double mutants between Dam1/DASH deletions and *Δmal3* were viable by random spore analysis and examination of the growth of *Δdam1mal3* cells on a serial dilution spot assay showed no apparent temperature sensitivity but the sensitivity to the spindle depolymerising drug TBZ was worsened (Figure 4.13B). This yet again hints at a possible role for Dam1 in microtubule stabilisation during mitosis.

There is some evidence from the budding yeast that the Ras pathway can act antagonistically to the Dam1/DASH complex (Li et al., 2005). In the fission yeast

there is one Ras protein, Ras1, which can interact with two effector proteins Byr2 or Scd1. There is some evidence that Scd1 may play a more direct role in microtubule regulation and mitosis. We envisioned that in *S. pombe* the Scd1 branch of the Ras pathway may play a role in mitotic regulation and perhaps can interact genetically with the fission yeast Dam1/DASH complex. It appeared that deletion of *scd1*$^{+}$ in Dam1/DASH deletion backgrounds results in a synthetically lethal phenotype (Table 4.1), however we were unable to examine the phenotype of these double mutants by plasmid loss experiments (Data not shown). We therefore cannot conclude what is the overlapping function between the Dam1/DASH complex and Scd1 during mitosis.

4.6 Discussion

Analysis of loss of function mutations in the Dam1/DASH complex in the budding yeast have implicated this complex in playing an essential role in bi-polar attachment of the spindle microtubules to the kinetochore and the subsequent bi-orientation of the sister kinetochores in metaphase and the regulation and maintenance of microtubule integrity in anaphase (Cheeseman et al., 2001; Hofmann et al., 1998; Janke et al., 2002; Jones et al., 1999; Jones et al., 2001).

In this chapter we addressed whether this complex may play a similarly vital role in mitotic kinetochore-microtubule regulation in the fission yeast. To assess this we carried out deletion of several subunits of this complex using a PCR based approach whereby a kanamycin resistant cassette was disruptively inserted into the locus of each Dam1/DASH member gene (Figure 4.1). We found that each of these Dam1/DASH genes was not essential in *S. pombe*. This result is not really surprising given that the centromere/kinetochore system in *S. pombe* is more complicated than that of *S. cerevisiae* and probably requires a concert of mitotic proteins to regulate attachment and bi-orientation. The centromere/kinetochore in budding yeast is a simple "point" centromere of 125bp in length, which is attached to microtubules from the SPB throughout the whole cell cycle. Indeed the kinetochores in this organism can only bind one microtubule per kinetochore, thus sister chromatids can only become syntelically or monotelically attached and complex merotelic attachments can never exist in this system (DeLuca et al., 2006). The fission yeast however, contains a more structurally complex centromere/kinetochore, closely resembling the centromeres from higher organisms, with repetitive centromeric DNA spanning from

35-110 kilobases in length. Each kinetochore in this organism can attach to between 2-4 microtubules allowing sister chromatids to become improperly attached in a more complex manner with syntelic, monotelic and merotelic attachment defects possible in this system. Finally the spindle microtubules are only nucleated during mitosis so kinetochores can only become attached in the mitotic phase. It seemed therefore likely that a complex that was essential in budding yeast perhaps functions redundantly with one or more other mitotic regulators in the fission yeast to facilitate kinetochore and attachment regulation.

Deletion of Dam1/DASH subunits in the fission yeast gives rise to cells that are slightly sensitive to the microtubule depolymerising drug TBZ. This sensitivity is not equally meted out between various Dam1/DASH deletion strains tested with *Δspc34* appearing strongly sensitive to TBZ, with *Δdam1* cells as sensitive as *Δmad2* or *Δalp14* cells, and *Δask1* cells hardly sensitive at all to the drug (Figure 4.2). It seems that the degree of sensitivity is dependent on which subunit is deleted and thus different components in this complex may function in slightly different ways with respect to mitotic regulation. Indeed this hints at the fact that the subunits are not all equal within the fission yeast complex. In the budding yeast it has been proposed that the complex forms a ring *in vitro* on spindle microtubules with which it can mediate spindle-kinetochore interactions and the pulling of the kinetochores to opposite poles in anaphase (Asbury et al., 2006; Miranda et al., 2005; Westermann et al., 2005; Westermann et al., 2006). In this organism as of yet there does not appear to be any distinct difference between the various subunits with respect to ring formation, localisation and phenotype. Our result, where different components show slight phenotypic differences, suggests that this complex may not form a ring within the fission yeast, as not all subunits are equal. This possibility is also reinforced by variations in the localisation and genetic interactions of Dam1/DASH subunits. We have previously shown a difference in localisation between constitutively kinetochore localised Dad1 and the other mitosis-specific Dam1/DASH subunits, hinting that Dad1 may have some mitotic role independent of the other complex members. Moreover, *cnp1-1* is synthetically lethal at all temperatures with *Δdad1* cells but viable with *Δdam1* or *Δask1*, thus inferring that Dad1 may somehow function in an overlapping essential pathway at the kinetochore with Cnp1, but that this is independent of the mitotic-specific Dam1/DASH members.

We have shown that Dad1 is dependent on the Mis6/Sim4 complex for its constitutive localisation to the kinetochore and Liu *et al* 2005 showed that Dad1 interacts directly with the Mis6/Sim4 complex in both Dad1-TAP and Sim4-TAP eluates (Liu et al., 2005; Sanchez-Perez et al., 2005). We therefore postulated whether a Dam1/DASH complex independent role for Dad1 might be related to its close association with the Mis6/Sim4 complex and perhaps Dad1 functions with Mis6 in Cnp1 loading to the centromere. We found however that Cnp1 loading was unaffected when Dad1 is deleted (Figure 4.12). Another possibility was that Dad1 might function along with Mis6 as an acceptor for the Mad2 spindle assembly checkpoint protein. Mad2 was shown to interact directly with Mis6 under conditions where the spindle assembly checkpoint is switched on and it is established that there is no spindle checkpoint activation in "*mis*" family mutants such as *mis6-302* or *mal2-1* (Saitoh et al., 2005). Perhaps Dad1 is also required for Mad2 binding at the kinetochore and therefore the spindle assembly checkpoint would not be maintained in *Δdad1* cells. We found however that upon treatment of *Δdad1* cells with MBC, the spindle assembly checkpoint mediated arrest is maintained as well as it is in wild-type cells (Figure 4.6). It seems therefore that the Dam1/DASH complex independent role of Dad1 at the kinetochore still remains elusive.

Consistent with the possibility that various Dam1/DASH subunits may have slightly differing roles in relation to kinetochore and/or spindle regulation there are also other disparities in genetic interactions between the mitosis-specific Dam1/DASH subunits. We showed that double mutants between *Δdam1, Δask1* or *Δdad1* and the *mis6-302* kinetochore "mis" mutant are synthetically lethal (Table 4.1). However a recent paper has shown that *Δhos2* mutant cells are viable in combination with the *mis6-302* mutant albeit with severe mitotic defects (Kobayashi et al., 2007). Indeed in this paper by Kobayashi *et al.* 2007 they also stated that a *Δhos2* mutation is synthetically lethal in combination with *nuf2-1, nuf2-2* or *nuf2-3* cells when we have found that *Δdam1, Δask1* and *Δdad1* cells are viable with *nuf2-2* or *nuf2-4* cells (Table 4.1, Figure 4.1) (Sanchez-Perez et al., 2005). This suggests that not all the mitosis-specific Dam1/DASH deletions behave identically in respect to penetrance of phenotype and/or genetic interactions either.

Deletion of *dam1*$^+$, *ask1*$^+$ or *dad1*$^+$ in a *Δklp5* or *Δklp6* strain results in synthetic lethality, indicating these proteins must perform an essential overlapping function (Table 4.1) (Sanchez-Perez et al., 2005). To gain a rudimentary understanding of

how these cells die Sanchez-Perez *et al* (2005) carried out a germination experiment on cells deleted for both *dam1*$^+$ and *klp5*$^+$ and *cen2*-GFP sister chromatid separation and Mad2-GFP foci formation were monitored. Multiple Mad2 foci were observed in these double mutants and are evidence that bi-polar kinetochore-microtubule attachment is defective in these cells (Sanchez-Perez et al., 2005). The double mutants showed a range of mitotic segregation defects indicative of several types of attachment errors, with some cells showing lagging chromosomes, syntelic mono-polar segregation of both sister chromatids to the same pole, or failure of one of the two sister chromatids to segregate to a pole indicating an unattached or merotelically attached kinetochore. In this experiment the single *Δdam1* cells showed only mono-polar syntelic segregation of sister chromatids whereas the single *Δklp5* strain showed only lagging chromosomes. It is therefore proposed that Klp5/6 and the Dam1/DASH complex function in an overlapping role to establish bi-polar kinetochore-microtubule attachment and chromosome bi-orientation through correction of mono-polar syntelic attachments through Dam1 and the correction of merotelic lagging chromosomes through Klp5 and Klp6. We will attempt to further address the lethality of these double mutants in the next chapter.

In *S. cerevisiae* there is some evidence to support the idea that the Ras/PKA pathway may act antagonistically in mitosis to the Dam1/DASH complex (Li et al., 2005). We attempted to address whether the Ras pathway in fission yeast may play a similar role in functioning antagonistically to the Dam1/DASH complex. The fission yeast contains only one Ras molecule, Ras1, which has been shown to interact with Scd1, a putative guanine nucleotide exchange factor for the Rho like GTPase Cdc42, to regulate sexual differentiation, polarized growth, and cell shape in *S. pombe* (Ahonen et al., 2005; Fukui et al., 1986; Fukui and Yamamoto, 1988). Indeed Scd1 has been proposed to function during mitosis. It has been shown to exacerbate the phenotype of tubulin mutants, is sensitive to the spindle de-polymerising drug TBZ, can interact with Klp5 and Klp6 both by immuno-precipitation experiments and genetically and has been shown to localise to the nucleus and along the spindle microtubules (Li et al., 2003; Li et al., 2000). We therefore tried to elucidate if Scd1 could interact genetically with the fission yeast Dam1/DASH complex. We were unable to construct double mutants between *Δdam1* or *Δask1* and *Δscd1*, suggesting these double mutants are synthetically lethal, however we were able to create a *Δdad1scd1* strain. It thus appears that a *Δscd1* mutant is synthetically lethal only with deletions of the mitosis-specific Dam1/DASH components. Our attempt to ascertain how these

double mutants die, however, did not yield any data about the possible overlapping functions of Dam1/DASH and Scd1. We tried to induce plasmid loss in the double mutant cells, but unfortunately there was only a modest loss of the plasmid in our strains. It would seem then that any mitotic role for Scd1 with the Dam1/DASH complex in the fission yeast is independent of Dad1 and only requires the mitosis-specific Dam1/DASH members. However that role of Scd1 with the Dam1/DASH complex in mitosis still remains elusive.

Deletions of Dam1/DASH components have also been show to be synthetically lethal when the chTOG protein Dis1 is absent. Dis1 is one of two chTOG family proteins in the fission yeast, the other being Alp14. Double mutants between *dis1*$^{+}$ and *alp14*$^{+}$ are synthetically lethal, but intriguingly double mutants of either *Δdam1*or *Δask1* are viable in an *Δalp14* background. These double mutants however are extremely sick, showing little growth even at the permissive temperature and absolutely no growth on plates treated with TBZ (Figure 4.11). There are severe chromosome segregation defects in these double mutants even at the permissive temperature with 68.15% of cells showing aberrant DAPI staining indicative of chromosome mis-segregation at 27°C in these cells. The microtubule structures in these cells are extremely disorganized with both interphase and mitotic cells having sometimes broken disturbed abnormal microtubule structures, or little or no microtubules (Figure 4.11).

Loss of Alp14 leads to destabilisation of microtubules with short interphase microtubules and mitotic spindles and perhaps removal of a functional Dam1/DASH complex exacerbates this stress on the microtubules leading to a complete disorganisation of microtubules. Further to this removal of Dam1 in a *Δmal3* background worsens the TBZ sensitivity of single *Δmal3* cells with the double *Δdam1mal3* cells extremely sensitive to the microtubule de-polymerising drug. (Figure 4.13B) Both these results hint at the intriguing possibility that the Dam1/DASH complex in fission yeast like its counterpart in budding yeast may have a microtubule integrity function.

Indeed when we analysed Sad1-dsRed and *cen2*-GFP dynamics in live *Δdam1* cells a population of cells showed a "spindle collapse" phenotype. In these cells the SPBs, which are marked by Sad1-dsRed, can duplicate and separate as normal but there are little centromere oscillations or movement of the sister *cen2*-GFP signals across the metaphase plate. As mitosis proceeds in these cells there is no segregation of the

cen2-GFP sister chromatids and the Sad1 marked SPBs begin to converge until there is complete collapse of the mitotic spindle (Figure 4.10C). We followed these cells for almost an hour past the point of collapse until signal bleach occurred, but these cells did not reform the spindle or undergo chromosome segregation.

There is a balance of force that occurs in normal cells, between the microtubule based forces that are pushing on the SPBs to move the two poles apart and the force that pulls the chromosomes towards the poles and the two poles together (Nabeshima et al., 1998). In normal cells this balance functions to maintain a constant spindle length in metaphase (Nabeshima et al., 1998), but in a subset of these *Δdam1* cells the "spindle collapse" defect probably occurs due to a disruption of this balance resulting in the pole-pole microtubules becoming de-stabilised which ultimately causes the two poles to converge and leads to a complete collapse of the spindle.

Deletion of Dam1/DASH subunits in the fission yeast results in chromosome segregation defects with DAPI staining in these cells showing aberrantly segregated DNA patterns (Figure 4.3A). Incorporation of a linear mini-chromosome shows an elevated level of loss of this mini-chromosome in Dam1/DASH deletion strains compared to wild-type cells with 7.8% plasmid loss for *Δdam1*, 5.3% plasmid loss for *Δask1* compared to 0.3% in wild-type cells (Figure 4.3B&C). The spindle assembly checkpoint is activated in these Dam1/DASH deletion mutants to induce a mitotic arrest. Bub1-GFP foci are visualised at an elevated rate in *Δdam1* cells compared to wild-type and the increased frequency of mitotic cells seen in Dam1/DASH null mutants is abolished when the spindle assembly checkpoint proteins Mad2 or Bub1 are deleted (Figure 4.4). Indeed if the spindle assembly checkpoint is removed in Dam1/DASH deletion mutants the resultant double mutants show synthetic growth defects in liquid culture, with Dam1/DASH null cells in which Bub1 is deleted showing extreme sensitivity to TBZ (Figure 4.5). This additional sensitivity seen when Bub1, but not Mad2, is removed in Dam1/DASH deletion strains highlights the obvious tension and bi-orientation defects in these cells.

The mitotic arrest seen in Dam1/DASH deletion mutants most likely occurs to give these cells time to promote proper attachment and repair spindle defects. We postulate that molecules like Klp5 or Klp6, Dis1 or Mal3 may function to try and promote proper bi-polar attachment in a stochastic manner. Despite this spindle assembly checkpoint activation however, a subset of Dam1/DASH null mutants still

undergo an aberrant mitosis and chromosome segregation defects occur (Figure 4.3). This result as expected shows that when this complex is non-functional chromosome segregation cannot occur with high fidelity and defects result.

Further to this our analysis of *cen2*-GFP sister chromatid separation in both fixed and live *Δdam1* cells shows a clear mono-polar segregation non-disjunction phenotype in this mutant at 20°C, 27°C or 36°C, indicative of kinetochore-microtubule bi-orientation defects (Figure 4.8, Figure 4.10). Indeed examination of *Δdam1* cells at 20°C reveals that at this low temperature an obvious "*dis*" phenotype appears with condensed chromatin, an increase in the frequency of chromosome mis-segregation and elongated spindles that cannot be maintained and break during anaphase (Figure 4.7). This phenotype is very similar to that seen in "*dis*" mutants, with a typical example being *Δdis1*. In these mutants the spindle assembly checkpoint is activated resulting in condensed sister chromatids but spindle elongation occurs despite checkpoint activation and non-disjunction of sister chromatids results (Nabeshima et al., 1995; Nabeshima et al., 1998; Ohkura et al., 1988).

As discussed above, the interaction between kinetochores and microtubules normally restrains the metaphase spindle length in wild-type cells. This occurs by maintaining the balance of microtubule-based forces within the cell between those that are pushing the opposite poles apart and those mediated by the interaction of kinetochores with the microtubules, which pull the poles closer (Nabeshima et al., 1998). However in "*dis*" mutants the spindle-kinetochore attachments are defective and this results in the poles becoming pushed apart and consequently the spindles abnormally elongate and can eventually break (Nabeshima et al., 1995; Nabeshima et al., 1998; Ohkura et al., 1988). We postulate that a similar disruption of this balance of force may be driving the elongation of metaphase spindles in the *Δdam1* cells at 20°C and therefore this protein must play an important role in attachment of the spindle microtubules to the kinetochores and probably works in concert with Dis1 to facilitate this. It is of note that this disruption of force in *Δdam1* cells gives rise to two distinct phenotypes, with the disruption of force that results in spindle collapse caused by a failure of pole-pole microtubule integrity whereas that which causes the spindle elongation and breakage occurs due to failure in kinetochore-microtubule attachments.

It seems that this complex in fission yeast functions in a similar manner to its counterpart in the budding yeast and is somehow involved in turnover of incorrect kinetochore-microtubule attachments and spindle integrity. We postulate that the Dam1/DASH complex in fission yeast functions predominantly to ensure syntelic mono-polar attachments are properly bi-oriented to form correct amphitelic attachments and in the subsequent maintenance of the mitotic spindle.

Chapter 5

5 Identification and characterisation of *dam1-A8* mutant allele

Introduction

In the previous chapter we examined the genetic relationship between Dam1/DASH null mutants and mutants of other mitotic regulators and found that deletion mutants of this complex were synthetically lethal when combined with mutants of the Mis6/Sim4 kinetochore complex or in *Δdis1*, *Δklp5* or *Δklp6* backgrounds. Interestingly deletions of either *klp5*$^+$ or *klp6*$^+$ have been shown to be lethal when *dis1*$^+$ is deleted (Garcia et al., 2002a). This indicates that the Dam1/DASH complex and Dis1, Klp5 and Klp6 must perform some essential overlapping function during mitosis.

In this chapter we attempt to address the reasons for the lethality of double mutants between *dam1*$^+$ and *klp5*$^+$. By analysing how these cells die we should gain further understanding of the essential overlapping function of both Klp5 and Klp6 and the Dam1/DASH complex in the fission yeast. We therefore screened for a temperature sensitive *dam1* mutant in a *klp5* null background and isolated a mutant we termed *dam1-A8*. This mutant appears to be a 'gain of function' mutant, which shows resistance to the microtubule drug TBZ, in sharp contrast to *Δdam1* cells, which are slightly sensitive. The temperature-sensitive double mutant *dam1-A8Δklp5* shows massive chromosome mis-segregation with mono-polar sister chromatid segregation defects, and activation of the spindle assembly checkpoint, however the temperature sensitivity of this double mutant can be rescued by the addition of the microtubule depolymerising agent TBZ. Indeed we show that the single *dam1-A8* mutant shows cells with congression defects, although there is little mis-segregation of chromosomes in these cells. We will demonstrate that despite the non-essentiality of the Dam1/DASH complex it plays a vital role in concert with the kinesins Klp5 and Klp6 to facilitate proper end on attachment of kinetochores to the spindle microtubules.

5.1 Mutagenesis screening for Dam1 mutants in a *Δklp5* background

In order to address the reasons for synthetically lethality between null mutants of the Dam1/DASH complex and *Δklp5* or *Δklp6*, we devised a screening strategy to isolate conditional temperature sensitive *dam1*$^{+}$*-GFP* mutants in a *Δklp5* background. The screening approach we formulated involves random mutagenesis of a template DNA fragment, which contains the *dam1* gene tagged with a GFP flourophore and a selectable drug resistance marker. The presence of the drug resistance marker allows us to select for correctly transformed strains rapidly, whereas the presence of the flourophore will allow visualisation of localisation of this mutant Dam1 protein at both the permissive and restrictive temperatures. The randomly mutagenised *dam1*$^{+}$ DNA fragment is then transformed to *Δklp5* cells and the subsequent transformants assessed for the presence of the selectable marker and temperature sensitivity when incubated at the restrictive temperature (Figure 5.1). Using this approach we expect to select for only mildly mutated *dam1*$^{+}$ alleles, severe mutations, which completely knock out Dam1 function, even at the permissive temperature, will in all probability be lethal in this *Δklp5* background and will not grow on the initial transformation selection plates.

The first step in our mutagenic screen for *dam1* mutants in a *klp5* null background, involved PCR amplification of *dam1*$^{+}$*-GFP-Kan* from a wild-type strain in which Dam1 was C-terminally tagged with GFP-kanamycin. This *dam1*$^{+}$*-GFP-Kan* fragment of DNA will serve as our template for the random mutagenic PCR. To ensure that this initial amplification proceeded accurately we carried out this PCR using a high-fidelity proofreading Taq enzyme, Vent polymerase, and also sequenced the subsequently amplified DNA fragment. As expected this fragment had no erroneous sequences, mutations or deletions (data not shown, Figure 5.1A), and was then used as a template for the subsequent mutagenic PCR (Figure 5.1B). The mutagenic PCR was carried out in an error-prone manner using TaKaRa LA Taq^{TM} and with 10xdGTP to unbalance the dNTP ratio. The resultant mutagenised PCR product was ethanol precipitated from the PCR reaction (sambrook, 1989) and then transformed into a total of ~$1x10^{10}$ *Δklp5* cells.

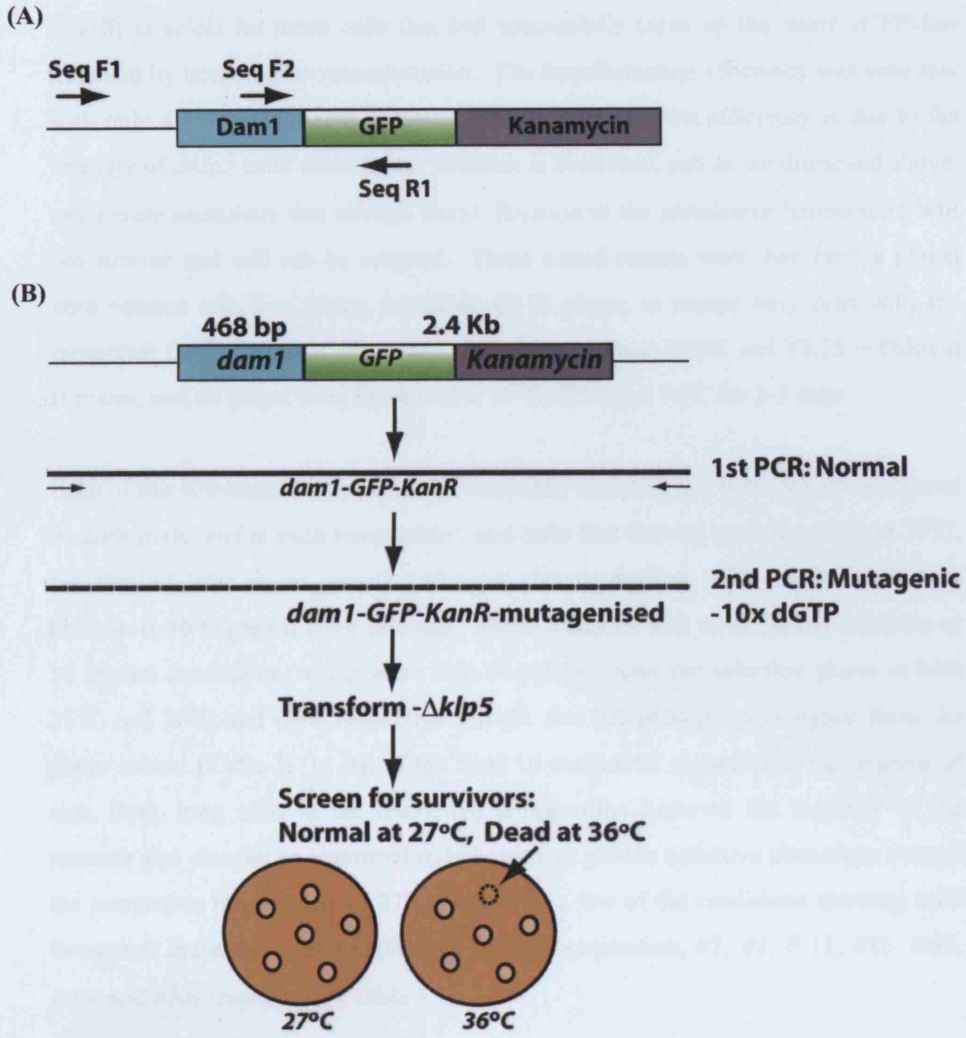

Figure 5.1: Schematic representation of mutagenic screening strategy

(A) Schematic showing region sequenced from *dam1*$^{+}$*-GFP-Kan* fragment. **(B)** Diagrammatic representation of strategy used to generate temperature sensitive conditional *dam1*$^{+}$ mutants in a *Δklp5* background.

The cells were plated onto rich medium YE5S plates containing the drug Geneticine (G418) to select for those cells that had successfully taken up the *dam1*$^{+}$*-GFP-kan* fragment by homologous recombination. The transformation efficiency was very low with only 400 transformants in total. We envisage this low efficiency is due to the lethality of *Δklp5* cells when Dam1 function is abolished, and as we discussed above, any severe mutations that abolish Dam1 function at the permissive temperature will not survive and will not be selected. These transformants were then replica plated onto various selection plates, including G418 plates, to ensure only cells with the integrated DNA fragment are selected, and rich medium YE5S and YE5S + Phloxin B plates, and all plates were incubated at 27°C, 30°C and 36°C for 2-3 days.

Each of the 400 transformant colonies were then analysed and their growth compared on each plate, and at each temperature, and cells that showed normal growth at 27°C, but showed little or no growth and were sick or dead at 36°C (appearing red on Phloxin B 36°C plates) were selected. These analyses lead to the initial selection of 16 mutant candidates, which were then re-patched onto the selection plates at both 27°C and 36°C and their respective growth and morphology phenotypes from the plates scored (Table 5.1). All of the final 16 candidates showed varying degrees of sick, bent, long cells at the restrictive temperature, however the majority of the mutants also showed an abnormal morphology or growth defective phenotype even at the permissive temperature of 27°C, with only a few of the candidates showing mild to normal growth or cell morphology at this temperature, #7, #9, # 11, #16, #A3, #A6, and #A8 respectively (Table 5.1).

To aid in the further selection of a stringent conditional mutant from our list of candidates a serial dilution plate spot assay was carried out to assess the growth of the remaining candidates compared against wild-type and *Δklp5* cells on YE5s, YE5S + Phloxin B plates at 27°C and 36°C and on TBZ 10μg/ml plates at 27°C (Figure 5.2). From this analysis we carefully examined the growth of the 7 candidates, #7, #9, # 11, #16, #A3, #A6, and #A8, that appeared from Table 5.1 to show a mild growth and morphology phenotype at the permissive temperature.

Mut	Growth 27°C	Morphology 27°C	Growth 36°C	Morphology 36°C
4	++-	Long, bent	---	Bent, branched, dead
7	+++	Longish	+--	Long, bent, sick
8	++-	Some long	+--	Long, bent, sick
9	+++	Some long	+--	Long, bent, sick
11	+++	Most normal	+--	Bent branched, long
16	+++	Longish	+--	Bent, branched, sick
18	++-	Some long	+--	Bent, branched, sick
20	++-	Some long	+--	Bent, branched, sick
24	++-	Some long	+--	Bent, branched, sick
A1	++-	Some long	---	Bent, branched, dead
A3	+++	Some long	---	Bent, branched, dead
A4	++-	Some long	---	Bent, branched, dead
A5	++-	Some long	---	Bent, branched, dead
A6	+++	Some long	---	Bent, branched, dead
A7	++-	Most normal	+--	Bent, branched, sick
*A8	+++	Normal	---	Bent, longish, dead

Table 5.1: Table of *dam1-GFP-Kan Δklp5* mutant candidates

Asterisk denotes mutant chosen for final further study.

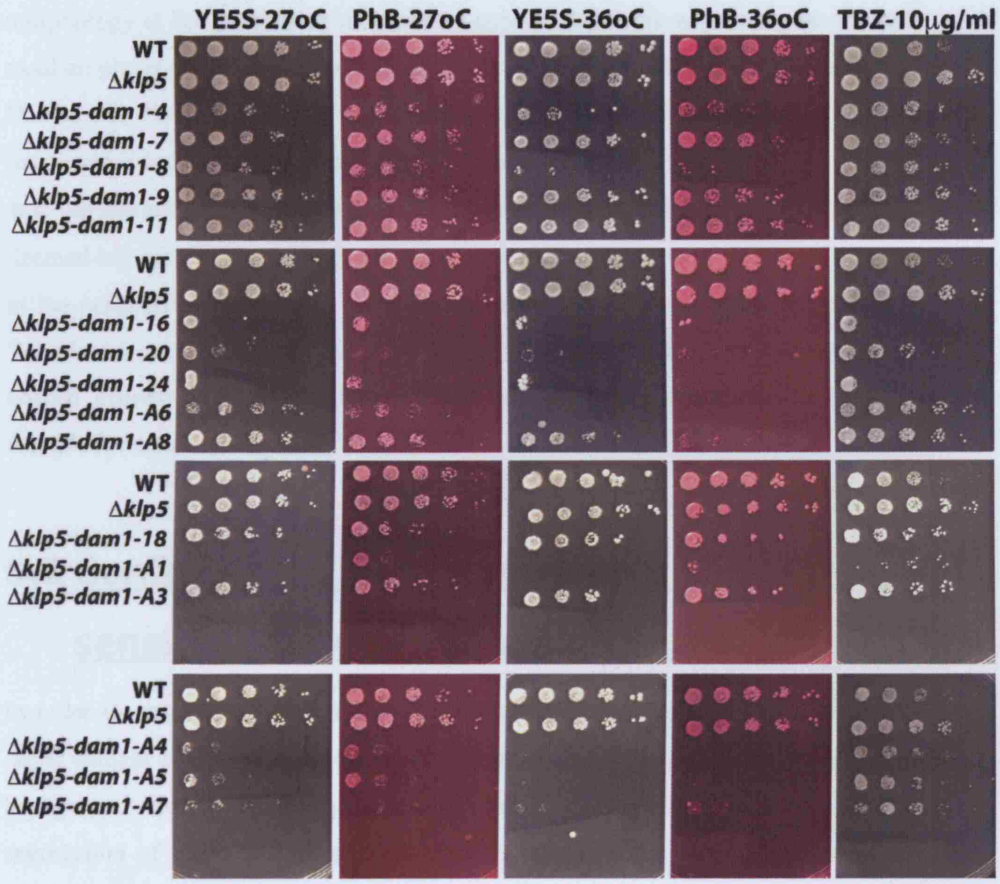

Figure 5.2: Serial dilution spot assay of final 16 *dam1Δklp5* mutant candidates.

A tenfold serial dilution spot assay with cells plated onto rich agar YE5S plates, YE5S & Phloxin B plates incubated at 27°C or 36°C and YE5S plates containing 10μg/ml TBZ incubated at 27°C. The growth of the final 16 candidates is compared to wild-type and *Δklp5* cells.

The 9 candidates from Table 5.1 that were scored as having abnormal growth or morphology at the permissive temperature appeared quite slow growing on the rich medium plates at either 27°C or 36°C and were immediately disregarded (Figure 5.1). Mutant #7, #9, #11 and #A3 while capable of growth at 27°C did not show strict temperature sensitivity at the restrictive temperature of 36°C and were disregarded, whereas mutant #16 did not show much, if any, growth at either temperature and was deemed too severe for analysis. Both mutants #A6 and #A8 were capable of growth at the permissive temperature and showed sensitivity at the restrictive temperature. We picked mutant A8, however, for further study as it seemed to have the most normal growth at 27°C of all the candidates and therefore was considered most suitable for conditional mutant analyses.

5.2 Confirmation of *dam1-A8* temperature sensitivity and sequencing the mutation

In order to ensure that the temperature sensitivity phenotype seen in our *dam1-A8 Δklp5* mutant was caused by the combination of the *dam1-A8* allele with a *Δklp5* background and not caused by some other unknown mutation we assessed the co-segregation of the ts^- phenotype with the double mutant by both backcrossing and tetrad analysis. We also carried out sequencing of the *dam1-A8* allele to check and and site the mutation responsible for the temperature sensitive phenotype.

The *dam1-A8* allele is tagged with a kanamycin marker, which confers resistance to the antibiotic drug Geneticine (G418), whereas the *klp5* gene has been deleted by the integration of a $Ura4^+$ marker, which disrupts the *klp5* locus, and enables the *Δklp5* cells to grown on minimal medium lacking uracil. If the temperature sensitive phenotype of the double mutant strain is not caused by an unlinked mutation then this phenotype should always and only, occur in cells that contain both the *dam1-A8* allele and are deleted for *klp5*. These double mutant cells can be selected for by the presence of both selectable markers, however, the wild-type cells (which will be auxotrophic for uracil and G418-) or the single *dam1-A8* or *Δklp5* mutant progeny resulting from either backcrossing or tetrad analysis should not demonstrate the temperature sensitivity. To assess whether this ts phenotype only co-segregates with the double mutant, the *dam1-A8Δklp5* strain was backcrossed to wild-type cells and the progeny analysed by random spore analysis and their growth assessed on YE5S

rich medium plates at both 27°C and 36°C, EMM-uracil plates and YE5S plates containing G418. As expected the Ura-G418- wild-type cells showed normal growth at both temperatures, the single *dam1-A8* Ura- G418+ cells appeared almost normal, the single mutant *Δklp5* Ura+ G418- cells were not temperature sensitive and only the double mutants containing both *dam1-A8Δklp5* appeared temperature sensitive at the restrictive temperature of 36°C (Data not shown, Figure 5.3A).

To confirm this result we also assessed the co-segregation of the temperature sensitivity with the double mutants by tetrad analysis. The *dam1-A8Δklp5* strain was crossed to a wild-type strain, which is auxotrophic for uracil, and the four spores from the ascii formed were dissected by a micromanipulator. The four spores from each ascus were separated into a line onto YE5S rich medium plates, incubated at 27°C for several days and allowed to form colonies. These plates were then replica plated onto G418, EMM-uracil and Phloxin B plates at both 27°C and 36°C and the segregation pattern of the different markers with the temperature sensitivity phenotype was examined. Using this approach it is quite clear that the temperature sensitivity phenotype always co-segregates with both kanamycin (G418) and uracil markers indicative of the double mutant *dam1-A8Δklp5* strain. Therefore this temperature sensitivity is not due to the presence of another background mutation and is solely dependent on the *dam1-A8* allele in a *Δklp5* background.

5.2.1 Sequencing the *dam1-A8* mutant allele

The *dam1-A8* allele was amplified by high-fidelity PCR and sequenced using the same oligos previously used to sequence the *dam1*$^{+}$*-GFP-Kan* fragment at the start of the screening process (Figure 5.1A). There are two C-G point mutations that were identified within the *dam1* ORF in this mutant. We expected to yield C-G mutations due to our screening strategy, which involved the usage of 10xdGTP to incur guanidine incorporation at a higher frequency. These point mutations resulted in a change of amino acids H126R and E149G, at the C-terminal of the Dam1 protein. Neither of these residues is conserved in the budding yeast protein (Figure 5.4).

(A)

Strain	Uracil	G418	Ts?
Wild-type	-	-	Normal
dam1-A8	-	+	Almost normal
Δklp5	+	-	Normal
dam1-A8Δklp5	+	+	TS red, dead

(B)

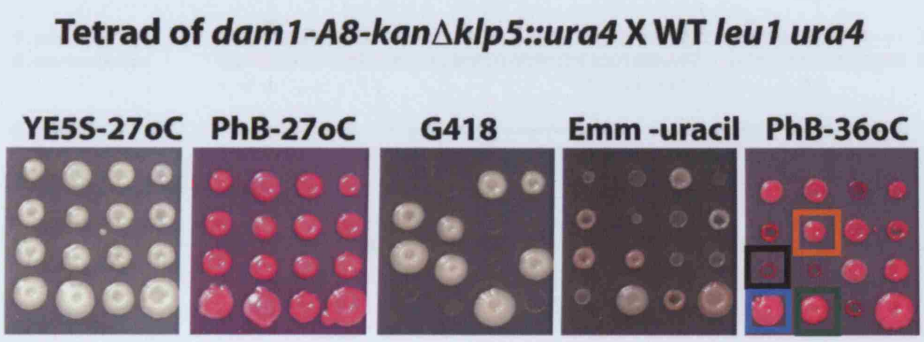

Figure 5.3: Co-segregation of ts⁻ phenotype with double *dam1-A8Δklp5* mutants.

(A) Table listing the various strain combinations identified from random spore analysis. Only the double mutants containing both *dam1-A8Δklp5* appeared temperature sensitive. **(B)** Tetrad analysis to confirm the co-segregation of the ts phenotype with the double mutants. Wild-type *leu1 ura4* and *dam1-A8-kanΔklp5::ura4* strains were crossed and after colony formation the resultant progenies were replica plated onto YE5S and Phloxin B plates at 27°C, Phloxin B plates at 36°C and G418 and EMM –uracil selection plates. Wild-type progeny are marked by a blue box, a green box marks *Δklp5* colonies, an orange box marks single *dam1-A8* progeny and the double mutants *dam1-A8Δklp5* colonies are marked by a black box.

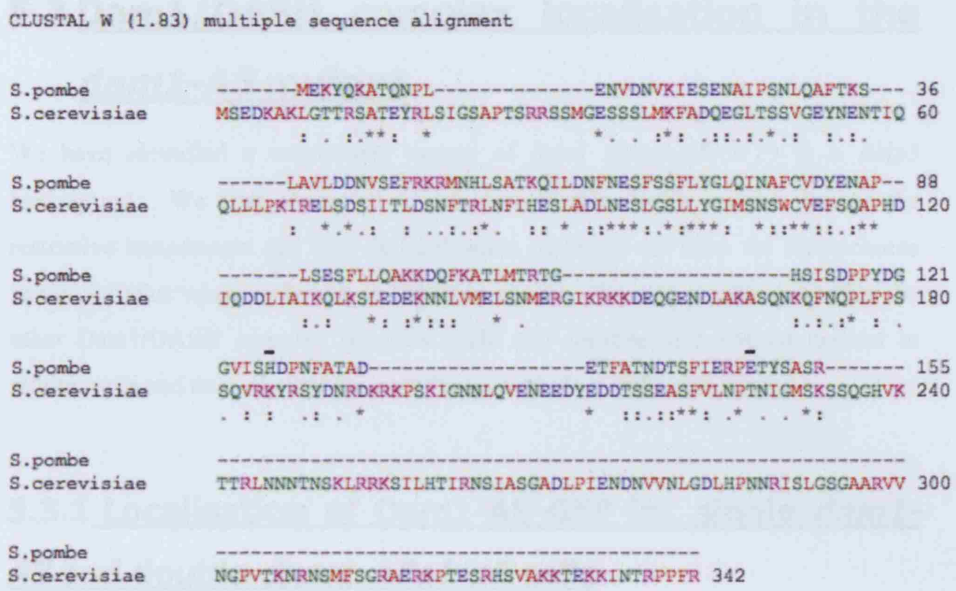

Figure 5.4: Analysis of mutation site in *dam1-A8* mutant.

Sequence alignment of the *S. pombe* and *S. cerevisiae* Dam1 proteins. The *dam1-A8* mutant allele contains two mutation sites in the C-terminal of the protein H126R and E149G. These are overlined in black.

5.3 Dam1/DASH complex localisation in the *dam1-A8* mutant

We have identified a conditional mutant of *dam1* (*dam1-A8-GFP)* in a *Δklp5* background. We first attempted to ascertain if this double mutant dies at the restrictive temperature due to a de-localisation of Dam1-A8 from the kinetochores and/or spindles when shifted up to this temperature. We also pondered whether the other Dam1/DASH complex subunits could still localise in a normal manner in mitotic cells and thus whether the complex as a whole may be still intact.

5.3.1 Localisation of Dam1-A8-GFP in single *dam1-A8* and double *dam1-A8Δklp5* cells

We examined the GFP localisation of this Dam1-A8 mutant protein in a wild-type and *Δklp5* background by fluorescence microscopy. The single *dam1-A8* and the double *dam1-A8Δklp5* mutant cells were cultured in rich medium overnight at 27°C, fixed and the localisation of Dam1-A8 visualised by fluorescence microscopy at both 27°C and 36°C. Even at the permissive temperature of 27°C the localisation of Dam1-A8 in either the single *dam1-A8* or double *dam1-A8Δklp5* cells was severely compromised. The signal in both backgrounds could be just barely visualised. It appeared very weak and became progressively weaker at the restrictive temperature, and after two hours incubation at the restrictive temperature the GFP signal was undetectable in either the single *dam1-A8* or double *dam1-A8Δklp5* cells (Figure 5.5). We conclude that even at the permissive temperature there is severly reduced localisation of Dam1-A8-GFP to the mitotic cells, however, the population of Dam1-A8 that can localise to the kinetochore and/or spindles albeit at a reduced frequency, seems to be sufficient for the growth and survival of this strain at 27°C when $klp5^{+}$ is deleted. Incubation of either the single *dam1-A8* or double *dam1-A8Δklp5* cells at the restrictive temperature completely abolishes localisation in mitotic cells.

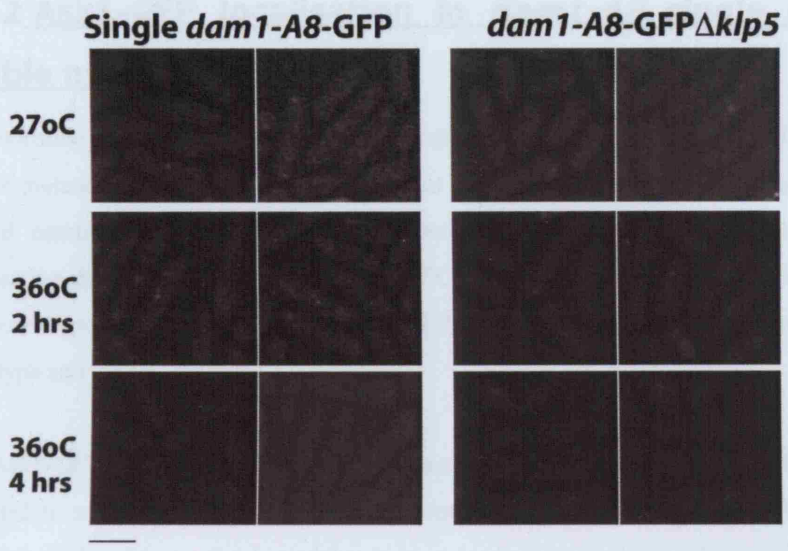

Figure 5.5: Localisation of Dam1-A8-GFP in single *dam1-A8* and double *dam1-A8Δklp5* mutants.

Single *dam1-A8* and double *dam1-A8Δklp5* mutant cells were cultured in rich medium overnight at 27°C. The cultures were split, incubated at 27°C or 36°C for four hours, fixed and visualised by fluorescence microscopy. The scale bar represents 10μm.

5.3.2 Ask1-GFP localisation in *dam1-A8* single and double mutants

To determine whether the Dam1/DASH complex remains intact in *dam1-A8Δklp5* double mutants we analysed if another subunit of this complex can still localise in a normal manner at the restrictive temperature. We thus examined Ask1-GFP localisation at 27°C, the permissive, and 36°C, the restrictive temperatures, in the *dam1-A8Δklp5* double mutant and compared this to Ask1-GFP localisation in both wild-type and *Δdam1* cells.

The Ask1-GFP in our wild-type control strain at both 27°C and 36°C, localised as expected to mitotic kinetochores and/or microtubules (Figure 5.6a&b). Ask1-GFP was able to localise to the kinetochores in *Δdam1* cells at 20°C, 27°C and 36°C respectively, indicating that Dam1 is dispensable for Ask1 localisation to the kinetochore and/or spindle microtubule plus ends (Figure 5.6c&d&e). The double mutant *dam1-A8Δklp5* showed normal Ask1-GFP localisation at 20°C (Figure 5.6f), however the localisation of Ask1-GFP to the kinetochores of mitotic *dam1-A8Δklp5* cells is slightly reduced when incubated at 27°C and strongly reduced after 4 hours incubation at the restrictive temperature of 36°C. Therefore while Ask-GFP can localise normally when *dam1*$^+$ is deleted there is a partial reduction in the strength of localisation signal in mitotic cells in the *dam1-A8Δklp5* mutant. Perhaps the Dam1/DASH complex is not fully intact under this mutant condition, however due to our failure to visualise any of the Dam1/DASH proteins biochemically we are unable to test whether the complex remains intact in a more direct manner. We therefore cannot definitively conclude that the Dam1/DASH complex is disrupted in this *dam1-A8* mutant despite a decrease in Ask1 signal at the kinetochore after prolonged incubation at high temperature.

What is of note however is the distinct difference between this *dam1-A8Δklp5* allele and a *Δdam1* strain with respect to Ask1-GFP localisation. Ask1 localises as normal in *Δdam1* cells at the various temperatures tested but there is a clear reduction in Ask1-GFP signal after incubation at the restrictive temperature in *dam1-A8Δklp5* cells. It would thus seem that this *dam1-A8Δklp5* allele may not be a simple loss of function Dam1 mutation and may behave differently to a complete *dam1*$^+$ deletion.

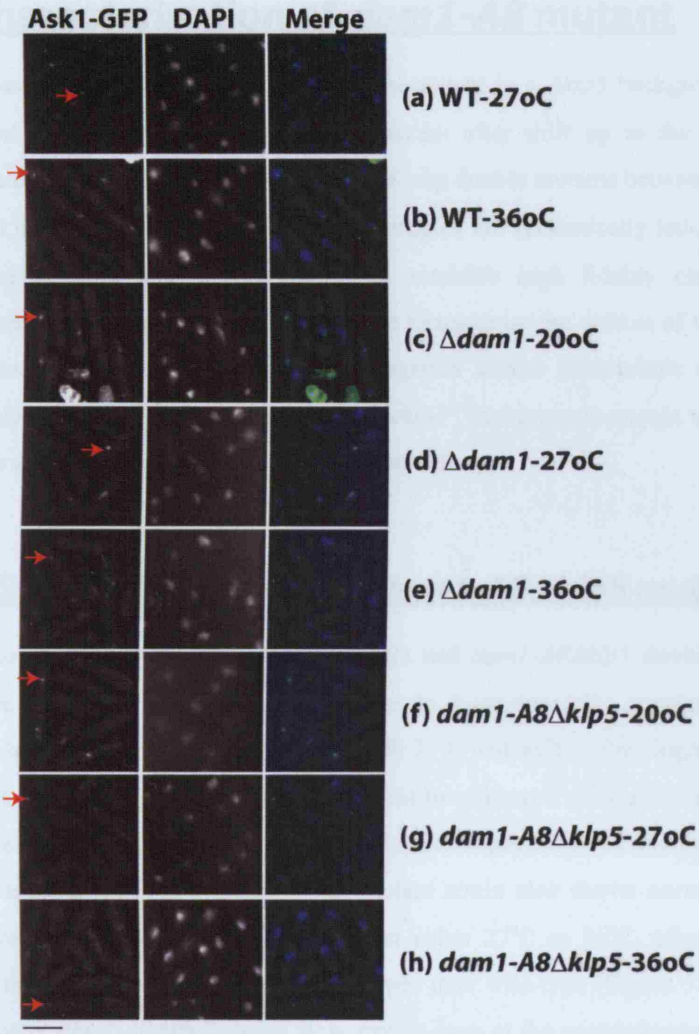

Figure 5.6: Ask1-GFP localisation in WT, *Δdam1* and *dam1-A8Δklp5* cells.

WT, *Δdam1* and *dam1-A8Δklp5* cells containing *ask1*$^{+}$*-GFP-kan* were cultured in rich medium at 27°C. The cultures were split and incubated at either 20°C for 8 hours, 27°C for 4 hours, or 36°C for 4 hours. The cells were fixed and Ask1-GFP and DAPI visualised by fluorescence microscopy. **(a&b)** Ask1-GFP visualised in wild-type cells at 27°C and 36°C respectively. **(c&d&e)** Ask1-GFP visualised in *Δdam1* cells at 20°C, 27°C and 36°C respectively. **(f&g&h)** Ask1-GFP visualised in *dam1-A8Δklp5* cells at 20°C, 27°C and 36°C respectively. The scale bar represents 10μm. The Red arrows highlight Ask1-GFP.

5.4 Characterisation of *dam1-A8* mutant

We successfully generated a *dam1* conditional mutant in a *Δklp5* background. The analysis of the mitotic phenotype of this mutant after shift up to the restrictive temperature should aid in our understanding of why double mutants between *Δklp5* or *Δklp6* and null mutants of the Dam1/DASH complex are synthetically lethal and thus how these proteins function in concert to establish high fidelity chromosome segregation. In this section we will attempt to characterise the defects of this double mutant *dam1-A8Δklp5* in chromosome segregation and/or microtubule regulation. We will also analyse the single *dam1-A8* (in a $klp5^+$ background) mutant to ascertain if it shows any mitotic chromosome segregation defects.

5.4.1 Growth defects of the *dam1-A8Δklp5* mutant

In order to ascertain how the *dam1-A8* single and *dam1-A8Δklp5* double mutants behave we first examined their growth rates in logarithmically growing cultures compared to wild-type and *Δdam1* cells at both 27°C and 36°C. The single *dam1-A8* mutant showed growth kinetics almost identical to wild-type cells at both 27°C and 36°C, indicating that in a $klp5^+$ background this strain does not show any proliferative defects (Figure 5.7A). The single *Δklp5* mutant strain also shows normal growth kinetics for the first 4 hours of incubation at either 27°C or 36°C, after this time however; the growth becomes marginally slower than wild-type (Figure 5.7A). The double mutant *dam1-A8Δklp5* shows slow growth even at the permissive temperature of 27°C, with a doubling time of approximately 4 hours, whilst wild-type cells have a doubling time of approximately 3 hours. Incubation of this strain at the restrictive temperature of 36°C severely compromises growth, with a doubling time now of approximately 6 hours (Figure 5.7A). It seems that this double mutant while able to grow at 27°C does not show normal growth kinetics and is functionally compromised at this permissive temperature.

We examined the *dam1-A8Δklp5* cell morphology by light microscopy at 27°C and every two hours after the shift up to 36°C. The majority of cells look relatively normal at 27°C although there are a few cells with aberrant morphology, however this is increased following the shift up to the restrictive temperature with the appearance of some multi-septated, bent or branched and dead cells (Figure 5.7B).

(A)

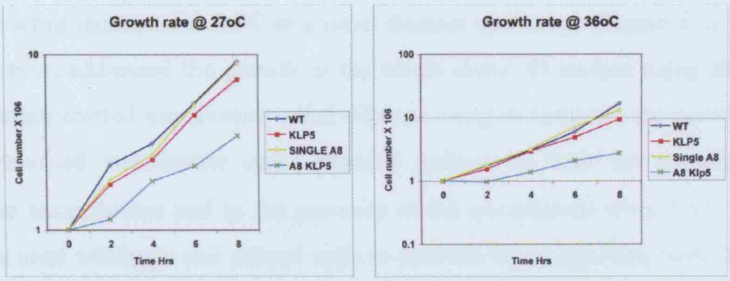

(B)

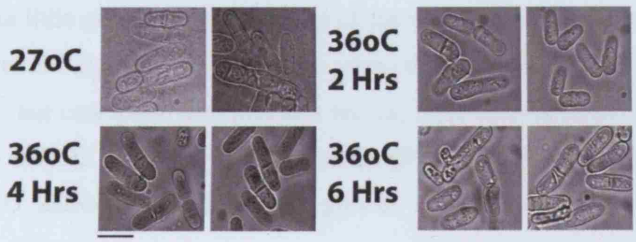

(C)

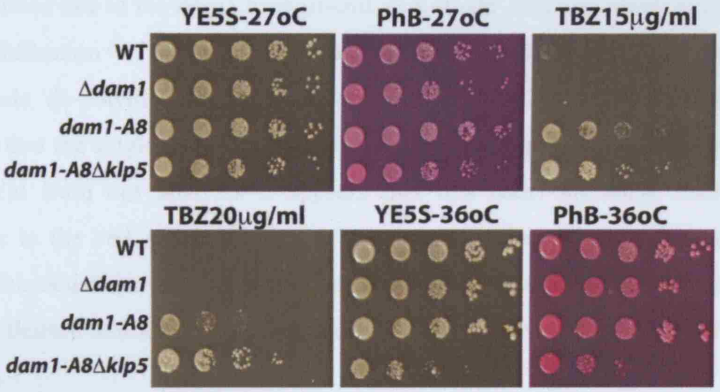

Figure 5.7: Growth defects in *dam1-A8Δklp5* cells at the restrictive temperature

(A) WT, *klp5Δ*, *dam1-A8* and *dam1-A8Δklp5* cells were cultured in rich medium at 27°C. The cultures were split, incubated at either 27°C or 36°C and the cell number was counted every 2 hours. The cell number was plotted against time. **(B)** Images of *dam1-A8Δklp5* cells from various time-points shown. The scale bar represents 10µm. **(C)** Tenfold serial dilution spot assay of WT, *Δdam1*, *dam1-A8* and *dam1-A8Δklp5* cells plated onto rich agar YE5S plates, YE5S & Phloxin plates and YE5S plates containing TBZ (Thiabendazole) 10µg/ml, or 20µg/ml concentrations.

We have previously shown that the *dam1-A8Δklp5* strain appears temperature sensitive when incubated at 36°C in a serial dilution spot assay (Figure 5.2). We had not, however, addressed the growth of the single *dam1-A8* mutant using this assay. We therefore carried out another serial dilution assay to compare the growth of the single *dam1-A8* and double *dam1-A8Δklp5* mutants at both the permissive and restrictive temperatures and in the presence of the microtubule drug TBZ. In this assay we used wild-type and *Δdam1* cells as controls for comparison with the *dam1-A8* single and double mutants. The wild-type cells showed normal growth at 27°C and 36°C, but little growth in the presence of the microtubule de-polymerising drug TBZ (Figure 5.7C). The *Δdam1* cells also showed normal growth at both temperatures, but consistent with previous results, these cells were more sensitive to the presence of TBZ than the wild-type strain (Figure 5.7C). The double mutant *dam1-A8Δklp5* showed almost normal growth 27°C but growth defects when incubated at 36°C. This double mutant can grow in the presence of TBZ, even at concentrations such as 20μg/ml or 50μg/ml (data not shown). This TBZ resistance was presumed due to the *Δklp5* background, as a single *Δklp5* or *Δklp6* mutant shows hyper-stabilisation of microtubules and strong resistance to TBZ and other microtubule de-polymerising drugs (Garcia et al., 2002b). We did not expect therefore that the single *dam1-A8* mutant in a *klp5*$^+$ background would be resistant to TBZ. Yet from our analysis it appears that this *dam1-A8* allele confers TBZ resistance to the cell, albeit this is not as strong as when Klp5 is deleted (Figure 5.7C). This resistance to TBZ is completely contrasting to the sensitivity seen when Dam1 is deleted and again suggests that this allele is not a simple loss of function mutation.

5.4.2 Mis-segregation of chromosomes in *dam1-A8Δklp5* mutant

It was previously shown that cells deleted for both *klp5*$^+$ and *dam1*$^+$ show kinetochore bi-orientation defects (Sanchez-Perez et al., 2005). It was presumed therefore that the reason for the lethality in these double deletion mutants was due to severe chromosome mis-segregation and an inability to establish correctly bi-oriented kinetochore attachments (Sanchez-Perez et al., 2005). We therefore examined whether the *dam1-A8Δklp5* mutant also yields cells with severe chromosome mis-segregation.

We firstly stained α-tubulin and DAPI of both wild-type and *dam1-A8Δklp5* cells, by immunoflourescence, at both the permissive temperature 27°C and at 2, 4 and 6 hours following shift up to the restrictive temperature of 36°C. The wild-type cells showed normal segregation of chromosomes, as marked by DAPI staining of the DNA, and also normal interphase and mitotic microtubule structures (Figure 5.8A). The double mutant *dam1-A8Δklp5* showed a typical *Δklp5/6* phenotype with respect to microtubule structure, with hyper-elongated interphase microtubules that often wind round the cell and with hyper-stabilised mitotic spindles. There were obvious chromosome segregation defects in these cells, which became extremely prominent after 4 and 6 hours incubation at the restrictive temperature (Figure 5.8A). The DNA in some cells at the 6 hour time-point looked extremely fragmented however it was not possible from this analyses to determine the types of segregation defects that gave rise to this severe mis-segregation phenotype.

In a similar experiment wild-type, *Δklp5, dam1-A8Δklp5* and *dam1-A8* single mutant cells were analysed for the frequency of mis-segregation of chromosomes following their incubation at either 27°C or 36°C for up to 6 hours. These cells were harvested every two hours after shift up to the restrictive temperature, fixed in formaldehyde and stained with DAPI to visualise any mis-segregation of chromosomes. The percentage of total cells that showed aberrantly segregated DNA for each strain at each time-point was calculated and graphed. Both wild-type and single *dam1-A8* cells show very little mis-segregation of chromosomes, while the single *dam1-A8* mutant does not behave as wild-type with respect to TBZ it does not show a high rate of chromosome mis-segregation (Figure 5.8B). The single *Δklp5* strain shows some segregation defects (approximately 9-13%) at either 27°C or 36°C.

The double mutant *dam1-A8Δklp5* shows a level of mis-segregation at the permissive temperature of 27°C, comparable to the single *Δklp5* mutant. The frequency of mis-segregation increases dramatically, however, following incubation at the restrictive temperature, with 71.7% of cells showing aberrantly separated DNA after 6 hours at 36°C. It would seem that these cells predominantly die at this temperature due to improper mis-segregation, however to address this more carefully we will examine segregation defects in synchronous *dam1-A8Δklp5* cells at the restrictive temperature.

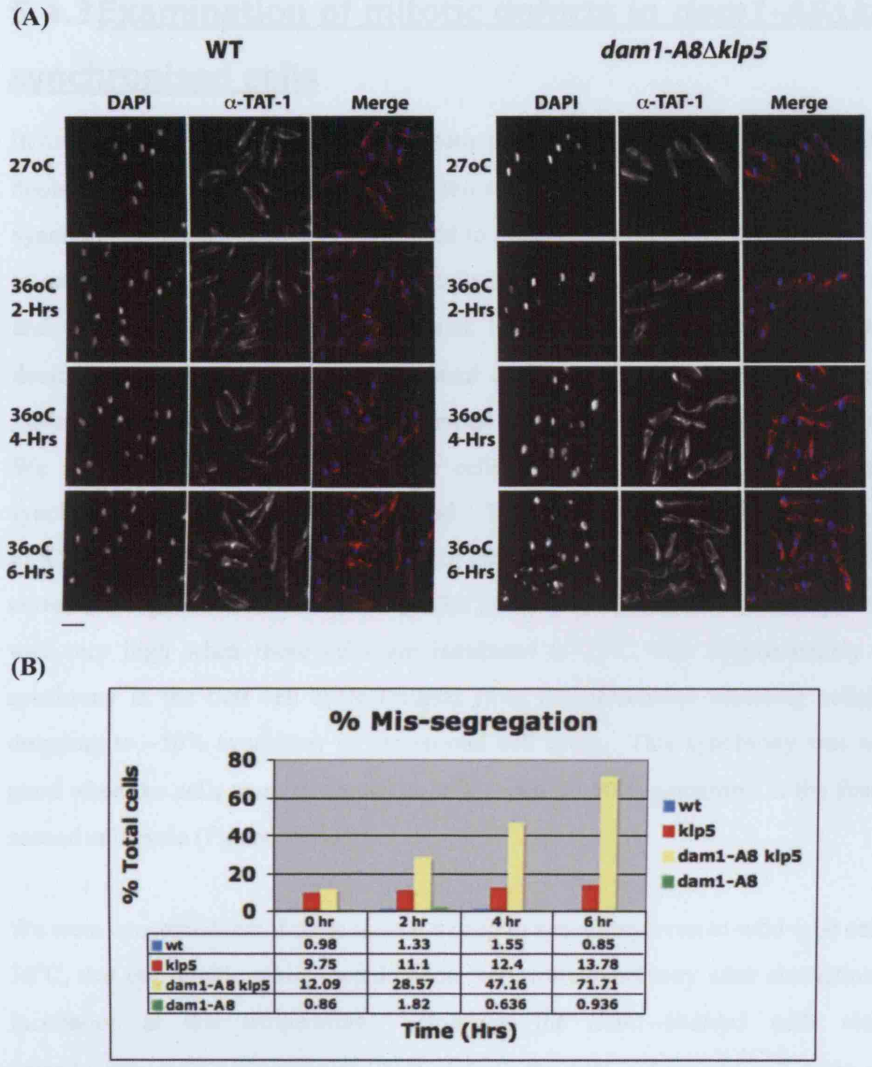

Figure 5.8: Chromosome segregation defects in *dam1-A8Δklp5* mutant.

(A) WT and *dam1-A8Δklp5* cells were cultured in rich medium overnight at 27°C. The cultures were split and incubated at either 27°C or 36°C for up to 6 hours. The cells were fixed and immunoflourescent staining of microtubules and DNA was carried out. The scale bar represents 10μm. **(B)** Graph of the frequencies of mis-segregation counted from fixed and DAPI stained WT, *Δklp5*, *dam1-A8Δklp5*, and *dam1-A8* single mutant cells (N>200 cells).

5.4.3 Examination of mitotic defects in *dam1-A8Δklp5* synchronised cells

In order to more carefully assess the mitotic phenotype seen when the *dam1-A8Δklp5* double mutant cells are shifted up to the restrictive temperature we attempted to synchronise the double mutant cells prior to incubation at the restrictive temperature to enrich for the mitotic population of cells and more carefully ascertain how, when and why these cells die. Due to the sick nature of these *dam1-A8Δklp5* cells we decided against using a cell cycle mutant or drug to induce an arrest, and opted instead for centrifugal elutriation as a mode of synchrony to collect early G2 cells. We first collected early G2 wild-type cells as a control to assess the degree of synchronisation when using this method. These cells were then incubated at both 27°C and 36°C for 5 hours, fixed every 20 minutes and the septation index counted to assess the degree of synchronisation. The level of synchrony in the wild-type strain was very high when these cells are incubated at 27°C with approximately 70% synchrony in the first cell cycle (judged from the percentage septating cells) and dropping to ~50% synchrony in the second cell cycle. This synchrony was not as good when the cells were incubated at 36°C, with 40-50% synchrony in the first and second cell cycle (Figure 5.9A).

We were concerned that if there is such a drop in synchrony even in wild-type cells at 36°C, that our double mutant would show very little synchrony after elutriation and incubation at this temperature. However the *dam1-A8Δklp5* cells showed reproducibly good synchrony of ~45% in both the first and second cell cycle when incubated at this temperature. We therefore perceived this to be an efficient method to synchronise our cells for the careful analysis of mitotic defects at the restrictive temperature in our double mutant.

Using this method we synchronised *dam1-A8Δklp5* cells in early G2 and incubated the collected cells at 36°C for 320 minutes. The cells were harvested every 20 minutes and the degree of synchronisation assessed by calcoflour staining as approximately 45%, with the time prior to the peak of septation indicative of the timing of mitosis. The frequency of mis-segregation at each time-point was then measured by DAPI staining and counting the number of cells displaying aberrant DNA.

(A)

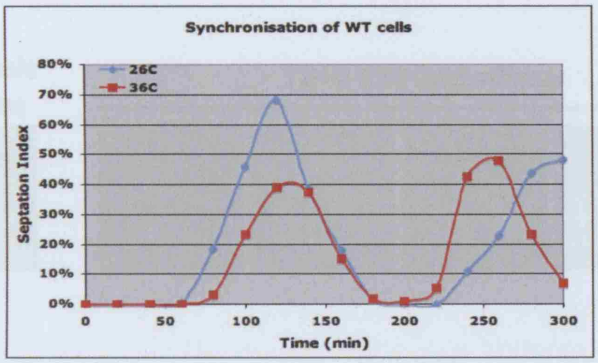
Synchronisation of WT cells
26C
36C
Septation Index
80%
70%
60%
50%
40%
30%
20%
10%
0%
0
50
100
150
200
250
300
Time (min)

(B)

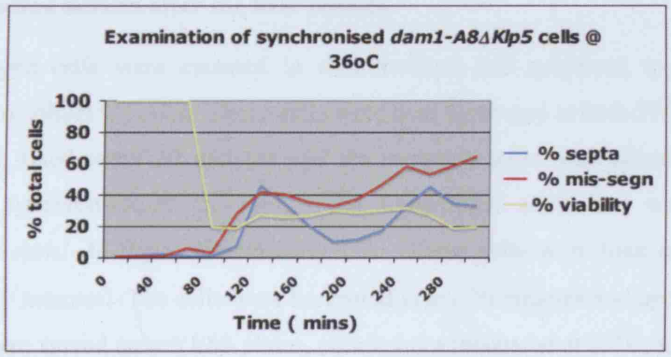
Examination of synchronised dam1-A8ΔKlp5 cells @ 36oC
% total cells
100
80
60
40
20
0
0
40
80
120
160
200
240
280
Time (mins)
% septa
% mis-segn
% viability

(C)

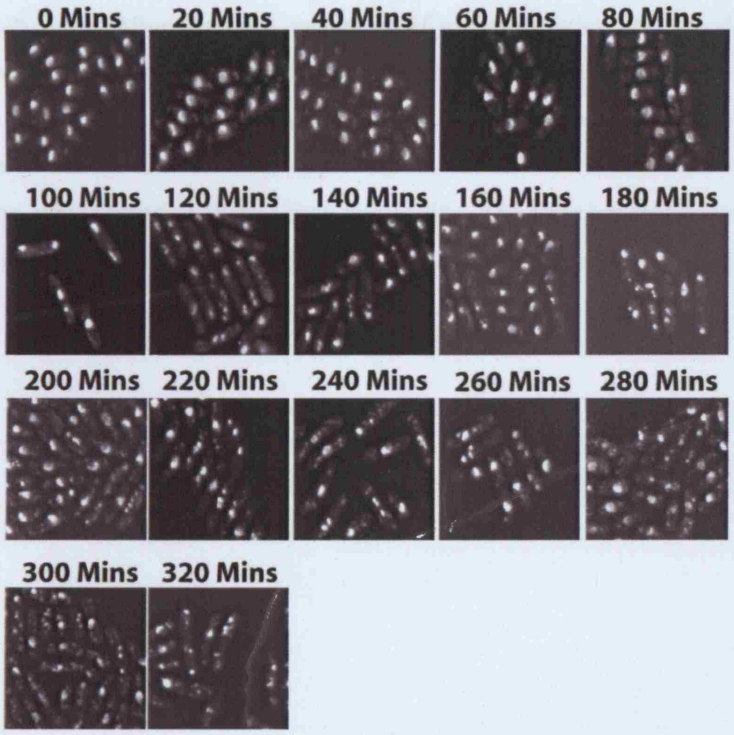
0 Mins
20 Mins
40 Mins
60 Mins
80 Mins
100 Mins
120 Mins
140 Mins
160 Mins
180 Mins
200 Mins
220 Mins
240 Mins
260 Mins
280 Mins
300 Mins
320 Mins

(D)

Figure 5.9: *dam1-A8Δklp5* mutants show loss of viability and severe chromosome mis-segregation defects after the first mitosis.

(A) Wild-type cells were cultured in rich medium and subjected to centrifugal elutriation to collect G2 cells. These cells were then incubated at both 27°C and 36°C for 5 hours; fixed every 20 minutes and the septation index was calculated as the degree of synchronisation (N>200). **(B)** Centrifugal elutriation was used to synchronise *dam1-A8Δklp5* cells in early G2. These cells were then incubated at 36°C for 320 minutes. The cells were harvested every 20 minutes and approximately 500 cells were spread onto YE5S plates, which were incubated at 27°C, to assess the viability of these cells at each time-point. The remaining cells were fixed, stained with DAPI or calcoflour and the frequency of mis-segregation and the degree of synchronisation calculated and graphed along with the frequency of viability (N>200). **(C)** Images of DAPI stained cells from each time-point. Chromosome segregation defects are obvious, appearing in cells from ~ 100 minutes after incubation, which coincided with a drop in viability. The scale bar represents 10 μm. **(D)** Images of cells containing calcoflour stained septa. The scale bar represents 10μm.

We can see that the frequency of mis-segregation rises to ~40% after the first mitosis, but this has increased dramatically to around 70% of cells displaying abnormal DNA after the second mitosis (Figure 5.9B). Indeed visualisation of these DAPI stained cells shows the clear appearance of mis-segregation and aberrant DNA from 100 minutes after incubation at the restrictive temperature. The severity of mis-segregation increases following the second mitosis at the restrictive temperature with cells from 220 minutes onwards showing extremely fragmented DNA (Figure 5.9C) .

Examination of those cells stained for calcoflour to highlight septa formation show normal septum structures after the first mitosis, however, the staining at later time-points, corresponding with the second mitosis, shows some cells with abnormal deposition of septa material, while some appear multi-septated (Figure 5.9D). We presume this is a secondary effect of the severe chromosome segregation defects in these cells. These cells were also subjected to a viability assay to determine the timing of when the majority of these cells die. At each time-point approximately 500 cells were plated onto YE5S plates and incubated for several days at 27°C. The number of viably growing colonies were then counted and calculated as a percentage against the viability (100%) at time-point zero. In our analyses it is clear that there is a huge drop in viability during the first mitosis, just prior to the first septation peak with the viability dropping down to ~20%. It thus appears as cells enter the first mitosis following shift up to the restrictive temperature that they are committed to a lethal mitotic event resulting in massive chromosome mis-segregation (Figure 5.9B).
We carefully assessed the microtubule structure in these synchronised *dam1-A8Δklp5* cells. These cells were synchronised in G2 and shifted up to the restrictive temperature. The cells were harvested every 20 minutes, fixed in methanol, microtubules and DAPI stained by immunoflourescence and examined by flourescence microscopy. The microtubules in this mutant appeared similar to those seen in a single *Δklp5/6* null mutant, or in asynchronous *dam1-A8Δklp5* cells (Figure 5.8), with strong tubulin staining in both interphase and mitotic cells indicative of very stable microtubules. Our analysis of microtubules at each timepoint did not highlight any defect that was previously unseen in our staining of microtubules in asynchronous *dam1-A8Δklp5* cells (Figure 5.10). It appears that the microtubule structure is not noticeably destabilised or altered in these cells.

We next categorised the mis-segregating mitotic cells according to type. We noticed four major mis-segregating phenotypes present in these cells. Type 1: reflects cells in

which the entire DNA is being segregated to one side of the cell. Type 2: these are the cells that are displaying a typical "*mis*" mutant phenotype of unequal segregation with large and small daughter nuclei. Type 3: Cells in which there are 3 or more bodies of DNA, some of which appear to be lagging. Type 4: Cells with only 2 DNA bodies in which one appears to be lagging behind during the segregation process. We quantified the distribution of the four types of mis-segregating cells visible during the first mitosis between 80 and 140 minutes when the cells were predominantly in mitosis (Figure 5.10B). Type 4 was only visible in the early stage of mitosis (80 mins) and the lagging DNA in these cells had obviously segregated in the manner of type 1, 2 or 3 by the time the next sample at 100 minutes was analysed. Overall throughout this first mitosis there was no type of aberrant DNA pattern that predominated, with Type 1 and Type3 showing an average for the four timepoints of ~33% and Type 2 showing ~26%, suggesting form our DAPI analyses that a range of chromosome segregation defects are occurring in these cells, including lagging chromosomes, unequal distribution of chromatin and fragmented DNA.

It is apparent in these cells that the DNA, which is in the process of being segregated, is always associated with the mitotic spindle. There are no incidences of DNA bodies completely un-associated from the mitotic spindle (Figure 5.10d-i). We can only assume that while there are obvious segregation defects in these cells the chromosomes are attached in some capacity to the spindle. Perhaps this association to microtubules is by a lateral attachment of the kinetochores to the mitotic microtubules, and end-on attachment is not fully established in these cells, resulting in severe mis-segregation of chromosomes. However this is simply speculative and no concrete evidence exists to corroborate this at this time.

5.5 The spindle assembly checkpoint and the *dam1-A8* mutant

Due to the slow doubling time of the *dam1-A8Δklp5* strain when grown at the permissive temperature and the massive mis-segregation of chromosomes at the restrictive temperature we presume that the spindle assembly checkpoint is also activated in these double mutant cells. We will assess whether there is a noticeable increased frequency of mitotic cells in our *dam1-A8Δklp5* double mutant and whether this delay is indeed dependent on the spindle assembly checkpoint.

(A)

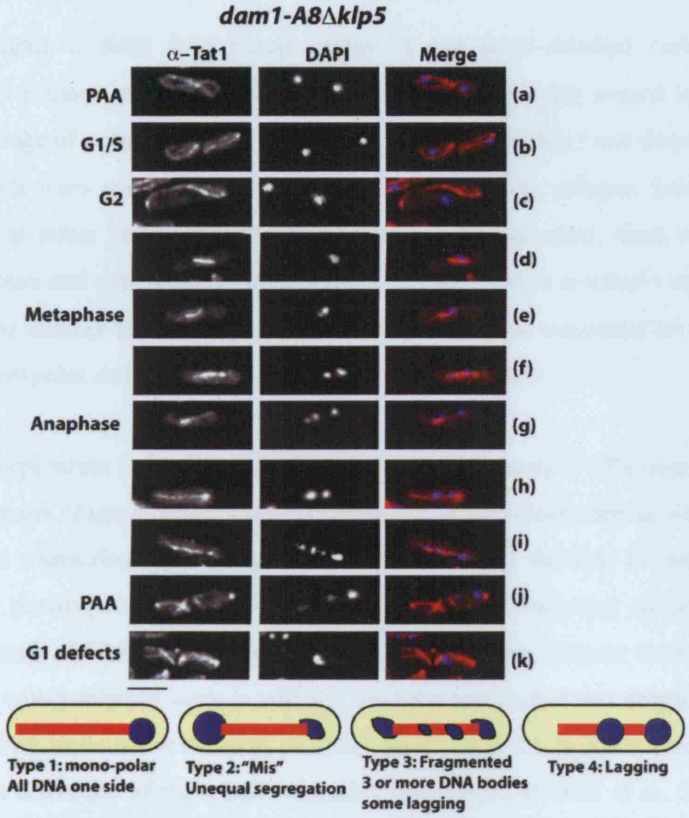

(B)

Time	Type 1	Type 2	Type 3	Type 4
80 mins	20%	13.3%	40%	26.6%
100 mins	45.45%	36.36%	18.18%	-
120 mins	27.58%	34.48%	37.93%	-
140 mins	41.6%	22.22%	36.11%	-
Average	33.675%	26.59%	33.055	6.65

Figure 5.10: Microtubule staining and chromosome mis-segregation of *dam1-A8Δklp5* cells

(A) Cells were synchronised in G2 by elutriation, shifted up to 36°C for 320 minutes, fixed and processed for immunoflourescence every 20 minutes. The microtubules were stained using α-TAT-1 primary antibody and DNA stained by DAPI. The cells were visualised by fluorescence microscopya. **(a-h)** Images which are representative of the aberrant *dam1-A8Δklp5* mitotic cells. The scale bar represents 10 μm. **(B)** Schematic and table showing frequency of four types of aberrant segregation pattern (N>200).

5.5.1 Increased mitotic index in *dam1-A8Δklp5* cells

To investigate if there is a mitotic delay in our *dam1-A8Δklp5* cells we first determined if there is an increased mitotic index in this double mutant by counting the percentage of mitotic cells. Wild-type, *Δklp5*, *dam1-A8Δklp5* and *dam1-A8* single mutant cells were cultured in rich YE5S medium at 27°C, cultures were split and incubated at either 36°C for 6 hours. The cells were harvested, fixed in methanol every 2 hours and processed for immunoflourescence to stain α-tubulin and DNA by DAPI. The number of cells displaying mitotic spindles was calculated for each strain at each time-point and measured as a percentage of total cells.

Our wild-type strain showed a mitotic index of approximately 5-10% over the course of the 6 hours (Figure 5.11). This is consistent with values seen in our previous experiment measuring the mitotic index in Dam1/DASH deletion mutants. (Figure 4.4) Our positive control *Δklp5* showed an increased frequency of mitotic cells (approximately 14-16%) compared to the wild-type strain (Figure 5.8A). This is consistent with published work in which it has been established that deletion of either Klp5 or Klp6 leads to localisation of either Mad2 or Bub1 to the kinetochore and subsequent activation of the spindle assembly checkpoint. (Garcia et al., 2002b) The single *dam1-A8* mutant showed a modest increase in the frequency of mitotic cells compared to wild-type, with approximately 12-13% mitotic cells over the 6 hour experimental period. Therefore while there is no chromosome mis-segregation in this single *dam1-A8* mutant (Figure 5.11A), there are obviously some defects present which leads to a mitotic delay in these cells. The double mutant *dam1-A8Δklp5* cells shows a frequency of mitotic cells comparable to the single mutant *dam1-A8* or the single *Δklp5* mutants when incubated at the permissive temperature of 27°C or just 2 hours after shift up to 36°C. The frequency increases dramatically, however, after 4-6 hours prolonged incubation at the restrictive temperature, rising to between 25-28% (Figure 5.11A). It is quite clear that this dramatic rise in the number of mitotic cells must be due to a mitotic delay and this is probably mediated by the spindle assembly checkpoint.

We next examined Mad2-GFP foci localisation in wild-type, *dam1-A8* single and *dam1-A8Δklp5* double mutants at 27°C and every two hours after shift-up to 36°C. Approximately 5% of wild-type cells displayed Mad2-GFP foci localisation at either 27°C or 36°C. The single *dam1-A8* mutant had approximately 9-15% of cells displaying Mad2-GFP foci at either 27°C or 36°C (Figure 5.11B). The double mutant

(A)

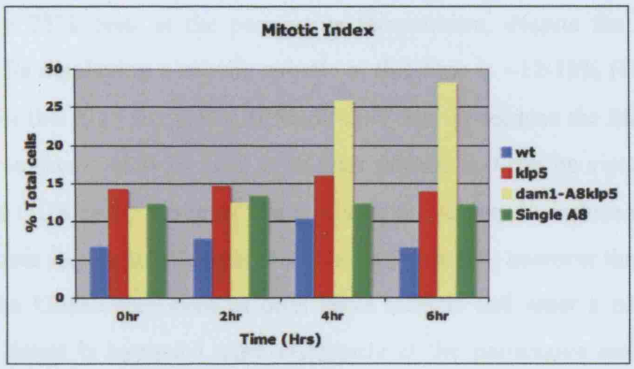

(B)

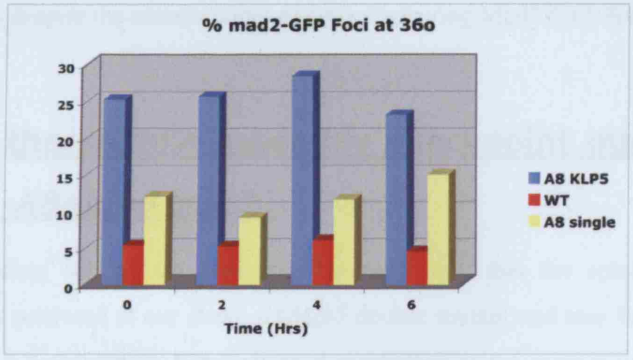

Figure 5.11: Mitotic delay induced by spindle assembly checkpoint in *dam1-A8* and *dan1-A8Δklp5* cells.

(A) WT, *Δklp5, dam1-A8Δklp5* and *dam1-A8* cells were cultured in rich YE5S medium at 27°C, split and incubated at 36°C for 6 hours. The cells were fixed and processed for immunoflourescence to stain α-tubulin and DAPI. The percentage of cells displaying mitotic spindles were counted and graphed at each time-point (N>200). **(B)** WT, *dam1-A8Δklp5* and *dam1-A8* single mutant cells containing *mad2*$^{+}$*-GFP* were cultured in rich YE5S medium at 27°C and shifted up to 36°C for 6 hours. The cells were fixed and examined for Mad2-GFP foci localisation by fluorescence microscopy. The scale bar represents 10 μm. (N>200).

dam1-A8Δklp5 shows an extremely elevated level of Mad2-GFP foci localisation of approximately 25% even at the permissive temperature, despite the fact that the number of cells displaying a mitotic spindle at this time is ~12-13% (Figure 5.11B). The reason for this high frequency of Mad2-GFP foci is because the Mad2-GFP foci persist in these *dam1-A8Δklp5* cells even after mitosis and can be visualised in post anaphase and G1/S cells. It seems that a mitotic arrest may be induced, but as there are chromosome segregation defects this arrest is bypassed, however the Mad2 signal remains at the kinetochore even as cells leave mitosis and enter a new cell cycle. Perhaps this arrest is bypassed more efficiently at the permissive temperature, but prolonged incubation at the restrictive temperature results in a greater frequency of arrested cells despite the same number of cells displaying Mad2-GFP foci.

5.5.2 Is the spindle assembly checkpoint maintained in *dam1-A8Δklp5* cells?

In the preceding section we discussed the possibility that the spindle assembly checkpoint is activated in our *dam1-A8Δklp5* double mutant and may be bypassed at the permissive temperature, but prolonged incubation at the restrictive temperature may lead to full activation of this checkpoint and an increased frequency of cells arrested in mitosis. We wondered whether the spindle assembly checkpoint would be maintained in these cells, in conditions where de-polymerisation of the mitotic spindle induces a mitotic arrest.

We arrested wild-type and *dam1-A8Δklp5* cells with 11mM HU for four hours. After washout, we re-suspended the cells in medium with or without MBC/CBZ (Carbendazim) at 50μg/ml and incubated at either 27°C or 36°C for 5 hours. Cells were harvested every hour, stained with DAPI and calcoflour to visualise DNA and septa, and the percentage of cells displaying "cut" DNA was calculated as a measure of the maintenance of mitotic arrest. Wild-type cells without MBC/CBZ at either 27°C or 36°C did not show "cut" cells. Incubation of wild-type cells at 27°C resulted in the appearance of "cut" cells between 2-3 hours after the addition of medium containing MBC/CBZ. This increased dramatically when these wild-type cells were incubated in the presence of MBC/CBZ at 36°C, with "cut" cells appearing as early as 1.5 hours after incubation. Therefore the stringency of the mitotic arrest is not very high when treated with MBC/CBZ 50μg/ml and incubated at 36°C.

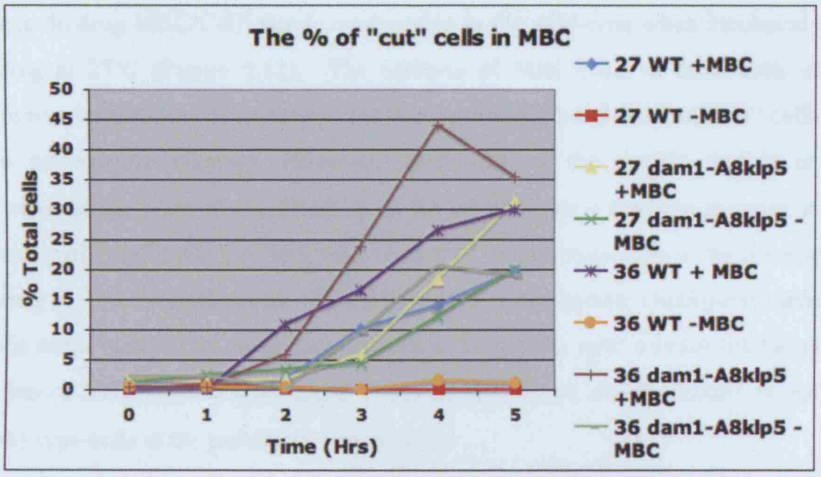

Figure 5.12: Is the spindle checkpoint maintained in *dam1-A8Δklp5* cells?

WT and *dam1-A8Δklp5* cells were cultured in rich medium at 27°C and arrested in S-phase by the addition of 11mM HU for 4 hours. The cells were filtered, washed and re-suspended in medium with or without 50μg/ml MBC/CBZ and incubated at either 27°C or 36°C for 5 hours. The cells were harvested every hour for 5 hours after MBC/CBZ addition, stained with DAPI and calcoflour to visualise DNA and septa and visualised by fluorescence microscopy. The percentage of cells displaying hypercondensed and "cut" DNA were counted at each time-point and plotted against time (N>200).

The double mutant *dam1-A8Δklp5* shows a level of "cut" cells even in the absence of the spindle drug MBC/CBZ that is comparable to the wild-type when incubated with the drug at 27°C (Figure 5.12). The addition of MBC/CBZ to these cells at the permissive temperature does not elevate this beyond the basal level of "cut" cells this strain intrinsically displays. However, incubation of the double mutant at the restrictive temperature in the presence of the drug causes a massive increase in the frequency of "cut" cells, yet the timing compared to wild-type cells in the presence of the drug at 36°C is unchanged. This indicates that the spindle checkpoint mediated mitotic arrest induced by de-polymerisation of the spindle microtubules following the addition of MBC/CBZ is maintained in the double mutant *dam1-A8Δklp5* as well as in wild-type cells at the restrictive temperature.

5.5.3 *dam1*-A8Δklp5 cells require *mad2*$^+$ for survival

We have shown that the spindle assembly checkpoint is activated in *dam1-A8Δklp5* cells. We theorised that the cells must need the checkpoint-induced delay to try and allow the cells to correct the kinetochore-microtubule interaction defects that are occurring in mitosis. If it were the case removal of this checkpoint through deletion of Mad2 or Bub1 proteins, which mediate the signalling cascade, must result in exacerbation of the mitotic defects seen in these *dam1-A8Δklp5* cells. We therefore attempted to construct a triple mutant strain by crossing the *dam1-A8Δklp5* double mutant to a strain in which *mad2* is deleted. We were unable to pick up the triple *dam1-A8Δklp5mad2* strain by random spore analysis and it thus appeared that deletion of *mad2* in this double mutant is synthetically lethal (data not shown).

We confirmed this synthetically lethality by tetrad analysis. The *dam1-A8Δklp5* strain, which contains a kanamycin (G418) marker tagged to the *dam1*-A8 and is protrophic for uracil, was crossed to a Δ*mad2* strain, which is protrophic for leucine, and the four spores from the ascii formed were dissected by a micromanipulator. The four spores from each ascus were separated linearly onto YE5S rich media plates, incubated at 27°C for several days and allowed to form colonies. These colonies were then replica plated onto G418, EMM-uracil, EMM-leucine and Phloxin B plates at both 27°C and 36°C and the segregation pattern of the different markers was examined.

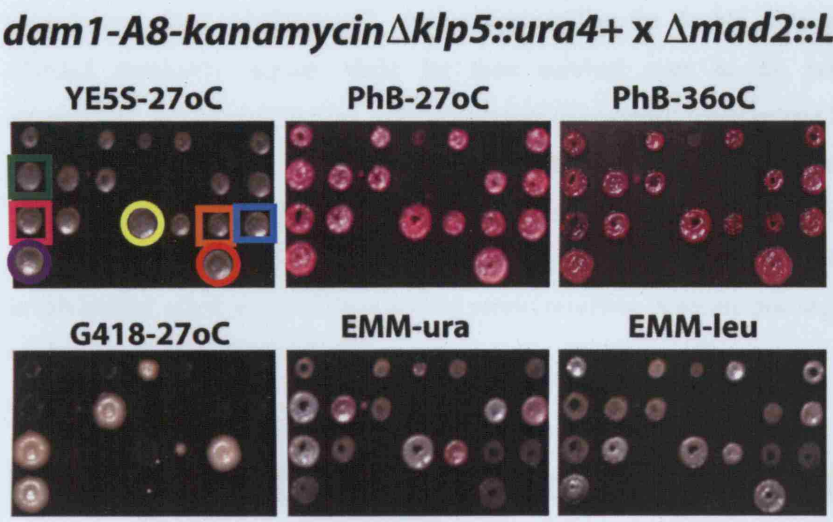

Figure 5.13: Deletion of Mad2 is synthetically lethal with the *dam1-A8Δklp5* mutant

Confirmation of the synthetic lethality of a *mad2*$^{+}$ deletion with the double mutant *dam1-A8Δklp5*. The double mutant strain *dam1-A8-kanΔklp5::ura4*$^{+}$ was crossed to a *Δmad2::LEU2* strain and after colony formation the resultant progenies were replica plated onto YE5S and Phloxin B plates at 27°C and 36°C, G418 EMM-leucine and EMM –uracil selection plates. The wild-type progeny are marked by a blue box, *Δklp5* colonies are marked by a green box, the single *dam1-A8* progeny are marked by an orange box, the double mutants *dam1-A8Δklp5* are marked by a pink box, the single *Δmad2* colonies are marked by a red circle, the *Δklp5mad2* colonies are marked by a yellow circle and the *dam1-A8Δmad2* colonies are marked by a purple circle.

Using this method we were able to select all combinations of progeny except the triple mutant *dam1-A8Δklp5mad2*. It thus appears that the double mutants *dam1-A8Δklp5* absolutely require Mad2 for their survival even at the permissive temperature. It is of note that we were also unable to construct triple mutant between *dam1-A8Δklp5* and *Δbub1* by random spore analysis (data not shown). The double mutants *dam1-A8Δklp5* appear to require the time provided by the spindle assembly checkpoint to perhaps activate some repair pathway to correct the attachment defects in this mutant, albeit many of these defects persist resulting in severe mis-segregation of chromosomes.

5.6 Analysis of types of segregation defects in fixed *dam1-A8* and *dam1-A8Δ klp5* cells

In this section we analyse whether the single *dam1-A8* mutant demonstrates a non-disjunction "*dis*" phenotype at 20°C, we also further examine the types of segregation defects seen in single *dam1-A8* and double *dam1-A8Δklp5* mutants by *cen2*-GFP analysis in fixed cells.

5.6.1 Does the single mutant *dam1-A8* show a non-disjunction "*dis*" phenotype at 20°C?

The single *dam1-A8* mutant does not behave like a *Δdam1* mutant with respect to TBZ sensitivity, however genetically it behaves in a similar manner, as it is synthetically lethal with *Δdis1* and shows exacerbated microtubule morphology and chromosome segregation defects with an *Δalp14* mutant. We examined whether the single *dam1-A8* mutant shows the *Δdam1* non-disjunction broken and elongated spindle phenotype when incubated at 20°C. We cultured the *dam1-A8* mutant cells in rich medium YE5S overnight at 27°C until log phase growth and then incubated the cells for 8 hours at 20°C. The cells were fixed in methanol, processed for immunoflourescence and tubulin and DAPI staining carried out.

The *dam1-A8* cells did not show a typical " *dis*" phenotype when incubated for a prolonged period of time at this temperature. The spindle microtubules appeared normal with no abnormally elongated mitotic spindles. Indeed the astral microtubules, which are notably absent in "*dis*" mutants when incubated at this

(A)

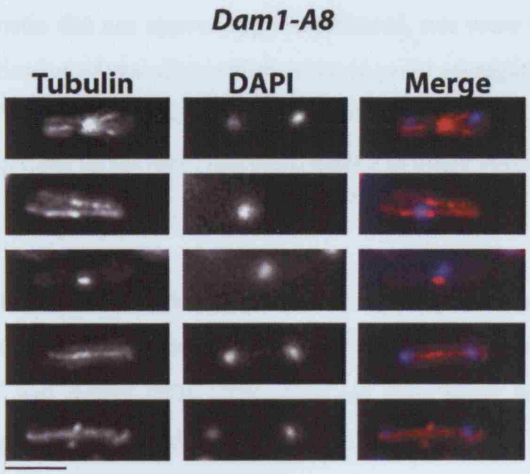

(B)

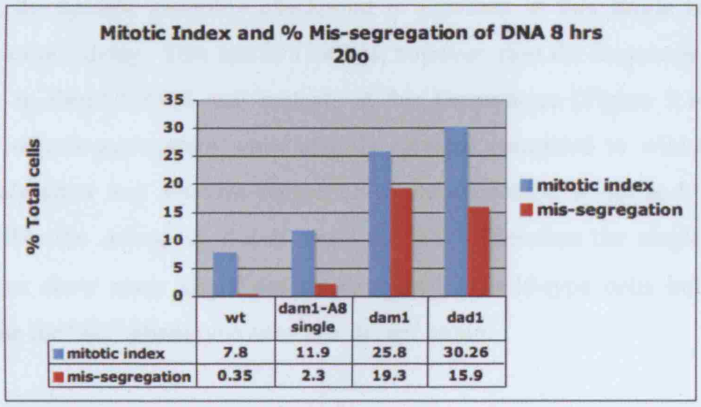

Figure 5.14: *dam1-A8* does not show a non-disjunction phenotype at 20°C.

(A) *dam1-A8* cells were cultured in rich medium, shifted to 20°C for 8 hours and fixed. The cells were processed and immunoflourescence of α-tubulin using α-Tat1 antibody and DAPI staining was carried out. Cells were viewed by fluorescence microscopy. The scale bar represents 10 μm. **(B)** Graph of the mis-segregation index as counted from WT, *Δdam1, Δdad1* and *dam1-A8* cells (N>200) in **(A).**

temperature, appeared normally positioned and intact. In the *dam1-A8* cells (Figure 5.14A), the chromatin did not appear hyper-condensed, nor were there any obvious DAPI patterns indicative of non-disjunction or mono-polar segregation, which can be seen in the Dam1/DASH deletion mutants when incubated at 20°C. The microtubules and chromatin structures in the *dam1-A8* cells looked in every respect normal (Figure 5.14A).

We next quantified the mitotic index and frequency of mis-segregation of chromosomes in these *dam1-A8* cells when incubated at 20°C and compared this to wild-type, *Δdam1* and *Δdad1* cells. The *dam1-A8* cells show an elevated rate of mitotic cells compared to the wild-type control. This is expected as we earlier saw approximately 9-15% Mad2-GF foci in this single mutant at either 27°C or 36°C indicating the spindle assembly checkpoint is activated in this single mutant and induces a mitotic delay. This rate is a lot less, however, than the frequency of mitotic cells seen in Dam1/DASH null mutants at this temperature (Figure 5.14B). The frequency of mis-segregation while slightly elevated compared to wild-type cells, which rarely show any aberrant separation of chromosomes, is not as high as that seen in either the *Δdam1* or *Δdad1* strain at 20°C. Therefore the single *dam1-A8* mutant does show some slight defects compared to wild-type cells but does not demonstrate the "*dis*" phenotype seen in a *Δdam1* strain.

5.6.2 Examination of sister-chromatid separation

To characterise further the types of chromosome segregation defects seen in the *dam1-A8Δklp5* double mutant we tried to construct a *dam1-A8Δklp5* strain containing *cen2*-GFP and Sad1-dsRed to carefully visualise sister-chromatid separation in these cells during mitosis. We were unable to easily construct a *dam1-A8Δklp5* strain containing cen2-GFP by random spore analysis as the *klp5* gene is linked to centromere two and homologous recombination always precludes the combination of both *Δklp5* and the integrated LacO array from being co-selected. Therefore we created a *dam1-A8Δklp6* strain containing *cen2*-GFP and Sad1-dsRed. Phenotypically there is no difference between *dam1-A8Δklp5* and *dam1-A8Δklp6* cells with both showing temperature sensitivity and mitotic defects (data not shown). We examined the separation pattern of *cen2*-GFP in asynchronous fixed *dam1-A8Δklp6* and *dam1-A8* single mutant cells at 27°C and 36°C and compared their

(A)

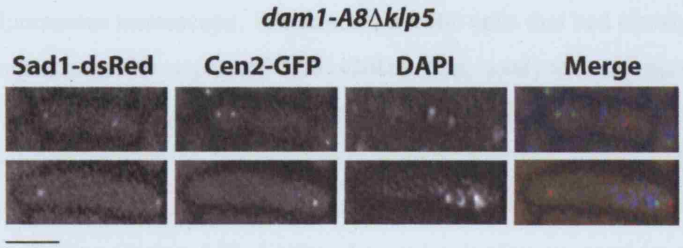

(B)

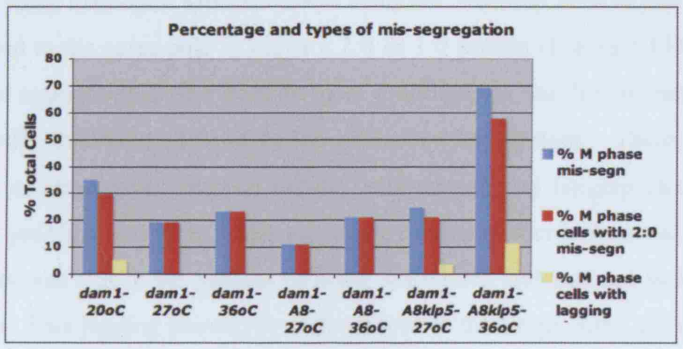

Figure 5.15: *dam1-A8Δklp5* mutant shows lagging chromosomes and mono-polar segregation of cen2-GFP sister chromatids

Δdam1, dam1-A8Δklp5 and *dam1-A8* single mutant cells containing *cen2*-GFP and Sad1-dsRed were cultured overnight in rich medium. The cultures were split and incubated at either 27°C for 4 hours, 36°C for 4 hours or 20°C for 8 hours prior to fixation. The cells were stained with DAPI and viewed under by fluorescence microscopy. **(A)** Images of Sad1-dsRed and *cen2*-GFP separation in *dam1-A8Δklp5* cells. The scale bar represents 10 μm. **(B)** The percentage of mitotic cells with mis-segregation were counted and graphed. The types of mitotic mis-segregation were further classified as mono-polar cells, i.e. cells with a 2:0 or 1:0 *cen2* separation pattern, or lagging cells and the frequencies of each graphed. (N>200)

segregation pattern to a *Δdam1* null mutant at 20°C, 27°C or 36°C on the Zeiss Axioplan fluorescent microscope. We selected mitotic cells that had clearly separated SPBS as represented by separated Sad1-dsRed foci, analysed and quantified the patterns of sister-chromatids *cen2*-GFP mis-segregation in these cells and graphed these frequencies for each of our mutants (Figure 5.15). The double mutant *dam1-A8Δklp5,* which showed a range of chromosome segregation defects from our DAPI and Tubulin staining (Figure 5.8), displayed a predominantly mono-polar segregation phenotype when *cen2*-GFP separation was analysed, whereby each of the two sisters is segregated to the same pole in either a 2:0 or 1:0 pattern (Figure 5.15A, B). This mono-polar segregation defect became more prominent in the double mutant *dam1-A8Δklp5* cells following shift up to the restrictive temperature. There is a small population of these double mutant mitotic cells that display lagging chromosomes, these were qualified as cells in which one of the *cen2*-GFP foci had moved to the pole but its sister was still in the process of being segregated and was not localised at or near a pole. This lagging phenotype is never seen in the single *dam1-A8* mutant and only ever seen in the *Δdam1* null mutant when incubated at 20°C, albeit the predominant phenotype in *Δdam1* at any temperature is a mono-polar segregation phenotype (Figure 5.15B). The frequency of mitotic cells that display mis-segregation in the single *dam1-A8* mutant containing *cen2*-GFP appears slightly increased compared to untagged *dam1-A8,* however this is still significantly lower than either the *Δdam1* or *dam1-A8Δklp5* mutants. Indeed these few instances of mitotic mis-segregation at either 27°C or 36°C appear to be cells in which mono-polar segregation occurs (Figure 5.15A, B).

It is intriguing that despite the obvious differences between the *Δdam1* and *dam1-A8* strains that the phenotype of Dam1/DASH null mutants and that of the double mutant *dam1-A8Δklp5* are essentially the same, with both mutants showing high rates of mono-polar segregation defects. The *Δdam1* cells which are sensitive to TBZ and form weak microtubule-kinetochore attachments give rise to defective syntelic mono-polar attachments, but also the *dam1-A8Δklp5* cells which are highly resistant to TBZ also give rise to these same syntelic mono-polar segregation defects. It thus appears that mono-polar segregation defects are not corrected in cells with attachments that are too weak as in *Δdam1* and other Dam1/DASH null mutants, or attachments that are too strong as is probably the case in the highly TBZ resistant *dam1-A8Δklp5* cells.

5.7 Live analysis of sister chromatid separation

We wished to carefully examine the mis-segregation phenotype in *dam1-A8Δklp5* cells to try and gain a further insight into how the double mutants are compromised in the formation of correct kinetochore attachments, and to more carefully analyse the single *dam1-A8* mutant cells during mitosis. We therefore decided to carry out live imaging of *cen2*-GFP and Sad1-dsRed in both the single *dam1-A8* and the double *dam1-A8Δklp6* strain using the Delta vision fluorescent inverted microscope. Filming (Timepoint 0:00) again started at prometaphase or metaphase when the two Sad1-dsRed signals had separated and was continued until after the sister-chromatids had segregated and anaphase B spindle elongation was carried out.

We first carried out live imaging of *cen2*-GFP and Sad1-dsRed in a control strain *Δklp6,* to ensure we were aware of the extent of the *Δklp6* phenotype and how it contributes to our double mutant *dam1-A8Δklp6*. It has been shown, by other members of this lab, that *Δklp6* cells have chromosome congression defects during mitosis. The *cen2*-GFP sister-chromatids in these cells never congress to the equator of the metaphase spindle but shuttle back and forth from one pole to the other before one sister separates right across the cell to the other pole (A. Unsworth personal communication). Consistent with this described phenotype we see a similar lack of congression of the *cen2*-GFP sisters to the equator and extreme oscillations of the pair of *cen2* signals from one pole to the next, before eventual separation by one of the sisters to the opposite pole (Figure 5.16A).

We next examined *cen2*-GFP and Sad1-dsRed separation in the double mutant *dam1-A8Δklp6* at room temperature (approximately 20°C-22°C). All of the cells examined (N=12) showed typical *Δklp6* congression defects and extreme oscillations of the sister-chromatids from one pole to the other prior to separation (Figure 5.16B). Within the *dam1-A8Δklp6* cells analysed (N=12) there is a population of cells (7/12, 58.33%) that segregated both sisters to opposite poles in a normal 1:1 manner. These cells are capable of carrying out equal separation of *cen2*-GFP at this temperature despite the obvious congression defects. The remaining *dam1-A8Δklp6* cells (5/12, 41.66%) showed a typical mono-polar segregation phenotype, whereby the *cen2*-GFP sister-chromatids failed to disjoin and are both segregated to the same pole (Figure 5.16B).

(A)

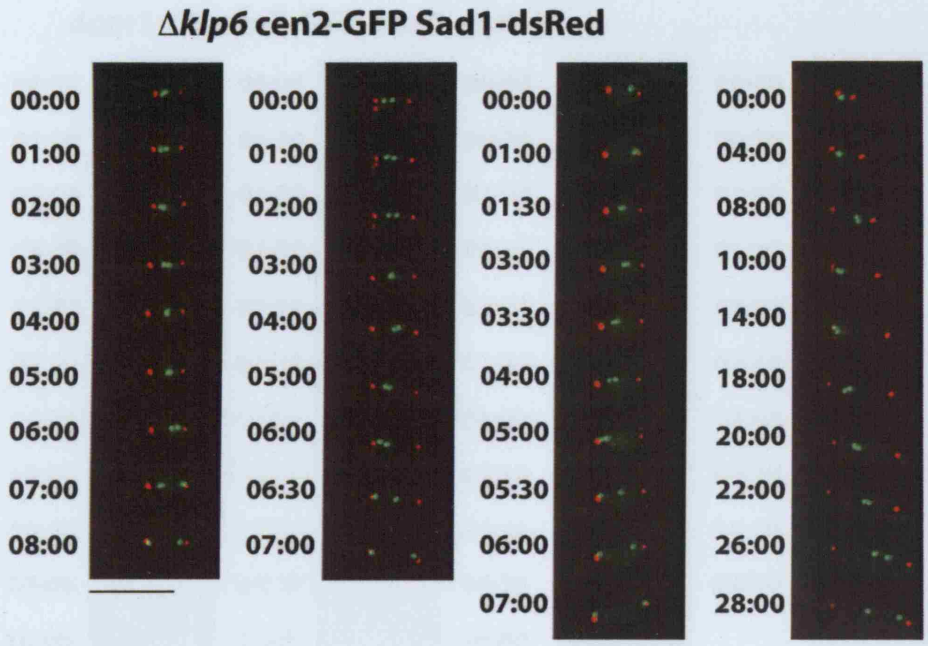
Δklp6 cen2-GFP Sad1-dsRed
00:00
01:00
02:00
03:00
04:00
05:00
06:00
07:00
08:00
00:00
01:00
02:00
03:00
04:00
05:00
06:00
06:30
07:00
00:00
01:00
01:30
03:00
03:30
04:00
05:00
05:30
06:00
07:00
00:00
04:00
08:00
10:00
14:00
18:00
20:00
22:00
26:00
28:00

(B)

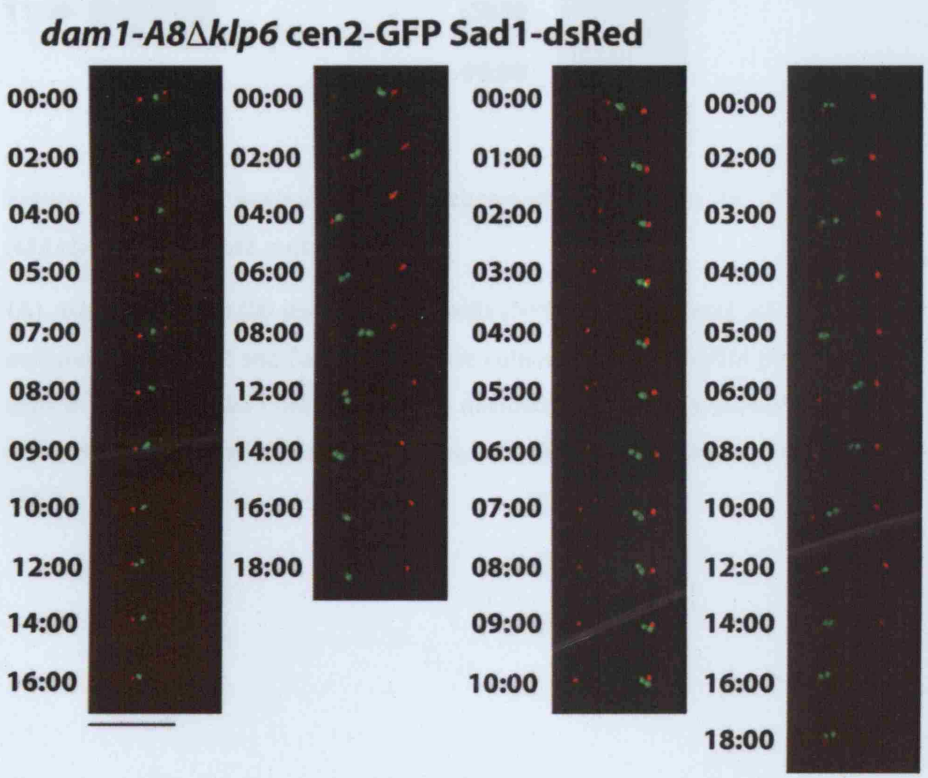
dam1-A8Δklp6 cen2-GFP Sad1-dsRed
00:00
02:00
04:00
05:00
07:00
08:00
09:00
10:00
12:00
14:00
16:00
00:00
02:00
04:00
06:00
08:00
12:00
14:00
16:00
18:00
00:00
01:00
02:00
03:00
04:00
05:00
06:00
07:00
08:00
09:00
10:00
00:00
02:00
03:00
04:00
05:00
06:00
08:00
10:00
12:00
14:00
16:00
18:00

(C)

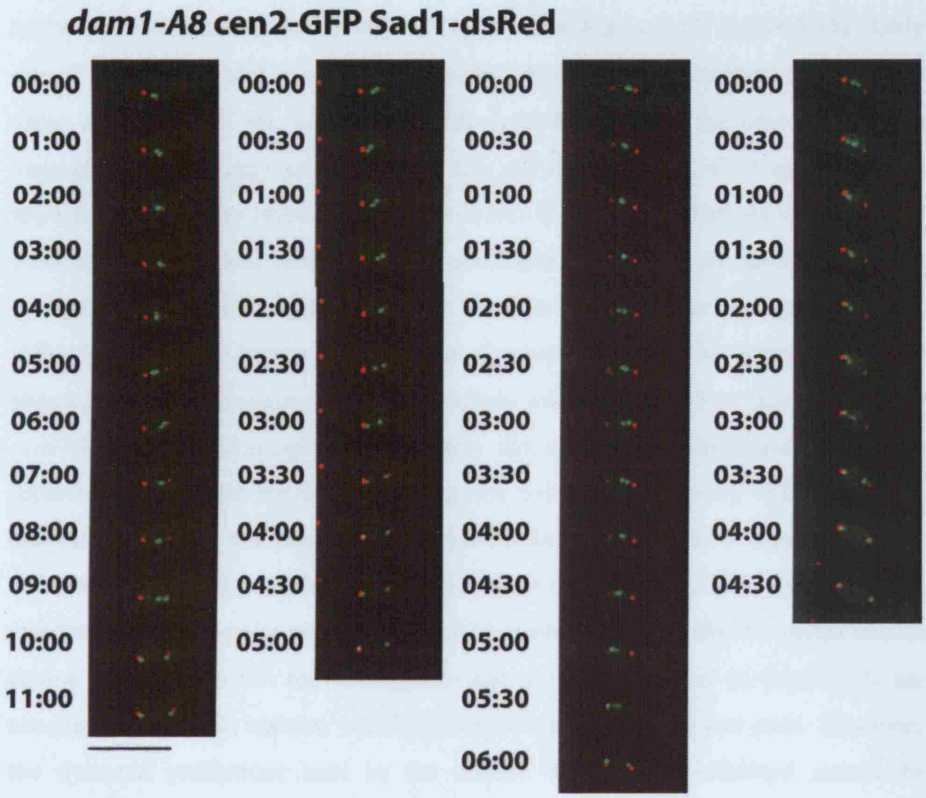

Figure 5.16: Live analysis of sister-chromatid separation in *Δklp6*, *dam1-A8Δklp6* and *dam1-A8* mutant cells

(A) *Δklp6* cells(N=6) **(B)** *dam1-A8Δklp6* cells (N=12) and **(C)** *dam1-A8* cells (N=10) containing *cen2*-GFP and Sad1-dsRed were cultured in rich medium overnight. The cells were immobilised onto lectin coated microscopy dish and *cen2*-GFP and Sad1-dsRed visualised on a Delta vision fluorescence microscope. The scale bars represent 10μm.

This corroborates the high frequency of mono-polar segregation visualised by both α-tubulin and DAPI staining of fixed synchronised *dam1-A8Δklp5* cells and cen2-GFP analysis of fixed asynchronous *dam1-A8Δklp6* cells (Figure 5.10, Figure 5.15). Only one of the *dam1-A8Δklp6* cells that displayed mono-polar segregation (1/5) did not show oscillations of the sister-chromatids from one pole to the next before both segregating to the same pole. Indeed in this cell once the *cen2*-GFP signals moved towards one pole they remained at that pole and no further oscillations were detected even when filming was continued for a prolonged period after the spindle started to elongate in anaphase B. This is similar to the type of mono-polar segregation seen in *Δdam1* cells. The remaining cells that displayed mono-polar segregation (4/5) showed varying degrees of congression defects with some extreme "shuttling" of the *cen2*-GFP signals form pole to pole before one of the sister-chromatids eventually separated right across the cell to the opposite pole. (Figure 5.16B) This "shuttling" movement suggests that the mono-polar attachments cannot be of a monotelic nature and that both sisters must be attached to spindle microtubules, albeit in a defective manner. The mono-polar segregation seen in *Δdam1* cells whereby the sisters remain at one pole and do not move, suggests that the chromosomes in these cells are attached in a syntelic manner, with both sisters attached to only one pole. However, the dynamic oscillations seen in the double mutant *dam1-A8Δklp6* cannot be explained by either of these attachment defects and indeed are more indicative of merotelic attachments that cannot be properly resolved to allow 1:1 equal sister segregation both instead result in separation of both sisters to the same pole. monotelic configurations. Perhaps in these double mutant cells the "merotelic" attachments, which are resolved to mono-polar attachments can then be resolved no further.

The *dam1-A8* single mutant cells examined (N=10) displayed segregation of the sister-chromatids to opposite poles in a normal 1:1 fashion (Figure 5.16C). However these cells nonetheless displayed some mitotic defects, albeit of a subtle nature.
These *dam1-A8* cells also displayed a tendency to "shuttle" their respective sister-chromatids from one pole to the other, but in a less dramatic fashion than in the double *dam1-A8Δklp6* or *Δklp6* mutants. Indeed some cells showed the typical congression defect seen in *Δklp6* or *dam1-A8Δklp6* cells, with both sisters located at one pole just prior to the segregation of one of the sisters right across the cell to the other pole (Figure 5.16C). This suggests that this *dam1-A8* mutant is also slightly defective in the congression of sister-chromatids to the equator during mitosis, most

likely due to the inability to correct merotelic attachments. However, as in *Δklp6* cells the chromosome attachments appear to eventually resolve to allow normal segregation of sister-chromatids in the single *dam1-A8* cells. Perhaps this reflects the overlapping role of both the Dam1/DASH complex and the kinesins Klp5/6 in erroneous kinetochore-microtubule attachment correction.

We then used the live images of all the strains examined in this chapter and in the previous chapter to examine mean spindle length in both anaphase A and anaphase B, to ascertain if there is any difference in the length of the spindle between *dam1-A8Δklp6* and the single *Δklp6* mutant. The intra SPB distance was measured as the distance between both Sad1-dsRed SPB foci and used as a representation of the spindle length. This measurement was carried out for wild-type, *Δdam1*, *Δklp6*, *dam1-A8* and *dam1-A8Δklp6* cells at anaphase A, when the *cen2*-GFP sister-chromatids just begin to separate, and anaphase B, when the sister-chromatids have separated and the SPB distance begins to elongate. The mean spindle length was calculated for each of these cells, however it should be pointed out that this measurement does not include *Δdam1* cells in which the 'spindle collapse' phenotype was observed. The wild-type cells showed an average anaphase-A spindle length of approximately 2.92 +/- 0.406μm and an anaphase B spindle length of 3.44 +/-0.46 μm. These results are consistent with previous established results for the anaphase spindle length in wild-type *S. pombe* cells as 2.5μm for phase 2 (metaphase – anaphase A). The *Δklp6* mutant shows much longer mitotic spindles than wild-type cells with an anaphase A spindle length of 4.7 +/- 1.36μm and an anaphase B length of 5.89 +/- 2.24μm, although there is a large deviation between spindle lengths when this strain is examined. This mutant appears to have decoupled spindle length from the timing of chromosome segregation. The double mutant *dam1-A8Δklp6* does not show any significant difference in spindle length compared to the single *Δklp6* cells.

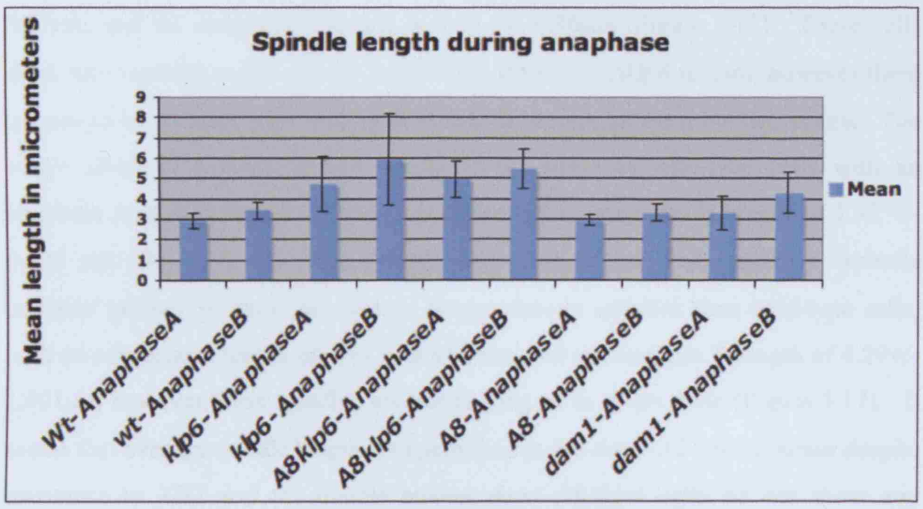

Figure 5.17 Mean spindle length of *dam1-A8Δklp6* cells

The mean spindle length of WT, *Δdam1, Δklp6, dam1-A8* and *dam1-A8Δklp6* cells was calculated as the distance between Sad1-dsRed SPB foci at anaphase A, when the *cen2*-GFP sister-chromatids begin to separate, and anaphase B, when the sisters have separated and the spindle is in the process of elongation. The mean length was calculated for each strain (N>5) and the standard deviation used to calculate error bars.

The anaphase A spindle for these *dam1-A8Δklp6* cells is approximately 4.95 +/- 0.87μm, and the anaphase B length is 5.46 +/- 0.96μm (Figure 5.17). These cells show less variation in the spindle length than the single *Δklp6* mutant; however there appears to be no significant difference in spindle length between the two strains. The single *dam1-A8* average spindle length is the same as wild-type cells with an anaphase A spindle length of 2.94 +/-0.28μm and an anaphase B length of 3.32 +/- 0.406 μm (Figure 5.17). The *Δdam1* cells that do not demonstrate a 'spindle collapse' phenotype show on average longer mitotic spindles than wild-type cells, with an anaphase A length of 3.31 +/-0.817 mm and an anaphase B length of 4.29+/- 1.001μμ, however these spindles are not as long as in *Δklp6* cells (Figure 5.17). It seems that average spindle length is unperturbed in the *dam1-A8* mutant strain despite resistance to TBZ and the double mutant *dam1-A8Δklp6* cells do not show any additive defects in spindle length compared to the single *Δklp6* cells. The spindle length in *Δdam1* cells is longer than wild-type cells, however we were unable to include those cells that underwent a 'spindle collapse' phenotype in this analysis, which would significantly reduce the spindle length.

5.8 Genetic interactions of the *dam1-A8* mutant

We examined the genetic interactions of both the double *dam1-A8Δklp5* and the single *dam1-A8* mutants with mutants of other mitotic regulators that function to co-ordinate chromosome segregation.

5.8.1 *dam1-A8* is synthetically lethal with *Δdis1*

We initially screened for conditional *dam1* mutants in a *Δklp5* background to understand why deletion of both these molecules is synthetically lethal to the cell. We also considered the idea of screening for *dam1* mutants in a *Δdis1* background to ascertain why these double mutants die, but unfortunately time-constraints prevented this possibility. We therefore crossed the other *dam1* alleles, to a strain, in which *dis1*$^{+}$ was deleted, hoping it would provide us with ready-made *dam1Δdis1* conditional mutants. This was not the case however, as all of the *dam1* alleles tested appeared to be synthetically lethal with *Δdis1* (data not shown). We then attempted to construct a *dam1-A8Δdis1* strain by random spore analysis, but again this *dam1*-A8

Strain	*dam1-A8*	*dam1-A8Δklp5*	*Δdam1*
Δdis1	SL	ND	SL
Δsgo2	V	V sick	V
Δmal3	V sick	V sick	V sick
Δalp14	V sick	ND	V sick

Table 5.2: Genetic interactions of *dam1-A8* and *dam1-A8Δklp5*

V: viable; SL: synthetically lethal; ND: not determined.

* Those strains designated ND were not tested because Klp5 and Dis1 deletions, or Klp5 and Alp14 deletions already known to be synthetically lethal

mutant was synthetically lethal with the *Δdis1* strain. We could not therefore generate a ready-made *dam1Δdis1* conditional mutant. It would seem that cells in which Dis1 is deleted are more sensitive to perturbations in Dam1 function than *Δklp5* or *Δklp6* cells.

5.8.2 Examination of *dam1-A8Δalp14* mutant

We previously determined that a *Δdam1alp14* mutant shows exacerbated microtubule and chromosome segregation defects compared to either of the single *Δdam1* or *Δalp14* mutants. In this section we examine the relationship between the *dam1* allele *dam1-A8* and the *Δalp14* null mutant. We were able to generate a viable double mutant between *Δalp14* and *dam1-A8* by random spore analysis. We examined the growth of this double mutant compared to wild-type, *dam1-A8*, *Δalp14*, *Δdam1*, and the *Δdam1alp14* strain at various temperatures and in the presence of TBZ by a serial dilution spot assay. It must be pointed out that the first 4 rows of this spot-test were used previously in figure 4.7B. when examining the *Δdam1alp14* strain. The *dam1-A8Δalp14* strain shows good growth at both 27°C and 30°C. This is in sharp contrast to the *Δdam1alp14* strain, which shows very little growth even at 27°C. The *dam1-A8Δalp14* strain does show perturbed growth at 36°C, which is slightly worse than the growth of a single *Δalp14* mutant at this temperature, but is much better than the *Δdam1alp14* strain, which doesn't grow at all when incubated at 36°C (Figure 5.18B). Intriguingly the *dam1-A8Δalp14* strain behaves like the single *dam1-A8* in that it is resistant to TBZ, whereas the single *Δalp14* cells are sensitive to the drug. We were interested therefore in how the morphology and microtubule structure of these double *dam1-A8Δalp14* cells would look.

We examined the morphology of these cells when cultured in rich medium at 36°C for 6 hours. These double mutants appear like *Δalp14* cells with altered polarity, showing bent and branched and T-shaped cells suggesting perturbation of the microtubule structures in these cells (Figure 5.18A). Visualisation of the microtubule structure of these cells by immunoflourescence staining of α-tubulin and DAPI revealed cells with strongly stained highly disorganised interphase microtubule arrays and perturbed spindle structures. The microtubules looked very similar to the *Δdam1alp14* double deletion mutants with many broken structures. Indeed the frequency of cells displaying mis-segregation of chromosomes was also very high in

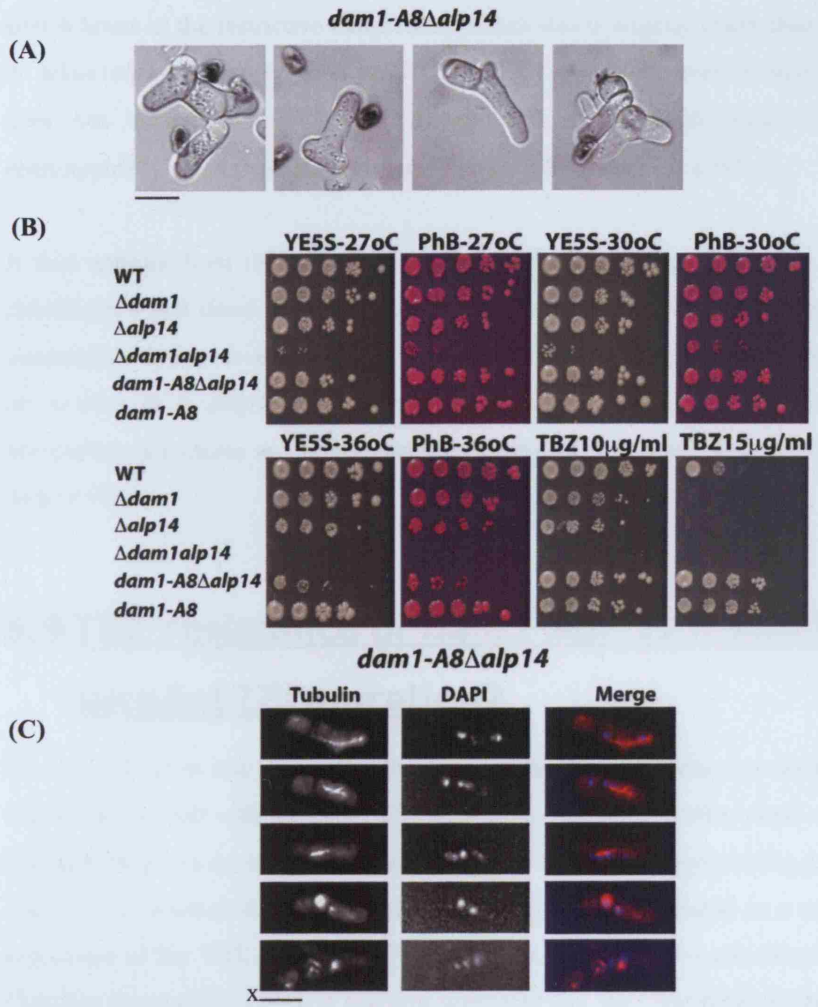

Figure 5.18: Deletion of Alp14 in *dam1-A8* mutant is viable but cells show TBZ resistance and mis-segregation

(A) Morphology defects of cells grown in rich medium liquid culture for 6 hours at the restrictive temperature 36°C. **(B)** Tenfold serial dilution spot assay plated onto rich agar YE5S plates, YE5S & Phloxin B plates, incubated at 27°C, 30°C or 36°C and YE5S plates containing 10μg/ml or 15μg/ml TBZ plated at 27°C and incubated for 3 days. **(C)** *dam1-A8Δalp14* cells were cultured in rich medium at 36°C for 6 hours. The cells were fixed and immunoflourescence of α-tubulin and DAPI staining was carried out. The scale bar represents 10 μm.

these *dam1-A8Δalp14* cells with approximately 52.9% of cells with aberrant DNA after 6 hours at the restrictive temperature, albeit this is slightly lower than that seen in *Δdam1alp14* cells (~68-69% at 27°C or 36°C). Therefore even though *dam1-A8* does not behave exactly like a *Δdam1* null mutant with respect to TBZ, phenotypically when crossed to an *Δalp14* strain it behaves very similarly.

It thus appears from the exacerbated microtubule morphology defects in both the *Δdam1alp14* and *dam1-A8Δalp14* strains that Dam1 has a role in the regulation of microtubule dynamics as the loss of function of Dam1 or the presence of this *dam1-A8* mutant in a *Δalp14* background results in an increased disorganisation of microtubule structures and mis-segregation of chromosomes compared to the single *Δalp14* strain.

5.9 TBZ resistance of *dam1-A8*. Is it similar to *dam1-127* truncation?

We have shown in this chapter that the single mutant *dam1-A8* does not behave like a *Δdam1* null mutant with respect to TBZ sensitivity. There is another *dam1* allele that has been shown to act in a resistant manner to the spindle de-polymerising drug TBZ. This is a C-terminal *dam1* truncation (*dam1-127*) that was isolated as a multi-copy suppressor of the TBZ sensitivity of the *cdc13-117* and a *mal3-1* conditional mutant (Sanchez-Perez et al., 2005). It was thus presumed that the C-terminal of Dam1 must play an important regulatory role in microtubule stability (Sanchez-Perez et al., 2005). In this section we compare our *dam1-A8* mutant allele to the C-terminal truncation allele *dam1-127*. We theorised that the *dam1-A8* allele was simply behaving as a loss of C-terminal mutant like the *dam1-127* strain, and therefore this truncation mutant would behave phenotypically the same as the *dam1-A8* mutant with respect to genetic interactions.

5.9.1 Growth comparison of *dam1-A8* and *dam1-127*

It is interesting to note that both of the point mutations that we identified in the *dam1-A8* allele are resident within the C-terminal region. Perhaps the C-terminal structure is disrupted in our Dam1-A8 protein, in a similar manner seen in the *dam1-127* C-

terminal truncation mutant. We presumed therefore that both mutants would behave in a similar manner with respect to growth in a serial dilution spot assay.

The wild-type strain shows good growth at either 27°C or 36°C and shows marginal growth in the presence of 15μg/ml TBZ. Consistent with previous results the *Δdam1* cells do not appear temperature sensitive but are slightly more sensitive to growth in the presence of TBZ than the wild-type cells. The *dam1-127* and *dam1-A8* strains behave identically with respect to growth at either 27°C or 36°C and both strains show a similar level of resistance to TBZ on plates (Figure 5.19).

5.9.2 Examination of *dam1-127Δklp5* and *dam1-127Δalp14* cells

The *dam1-127* and *dam1-A8* strains appear to grow in a similar manner on YE5S plates at either 27°C or 36°C or in the presence of TBZ. We next assessed if the *dam1-127* mutant will show the same severity of phenotype as a *dam1-A8* mutant when combined with either *Δklp5* or *Δalp14* null mutants. We generated the double *dam1-127Δklp5* or *dam1-127Δalp14* strains by random spore analysis and carried out immunoflourescent staining of α-tubulin on methanol fixed cells, 6 hours after shift up to 36°C.

The *dam1-127Δklp5* cells showed strong staining of both interphase and mitotic microtubules with a typical *Δklp5* phenotype of elongated mitotic spindles that sometimes curve around the cells (Figure 5.20). However, some of the interphase microtubules demonstrated disorganised microtubule arrays unseen in the single *Δklp5* cells (data not shown). The *dam1-127Δalp14* strain showed cells with shorter, weaker stained microtubules, typical of an *Δalp14* phenotype. The microtubule structures of these cells did not look like either the *dam1-A8Δalp14* or *Δdam1alp14* double mutants, which have extremely disorganised and broken microtubule structures (Figure 5.20A). Furthermore we counted the frequency of mis-segregation in both *dam1-127Δklp5* and *dam1-127Δalp14* cells and while there is a significant frequency of aberrant segregation of DNA in these cells it is much less severe than double mutants of either *Δklp5* or *Δalp14* cells combined with *dam1-A8* (Figure 5.20B). Therefore it seems while both alleles *dam1-127* and *dam1-A8* cause resistance to the microtubule-depolymerising drug TBZ, they do not behave similarly

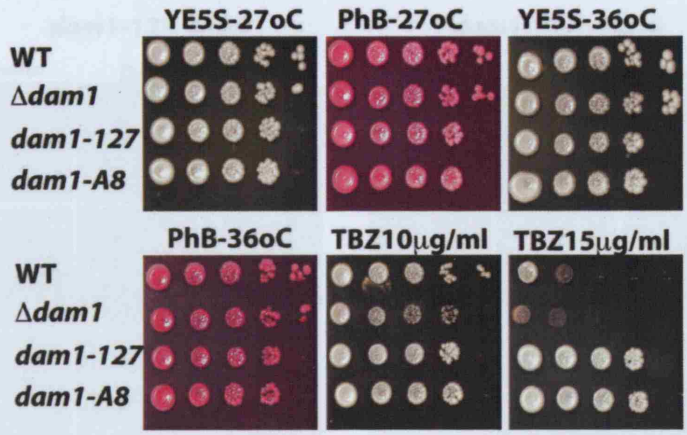

Figure 5.19: Spot assay comparing *dam1-A8* and *dam1-127* growth

Tenfold serial dilution spot assay plated onto rich agar YE5S plates, YE5S & Phloxin B plates incubated at 27°C or 36°C and YE5S plates containing 10μg/ml or 15μg/ml TBZ plated at 27°C and incubated for 3 days.

(A)

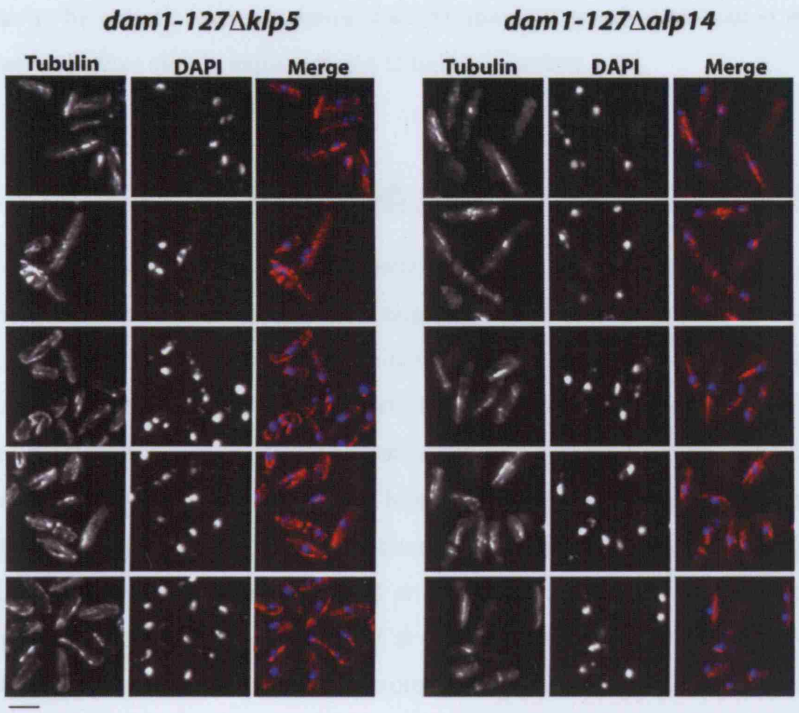

(B)

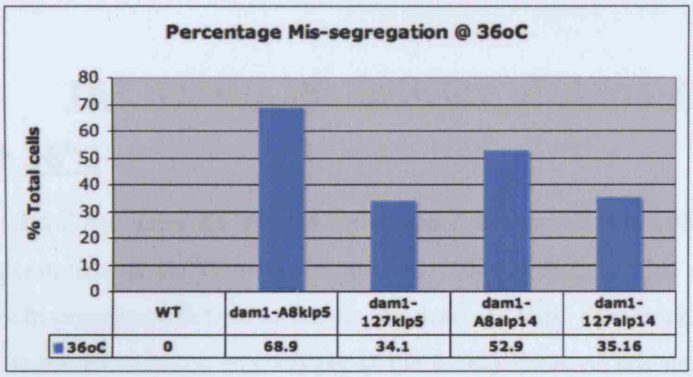

Figure 5.20: *dam1-127Δklp5* and *dam1-127Δalp14* cells show microtubule and chromosome segregation defects

(A) *dam1-127Δklp5* and *dam1-127Δalp14* cells were cultured in rich medium at 36°C for 6 hours. The cells were fixed and immunoflourescence of α-tubulin using α-TAT-1 antibody and DAPI staining was carried out and cells were viewed by fluorescence microscopy. The scale bar represents 10 μm. **(B)** Graph showing the frequency of mis-segregation of chromosomes in WT, *dam1-A8Δklp5, dam1-A8Δalp14*, *dam1-127Δklp5* and *dam1-127Δalp14* cells (N>200).

in terms of their genetic interactions with *Δklp5* or *Δalp14*. The *dam1-A8* mutant appears to be a more severe mutation than the simple C-terminal truncation mutant and cannot be thus simply explained as a C-terminal mutant.

5.10 Suppression of the *dam1-A8Δklp5* mutant

The *dam1-A8Δklp5* mutant shows severe growth and chromosome segregation defects when incubated at the restrictive temperature. To gain a different perspective on the reasons for the lethality of these double mutant cells and an insight into the overlapping functions of both the Dam1/DASH complex and Klp5 and Klp6, we carried out a multi-copy suppressor screen on the *dam1-A8Δklp5* double mutant. We also examined whether the severity of bi-orientation defects in the double mutant might be due to extremely stable kinetochore-microtubule attachments in these cells as indicated by hyper-resistance to TBZ at the permissive temperature. To address this we examined if the addition of TBZ at the restrictive temperature, which would de-polymerise the rigidly attached microtubules, would cause suppression of the temperature sensitive growth defect in these cells.

5.10.1 TBZ rescues the lethality of *dam1-A8Δklp5* cells at 36°C

The single *Δklp5* and *dam1-A8* mutants both display resistance to the addition of the spindle microtubule de-polymerising drug TBZ. We postulated that the severe kinetochore bi-orientation defects in the double *dam1-A8Δklp5* cells might be due to extremely stable microtubule attachments at the kinetochores of this mutant. The attachments to the kinetochores in these cells may be of such a stable nature with no dynamic instability that any incorrect merotelic or syntelic attachments to the kinetochores that occur would not be resolved due to the rigidity of the spindle microtubules, preventing turn-over of attachments and the establishment of bipolar attachments. We hypothesized that induction of dynamic instability in these spindle microtubules through the addition of TBZ, that causes microtubule de-polymerisation, could suppress the inability of these cells to correct erroneous kinetochore attachments and rescue the temperature sensitive growth defect at the restrictive temperature. We therefore carried out a serial dilution spot assay to assess

the growth of our double mutant at the restrictive temperature in the absence and presence of varying concentrations of TBZ.

In this assay we included several control strains such as wild-type, *Δdam1, Δklp5* and the single mutant *dam1-A8*. The wild-type and *Δdam1* cells grew normally at either 27°C or 36°C on rich medium in the absence of TBZ, but showed no growth in the presence of 20μg/ml TBZ at 27°C. These strains were able to grow, however, on 20μg/ml TBZ when incubated at 36°C, highlighting that the efficacy of the drug is reduced at this higher temperature (Figure 5.21). Likewise the single mutant *dam1-A8* grew normally on rich medium at either 27°C or 36°C and showed better growth than the wild-type strain on TBZ at either 27°C or 36°C. The *Δklp5* strain showed strong growth, as expected, in the presence of TBZ at 27°C and could grow on concentrations up to 75μg/ml of TBZ at 36°C. The double mutant *dam1-A8Δklp5* showed TBZ resistance at 27°C, growing on plates containing a concentration of 20μg/ml and consistent with previous results showed severe growth defects on both YE5S and Phloxin B plates when incubated at the restrictive temperature 36°C. This temperature sensitivity was rescued by the addition of TBZ, with *dam1-A8Δklp5* cells able to grow as well as *Δklp5* cells at the restrictive temperature, on plates containing 20, 50 or 75μg/ml concentration of TBZ (Figure 5.21). It seems that the addition of this microtubule de-polymerising drug can suppress the growth defects seen when the double *dam1-A8Δklp5* cells are incubated at the restrictive temperature. We theorise that addition of TBZ to these cells at this temperature allows the stable rigid microtubule-kinetochore attachments to undergo dynamic instability, and thus allow turnover of erroneous attachments at the kinetochore and the subsequent establishment of properly bi-oriented kinetochores.

We wished to understand the reasons why the addition of TBZ to *dam1-A8Δklp5* cells at the restrictive temperature resulted in suppression of the temperature sensitive growth defects. We therefore attempted to carry out a rescue experiment on *dam1-A8Δklp5* cells in liquid culture at the restrictive temperature through the addition of MBC/CBZ. We first tried examining both wild-type and *dam1-A8Δklp5* cells at 27°C or 36°C before and following the addition of 50μg/ml MBC/CBZ, to assess whether the addition of this drug would reduce the incidence of chromosome mis-segregation in the double mutants at 36°C. This concentration was far too high and resulted in a high frequency of even wild-type cells at 27°C with chromosome mis-segregation and "cut" phenotype. We reduced the concentration of the drug to 25μg/ml and 20μg/ml

and tried several times to develop an optimised experimental system to assess the physiological reasons for suppression of the double mutant following microtubule de-polymerisation, however, we could not find a concentration of MBC/CBZ sufficient to induce microtubule de-polymerisation without causing a high frequency of chromatin defects in the wild-type or *dam1-A8Δklp5* strain. Therefore while we can reproducibly see that the addition of TBZ rescues the growth defects of our double mutant at the restrictive temperature we cannot visualise which aspects of the *dam1-A8Δklp5* phenotype are suppressed under these conditions.

5.10.2 Does *Δmal3* suppress *dam1-A8Δklp5* cells?

The suppression of the temperature sensitivity of *dam1-A8Δklp5* cells by the addition of TBZ caused us to wonder if a mitotic mutant that results in destabilised microtubule plus ends might also suppress the ts phenotype in *dam1-A8Δklp5* cells. Mal3 is the fission yeast EB1 homologue. It acts as a plus end microtubule binding protein and plays an important role in cell polarity, cytoplasmic microtubule and mitotic spindle integrity and chromosome stability in mitosis (Asakawa and Toda, 2006; Beinhauer et al., 1997; Busch and Brunner, 2004; Chen et al., 2000; Kerres et al., 2004; Sandblad et al., 2006). Deletion of Mal3 results in short interphase microtubule structures, abnormal mitotic spindles, and the failure of cells to resolve syntelic attachments resulting in mono-polar segregation defects (Asakawa and Toda, 2006; Asakawa et al., 2005). We therefore pondered whether deletion of Mal3 in a *dam1-A8Δklp5* background would also suppress the growth defects of this double mutant at the restrictive temperature in a similar manner to the addition of TBZ. We constructed the triple mutant strain *dam1-A8Δklp5mal3*. This strain was viable but did not result in suppression of our *dam1-A8Δklp5* mutant. We then carried out a serial dilution spot assay to assess the growth of this triple mutant and compared it against wild-type, the single mutants *Δmal3, Δklp5*, *dam1-A8*, the double mutant *dam1-A8Δklp5* and *dam1-A8Δmal3* and *Δmal3klp5* which we also generated by random spore analysis selection. Deletion of *mal3* in the *dam1-A8Δklp5* strain does not result in suppression of the temperature sensitive growth defect of the double *dam1-A8Δklp5* mutant. The triple mutant cells grow even more slowly than the double *dam1-A8Δklp5* mutant when incubated on plates at the permissive temperature (Figure 5.22A). The double *dam1-A8Δmal3* mutant shows some synthetic growth defects at 36°C

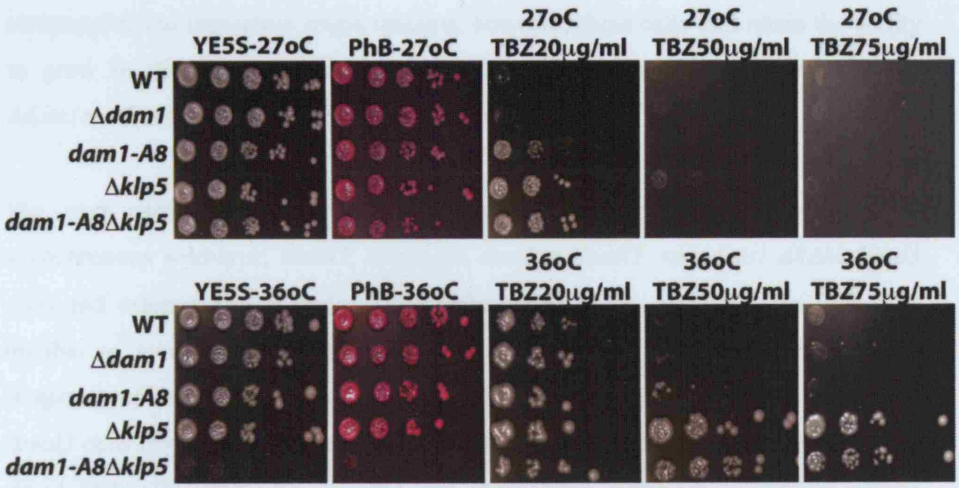

Figure 5.21: The addition of TBZ rescue the temperature sensitive growth defects of *dam1-A8Δklp5* cells at the restrictive temperature

Tenfold serial dilution spot assay of WT, *Δdam1*, *dam1-A8*, *Δklp5*, and *dam1-A8Δklp5* cells in the presence and absence of TBZ. The cells are plated onto rich agar YE5S plates , YE5S & Phloxin B plates incubated at 27°C or 36°C and YE5S plates containing 20μg/ml, 50μg/ml or 75μg/ml TBZ plated at 27°C or 36°C and incubated for 3 days.

compared to the respective single mutants, however, these cells still retain the ability to grow in the presence of TBZ as well as the single *dam1-A8* cells, unlike *Δdam1mal3* cells which show an exacerbated sensitivity to TBZ.

We next carried out immunoflourescence staining of microtubules in fixed asynchronous wild-type, *Δmal3*, *dam1-A8*, *dam1-A8Δmal3*, and *dam1-A8Δklp5mal3* cells and examined cells under Zeiss fluorescent microscope. We quantified the number of mitotic spindles to indicate the mitotic index, and also quantified the frequency of chromosome mis-segregation in these cells. The microtubule staining of *Δmal3* cells revealed short interphase microtubules and weakly stained spindles. The *dam1-A8Δmal3* cells however, did not show short interphase or weak spindle microtubules, which is consistent with the retained resistance to TBZ in these cells (Figure 5.22B). The *dam1-A8Δmal3* cells did not show an increased frequency of mitotic cells compared to the single *Δmal3* or *dam1-A8* mutants, however the incidence of mis-segregation in the *dam1-A8Δmal3* cells increased dramatically (Figure 5.22C). The triple mutant *dam1-A8Δklp5mal3* cells showed a substantially high level of chromosome mis-segregation even at the permissive temperature, which was expected due to the poor growth of this strain on plates at 27°C.

There is a decrease in the mitotic index in this triple mutant strain compared to the *dam1- A8Δklp5* cells, this is probably due to the high frequency of dead cells with abnormal microtubule staining and mis-segregated chromosomes, which are included in the quantification of total cells (Figure 5.22B&C). Therefore we can conclude that deletion of Mal3 does not suppress the temperature sensitive growth and mitotic defects seen in *dam1-A8Δklp5* cells.

5.10.3 Suppressor screen for *dam1-A8Δklp5* cells

We carried out a multi-copy suppressor screen on the *dam1-A8Δklp5* mutant to garner an insight into how the Klp5 and Klp6 kinesins and the Dam1/DASH complex function to regulate bi-orientation of kinetochores in mitosis. We transformed our *dam1-A8Δklp5* mutant cells with a genomic library, cloned into the PAL-SK vector, which spanned the entire genome of *S. pombe*. The vector contained *LEU2* and ampicillin markers to enable selection of transformed cells on EMM –leucine plates. The transformants (approximately 4000) were then replica plated onto YE5S and Phloxin B plates, incubated at 27°C, 34°C, 35°C and 36°C for approximately 3 days

(A)

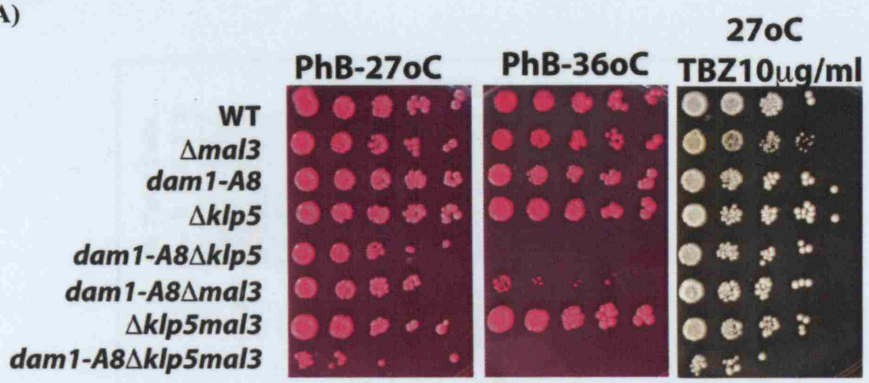
PhB-27oC
PhB-36oC
27oC
TBZ10μg/ml
WT
Δmal3
dam1-A8
Δklp5
dam1-A8Δklp5
dam1-A8Δmal3
Δklp5mal3
dam1-A8Δklp5mal3

(B)

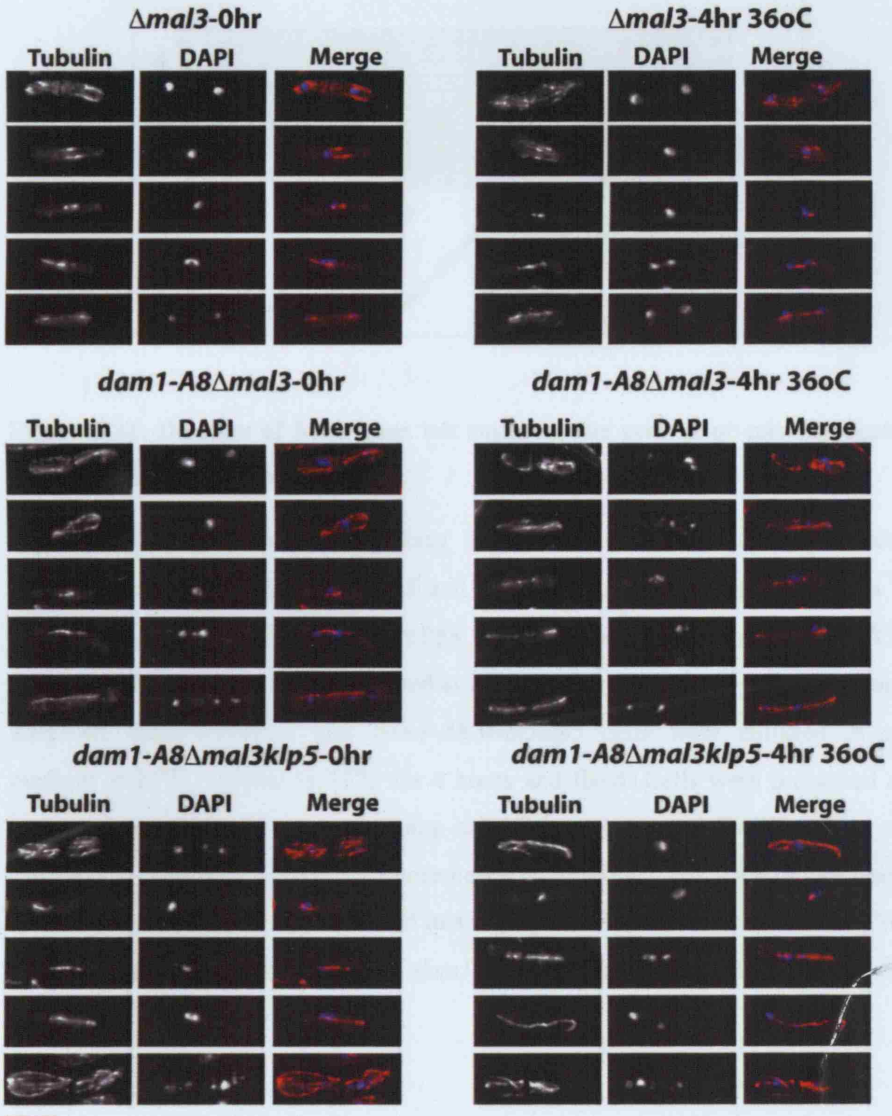
Δmal3-0hr
Tubulin
DAPI
Merge
Δmal3-4hr 36oC
Tubulin
DAPI
Merge
dam1-A8Δmal3-0hr
Tubulin
DAPI
Merge
dam1-A8Δmal3-4hr 36oC
Tubulin
DAPI
Merge
dam1-A8Δmal3klp5-0hr
Tubulin
DAPI
Merge
dam1-A8Δmal3klp5-4hr 36oC
Tubulin
DAPI
Merge

(C)

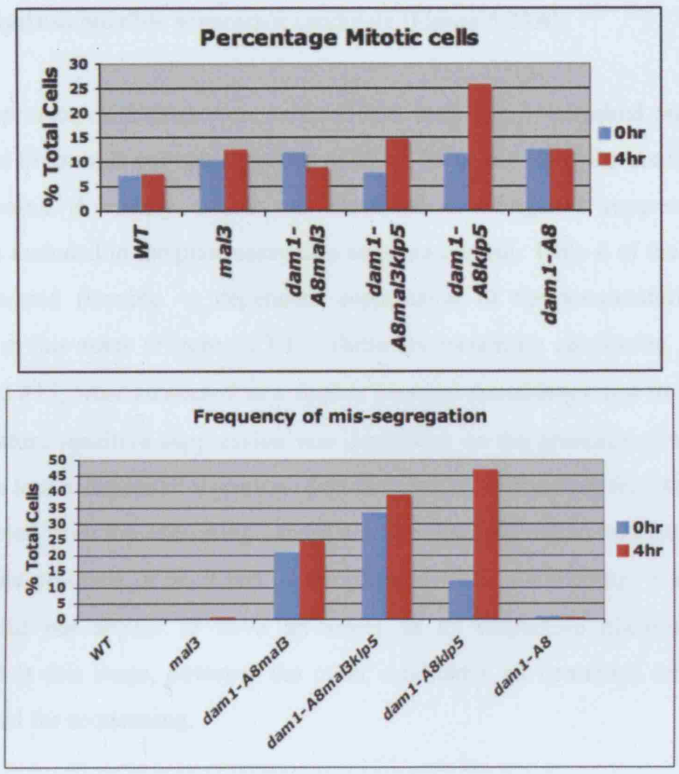

Figure 5.22: Deletion of Mal3 does not suppress the growth or mis-segregation defects of *dam1-A8Δklp5* cells

(A) Tenfold serial dilution spot assay of WT, *Δmal3*, *dam1-A8*, *Δklp5*, *dam1-A8Δklp5*, *dam1-A8Δmal3*, *Δmal3klp5* and *dam1-A8Δklp5mal3* cells. The cells are plated onto rich agar YE5S plates, YE5S & Phloxin B plates incubated at 27°C or 36°C and YE5S + 10μg/ml, TBZ plated at 27°C and incubated for 3 days. **(B)** *Δmal3*, *dam1-A8*, *dam1-A8Δmal3* and *dam1-A8Δmal3klp5* cells were cultured in rich medium at 27°C , shifted to 36°C for 4 hours and fixed. Cells were processed and immunoflourescence of α-tubulin using α-TAT-1 antibody and DAPI staining was carried out. Cells were viewed by fluorescence microscopy. The scale bar represents 10 μm. **(C)** Graphs of the mitotic and mis-segregation indexes as counted from WT, *Δmal3*, *dam1-A8*, *dam1-A8Δmal3*, *dam1-A8Δklp5* and *dam1-A8Δmal3klp5* cells (N>200).

and growth of each colony at each temperature carefully analysed. Colonies that were now capable of growth when incubated at 34°C, 35°C or 36°C were selected for further analysis as possible suppressor candidate (Figure 5.23A).

Fifteen suppressor candidates were selected and were then re-streaked onto EMM – leucine, and Phloxin B containing plates at 27°C, 35°C and 36°C for confirmation of the suppression. A colony, which was identified as a negative suppressor in our screen, was included in the plate assay as a negative control. Only 6 of the candidates showed plasmid (leucine +) dependent suppression of the temperature sensitive phenotype in this assay (Figure 5.23B). These six remaining candidates, #2, #6, #7, #9, #10 and #15, were subjected to a further plasmid dependency test to ensure that the temperature sensitive suppression was dependent on the presence of the plasmid and not due to a background mutation (data not shown). Following this, the plasmids were extracted from the remaining candidates and digested with a restriction enzyme to ensure the presence of an insert in the plasmid (data not shown). Candidate #7 strangely did not appear to have an insert in its respective plasmid and was disregarded at this stage, however the other candidates all contained an insert and were selected for sequencing.

Sequencing of the remaining 5 candidates was carried out with candidates #2 and #15 identified as carrying the *klp5*$^+$ gene, and candidates #6 and #9 were identified as carrying the *dam1*$^+$ gene (Figure 5.23C). We were pleased to identify *klp5*$^+$ in our screen, as expected; as this highlighted that the screen was indeed working. The identification of *dam1*$^+$ also validated the screen, however we had not been sure whether this would be identified due to the complex "gain of function" nature of the *dam1-A8* allele. Candidate #10 was identified as a gene called *dsk1* (Figure 5.23C). The *dsk1*$^+$ gene was first identified as a multi-copy suppressor of cold-sensitive Dis1 mutants (Ohkura et al., 1988). It was presumed that "*dis*" mutants could enter mitosis but due to the chromosome non-disjunction and spindle elongation phenotype that these cells could not exit properly from mitosis. It had been shown that over-expression of Dsk1 causes a delay in G2/M progression and therefore overproduction of Dsk1 could somehow allow these cells to sufficiently exit mitosis (Ohkura et al., 1988; Takeuchi and Yanagida, 1993). Dsk1 is a serine/threonine protein kinase that is itself phosphorylated in G2/M by Cdc2. This protein is not essential for viability but plays a possible a role in mitotic regulation (Takeuchi and Yanagida, 1993). Dsk1 localises to the cytoplasm in interphase but in mitosis it becomes localised to the

(A)

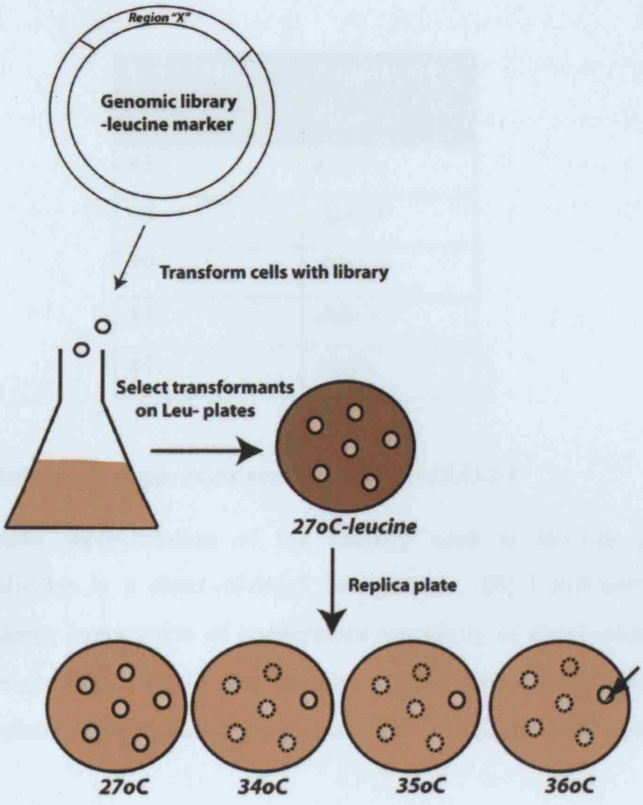

(B)

Select colonies that can grown at restrictive temperature

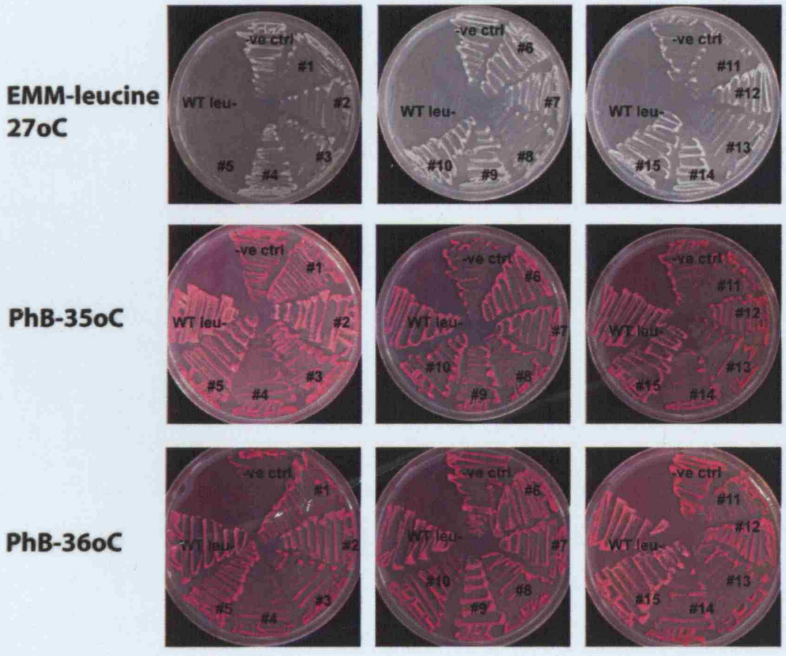

(C)

Candidate #	Suppressor Gene
#2	*klp5+*
#6	*dam1+*
#9	*dam1+*
#10	*dsk1+*
#15	*klp5+*

Figure 5.23: Multi-copy suppressor screen of *dam1-A8Δklp5*

(A) Diagrammatic representation of the strategy used to identify multi-copy suppressor candidates in a *dam1-A8Δklp5* background. **(B)** Confirmation of the plasmid dependency suppression of temperature sensitivity of *dam1-A8Δklp5* cells. WT, suppressor candidates #1-15 and negative control strains were streaked onto EMM –leucine plates at 27°C, Phloxin B plates at 27°C, 35°C and 36°C and incubated for 3 days.

nucleus where it associates with spindle microtubules and the SPBS (Nabeshima et al., 1995).Intriguingly Dsk1 has more recently been identified as a multi-copy suppressor for the "*hos*" family of mutants including *Δhos3* (Fission yeast Hsk3 Dam1/DASH component) (Aoyama et al., 2000). Therefore it is not surprising that Dsk1 also suppresses a mutant defective in proper Dam1 function, as this Dsk1 protein may play an important regulatory role in chromosome segregation and mitotic regulation.

5.11 Discussion

We previously showed that deletion of Dam1/DASH subunits in a *Δklp5* or *Δklp6* background is synthetically lethal, a result which was also corroborated by Sanchez-Perez *et al.* To gain an understanding of why these cells die a germination grow-out experiment was carried out on cells doubly deleted for both *klp5* and *dam1*. (Sanchez-Perez et al., 2005) These double null mutants could only undergo a few divisions before lethality. These cells were defective in forming proper bi-polar attachments of the spindle to the kinetochores, with multiple Mad2-GFP foci often visualised per cell (Sanchez-Perez et al., 2005). Sister chromatid *cen2*-GFP separation was monitored both in these double deletion mutants and in the single *Δklp5* and *Δdam1* mutants. The single *Δdam1* mutant cells displayed mono-polar segregation with a predominantly 2:0 or 1:0 separation pattern of *cen2*-GFP. The *Δklp5* cells displayed a phenotype consisting of 'lagging' chromosomes, with mono-polar segregation defects never visualised in this cells. The double null mutants *Δdam1klp5* showed a range of mitotic *cen2*-GFP separation defects. Some of these double null mutant cells, approximately 20%, showed a normal 1:1 segregation pattern of the *cen2*-GFP sisters but not all the DNA was separated normally. Approximately 19% of the cells displayed a typical non-disjunction phenotype, 25% of the cells separated their chromosomes in a mono-polar manner to the same pole, and 34% of the cells displayed a 'lagging' phenotype whereby one of the two *cen2*-GFP sisters failed to separate to a pole (Sanchez-Perez et al., 2005). It was therefore proposed that the Dam1/DASH complex and Klp5 and Klp6 play an essential overlapping role in the correction of mal-oriented sister kinetochores, whereby the Dam1/DASH complex predominantly corrects mono-polar syntelic attachments in a similar manner to its homologous complex in the budding yeast, and the kinesins Klp5 and Klp6 function to turn-over merotelically attached kinetochores.

In this chapter we attempted to further address the reasons for the synthetically lethality between the Dam1/DASH complex and Klp5 and Klp6. We carried out a mutagenesis screen for *dam1* mutants in a *Δklp5* background. We expected a poor transformation efficiency due to the lethal nature of the double *Δdam1klp5* null cells; any mutations that severely impaired Dam1 function at the permissive temperature in this *Δklp5* background would also result in lethality. Therefore we expected that any mutant selected would show a strong mutant phenotype in the *Δklp5* background but in a *klp5*$^{+}$ background would show a negligible phenotype. This turned out to be the case with screening leading to the identification of a mutant *dam1* allele we termed *dam1-A8* that showed a strongly temperature sensitive phenotype when combined with a *Δklp5* background but that did not show a very strong phenotype as a single *dam1-A8* mutant in a *klp5*$^{+}$ background.

We ensured that the temperature sensitivity of this double *dam1-A8Δlp5* mutant was due to the presence of both *dam1-A8* and *Δklp5* and not some background mutation, confirming the co-segregation of the ts^{-} phenotype with markers for both mutants by tetrad analysis and random spore analysis (Figure 5.3). The *dam1-A8* mutant was sequenced and found to contain two point mutations in the C-terminal region of the Dam1 protein, resulting in amino acid changes H126R and E149G. Neither of these residues are conserved in the *S. cerevisiae* sequence, however the area around both these residues seems quite conserved amongst the two fungal species, possibly indicating an important role for this region of the Dam1 C-terminal in mitotic regulation (Figure 5.4).

This *dam1-A8* mutant demonstrated resistance to the addition of the microtubule spindle poison TBZ independent of the *Δklp5* background. A C-terminal *dam1* truncation mutant *dam1-127* exists which is also resistant to TBZ and was originally identified as a multi-copy suppressor for *mal3-1* and *cdc13-117* mutants. We postulated whether the *dam1-A8* mutant is disrupted in its C-terminal by the presence of the two mutation sites and thus acts in a similar manner to a C-terminal disruption, pheno-copying the *dam1-127* truncation. We first compared both the *dam1-A8* and *dam1-127* mutants and found both to be strongly resistant to the presence of TBZ. We then compared the genetic interactions of both *dam1-A8* and *dam1-127* mutants in a *Δklp5* and *Δalp14* mutant background. The *dam1-A8Δklp5* and *dam1-A8Δalp14* cells showed a more severe and dramatic phenotype than the *dam1-127Δklp5* or *dam1-127Δalp14* cells (Figure 5.20). Therefore there appears to be some differences

between the *dam1-A8* and *dam1-127* allele with respect to genetic interactions. The *dam1-A8* mutant seems to be a more severe mutation than the *dam1-127* mutant, when combined with either *Δklp5* or *Δalp14* backgrounds, indicating it is not just a simple C-terminal disruption mutation.

We examined the localisation of the Dam1-A8 protein in both single *dam1-A8* and *dam1-A8Δklp5* cells at both the permissive and restrictive temperature to ascertain if its localisation is abolished following incubation at the restrictive temperature. Dam1-A8-GFP kinetochore localisation appeared to be compromised even at the permissive temperature in both strains (Figure 5.5). The localisation was further dramatically reduced in both strains following incubation at the restrictive temperature. We postulate that the reason for the lethality of this *dam1-A8Δklp5* strain at the restrictive temperature and its slow growth at even the permissive temperature is due to the decrease in localisation of the Dam1-A8 protein at the kinetochore. We cannot however, exclude the possibility that a small amount of Dam1-A8 is still retained at the kinetochore at the restrictive temperature.
We wished to ascertain whether the Dam1/DASH complex itself was intact in the *dam1-A8Δklp5* mutant following incubation at the restrictive temperature. We were unable to visualise various Dam1/DASH subunits by western blotting and tried various protein extraction methods to enable the detection of the complex in extracts but to no avail. Therefore we examined Ask1-GFP localisation in the double mutant at both permissive and restrictive temperature, and in *Δdam1* cells. Ask1 does not require Dam1 for its kinetochore localisation, as it could still localise to mitotic cells in *Δdam1* cells at 20°C, 27°C or 36°C. Intriguingly the signal intensity of Ask1-GFP was reduced in *dam1-A8Δklp5* cells at the permissive temperature and almost completely abolished following incubation at the restrictive temperature (Figure 5.6). Perhaps residual kinetochore localised Dam1-A8 interferes with the Dam1/DASH complex structure or integrity in a way that is not seen when the Dam1 protein is deleted, however our understanding of the reasons for this remain elusive. It seems that the *dam1-A8* mutant is not a loss of function mutant as the *Δdam1* null strain, but behaves more as a 'gain of function' mutant.

This evidence that *dam1-A8* does not behave as a loss of function mutation is further corroborated by the differences between the *Δdam1* cells and *dam1-A8* cells with respect to TBZ. The *Δdam1* strain is slightly sensitive to the addition of TBZ, however the single *dam1-A8* mutant is strongly resistant to the microtubule de-

polymerising drug. Furthermore, incubation of the *dam1-A8* mutant at 20°C does not cause the appearance of the typical "*dis*" mutant phenotype seen in *Δdam1* and other Dam1/DASH null mutants at this temperature, indicating that this *dam1-A8* mutant is quite distinct phenotypically from a Dam1 deletion. Moreover analysis of *cen2*-GFP separation in live mitotic cells reveals the major phenotype of *Δdam1* to be mono-polar sister-chromatid separation and 'spindle collapse' phenotype that is never seen in *dam1-A8* cells. The *dam1-A8* mutant instead displays a slight chromosome congression defect with sister-chromatids showing slight oscillations and "shuttling" between the two poles before one of the sisters separates to the opposite pole (Figure 5.16). It would seem therefore that several lines of evidence underline the fact that the novel *dam1* allele identified in our mutant screen behaves differently from a complete *dam1*$^+$ deletion. There are some similarities however between the two *dam1* alleles. Both strains *Δdam1* and *dam1-A8* are synthetically lethal in combination with deletion of the chTOG protein Dis1. Deletion of the other chTOG member, *alp14*$^+$ in either *Δdam1* or *dam1-A8* is not lethal but yields cells that are extremely sick. The *Δdam1alp14* cells show little growth even at the permissive temperature and are extremely sensitive to the addition of TBZ. These cells show severe microtubule morphology defects and a huge rate of chromosome mis-segregation. The *dam1-A8Δalp14* cells are not as sick as the double null mutants; they can grow when incubated at 27°C but show temperature sensitivity when incubated at 36°C with chromosome mis-segregation defects, albeit at a reduced frequency than the double null mutants (Figure 5.18). It is interesting to note that despite the fact that these double mutant cells show resistance to TBZ, analysis of their microtubule structures reveals similar microtubule structures as seen in *Δdam1mal3* cells with broken and disorganised microtubules (Figure 5.22). Perhaps in both strains a disruption in the balance of microtubule dynamics causes the same phenotypic outcome in relation to microtubule integrity and chromosome segregation.

The spindle assembly checkpoint is absolutely required for the viability of the double mutant *dam1-A8Δklp5* at even the permissive temperature (Figure 5.13). The spindle assembly checkpoint must be required to provide these mutant cells with time to activate an error repair pathway to correct some of the attachment and/or bi-orientation defects in these double mutant cells. Perhaps this pathway involves the Aurora B kinase homologue in *S. pombe* Ark1, in a similar manner to the important role Ipl1 (budding yeast Aurora B) plays in Dam1/DASH function and error correction in the budding yeast. Ark1 is an essential protein in the fission yeast and it

was therefore not possible prior to writing to test any possible role for this kinase with the Dam1/DASH complex in establishing proper bi-polar attachments and bi-oriented chromosomes. Recently however Ark1 temperature sensitive mutants have become available, so it would be interesting to see how these mutants interact genetically with both *Δdam1* and other Dam1/DASH nulls and our *dam1-A8Δklp5* strain.

We demonstrated that the spindle assembly checkpoint is activated, not only in the double mutant *dam1-A8Δklp5,* but also in the single *dam1-A8* mutant at both permissive and restrictive temperatures, with an increase in the frequency of mitotic cells and cells displaying Mad2-GFP foci (Figure 5.11). This indicates that, despite the low incidence of chromosome segregation defects seen in these cells, some mitotic defect is present that leads to the activation of the checkpoint. Indeed this is attested to by our visualisation of chromosome congression defects in this single mutant, with oscillations in the *cen2*-GFP signals prior to separation of the sister-chromatids. The double mutant *dam1-A8Δklp5* showed a similar level of mitotic cells as the single *dam1-A8* at the permissive temperature, but this rapidly increased following incubation at the restrictive temperature. The frequency of double mutant cells displaying Mad2-GFP foci however remained unchanged at either temperature with approximately 25% of cells with one or more Mad2 signal. It also appears that these Mad2 foci persist in these double mutant cells beyond mitosis and can be visualised in post-anaphase and G1/S phase cells. The spindle assembly checkpoint is activated in these cells but for some reason mitosis proceeds in a defective manner, leading to mis-segregation of chromosomes, however, the Mad2-GFP signals still remains associated with the kinetochores even as cells exit mitosis and enter a new round of the cell cycle. We postulated that the spindle assembly checkpoint may be bypassed in these cells, and perhaps it is bypassed more efficiently at the permissive temperature leading to an accumulation of mitotic cells at the restrictive temperature despite the frequency of cells displaying Mad2-GFP foci remaining unchanged.

To examine if the spindle assembly checkpoint is maintained in these double mutant cells we arrested the double mutant and wild-type cells with hydroxyurea and then treated the cells with CBZ/MBC at 27°C or 36°C for 5 hours to induce a mitotic arrest due to de-polymerisation of the microtubules. Incubation of the double mutant in the spindle drug caused a massive increase in the frequency of "cut" cells compared to the mutant without the drug, or wild-type cells. The timing of the appearance of

"cut" cells was the same as wild-type, however, which indicates that the spindle assembly checkpoint mediated mitotic arrest is maintained as well in the double mutants as in wild-type cells. Perhaps it would be more relevant to test the maintenance of the spindle assembly checkpoint in these cells under conditions where a mitotic arrest is induced through the disruption of tension, however due to time and strain constraints this was not assessed.

Careful analysis of the aberrant separation pattern of DNA in the synchronised and fixed *dam1-A8Δklp5* cells, showed a range of mitotic mis-segregation defects including lagging chromosomes, unequal distribution of chromatin, mono-polar separation of chromosomes and fragmented DNA. This result is consistent with the germination grow-out experiment carried out by Sanchez-Perez *et al.* whereby they visualised lagging chromosomes and mono-polar segregation defects in *Δdam1klp5* cells prior to cell death, indicating that perhaps Klp5/6 and the Dam1/DASH complex play distinct but overlapping roles in error correction and the resolution of attachments to promote proper bi-orientation.

We carried out live analysis of cen2-GFP sister-chromatid separation in the double mutant cells and in single *Δklp6* cells as a control. The *Δklp6* cells displayed a "shuttling" phenotype whereby the cen2-GFP sister-chromatids oscillated from one pole to the other prior to the separation of one of the sisters across the cell to the opposite pole. These cells did not demonstrate any real congression of the sister-chromatids on the spindle prior to anaphase A (Figure 5.16). It is presumed that these "shuttling" chromosomes in *Δklp6* cells are merotelically oriented, with each kinetochore attached to one or more microtubules from each pole, thus causing the cells to be pulled from one pole to the other. However, many of these *Δklp6* cells do undergo equal chromosome segregation and considering that all of the mitotic *Δklp6* cells display these mal-oriented congression deficient chromosomes, there must therefore exist a further redundant error correction pathway apart from Klp5/6 to facilitate the repair of some of these "shuttling" chromosomes.

The double *dam1-A8Δklp6* cells also displayed this "shuttling" phenotype showing oscillations of the cen2-GFP sisters from one pole to the other prior to anaphase onset. More than half of the cells (7/12) separated their sister-chromatids in an equal 1:1 manner despite the "shuttling" congression defect. The remaining cells (5/12) displayed a mono-polar segregation pattern with both *cen2*-GFP sister-chromatids

segregating to the same spindle pole. Four of these five cells displayed congression defects and typical "shuttling" of the sister-chromatids prior to the *cen2*-GFP sisters remaining associated with only one pole. The other cell did not demonstrate the "shuttling" phenotype and the cen2-GFP sisters became associated with one pole and did not undergo any further oscillations in a manner reminiscent of *Δdam1* cells (Figure 5.16). It would seem that in this and *Δdam1* cells the sister-chromatids are attached in a syntelic manner with each sister-kinetochore attached to the same pole. The *dam1-A8Δklp6* cells that display an oscillatory phenotype cannot be syntelically or monotellically attached and must be attached in a merotelic fashion. It would seem that these cells that display "shuttling" followed by mono-polar segregation may be highlighting the sequential steps involved in resolution of erroneous attachments in fission yeast cells, whereby merotelic attachments may be first resolved to attachments of a mono-polar nature in a stochastic manner before proper bi-polar attachments can be established. Perhaps this population of *dam1-A8Δklp6* cells can somehow resolve the merotelic attachments but are unable to resolve the mono-polar attachments thus causing segregation of a mono-polar nature. It is worth pointing out, however, that another redundant error correction mechanism must exist in these cells as 7/12 of these cells can resolve both attachment defects to undergo normal *cen2*-GFP separation. It is tempting to speculate as to which proteins might play a role in such a process, Dis1, Mal3, some novel unknown protein, however as of yet this sequential model is speculative and more work needs to be done to establish a concrete model of error-correction in the fission yeast mitosis.

While we have not, due to time constraints, examined *cen2*-GFP sister-chromatid separation in the triple *dam1-A8Δklp6mal3* cells. We have carried out some preliminary examination of *dam1-A8Δklp5mal3* triple mutant cells. These triple mutant cells appear more defective than the double *dam1-A8Δklp5* cells with very poor growth and a high frequency of chromosome mis-segregation even when incubated at the permissive temperature, suggesting that deletion of Mal3 exacerbates the growth and mitotic defects seen in *dam1-A8Δklp5* cells. Indeed the double mutant *dam1-A8Δmal3* show synthetic growth defects and dramatic increase in the frequency of chromosome mis-segregation at 36°C compared to the single *dam1-A8* or *Δmal3* mutants (Figure 5.22). These results could be an indicator that Mal3 also plays an important overlapping role in error-correction and kinetochore-microtubule attachment in concert with Klp5/6 and the Dam1/DASH complex. It would be interesting to examine the separation pattern on *cen2*-GFP sister-chromatids in these

dam1-A8Δmal3 and *dam1-A8Δklp6mal3* cells to understand if Mal3 is participating in another facet of this error correction and bi-polar establishment pathway.

Finally it is worth considering our suppression studies on our *dam1-A8Δklp5* double mutant. We demonstrated that the addition of TBZ at the restrictive temperature suppresses the temperature sensitive growth defects of the *dam1-A8Δklp5* mutant. This seems to suggest that the reasons for the extreme lethality of these cells at the restrictive temperature is due to the rigidity and hyper-stabilised nature of the spindle microtubules in these cells, which prevents proper end on bi-oriented attachments to the kinetochore. Therefore it would seem that the addition of TBZ to these cells allows these rigid microtubules to become more dynamic and perhaps in this way facilitate turnover of the improperly attached kinetochores and the establishment of properly bi-oriented sister chromatids.

We carried out a multi-copy suppressor screen on our *dam1-A8Δklp5* mutant. We identified two copies of $klp5^+$ and two copies of $dam1^+$ as suppressors of our double mutant. This validated the effectiveness of the screen as a method to identify genes that may interact genetically with *dam1* and *klp5/6*. We were mildly surprised to identify $dam1^+$ in this screen as we had been unsure whether it would be identified, due to the complex nature of the *dam1-A8* mutant. We further identified a gene termed $dsk1^+$, which is a serine/threonine kinase that has been implicated in mitotic regulation. Intriguingly Dsk1 was identified both as a multi-copy suppressor of Dis1 mutants, but also as a multi-copy suppressor of *Δhos3* (fission yeast Hsk3). It had been shown that over-expression of Dsk1 causes a delay in G2/M progression and it was presumed that over-expression of this gene suppresses Dis1 mutants, which can enter mitosis but are presumed unable to exit mitosis, by allowing these mutants to exit mitosis (Ohkura et al., 1988; Takeuchi and Yanagida, 1993). Dsk1 has not been extensively characterised. It is known that it can localise to the nucleus in mitosis, where it is thought to associate with spindles and SPBS. It has been shown that Dsk1 itself is phosphorylated, possibly in a Cdc2 dependent manner and it is thought that this somehow may regulate its localisation and/or kinase function. Perhaps Dsk1 is an important regulatory kinase not just in the G2/M transition but also in mediating proper kinetochore attachments and orientation and ensuring accurate sister chromatid separation during mitosis. However, as of yet the role for Dsk1 remains to be seen.

Chapter 6

6 Discussion

6.1 Conservation of the Dam1/DASH complex

The Dam1/DASH complex was first identified in the budding yeast *S. cerevisiae* and shown to be an essential 10 component complex required for the attachment of spindle microtubules to the kinetochore in a bi-oriented manner and to ensure the resolution of incorrect kinetochore configurations to an amphitelic bipolar attachment state (Cheeseman et al., 2002; Janke et al., 2002; Kang et al., 2001). We investigated whether this complex is conserved in the fission yeast by identifying homologous proteins by searching through the sequence databases. We initially identified 6 of the 10 fission yeast Dam1/DASH subunits with the remaining four proteins subsequently identified by Sanchez-Perez & J Millar. We demonstrated that the *S. pombe* Dam1/DASH proteins showed low but significant homology to their *S. cerevisiae* counterparts and that several of the residues and motifs shown to be required for Dam1/DASH function in the budding yeast are conserved highlighting a possible conservation of the nature and function of this complex in the fission yeast. However we also identified several budding yeast Dam1/DASH motifs and residues that were shown to be important for the function of the complex that are not conserved in the fission yeast indicating that despite an overall conservation of the complex and function between the two organisms there are differences and divergences in structure and function of the complex between the two species.

6.2 Localisation of the Dam1/DASH complex

The budding yeast Dam1/DASH complex localises to the kinetochores and SPBs throughout the cell cycle and to the mitotic spindle (Cheeseman et al., 2001; Enquist-Newman et al., 2001; Hofmann et al., 1998; Janke et al., 2002; Jones et al., 1999; Li et al., 2002). In the fission yeast the kinetochores only become attached to the microtubules during mitosis, but in the budding yeast the kinetochores are attached to microtubules throughout the cell cycle. We expected therefore that the fission yeast

Dam1/DASH complex would show only mitotic specific kinetochore and/or spindle localisation due to the nature of the fission yeast system. As expected the majority of the fission yeast Dam1/DASH complex localises to the kinetochores and plus ends of the microtubules only during mitosis. However, Dad1 localises in a constitutive manner to the kinetochore throughout the cell cycle. This suggests that Dad1 may act as an anchor for the recruitment of the mitotic specific Dam1/DASH members during mitosis. Indeed we demonstrated that Dam1-GFP localisation to the kinetochore is abolished in *Δdad1* cells but not vice versa. Furthermore in a recently published paper Kobayashi *et al.* demonstrated that Dad2 and Ask1 localisation to the kinetochore is abolished in *Δdad1* cells (Kobayashi et al., 2007). Therefore it seems that Dad1 acts as a platform to facilitate the docking of the mitotic specific Dam1/DASH complex to the kinetochore during mitosis.

In the budding yeast recruitment of outer kinetochore components such as the Dam1/DASH complex requires a stable and intact kinetochore structure. Indeed the budding yeast Dam1/DASH complex has been shown to localise to the kinetochore in a CBF3 and Ndc80 complex dependent manner (Janke et al., 2002; Jones et al., 2001). We examined the kinetochore requirements for the localisation of Dad1 to the fission yeast kinetochore and demonstrated that the Mis6/Sim4 complex is required to tether Dad1 to the kinetochore in a constitutive manner thus enabling the docking of the mitotic specific Dam1/DASH members. We saw that Dad1-GFP localisation is abolished following a shift up to the restrictive temperature in *mal2-1* and *mis6-302* cells. Furthermore Liu *et al* showed that Dad1 can co-purify with the Mis6/Sim4 complex and seems to bind this core kinetochore structure throughout the cell cycle (Liu et al., 2005). We did not see delocalisation of Dad1 from the kinetochore in *cnp1-1, mis12-537, nuf2-2* or *nuf2-4* cells however, in a recent paper it was shown that Hos2(Dad2)-GFP is delocalised in *nuf2-1* cells following incubation at the restrictive temperature and thus Nuf2 is required for the kinetochore localisation of the Dam1/DASH complex (Kobayashi et al., 2007). It may be that the Ndc80 complex is indeed required to tether both Dad1 and the mitotic Dam1/DASH complex to the kinetochore or perhaps more specifically the mitotic Dam1/DASH members. We cannot completely exclude this possibility at this time.

The budding yeast Dam1/DASH complex has been shown to require an intact mitotic spindle for its association with the kinetochores during G2/M phase (Li et al., 2002). We analysed the microtubule dependency of the Dam1/DASH complex by examining the localisation of Dam1-GFP in the temperature sensitive β-tubulin mutant *nda3-*

1828 at the restrictive temperature and demonstrated that Dam1-GFP is delocalised at the restrictive temperature in these cells. At this time a conflicting report was published that suggested that the fission yeast Dam1/DASH complex was not dependent on microtubules. In this paper Ask1-GFP localisation was examined in the cold sensitive *nda3-311* cells and shown to accumulate in over 80% of these mitotically arrested cells (Liu et al., 2005). We examined Dam1-GFP in this *nda3-311* background and obtained the same result. We postulated that difference between the results in both strains might be due to the presence of residual microtubules in the *nda3-311* strain even at the restrictive temperature. To remove any residual microtubules we ice-treated and fixed the *nda3-311* cells following incubation at the restrictive temperature and then saw that Dam1-GFP was no longer able to localise in this strain, indicating that intact microtubules are required for the kinetochore localisation of the Dam1/DASH complex during mitosis. This microtubule dependency provides an attractive model whereby the mitotic specific Dam1/DASH subunits 'surf' in on the incoming spindle microtubule, bind to Dad1, which is already kinetochore localised and facilitate the tethering of the microtubule to the kinetochore (Figure 6.1).

6.3 Dam1/DASH complex function

The essential budding yeast Dam1/DASH complex plays a crucial role in the proper attachment of kinetochores to spindle microtubules during mitosis and ensures 'turnover' of mal-oriented kinetochore configurations to facilitate bi-orientations and tension establishment. We deleted several components of the fission yeast Dam1/DASH complex and found that this complex is not essential in this organism. Upon reflection this result does not seem that surprising given that the fission yeast centromere/kinetochore structure is a more complicated than that of the budding yeast and probably requires a myriad of mitotic regulators to ensure proper kinetochore architecture and functioning during mitosis. Perhaps the Dam1/DASH complex functions in concert with several other proteins to facilitate proper kinetochore-microtubule interactions and bi-orientation. Indeed we showed that Dam1/DASH deletion mutants are synthetic lethal with deletions of the kinesin-8 proteins

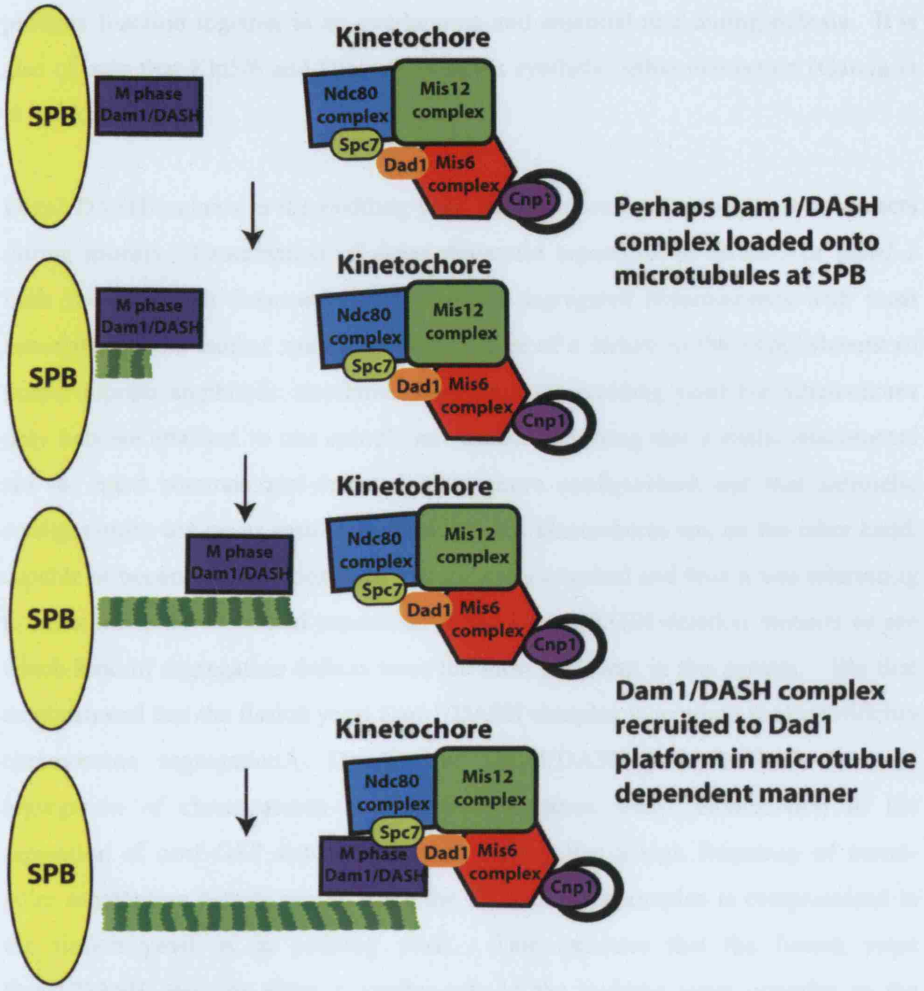

Figure 6.1: Model of microtubule dependent 'surfing' of mitotic specific Dam1/DASH complex to Dad1 platform at the kinetochore during mitosis

Klp5 and Klp6 and the TOG family member Dis1 perhaps highlighting that these proteins function together in an overlapping and essential role during mitosis. It is also of note that Klp5/6 and Dis1 also show a synthetic lethal interaction (Garcia et al., 2002).

Dam1/DASH mutants in the budding yeast display chromosome segregation defects during mitosis. Examination of sister-chromatid separation in *spc34-3* or *dam1-1* cells shows a high frequency of mono-polar segregated chromosomes with most associated to the mother spindle pole indicative of a failure in the establishment of proper bipolar amphitelic attachments. Within the budding yeast the kinetochores only become attached to one spindle microtubule ensuring that syntelic attachments are the most common mal-oriented kinetochore configuration and that merotelic configurations are never seen. The fission yeast kinetochores are, on the other hand, capable of becoming syntelically or merotelically attached and thus it was interesting to visualise sister chromatid separation in the Dam1/DASH deletion mutants so see which kind of segregation defects were the most prevalent in this system. We first demonstrated that the fission yeast Dam1/DASH complex is required for high-fidelity chromosome segregation. Deletion of Dam1/DASH subunits leads to mis-segregation of chromosomes and mini-chromosome loss. Examination of the separation of *cen2*-GFP sister chromatids showed that a high frequency of mono-polar segregation defects occurs when the Dam1/DASH complex is compromised in the fission yeast as in budding yeast. This indicates that the fission yeast Dam1/DASH complex plays a similar role to the budding yeast complex in the resolution of syntelically mal-oriented kinetochores.

Examination of Dam1/DASH deletion mutants in the fission yeast at 20°C revealed a '*dis*' phenotype of chromosome non-disjunction and broken spindles highlighting the importance of this complex for not only correct kinetochore attachment but also, anaphase spindle integrity as in the budding yeast. Typical '*dis*' mutants phenotypically show condensed non-disjoined sister chromatids with elongation of the mitotic spindle, despite activation of the spindle assembly checkpoint, which can then collapse and break (Nabeshima et al., 1995; Nabeshima et al., 1998; Ohkura et al., 1988). This abnormal spindle elongation occurs due to a disruption in the balance of force between microtubule based pushing forces and the force that pulls the kinetochores towards the poles. When this force is disrupted in these mutants due to defective kinetochore-microtubule interactions it causes the abnormal elongation of prophase spindles and their breakage (Nabeshima et al., 1998). A similar disruption

in this balance of force probably occurs in the Dam1/DASH deletion cells causing the elongation and breakage of the mitotic spindle.

The budding yeast Dam1/DASH mutants activate the spindle assembly checkpoint to induce a mitotic delay. We also demonstrated the activation of the spindle assembly checkpoint and an increase in the mitotic index in fission yeast Dam1/DASH deletion mutants. We also investigated whether Dad1 may have a Dam1/DASH complex independent role at the kinetochore in conjunction with the Mis6/Sim4 complex, in spindle assembly checkpoint signalling. Mis6 has been implicated as the kinetochore binding receptor for Mad2, with no checkpoint activation in Mis6/Sim4 mutants (Saitoh et al., 2005). We postulated therefore that Dad1 may play an active role with the Mis6/Sim4 complex in the Mad2 checkpoint, however we discovered that the spindle assembly checkpoint is activated and maintained in *Δdad1* cells under conditions of induced microtubule depolymerisation. However as a *dad1* deletion, but not *dam1*, shows a synthetic lethal interaction with a temperature sensitive *cpn1* mutant, Dad1 might play a centromere-related role independent of the Dam1/DASH complex.

It is probable that the activation of the spindle assembly checkpoint occurs to provide the Dam1/DASH mutant cells with sufficient time to repair any erroneous attachments and thus allow a normal segregation of chromosomes to proceed. In the budding yeast the spindle assembly checkpoint is activated and maintained through Aurora B/Ipl1 kinase activity. Ipl1 senses mal-oriented kinetochore configurations and induces the detachment of the spindle microtubule from the kinetochore, which facilitates the checkpoint signalling. It appears that Ipl1 creates unattached kinetochores through the phosphorylation of Dam1 and Spc34 and Ndc80 disrupting the interaction of the Ndc80 and Dam1/DASH complexes and the interaction of the microtubule to the kinetochore (Pinsky et al., 2006; Shang et al., 2003). In the fission yeast there is as of yet no evidence that the Dam1/DASH complex is regulated by Aurora B/Ark1 kinase activity. Any error correction pathway may act in a similar manner as in the budding yeast by detaching mal-oriented microtubule configurations and allowing new attachments to form, however as of yet the mechanics of such a system are unknown. We presume however, that such an error correction pathway may function through various mitotic regulators such as Klp5 and Klp6 to 'turnover' merotelic attachments and Mal3 to 'turnover' syntelic mono-polar attachments. Indeed further evidence for a possible functional overlap in erroneous attachment correction comes from studies on our double mutant *dam1-A8Δklp5*.

To understand the reasons for the synthetic lethality between the Dam1/DASH complex and the kinesins Klp5 and Klp6 we generated a temperature sensitive *dam1* mutant in a *Δklp5* background. The double mutant *dam1-A8Δklp5* shows severe chromosome segregation defects following incubation at the restrictive temperature and is dependent on the spindle assembly checkpoint protein Mad2 for survival even at the permissive temperature. This indicates that these cells require the time provided by the spindle assembly checkpoint to activate a repair pathway in an attempt to 'turnover' erroneous kinetochore-microtubule configurations. Live analysis of *cen2*-GFP sister chromatid separation in these *dam1-A8Δklp6* cells showed a typical *klp6* phenotype of chromosome congression defects with oscillations of the sister chromatids from one pole to other pole prior to anaphase onset. More than half of the double mutant cells eventually went on to segregate their cells normally following the oscillations, however, 5/12 cells did not segregate their sister chromatids properly and mono-polar segregation defects occurred. It is presumed that the chromosome oscillation and shuttling phenotype in *Δklp6* cells is indicative of the presence of merotelic attachments which cause the sisters to be pulled from one pole to the other. The double *dam1-A8Δklp6* mutants that display an oscillatory phenotype must be attached in a merotelic manner and those that go on to segregate in a mono-polar fashion are highlighting the possible sequential steps involved in the resolution of these mal-orientations, whereby merotelic configurations may be first resolved to monotelic or syntelic mono-polar states before complete resolution to a proper bipolar attachment state. If the detachment of mal-connected microtubules occurred in a stochastic manner then merotelic kinetochores could be turned over to amphitelic, monotelic or syntelic configurations. These mono-polar connections could be then further processed to ensure the establishment of amphitelic bipolar and bi-oriented configurations (Figure 6.2). This mutant shows the important overlapping but distinct role that both Klp5 and Klp6 play with the Dam1/DASH complex in the 'turnover' of mal-oriented attachments and bi-oriented kinetochores.

Our *dam1-A8* mutant contains two mutations sites in the C-terminal region H126R and E149G. The single *dam1-A8* mutant in a *klp5*$^{+}$ background is resistant to the spindle depolymerising drug TBZ. The *dam1-127* C-terminal truncation mutant identified as a multicopy suppressor of *cdc13-117* and *mal3-1* cells also demonstrates resistance to TBZ (Sanchez-Perez et al., 2005).

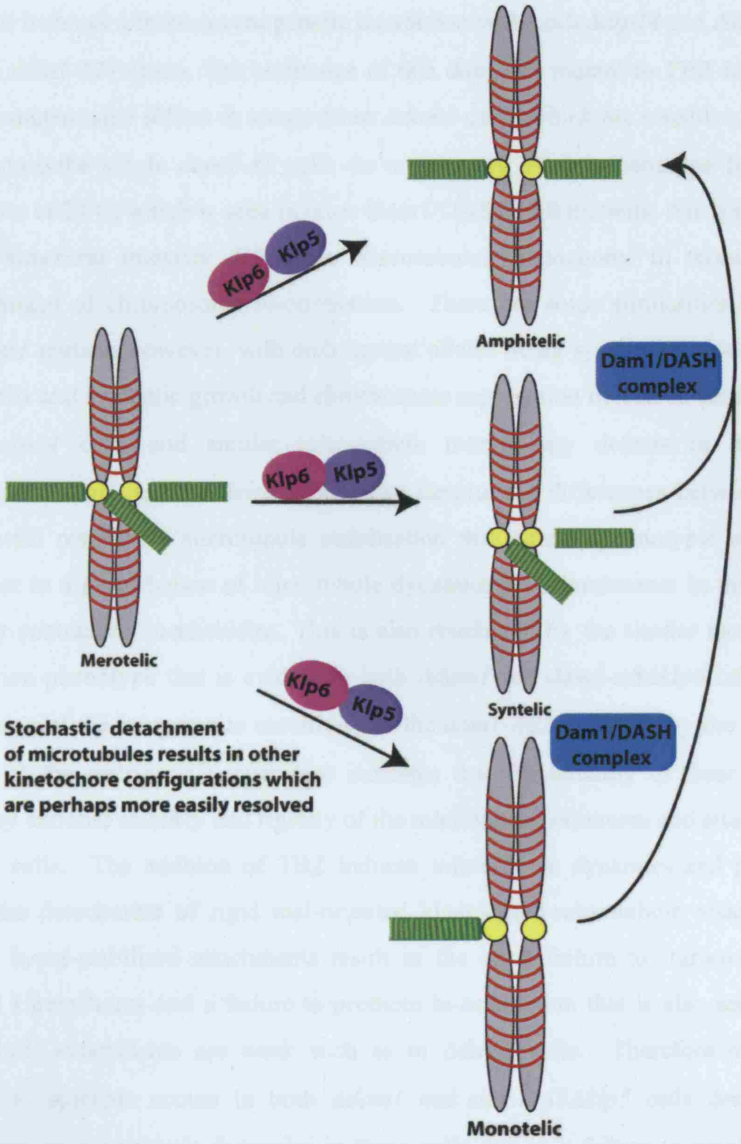

Figure 6.2: Model of 'turnover' of merotelic kinetochore configurations in a stochastic manner

Resolution of merotelic kinetochores may occur through disassembly of mal-oriented microtubules from the kinetochore. This probably occurs in a stochastic manner which give rise to monotelic, syntelic and amphitelic configurations. The mono-polar monotelic and syntelic configurations are perhaps further resolved to yield bipolar amphitelic configurations.

We showed that our *dam1-A8* mutant does not act simply as a C-terminal disruption mutant as it shows a more severe genetic interaction with both *Δalp14* and *Δklp5* cells than the *dam1-127* strain. The resistance of this *dam1-A8* mutant to TBZ highlights that this mutant also differs in nature from *Δdam1* cells, which are sensitive to TBZ. Furthermore the single *dam1-A8* cells do not display a '*dis*' phenotype following incubation at 20°C, which is seen in other Dam1/DASH null mutants, this is probably due to structural integrity defects in microtubules/kinetochores in terms of the establishment of chromosome bi-orientation. There are some similarities between both *dam1* mutants however, with both mutant alleles being synthetically lethal with *Δdis1* cells and synthetic growth and chromosome segregation defects in combination with *Δalp14* cells and similar microtubule morphology defects in a *Δmal3* background. This perhaps demonstrates that despite the differences between these strains with respect to microtubule stabilisation that similar phenotypic outcomes result due to a perturbation of microtubule dynamics and attachments in these cells albeit by contrasting mechanisms. This is also reinforced by the similar mono-polar segregation phenotype that is evident in both *Δdam1* and *dam1-A8Δklp6* cells. The suppression of the temperature sensitivity of the *dam1-A8Δklp5* cells by the addition of TBZ at the restrictive temperature indicates that the lethality of these cells is caused by extreme stability and rigidity of the microtubule structures and attachments in these cells. The addition of TBZ induces microtubule dynamics and probably allows the detachment of rigid mal-oriented kinetochore-microtubule attachments. Perhaps hyper-stabilised attachments result in the same failure to 'turnover' mal-oriented kinetochores and a failure to promote bi-orientation that is also seen when microtubule attachments are weak such as in *Δdam1* cells. Therefore the same phenotypic outcome occurs in both *Δdam1* and *dam1-A8Δklp5* cells despite the differences in microtubule dynamics in these cells due to a failure to resolve mal-oriented kinetochore states. It would seem that the Dam1/DASH complex, while dispensable for viability, is required in concert with other mitotic regulators to ensure high fidelity microtubule attachments and proper chromosome segregation.

We have demonstrated that the Dam1/DASH complex is conserved in the fission yeast and plays an important role in accurate chromosome segregation during mitosis by ensuring correctly configured kinetochore-microtubule interactions through the resolution and 'turnover' of mal-oriented mono-polar attachment states. It is of interest that this complex is not essential in the fission yeast and begs the question as to the conservation of this complex in higher organisms, which also contain

structurally and functionally complex centromere/kinetochore systems. There is one report of an Ask1 homologue in the fruitfly however this has not been confirmed. Currently the existence and identification of Dam1/DASH members in higher organisms remains elusive. Perhaps if this complex is conserved amongst vertebrates then it is also non-essential and functions in concert with a myriad of other mitotic regulators to ensure correct microtubule-kinetochore attachments, although this remains to be seen.

Chapter 7

7 Materials & Methods

7.1 Stocks & Solutions

The Cancer Research UK Central Services provided all media; pipette tips, autoclaved glassware, and some commonly used chemical solutions.

7.1.1 Media recipes

Media Type	Ingredients
EMM (Minimal media used for proto/auxotrophic selection)	14.7 mM KH phthalate, 15.5 mM Na_2HPO_4, 93.5 mM NH_4Cl, 111 mM dextrose, salt and vitamin stocks.
DV clear media	EMM
N_2 starvation media	EMM – NH_4Cl
L Broth (for bacteria)	170 mM NaCl, 0.5% (w/v) yeast extract, 1% (w/v) bacto-tryptone, pH 7.0.
YE (rich fission yeast media)	0.5% Difco yeast extract, 3% dextrose
YE5S (rich fission yeast media)	0.5% Difco yeast extract (yeast nitrogen base – amino acids not yet added), 3% dextrose +250 μg/ml, histidine, leucine, uracil, adenine, and lysine.
YFM (fission yeast freezing media)	YE5S with 15% glycerol

7.1.2 Immunoflourescent reagents

Immunoflourescent reagents	
PBSA (washing and mounting cells)	170 mM NACl, 3 mM KCl, 10 mM Na_2HPO_4, 2 mM KH_2PO_4. pH 7.0.
PEM (pH 6.9)	100 mM PIPES, 1 mM EGTA, 1 mM $MgSO_4$.
1.2 M Sorbitol	1.2 M Sorbitol
PEMS	PEM + 1.2 M Sorbitol.
PEMBAL (pH 6.9)	PEM +1%BSA, 0.1% NaN_3, 100 mM lysine hydrochloride. Filter sterilised.

7.1.3 DNA reagents

DNA reagents	
TE	10 mM Tris-HCl, pH 7.0, 0.1 M EDTA.
TBE	0.02M Tris borate, 0.4 mM Na_2EDTA
TAE	0.08M Tris acetate, 2 mM Na_2EDTA
10X loading buffer	60% (w/v) sucrose, 0.1% (w/v) bromophenol blue.

7.1.4 Commercial Kits

TaKaRa LA Taq™:

PCR kit for amplification of long DNA fragments (5-17kb).

QIAquick Gel extraction kit:

DNA purification system for extraction and clean-up of linear DNA (70bp-10kb) from agarose gels.

Promega Wizard® DNA clean-up system:

DNA purification system for linear and circular DNA (200bp-50kb). Used in this study for purification of DNA from PCR reactions and plasmid recovery from fission yeast transformants in multi-copy suppressor screen.

7.2 Yeast Physiology

7.2.1 Fission yeast nomenclature

The nomenclature used for fission yeast in this thesis is as follows. Gene names and other *cis* elements are represented in italics, e.g. *dam1*. The wild-type allele of a gene is denoted in italics with a superscript plus sign following the gene name e.g. *dam1*$^{+}$. Mutant alleles of the gene are indicated in italics followed by the allele number e.g. *dam1-A8*, *dam1-127*. When a gene has been deleted by the integration of a specific marker gene this is represented by the gene name written in italics, followed by the marker name that is replacing it, and separated by '::' e.g. *klp5::Ura4* . Resistance to the selectable marker is denoted by the presence of a superscript 'r' e.g. *dam1::kan*^{r}. Deleted genes in this thesis are often referred to by the presence of a 'Δ' before the italiised gene name e.g. *Δdam1*. A gene that has been C-terminally tagged is represented by the italicised gene name followed by the name of the tag and its selectable marker e.g. *dam1*$^{+}$*-GFP-kan*^{r}. Protein names are not italicised in the fission yeast. The gene products are given the same name as the gene name, however, the first letter is written in the upper-case e.g. Dam1. Tagged gene products are also not written in italics and are represented by the protein name followed by the name of the tag and its selectable marker e.g. Dam1-GFP-Kan.

7.2.2 Budding yeast nomenclature

Gene names within the budding yeast are represented in upper-case italics e.g. *DAM1*. Mutant alleles are denoted in lower-case italics followed by the allele number e.g. *dam1-1*. Gene deletions and protein names follow the fission yeast format.

7.2.3 Strain growth and maintenance

Fission yeast strains were frozen and stored, revived, grown and maintained according to well-described methods (Moreno et al., 1991). *S. pombe* cells were grown either in liquid culture media or on agar plates containing 1.6% agar. The recipes for different media types are listed above in section 7.1. Stocks of yeast strains were stored in YFM media at -70°C. Selection media containing the drug Geneticine (G418), to assay for Kanamycin resistance, were made by the addition of 100μg/ml G418 to molten YE5S agar. Selection plates containing the dye phloxin B

(Sigma # P4030), to assess dead or dying cells, were made by the addition of 5mg/L phloxin B to cooled YE5S molten agar. Selection plates containing the drug Hygromycin B (Hph, Roche) were made by the addition of 300μg/ml hygromycin B to molten YE5S agar. Selection plates containing the drug nourseothricin (clonNAT, Werner Bio-agents) were made by the addition of 100μg/ml clonNAT to YE5S molten agar.

7.2.4 Transformation of DNA into *S. pombe* cells

Transformation of fission yeast cells was carried out to introduce plasmid DNA or to integrate a PCR product into the genome. The protocol used for the transformation of DNA into *S. pombe* cells is based on well-described methods (Bahler et al., 1998; Keeney and Boeke, 1994). This protocol uses lithium acetate (10x LiAc: 1M lithium acetate, pH 7.5; 10x TE: 0.1 M Tris-HCl, 0.01 M EDTA, pH 7.5), fresh PEG 40% and DMSO.

A 50ml culture was grown to log phase (approximately $1x10^7$ cells/ml) in YE5S media. Cells were pelleted and washed in an equal volume of ddH_2O, followed by 1ml ddH_2O and then 1ml LiAc/TE solution. Cells were resuspended in ~200μl LiAc/TE solution and 100μl used for each transformation. Salmon sperm DNA (10μg/ml, Stratagene) was added (approximately 2μl) to cell mix. Approximately 3-10 μg PCR fragments, or ~1 μg plasmid DNA, added to the mix. Cells were incubated with the DNA at room temperature for 10 mins. 260μl PEG4000/LiAc/TE (40% in LiAc/TE solution) was added, mixed gently by pipetting, and then incubated for 30-60 mins at 30°C (25°C for temperature sensitive strains). 43μl of pre-warmed DMSO was added and the cells heat-shocked at 42°C for 5 mins. Cells were pelleted, washed in 1ml ddH_2O then resuspended in 500μl ddH_2O. 250μl was plated onto the appropriate media and incubated at 30° (25°C for temperature sensitive strains) for selection. For drug resistant selection, cells were first plated onto YE5S and incubated overnight before replica plating onto selection plates. Selective markers used include, *LEU2*, *ura4*$^+$, *his7*$^+$, *kan*^{r}, *nat*^{r} and *hph*^{r}. Transformants were selected, restreaked onto selective media and their phenotypes and/or genotypes verified. Oligonucleotides used for amplifying PCR fragments, and plasmids used for transformation listed in sections 7.5 and 7.6.

7.2.5 Random spore analysis and tetrad dissection

Most of the strains used in this study were constructed by random spore analysis. Strains of different mating types and different genotypes were crossed on EMM plates lacking nitrogen (conjugation and sporulation do not take place in fission yeast except under conditions of nutrient starvation) and allowed to sporulate for 3 days. Once mated and ascii observed, cells treated with 0.5% helicase (a crude snail gut enzyme that can break down the ascus wall) for between 1-5 hours. The ascii/cells are then pelleted, washed in ddH_2O and plated onto YE5S plates to grown unassorted for several days before replica plating to selection media to obtain desired strain.

For tetrad dissection a two-day-old cross is most normally used, as the ascus wall has not yet begun to break down at this stage. Asci are selected using a micromanipulator and placed in a vertical line about 3mm apart on a YE5S plate and left to breakdown at 30°C for approximately 3-5 hours. All four spores from each ascus are separated on plates by the micromanipulator to give a line of four isolated spores separated by about 3-5mm. These plates are incubated at an appropriate temperature until colonies form and desired strain selected by replica plating to selection media. Strains generated from both ransom spore analysis and tetrad dissection, which are used in this study, are listed along with externally obtained strains in section 7.3.

7.2.6 Cell number counting and viability assays

Cell number of fission yeast cultures were counted using Sysmex Microcell counter F-800. 20µl or 200µl of cell culture added to 10ml of Isoton (Beckman Coulter), sonicated (soniprep 150 sonicator MSE, setting 5) for approximately 45 seconds and counted on Sysmex F-800. For viability assays cells were counted, diluted into YE5S broth and plated out on YE5S plates at a concentration of ~500 cells per plate. Plates were incubated at 26°C and colonies that grew were counted and calculated as a percentage of the 500 plated cells.

7.2.7 Production of synchronous cultures

To synchronise cells in G2 or M phase for various experimental procedures we used either hydroxyurea (HU) treatment or centrifugal elutriation.

7.2.7.1 HU induced S-phase arrest

To examine populations of mitotic cells in assorted strains we used HU block and release experiments. HU is a drug that stalls DNA replication through the inhibition of ribonucleotide reductase, leading to a depletion of the cellular level of dNTP's and an early S-phase arrest through the activation of the S-phase checkpoint. The addition of HU allows cells to accumulate in early S-phase and upon release into HU-free media they can resume the cell cycle at late S-phase. In our experiments 11mM HU (must be made fresh) was added to an exponentially growing culture (approximately $2x10^6$ cells/ml) and incubated for 4 hours at 26°C. Cells were then filtered and washed 2-3 times in YE5S broth and re-suspended in HU-free media.

7.2.7.2 Centrifugal elutriation-synchrony in early G2

Centrifugal elutriation was carried out using a Beckman Coulter Avanti J-20 centrifuge as described by the manual and as previously published (Moreno et al., 1991). Centrifugal elutriation is a process whereby cells are separated according to size. The opposing centrifugal force and the pressure created by the use of a pump within the elutriation chamber, causes the sedimentation of the cells by size, with the smallest cells (G2 cells in fission yeast) sedimenting at a slower rate. Increasing the pressure from the pump causes these G2 cells to be elutriated out of the chamber where they can be harvested. A 3 litre culture of cells is grown in YE5S to a mid-log phase cell number of approximately $2x10^{10}$ cells in total. Cells are pumped into the elutriation chamber, which is maintained at 26°C, at a pump rate of ~85 ml/min and increased to ~110ml/min to build up sedimentation front of cells within the chamber. When all cells are loaded reservoir is switched to fresh media and pump rate adjusted to between 60-110 ml/min to allow elutriation and collection of smallest G2 cells. Elutriated cultures then split in half, filtered, re-suspended in pre-warmed media at 26°C or 36°C for several hours. Synchrony was measured as a percentage of septated to non-septated cells.

7.2.8 Microtubule drug treatment & cold shock

To assess sensitivity or resistance of strains to microtubule de-polymerising drugs we used plates containing thiabendazole (TBZ). TBZ was added to YE5S plates at a concentration of 10, 15, 20, 50 or 75 μg/ml, depending on the individual experiment.

Stock solutions of TBZ were prepared to a concentration of 20mg/ml in DMSO and stored at -20°C. To visualise the physiology of cells in liquid culture following incubation with a microtubule de-polymerising drug we used carbendazim (MBC/CBZ). MBC/CBZ was added to HU arrested and released cells at a concentration of 50μg/ml as previously described (Hardwick et al., 2000). Stock solutions of MBC/CBZ were stored at 5mg/ml concentrations in DMSO at -20°C.

Cold shock treatment to de-polymerise microtubules was carried out by incubation of cells on ice for 30 minutes. Cells were then fixed in 3% formaldehyde while on the ice to prevent rapid re-polymerisation of microtubules.

7.2.9 Mini-chromosome loss assay

Mini-chromosome loss assay was carried out to assess the fidelity of chromosome segregation in various Dam1/DASH null mutants compared to wild-type cells. For this assay we used a well-established method (Niwa et al., 1989), whereby a non-essential linear mini-chromosome (Ch16) was incorporated into the strains to be tested. This nonessential minichromosome (Ch16) derives from the centromeric region of chromosome 3 in the fission yeast and contains the *ade6-m216* allele, which can compensate for the *ade6-m210* adenine mutation, which is carried endogenously in the genome of the strains to be tested. Cells were grown on selective media (EMM-adenine) lacking adenine to retain the mini-chromosome and were then cultured overnight and plated onto rich YE media and incubated at 30°C for 4 days. The mini-chromosome is normally stably maintained in mitosis, however when chromosome segregation or DNA replication defects occur the mini-chromosomes are lost and the cells appear as red auxotrophs on the YE plates. The percentage of chromosome loss is calculated by quantifying the number of colonies with red sectors against the total number of colonies.

7.2.10 Spot test growth assay

To examine the growth of mutant strains at various temperatures, or in the presence of microtubule drugs, compared to wild-type and other control strains, we carried out a serial dilution spot test assay. Strains were streaked fresh onto rich media YE5S plates overnight and then suspended in ddH_2O and cell number calculated. Cell concentration was adjusted to 1 x 10^7 cells/ml as the starting concentration and

serially diluted in a ten-fold manner in a 96 well micro-titre plate. 5µl of each dilution was spotted onto appropriate agar plates such that the first spot contains 5 x 10^4 cells/ml. Plates used varied depending on individual experiments but often included YE5S, YE5S& phloxin B and TBZ containing plates of varying concentrations.

7.2.11 Plasmid loss assay on plates and liquid culture

Plasmid loss assay on plates was carried out by culturing various mutant strains and wild-type (control) cells, containing plasmid to be lost, overnight in selective media, EMM- leucine (plasmid contains *LEU2* marker). Cell number was calculated and approximately 500 cells were plated onto rich agar YE5S, incubated at 26°C for 4 days, followed by replica plating onto minimal media lacking leucine (EMM – leucine) for 3 days. The number of colonies that could no longer grow in the absence of leucine (EMM- leucine) was calculated as a percentage of the total 500 colonies. This represented the percentage of cells that had lost the plasmid.

To study the phenotypic defects of plasmid loss in mutant and wild-type strains we carried out nitrogen starvation and re-feeding to induce plasmid loss in liquid culture. Cells containing plasmid to be lost were starved of nitrogen for ~ 12 hours overnight by incubation in minimal media lacking nitrogen (EMM-NH_4Cl), washed and re-suspended in rich media YE5S broth at 36°C for 8 hours. Samples were harvested every hours and processed for immuno-flourescent staining.

7.3 Fission yeast strain list

Name	Genotype	Derivation
513	*h⁻ leu1 ura4*	Lab stock
TP108-3D	*h⁺ leu1 ura4 his2*	Lab stock
CHP428	*h⁺ leu1 ura4 his7 ade6-210*	Dr.Hoffmann
CHP429	*h⁻ leu1 ura4 his7 ade6-m216*	Dr. Hoffmann
HM248	*h⁻ his2 ade6-210* containing Ch16	Dr. Niwa
HM?	*h⁺ ade6-210* containing Ch16	Dr. Niwa
KC29	*h⁻ leu1 ura4 dam1⁺-GFP-Kan^r*	This study

KC56	*h⁻ leu1 ura4 dad1⁺-GFP-Kan^r*	This study
KC57	*h⁻ leu1 ura4 ask1⁺-GFP-Kan^r*	This study
KC58	*h⁻ leu1 ura4 duo1⁺-GFP-Kan^r*	This study
MA217	*h⁺ leu1 ura4 his2 nuf2⁺-CFP-Kan^r*	Lab stock
KC164	*h⁺ leu1 ura4 his2 nuf2⁺-CFP-Kan^r dad1⁺-GFP-Kan^r*	This study
KC175	*h⁺ leu1 ura4 his2 dam1⁺-GFP-Kan^r Sad1⁺-dsRed-LEU2⁺*	This study
MA194	*h⁻ leu1 ura4 sad1⁺-dsRed-LEU2⁺*	Lab stock
KC396	*h⁻ leu1 ura4 dam1⁺-GFP-Kan^r dad1:: Kan^r*	This study
Mal2-1	*h⁻ leu1 ura4 ade6-210 mal2-1^ts*	Dr. Fleig
KC201	*h⁺ leu1 ura4 ade6-210 dad1⁺-GFP-Kan^r mal2-1^ts*	This study
SP540	*h⁻ leu1 ade6-216 mis6-302^ts*	Dr. Takahashi
SP142	*h⁺ leu1 his2 mis6-302^ts*	Dr. Takahsahi
KC181	*h⁻ leu1 ura4 dad1⁺-GFP-Kan^r* mis6-302^ts	This study
SP920	*h⁻ leu1 ura4 mis12-537^ts*	Dr. Takahashi
SP306	*h⁺ leu1 ura4 his2 mis12-537^ts*	Dr. Takahashi
KC179	*h⁻ leu1 ura4 dad1⁺-GFP-Kan^r mis12-537^ts*	This study
SP525	*h⁻ leu1 ura4 cnp1::ura4⁺lys1⁺-cnp1-1^ts*	Dr. Takahashi
KC200	*h⁻ leu1 ura4 cnp1::ura4⁺lys1⁺-cnp1-1^ts dad1⁺-GFP-Kan^r*	This study
FY5232	*h⁺ arg3 leu1 ura4 ade6-216 sim4-193^ts*	Dr. Fleig
FY5233	*h⁻ arg3 leu1 ura4 ade6-216 sim4-193^ts*	Dr. Fleig
KC202	*h⁺ leu1 ura4 his2 dad1⁺-GFP-Kan^r sim4-193^ts*	This study
ANF254-3A	*h⁺ ura4 nuf2-4- ura4⁺*	Dr. Takahashi
KC199	*h⁺ leu1 ura4 nuf2-4- ura4^ts⁺ dad1⁺-GFP-Kan^r*	This study
alp12	*h⁺ leu1 ura4 his2 nda3-1828^ts*	Lab stock
KC184	*h⁺ leu1 ura4 his2 dam1⁺-GFP-Kan^r nda3-1828^ts*	This study
KC207	*h⁻ leu1 ura4 dad1⁺-GFP-Kan^r nda3-1828^ts*	This study
KC210	*h⁻ leu1 ura4 dad1::kan^r cnp1⁺-GFP::lys1⁺*	This study
Cnp1-GFP	*h⁻ leu1 ura4 cnp1⁺-GFP::lys1⁺*	Lab stock
nda3-311	*h⁻ arg1 leu1 ura4 nda3-311^cs*	Lab stock
KC211	*h⁺ leu1 ura4 his2 dam1⁺-GFP-Kan^r nda3-311^cs*	This study
	h⁻ leu1 ura4 dis1::ura4⁺	Dr. Yanagida
MA131	*h⁺ leu1 ura4 his7 dis1::ura4⁺*	Lab stock
MA130	*h⁻ leu1 ura4 ade6-210 alp14::kan^r*	Lab stock

NK162	*h⁻ leu1 ura4 alp14::kan::ura4⁺*	Lab stock
MA060	*h⁺ leu1 ura4 his7 ade6-216 klp5::ura4⁺*	Lab stock
MA061	*h⁻ leu1 ura4 his7 ade6-210 klp6:: ura4⁺*	Lab stock
KC137	*h⁺ leu1 ura4 his2 dam1⁺-GFP-Kan^r dis1::ura4⁺*	This study
KC397	*h⁻ leu1 ura4 dam1⁺-GFP-Kan^r alp14::kan::ura4⁺*	This study
KC213	*h⁺ leu1 ura4 his7 dam1⁺-GFP-Kan^r klp5::ura4⁺*	This study
KC60	*h⁺ leu1 ura4 ade6-216 dam1:: kan^r*	This study
KC392	*h⁺ leu1 ura4 ade6-216 dam1::kan::hph^r*	This study
KC63	*h⁻ leu1 ura4 ade6-210 dad1::kan^r*	This study
KC62	*h⁻ leu1 ura4 ade6-210 SPC34::kan^r*	This study
KC61	*h⁻ leu1 ura4 ade6-216 ask1::kan^r*	This study
MS197	*h⁺ leu1 ura4 mad2:: LEU2⁺*	Lab stock
	h⁻ leu1 ura4 mad2:: LEU2⁺	Lab stock
343	*h⁻ leu1 ura4 ade6-216 bub1::ura4⁺*	Dr. Javerzat
KC154	*h⁺ leu1 ura4 ade6-216 dam1::kan^r* containing Ch16	This study
KC155	*h⁺ leu1 ura4 ade6-216 ask1::kan^r* containing Ch16	This study
KC106	*h⁻ leu1 ura4 dam1::kan^r bub1::ura4⁺*	This study
KC107	*h⁺ leu1 ura4 dam1::kan^r bub1::ura4⁺*	This study
KC108	*h⁻ leu1 ura4 dam1::kan^r mad2::LEU2⁺*	This study
KC109	*h⁺ leu1 ura4 dam1::kan^r mad2::LEU2⁺*	This study
KC112	*h⁺ leu1 ura4 dad1::kan^r mad2::LEU2⁺*	This study
KC111	*h⁻ leu1 ura4 dad1::kan^r bub1::ura4⁺*	This study
MA239	*h⁻ leu1 ura4 bub1⁺-GFP-Kan^r*	Lab stock
KC409	*h⁻ leu1 ura4 dam1::kan^r bub1⁺-GFP-Kan^r*	This study
KC89	*h⁺ leu1 ura4 ask1::kan^r bub1::ura4⁺*	This study
KC87	*h⁺ leu1 ura4 ask1::kan^r mad2::LEU2⁺*	This study
KC85	*h⁻ leu1 ura4 spc34::kan^r bub1::ura4⁺*	This study
KC83	*h⁻ leu1 ura4 spc34::kan^r mad2::LEU2⁺*	This study
KC197	*h⁺ leu1 ura4 dam1::kan^r alp14::kan::ura4⁺*	This study
KC187	*h⁺ leu1 ura4 dam1::kan^r mis12-537^ts*	This study
KC158	*h⁺ leu1 ura4 ask1::kan^r mis12-537^ts*	This study
KC195	*h⁺ leu1 ura4 dam1::kan^r mal3::kan::ura4⁺*	This study
	h⁻ leu1 ura4 mal3::kan::ura4⁺	Lab stock
	h⁻ leu1 ura4 sgo2::kan^r	Lab stock
	h⁺ leu1 ura4 sgo2::kan^r	This study

KC410	*h⁻ leu1 ura4 sgo2::kan^r dam1:: ura4^+*	This study
KC190	*h^+ leu1 ura4 ask1::kan^r cnp1::ura4^+ lys1^+- cnp1-1^ts*	This study
KC188	*h^+ leu1 ura4 dam1::kan^r cnp1::ura4^+ lys1^+- cnp1-1^ts*	This study
KC415	*h⁻ leu1 ura4 ade6-216 dam1::kan^r sim4-193^ts*	This study
KC416	*h⁻ leu1 ura4 ade6-216 dad1::kan^r sim4-193^ts*	This study
KC220	*h⁻ leu1 ura4 dad1::kan^r nuf2-2:: ura4^+*	This study
KC221	*h⁻ leu1 ura4 dad1::kan^r nuf2-4:: ura4^+*	This study
Δ*scd1*	*h^90 leu1 ura4 ade6-210 scd1:: ura4^+*	Dr. Chang
KC216	*h^90 leu1 ura4 ade6-210 scd1:: ura4^+* containing p*scd1^+-LEU2^+*	This study
KC217	*h^+ leu1 ura4 ade6-210 dam1::kan^r scd1:: ura4^+* containing p*scd1^+-LEU2^+*	This study
KC218	*h^+ leu1 ura4 ade6-210 dad1::kan^r scd1:: ura4^+* containing p*scd1^+-LEU2^+*	This study
KC413	*h^+ leu1 ura4 ade6-210 ask1::kan^r scd1:: ura4^+* containing p*scd1^+-LEU2^+*	This study
KC414	*h^+ leu1 ura4 ade6-210 spc34::kan^r scd1:: ura4^+* containing p*scd1^+-LEU2^+*	This study
KZ85	*h^+ leu1 his7+::lacI-GFP ura4 cen2::Kan-ura4^+-lacOp sad1^+-dsRed-LEU2^+*	Lab stock
KC411	*h^+ leu1 dam1::hph^r his7+::lacI-GFP ura4? cen2::Kan-ura4^+-lacOp sad1^+-dsRed-LEU2^+*	This study
MA042	*h⁻ leu1 ura4 dis1^+-GFP-Kan^r*	Lab stock
KC398	*h⁻ leu1 ura4 dam1::hph^r dis1^+-GFP-Kan^r*	This study
KC367	*h^+ leu1 ura4 his7 dam1-A8^ts*-GFP- *hph^r klp5::ura4^+*	This study
KC366	*h^+ leu1 ura4 his7 dam1-A8^ts*-GFP- *nat^r klp5::ura4^+*	This study
KC344	*h^+ leu1 ura4 his7 dam1-A8^ts*-GFP- *kan^r klp5::ura4^+*	This study
KC301	*h^+ leu1 ura4 his7 dam1-4^ts*-GFP- *kan^r klp5::ura4^+*	This study
KC302	*h^+ leu1 ura4 his7 dam1-7^ts*-GFP- *kan^r klp5::ura4^+*	This study

KC303	*h⁺ leu1 ura4 his7 dam1-8 ts*-GFP- *kan^r* *klp5::ura4⁺*	This study
KC304	*h⁺ leu1 ura4 his7 dam1-9 ts*-GFP- *kan^r* *klp5::ura4⁺*	This study
KC306	*h⁺ leu1 ura4 his7 dam1-11 ts*-GFP- *kan^r* *klp5::ura4⁺*	This study
KC308	*h⁺ leu1 ura4 his7 dam1-16 ts*-GFP- *kan^r* *klp5::ura4⁺*	This study
KC310	*h⁺ leu1 ura4 his7 dam1-18 ts*-GFP- *kan^r* *klp5::ura4⁺*	This study
KC311	*h⁺ leu1 ura4 his7 dam1-20 ts*-GFP- *kan^r* *klp5::ura4⁺*	This study
KC314	*h⁺ leu1 ura4 his7 dam1-24 ts*-GFP- *kan^r* *klp5::ura4⁺*	This study
KC329	*h⁺ leu1 ura4 his7 dam1-A1 ts*-GFP- *kan^r* *klp5::ura4⁺*	This study
KC331	*h⁺ leu1 ura4 his7 dam1-A3 ts*-GFP- *kan^r* *klp5::ura4⁺*	This study
KC332	*h⁺ leu1 ura4 his7 dam1-A4 ts*-GFP- *kan^r* *klp5::ura4⁺*	This study
KC333	*h⁺ leu1 ura4 his7 dam1-A5 ts*-GFP- *kan^r* *klp5::ura4⁺*	This study
KC336	*h⁺ leu1 ura4 his7 dam1-A6 ts*-GFP- *kan^r* *klp5::ura4⁺*	This study
KC335	*h⁺ leu1 ura4 his7 dam1-A7 ts*-GFP- *kan^r* *klp5::ura4⁺*	This study
KC400	*h⁺ leu1 ura4 his7 dam1-A8 ts*-GFP- *hph^r* *klp5::ura4⁺ ask1⁺-GFP-Kan^r*	This study
KC346	*h⁻ leu1 ura4 dam1-A8 ts*-GFP- *kan^r*	This study
KC345	*h⁺ leu1 ura4 his7 dam1-A8 ts*-GFP- *kan^r*	This study
KC399	*h⁺ leu1 ura4 his7 dam1-A8 ts*-GFP- *hph^r*	This study
KC356	*h⁺ leu1 ura4 his7 dam1-A8 ts*-GFP- *hph^r* *klp5::ura4⁺ mad2⁺-GFP-LEU2⁺*	This study
MA?	*h⁻ leu1 ura4 mad2⁺-GFP-LEU2⁺*	Lab stock
KC401	*h⁺ leu1 ura4 ura4 his7 dam1-A8 ts*-GFP- *hph^r* *mad2⁺-GFP-LEU2⁺*	This study

KC402	*h⁻ leu1 ura4 ura4 dam1-A8*^{ts}-GFP- *hph*^{r} *sgo2::kan*^{r}	This study
KC403	*h*$^{+}$ *leu1 ura4 his7 dam1-A8*^{ts}-GFP- *hph*^{r} *klp5::ura4*$^{+}$ *sgo2::kan*^{r}	This study
KC404	*h⁻ leu1 ura4 dam1-A8*^{ts}-GFP- *hph*^{r} *klp5::ura4*$^{+}$ *mal3::kan*^{r}	This study
KC405	*h⁻ leu1 ura4 dam1-A8*^{ts}-GFP- *hph*^{r} *mal3::kan*^{r}	This study
KC391	*h⁻ leu1 ura4 dam1-A8*^{ts}-GFP- *hph*^{r} *alp14::kan::ura4*$^{+}$	This study
dam1-127	*h⁻ leu1 ura4 dam1-127-kan*^{r}	Dr. Millar
KC407	*h*$^{+}$ *leu1 ura4 dam1-127-kan*^{r} *alp14::kan::ura4*$^{+}$	This study
KC408	*h*$^{+}$ *leu1 ura4 dam1-127-kan*^{r} *klp5::ura4*$^{+}$	This study
KC359	*h*$^{+}$ *leu1 ura4 his7+::lacI-GFP ura4? Cen2::Kan-ura4*$^{+}$*-lacOp Sad1*$^{+}$*-dsRed-LEU2*$^{+}$ *dam1-A8*^{ts}-GFP- *hph*^{r} *klp6::kan*^{r}	This study
KC412	*h*$^{+}$ *leu1 ura4 his7+::lacI-GFP ura4? Cen2::Kan-ura4*$^{+}$*-lacOp Sad1*$^{+}$*-dsRed-LEU2*$^{+}$ *dam1-A8*^{ts}-GFP- *hph*^{r}	This study
AR030	*h*$^{+}$ *leu1 ura4 his7+::lacI-GFP ura4? Cen2::Kan-ura4*$^{+}$*-lacOp Sad1*$^{+}$*-dsRed-LEU2*$^{+}$ *klp6::kan*^{r}	Lab stock
KC420	*h*$^{+}$ *leu1 ura4 his7 dam1-A8*^{ts}-GFP- *hph*^{r} *klp5::ura4*$^{+}$ contains suppressor plasmid #2-p*klp5*$^{+}$	This study
KC421	*h*$^{+}$ *leu1 ura4 his7 dam1-A8*^{ts}-GFP- *hph*^{r} *klp5::ura4*$^{+}$ contains suppressor plasmid #6-p*dam1*$^{+}$	This study
KC422	*h*$^{+}$ *leu1 ura4 his7 dam1-A8*^{ts}-GFP- *hph*^{r} *klp5::ura4*$^{+}$ contains suppressor plasmid #9-p*dam1*$^{+}$	This study
KC423	*h*$^{+}$ *leu1 ura4 his7 dam1-A8*^{ts}-GFP- *hph*^{r} *klp5::ura4*$^{+}$ contains suppressor plasmid #10-p*dsk1*$^{+}$	This study
KC424	*h*$^{+}$ *leu1 ura4 his7 dam1-A8*^{ts}-GFP- *hph*^{r} *klp5::ura4*$^{+}$ contains suppressor plasmid #15-p*klp5*$^{+}$	This study

7.4 Molecular biological techniques

Molecular biology techniques were carried out according to well-described methods (Maniatis et al., 1982). This included the growth and transformation of competent bacterial cells, restriction enzyme digests, minipreps, and gel electrophoresis of DNA in TBE buffer.

7.4.1 Nucleic acid preparation and manipulation

Yeast genomic DNA was prepared using a well-established method (Burke et al., 2000). A 5 ml culture in YE5S was grown over-night to saturation. Cells collected by centrifugation for 5 mins, washed in 500µl ddH_2O, centrifuged for 5 secs and re-suspended in 200µl 'breaking buffer' (2% Triton X-100, 1% SDS, 100mM NaCl, 10mM Tris-HCl-pH8.0, 1mM Na_2EDTA-pH8.0). 200µl phenol:chloroform:isoamyl alcohol was added along with 0.3g of acid washed beads and mixture vortexed for 3-4 mins using the Bio101 Fastprep FP120 cell disruptor (Anachem). 200µl TE (pH 8.0) was then added and mixture centrifuged for further 5 mins. The top aqueous layer was then carefully transferred to a fresh eppendorf, 1ml EtOH added and mixed by inversion. Mixture was incubated at room temperature for 5 mins, centrifuged for 2 mins and supernatant discarded. 500µl of 70% EtOH was added and mixed by inversion. Tube centrifuged for 5 secs, supernatant discarded and pellet air dried at room temperature. The pellet was resuspended in 20µl TE.

Enzymatic digestion of DNA with restriction enzymes carried out as recommended by suppliers (New England Biolabs). DNA fragments were examined on a 1% (w/v) agarose gel in 1xTBE buffer. Electrophoresis was carried out at 100V in 1x TBE buffer.

7.4.2 Polymerase Chain reaction

7.4.2.1 Non-mutagenic PCR

Normal PCR reactions were carried out using LA Taq™ (TaKaRa) and Vent (New England Biolabs) polymerase for high-fidelity amplification when the product was to be used for yeast transformation, including gene-tagging and marker switching. Buffers were supplied by the manufacturers and used as recommended. High-fidelity

PCR reactions for transformation were performed in 50µl volumes with 1 mM $MgSO_4$, 1µM of each oligonucleotide primer, ~ 10ng of template DNA, 0.2 mM dNTPs and 2.5 units of enzyme. Colony PCR samples were prepared in a similar manner, however, without the addition of enzyme. Yeast cells were first added to the reaction mix before boiling at 95°C for 5 mins. The enzyme was subsequently added to reaction mix and PCR reaction started. For colony PCRs a generic in-house prepared Taq polymerase supplied by Cancer Research UK central services was used. PCR reactions were carried out on a Peilter Thermal Cycler-200. PCR products were purified using EtOH precipitation and/or Promega Wizard® DNA clean-up system. PCR products were subsequently run on 1% agarose gel to check for correct product size. If template was used for subsequent sequencing DNA fragment was gel purified using Qiagen QIAquick gel extraction kit.

7.4.2.2 Mutagenic PCR

PCR was carried out under modified 'error-prone' conditions to create DNA fragments containing random mutations. The 'error-prone' PCR was carried out using TaKaRa LA Taq™ Taq polymerase and 10xdGTP. In these reactions the concentration of dGTP was increased to 2mM, whilst the remaining dNTPs were supplied at a concentration of 0.2mM per reaction. The total reaction volume used was 100µl with 1 mM $MgSO_4$, 1µM of each oligonucleotide primer, ~10-50ng of template DNA and ~5units of enzyme.

7.4.3 Sequencing

Forward and reverse oligonucleotide primers of ~20 base pairs each were designed based on the known sequence of the *dam1*$^+$ gene in *S. pombe*, and the GFP-kanamycin vector to which *dam1*$^+$ is tagged. The *dam1*$^+$ gene in *S. pombe* is extremely small (468bp) so a single oligonucloetide was sufficient to read the whole ORF. PCR reactions including each of these oligonucleotide primers (3.2pmol) and *dam1-A8* mutant amplified DNA (150-200ng) were carried out with ABI Prism Dye Terminator Cycle Sequencing Ready Reaction Kit followed by automated readout using a Perkin Elmer sequencer, ABI prism 3730.

7.4.4 Gene Disruption & C-terminal tagging

Genes were disrupted using PCR generated *kan*^{r} containing fragments (Bahler et al., 1998). N. Koonrugsa & S. Dhut carried out deletion of Dam1/DASH genes by insertion of a kanamycin resistance gene (Kan^{R}) into the gene locus within a diploid strain.

C-terminal tagging of genes with HA, Myc or GFP epitopes was also carried out by insertion of PCR generated fragments in the same manner as described above (Bahler et al., 1998). Sequences encoding the epitopes were inserted at the 3' region of the gene just prior to the stop codon, to allow epitope expression. All tagging was confirmed by colony PCR to look for increased gene size.

7.4.5 Transformation and isolation of plasmid DNA in *E. coli*

Competent *E. coli* cells stored at -70°C were thawed on ice and incubated with ~10-50ng of plasmid DNA on ice for 10-30 mins. Cells were then heat shocked at 42°C for 90 secs and incubated on ice for 1-2mins. ~800µl-1ml of LB broth was added, and cells allowed to recover at 37°C for approximately 45 mins. Cells were then plated onto LB plates containing 100µg/ml ampicillin and incubated at 37°C.

5ml of transformed *E. coli* were grown overnight in LB broth containing 100µg/ml ampicillin at 37°C. Cells were then harvested by centrifugation at 5000rpm for 5 mins. Plasmid isolation was carried out internally by Cancer Research UK central services.

7.5 Oligonucleotides

The oligonucelotides designed for use in this study were based on methods and plasmids from Bähler *et al.* (1998). Capitalised letters represent genome binding sequences, whereas italics represent DNA sequences designed to bind to plasmids from Bähler *et al.* (1998). The plasmid binding sequences facilitate the amplification of epitope tags and/or selection markers. The genome binding sequence facilitates the integration of the DNA fragment by homologous recombination into the fission yeast genome.

7.5.1 Deletion oligos

ask1(kan)fwd

CATCGCTAATAATGGACGCTAGTATACCTACACCTCAGTTGCAGTTCGCC
ATAAATTTCACCATTGAGAGTTTCTATACT*CGGATCCCCGGGTTAATTAA*

ask1(kan)rev

CTGCTTAGAAAATAAATAGAAAAAATGCGAAAGTAAGGTTCACTACTAA
GGCGAAACGAAGGTGATAACTTCAGCAGTGC*GAATTCGAGCTCGTTTAAAC*

dad1(kan)fwd

CTATGCATAACATGTCTCTTTTGACTAATATTCTATGCTCGTACGGAAGCT
TCAATTTTGGCATTTAATTATGAAGATAGT*CGGATCCCCGGGTTAATTAA*

dad1(kan)rev

CAGGTTTGTGTATTGTAATATGTAAGTTAATTTAAAAGAATCCTGACCTTT
GACCAATTTTTGAGGACGCTATTAAATTTA*GAATTCGAGCTCGTTTAAAC*

dad2(kan)fwd

CCAAAACCGAAATCGCCTTATATGGTGTAGGAGATAAATCTAGTAAATTT
CGTACCTTCTTCTACAAACATTTGGCGTGAA*CGGATCCCCGGGTTAATTAA*

dad2(kan)rev

CGATACTTGGAACTTGGGTTTGCTGTCGGCTTTACCAATTCTGAAATAGAA
GAAACAATATGAATAAATGGACAGAACAAT*GAATTCGAGCTCGTTTAAC*

dam1(kan)fwd

CGTCTACAGTCTCAGGCTCAGGCTGTTTTTGAGAACGTCGGAAGAAAAAT
GTTCCTGCTGCTGCTGCCGAAAGCGCTGTAG*CGGATCCCCGGGTTAATTA*

dam1(kan)rev

CAATGATCATTATGATTCCGTTGTTTCATTATCCAACCTGATATGCTAGGT
TATTCCCTTCGACTATTATAATAATAAATG*GAATTCGAGCTCGTTTAAAC*

duo1(kan)fwd

CCCTTCGTCTACTCTTTGTACTGAATTTCTTTAAACAATTCGCACATCTTCA
ATCGAATACTTTGTTAGGCTTAAATTGCA*CGGATCCCCGGGTTAATTAA*

duo1(kan)rev

CTATAGTAGGAGCAGAGGAGGTGGCCGATTTTGGAATTGCGGATTGGCGA
TGACTTGCAAAAGATGAAGAAGGAGTCCTAA*GAATTCGGCTCGTTTAAAC*

spc34(kan)fwd

CCCCAGAGATTGCATACACTTTTGGCAACTCTGGTAAAGTGAATTGAAAC
ATACCTTTTACTAATTACGAGTCGAATTAGT*CGGATCCCCGGGTTAATTAA*

spc34(kan)rev

CCTCAAATCCATGATAAAACAACGACCTCGCTTCTCCTTTTCTAAATGTTC
ACCAATACGAAAAGTCGATCTGACTACCAA*GAATTCGAGCTCGTTTAAAC*

7.5.2 C-terminal tagging oligos

ask1-fwd-tag

GCCTGTCTTTGCAGAGGAAATTAGAAACCTTGAATGATTCTAATGATAGT
TTTGTCAAAGAAGAAGATAGTTGGGAACTC*CGGATCCCCGGGTTAATTAA*

ask1-rev-tag

TTTACTTGGTTTACAGTATTTATACCGTGACTTATGATTCTCTTAAAAGAA
GAATTTTCCAAATTAAATAGAACGTACAG*GAATTCGAGCTCGTTTAAAC*

dad1-fwd-tag

TTGAAAATGTCGCGTCTCTTTGGAAGGAGTTTCAAAATTCAGTGTTACAG
AAGAAAGATCGTGAAATGCTAGATGCACCT*CGGATCCCCGGGTTAATTAA*

dad1-tag-rev

GAAGTGACTTAAGGTTTGTGTATTGTAATATGTAAGTTAATTTAAAAGAA
TCCTGACCTTTGACCAATTTTTGAGGACGC*GAATTCGAGCTCGTTTAAAC*

dam1-tag-fwd

ATTTTGCAACTGCAGACGAAACATTTGCTACAAATGACACTTCTTTCATTG
AACGGCCAGAAACCTATTCCGCTTCCAGA*CGGATCCCCGGGTTAATTAA*

dam1-tag-rev

GATTGGAGAAGCTATTACATATGAGTTTACTGAACGCTTTCTAGAACTTTT
AAAGCAATTGTCTACAGTTCACTTCGCTG*GAATTCGAGCTCGTTTAAAC*

duo1-tag-fwd

GAAGAGCCGCATCTTCATATGTACCTTCTAGGCCTTCCCATGTTCCCAAGG
TCTTCATCCATGAATGTGCGTTCTCGGGT*CGGATCCCCGGGTTAATTAA*

duo1-tag-rev

CTGAGGAACGGAGGGCACATTACTGACTCGTGAAGGTGGACGAAGTCTA
GAGGAAGTTTTAGAAATTATACTTTTTCTAT*GAATTCGAGCTCGTTTAAAC*

7.5.3 Dam1 mutagenic and sequencing oligos

Fwddam1: CAACACCTGTATCTACGCGCCATTGTAGCG

Revdam2: GAGCCACTGAAGTTGTAAATGTGAGTATCG

FdamSeq2: GACTTGCTTCATGTGAATCGTTATTGC

FdamSeq3: CGTACTAAGATAGCGTCGGGTG

Revdam3: CAGTTCACTTCGCTGAAGAAAAATGTGC

7.6 Plasmids

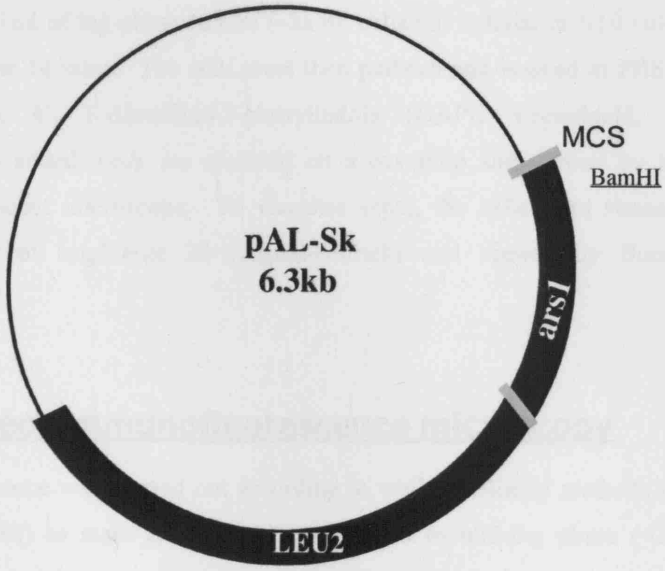

pAL-SK vector containing *S. pombe* genomic library received from Dr. Shimoda &Dr.Nakmura. This plasmid library used for multi-copy suppressor screening in this study. pDB248 *S. pombe* genomic library plasmid containing $scd1^{+}$ used in p*scd1* plasmid loss experiments.

7.7 Microscopic analysis

7.7.1 Visualisation of DNA and septa

Prior to visualisation of septa or DNA cells must be fixed in formaldehyde. Approximately 1ml of log-phase culture (~$2x10^6$ cells/ml) is fixed in 1/10 volume of formaldehyde for 10 mins. The cells were then pelleted and washed in PBSA. To visualise DNA 4', 6-diamidino-2-phenylindole (DAPI, Vectashield, Vector Laboratories) is added, cells are mounted on a coverslip and viewed by a Zeiss axioplan fluorescent microscope. To visualise septa, the cells were stained with F3543 Flourescent brightener 28 (Sigma-Aldrich) and viewed by fluorescent microscopy.

7.7.2 Indirect immunofluorescence microscopy

Immunofluorescence was carried out according to well-established methods (Hagan and Hyams, 1988) to stain α-tubulin. Cells grown to mid-log phase (~2-$5x10^6$ cells/ml) and a total of ~$5x10^7$ cells filtered and fixed in 10ml MeOH at –70°C for 10 minutes. Cells then harvested from MeOH, washed in PEM and cell wall digested with 0.6 mg/ml zymolyase 20T in PEMS for 70 mins at 37°C (shaking). Cells then pelleted and re-suspended in 1%TritonX in PEMS for 5 minutes at room temperature. Cells washed in PEM x3 and then incubated in PEMBAL for ~30 mins at room temperature. Primary antibody added in 50 µl of PEMBAL and cells left overnight at room temperature on shaker. Cells washed in PEMBAL to remove primary antibody, secondary antibody added in 200µl PEMBAL and cells incubated in dark for 2 hours at room temperature. Cells are again washed in PEMBAL x3 and then re-suspended in PBSA + 0.2 µg/ml NaN_3. Images were viewed under Zeiss Axioplan fluorescent microscope using Velocity Improvision software.

7.7.2.1 Primary antibodies

α-tubulin (TAT-1)	Dr. Keith Gull	monoclonal	1:40

7.7.2.2 Secondary antibodies

Cy3-conjugated sheep	anti-mouse IgG (Sigma C2128)	1:500
Fluorescein-linked sheep	anti-rabbit IgG (Amersham F0208)	1:40

7.7.3 Flourescence microscopy of live and fixed cells

Live imaging was carried out according to well-established methods (Brunner and Nurse, 2000), using a thin layer of lectin on the surface of a dish to prevent cell movements. All the imaging was carried out by the use of a chilled camera connected to a computer and microscope. The imaging of fixed cells, including cells subjected to immuno-flourescent staining, was carried out on a Zeiss Axioplan fluorescent microscope using Improvision Velocity software (Zeiss). For all imaging of fixed cells, Z-stacks (200-400nm steps) were taken and the images were subjected to deconvolution to remove any background haze. The imaging of live cells was carried out on a Deltavision inverted fluorescence microscope (Olympics) with 8 Z-stacks (200nm steps) taken every 30seconds for each channel. The Z-stacks were then compressed into a projection for each time-point, deconvolved and the channels for each time-point merged to produce a series of time-lapse images. All images were processed by Adobe® Photoshop CS2.

8 Bibliography

Adachi, Y., T. Toda, et al. (1986). "Differential expressions of essential and nonessential alpha-tubulin genes in Schizosaccharomyces pombe." Mol Cell Biol 6(6): 2168-78.

Ahonen, L. J., M. J. Kallio, et al. (2005). "Polo-like kinase 1 creates the tension-sensing 3F3/2 phosphoepitope and modulates the association of spindle-checkpoint proteins at kinetochores." Curr Biol 15(12): 1078-89.

Al-Bassam, J., M. van Breugel, et al. (2006). "Stu2p binds tubulin and undergoes an open-to-closed conformational change." J Cell Biol 172(7): 1009-22.

Alberts, B., D. Bray, et al. (1994). Molecular Biology of the Cell, New York, Garland publishing Inc.

Allshire, R. C., E. R. Nimmo, et al. (1995). "Mutations derepressing silent centromeric domains in fission yeast disrupt chromosome segregation." Genes Dev 9(2): 218-33.

Aoki, K., Y. Nakaseko, et al. (2006). "CDC2 phosphorylation of the fission yeast dis1 ensures accurate chromosome segregation." Curr Biol 16(16): 1627-35.

Aoyama, K., R. Kawaura, et al. (2000). "Identification and characterization of a novel gene, hos3+, the function of which is necessary for growth under high osmotic stress in fission yeast." Biosci Biotechnol Biochem 64(5): 1099-102.

Asakawa, K. and T. Toda (2006). "Cooperation of EB1-Mal3 and the Bub1 spindle checkpoint." Cell Cycle 5(1): 27-30.

Asakawa, K., M. Toya, et al. (2005). "Mal3, the fission yeast EB1 homologue, cooperates with Bub1 spindle checkpoint to prevent monopolar attachment." EMBO Rep 6(12): 1194-200.

Asbury, C. L., D. R. Gestaut, et al. (2006). "The Dam1 kinetochore complex harnesses microtubule dynamics to produce force and movement." Proc Natl Acad Sci U S A 103(26): 9873-8.

Bahler, J., J. Q. Wu, et al. (1998). "Heterologous modules for efficient and versatile PCR-based gene targeting in Schizosaccharomyces pombe." Yeast 14(10): 943-51.

Barton, N. R. and L. S. Goldstein (1996). "Going mobile: microtubule motors and chromosome segregation." Proc Natl Acad Sci U S A 93(5): 1735-42.

Basto, R., R. Gomes, et al. (2000). "Rough deal and Zw10 are required for the metaphase checkpoint in Drosophila." Nat Cell Biol 2(12): 939-43.

Becker, B. E. and L. Cassimeris (2005). "Cytoskeleton: microtubules born on the run." Curr Biol 15(14): R551-4.

Beinhauer, J. D., I. M. Hagan, et al. (1997). "Mal3, the fission yeast homologue of the human APC-interacting protein EB-1 is required for microtubule integrity and the maintenance of cell form." J Cell Biol 139(3): 717-28.

Belmont, L. D. and T. J. Mitchison (1996). "Identification of a protein that interacts with tubulin dimers and increases the catastrophe rate of microtubules." Cell 84(4): 623-31.

Bernard, P., J. F. Maure, et al. (2001). "Requirement of heterochromatin for cohesion at centromeres." Science 294(5551): 2539-42.

Biggins, S. and A. W. Murray (2001). "The budding yeast protein kinase Ipl1/Aurora allows the absence of tension to activate the spindle checkpoint." Genes Dev 15(23): 3118-29.

Biggins, S., F. F. Severin, et al. (1999). "The conserved protein kinase Ipl1 regulates microtubule binding to kinetochores in budding yeast." Genes Dev 13(5): 532-44.

Bomont, P., P. Maddox, et al. (2005). "Unstable microtubule capture at kinetochores depleted of the centromere-associated protein CENP-F." Embo J 24(22): 3927-39.

Brunner, D. and P. Nurse (2000). "CLIP170-like tip1p spatially organizes microtubular dynamics in fission yeast." Cell 102(5): 695-704.

Buffin, E., C. Lefebvre, et al. (2005). "Recruitment of Mad2 to the kinetochore requires the Rod/Zw10 complex." Curr Biol 15(9): 856-61.

Burke, D., D. Dawson, et al. (2000). Methods in Yeast Genetics., Cold Spring Harbour Laboratory Press.

Busch, K. E. and D. Brunner (2004). "The microtubule plus end-tracking proteins mal3p and tip1p cooperate for cell-end targeting of interphase microtubules." Curr Biol 14(7): 548-59.

Buvelot, S., S. Y. Tatsutani, et al. (2003). "The budding yeast Ipl1/Aurora protein kinase regulates mitotic spindle disassembly." J Cell Biol 160(3): 329-39.

Cai, M. and R. W. Davis (1990). "Yeast centromere binding protein CBF1, of the helix-loop-helix protein family, is required for chromosome stability and methionine prototrophy." Cell 61(3): 437-46.

Cairns, N. J., V. M. Lee, et al. (2004). "The cytoskeleton in neurodegenerative diseases." J Pathol 204(4): 438-49.

Carroll, C. W. and A. F. Straight (2006). "Centromere formation: from epigenetics to self-assembly." Trends Cell Biol 16(2): 70-8.

Cassimeris, L. (2002). "The oncoprotein 18/stathmin family of microtubule destabilizers." Curr Opin Cell Biol 14(1): 18-24.

Chan, G. K., S. A. Jablonski, et al. (2000). "Human Zw10 and ROD are mitotic checkpoint proteins that bind to kinetochores." Nat Cell Biol 2(12): 944-7.

Chan, G. K., B. T. Schaar, et al. (1998). "Characterization of the kinetochore binding domain of CENP-E reveals interactions with the kinetochore proteins CENP-F and hBUBR1." J Cell Biol 143(1): 49-63.

Chan, G. K. and T. J. Yen (2003). "The mitotic checkpoint: a signaling pathway that allows a single unattached kinetochore to inhibit mitotic exit." Prog Cell Cycle Res 5: 431-9.

Chang, E. C., M. Barr, et al. (1994). "Cooperative interaction of S. pombe proteins required for mating and morphogenesis." Cell 79(1): 131-41.

Chang, P. and T. Stearns (2000). "Delta-tubulin and epsilon-tubulin: two new human centrosomal tubulins reveal new aspects of centrosome structure and function." Nat Cell Biol 2(1): 30-5.

Cheeseman, I. M., S. Anderson, et al. (2002). "Phospho-regulation of kinetochore-microtubule attachments by the Aurora kinase Ipl1p." Cell 111(2): 163-72.

Cheeseman, I. M., C. Brew, et al. (2001). "Implication of a novel multiprotein Dam1p complex in outer kinetochore function." J Cell Biol 155(7): 1137-45.

Cheeseman, I. M., J. S. Chappie, et al. (2006). "The conserved KMN network constitutes the core microtubule-binding site of the kinetochore." Cell 127(5): 983-97.

Cheeseman, I. M., D. G. Drubin, et al. (2002). "Simple centromere, complex kinetochore: linking spindle microtubules and centromeric DNA in budding yeast." J Cell Biol 157(2): 199-203.

Cheeseman, I. M., M. Enquist-Newman, et al. (2001). "Mitotic spindle integrity and kinetochore function linked by the Duo1p/Dam1p complex." J Cell Biol 152(1): 197-212.

Cheeseman, I. M., S. Niessen, et al. (2004). "A conserved protein network controls assembly of the outer kinetochore and its ability to sustain tension." Genes Dev 18(18): 2255-68.

Chen, C. R., J. Chen, et al. (2000). "A conserved interaction between Moe1 and Mal3 is important for proper spindle formation in Schizosaccharomyces pombe." Mol Biol Cell 11(12): 4067-77.

Chen, C. R., Y. C. Li, et al. (1999). "Moe1, a conserved protein in Schizosaccharomyces pombe, interacts with a Ras effector, Scd1, to affect proper spindle formation." Proc Natl Acad Sci U S A 96(2): 517-22.

Chen, R. H., A. Shevchenko, et al. (1998). "Spindle checkpoint protein Xmad1 recruits Xmad2 to unattached kinetochores." J Cell Biol 143(2): 283-95.

Ciferri, C., J. De Luca, et al. (2005). "Architecture of the human ndc80-hec1 complex, a critical constituent of the outer kinetochore." J Biol Chem 280(32): 29088-95.

Cimini, D., L. A. Cameron, et al. (2004). "Anaphase spindle mechanics prevent mis-segregation of merotelically oriented chromosomes." Curr Biol 14(23): 2149-55.

Cimini, D., B. Howell, et al. (2001). "Merotelic kinetochore orientation is a major mechanism of aneuploidy in mitotic mammalian tissue cells." J Cell Biol 153(3): 517-27.

Cimini, D., B. Moree, et al. (2003). "Merotelic kinetochore orientation occurs frequently during early mitosis in mammalian tissue cells and error correction is achieved by two different mechanisms." J Cell Sci 116(Pt 20): 4213-25.

Cimini, D., X. Wan, et al. (2006). "Aurora kinase promotes turnover of kinetochore microtubules to reduce chromosome segregation errors." Curr Biol 16(17): 1711-8.

Ciosk, R., W. Zachariae, et al. (1998). "An ESP1/PDS1 complex regulates loss of sister chromatid cohesion at the metaphase to anaphase transition in yeast." Cell 93(6): 1067-76.

Clarke, L., M. Baum, et al. (1993). "Structure and function of Schizosaccharomyces pombe centromeres." Cold Spring Harb Symp Quant Biol 58: 687-95.

Clarke, L. and J. Carbon (1980). "Isolation of a yeast centromere and construction of functional small circular chromosomes." Nature(287): 504-9.

Cleveland, D. W., Y. Mao, et al. (2003). "Centromeres and kinetochores: from epigenetics to mitotic checkpoint signaling." Cell 112(4): 407-21.

Collins, K. A., A. R. Castillo, et al. (2005). "De novo kinetochore assembly requires the centromeric histone H3 variant." Mol Biol Cell 16(12): 5649-60.

Cooke, C. A., B. Schaar, et al. (1997). "Localization of CENP-E in the fibrous corona and outer plate of mammalian kinetochores from prometaphase through anaphase." Chromosoma 106(7): 446-55.

Cottarel, G., J. H. Shero, et al. (1989). "A 125-base-pair CEN6 DNA fragment is sufficient for complete meiotic and mitotic centromere functions in Saccharomyces cerevisiae." Mol Cell Biol 9(8): 3342-9.

Cottingham, F. R. and M. A. Hoyt (1997). "Mitotic spindle positioning in Saccharomyces cerevisiae is accomplished by antagonistically acting microtubule motor proteins." J Cell Biol 138(5): 1041-53.

Courtwright, A. M. and X. He (2002). "Dam1 is the right one: phosphoregulation of kinetochore biorientation." Dev Cell 3(5): 610-1.

De Antoni, A., C. G. Pearson, et al. (2005). "The Mad1/Mad2 complex as a template for Mad2 activation in the spindle assembly checkpoint." Curr Biol 15(3): 214-25.

De Wulf, P., A. D. McAinsh, et al. (2003). "Hierarchical assembly of the budding yeast kinetochore from multiple subcomplexes." Genes Dev 17(23): 2902-21.

DeLuca, J. G., W. E. Gall, et al. (2006). "Kinetochore microtubule dynamics and attachment stability are regulated by Hec1." Cell 127(5): 969-82.

DeLuca, J. G., B. J. Howell, et al. (2003). "Nuf2 and Hec1 are required for retention of the checkpoint proteins Mad1 and Mad2 to kinetochores." Curr Biol 13(23): 2103-9.

DeLuca, J. G., B. Moree, et al. (2002). "hNuf2 inhibition blocks stable kinetochore-microtubule attachment and induces mitotic cell death in HeLa cells." J Cell Biol 159(4): 549-55.

Desai, A., S. Rybina, et al. (2003). "KNL-1 directs assembly of the microtubule-binding interface of the kinetochore in C. elegans." Genes Dev 17(19): 2421-35.

Desai, A., S. Verma, et al. (1999). "Kin I kinesins are microtubule-destabilizing enzymes." Cell 96(1): 69-78.

Dewar, H., K. Tanaka, et al. (2004). "Tension between two kinetochores suffices for their bi-orientation on the mitotic spindle." Nature 428(6978): 93-7.

DeZwaan, T. M., E. Ellingson, et al. (1997). "Kinesin-related KIP3 of Saccharomyces cerevisiae is required for a distinct step in nuclear migration." J Cell Biol 138(5): 1023-40.

Ding, R., K. L. McDonald, et al. (1993). "Three-dimensional reconstruction and analysis of mitotic spindles from the yeast, Schizosaccharomyces pombe." J Cell Biol 120(1): 141-51.

Ding, R., R. R. West, et al. (1997). "The spindle pole body of Schizosaccharomyces pombe enters and leaves the nuclear envelope as the cell cycle proceeds." Mol Biol Cell 8(8): 1461-79.

Ditchfield, C., V. L. Johnson, et al. (2003). "Aurora B couples chromosome alignment with anaphase by targeting BubR1, Mad2, and Cenp-E to kinetochores." J Cell Biol 161(2): 267-80.

Dohmen, R. J., P. Wu, et al. (1994). "Heat-inducible degron: a method for constructing temperature-sensitive mutants." Science 263(5151): 1273-6.

Egel, R., J. Kohli, et al. (1980). "Genetics of the fission yeast Schizosaccharomyces pombe." Annu Rev Genet 14: 77-108.

Ekwall, K., E. R. Nimmo, et al. (1996). "Mutations in the fission yeast silencing factors clr4+ and rik1+ disrupt the localisation of the chromo domain protein Swi6p and impair centromere function." J Cell Sci 109 (Pt 11): 2637-48.

Ekwall, K., T. Olsson, et al. (1997). "Transient inhibition of histone deacetylation alters the structural and functional imprint at fission yeast centromeres." Cell 91(7): 1021-32.

Ekwall, K. and T. Ruusala (1994). "Mutations in rik1, clr2, clr3 and clr4 genes asymmetrically derepress the silent mating-type loci in fission yeast." Genetics 136(1): 53-64.

Enquist-Newman, M., I. M. Cheeseman, et al. (2001). "Dad1p, third component of the Duo1p/Dam1p complex involved in kinetochore function and mitotic spindle integrity." Mol Biol Cell 12(9): 2601-13.

Espelin, C. W., K. B. Kaplan, et al. (1997). "Probing the architecture of a simple kinetochore using DNA-protein crosslinking." J Cell Biol 139(6): 1383-96.

Fang, G. (2002). "Checkpoint protein BubR1 acts synergistically with Mad2 to inhibit anaphase-promoting complex." Mol Biol Cell 13(3): 755-66.

Fantes, P. and J. Beggs (2000). The Yeast Nucleus, Oxford University Press.

Feng, J., H. Huang, et al. (2006). "CENP-F is a novel microtubule-binding protein that is essential for kinetochore attachments and affects the duration of the mitotic checkpoint delay." Chromosoma 115(4): 320-9.

Fitzgerald-Hayes, M., L. Clarke, et al. (1982). "Nucleotide sequence comparisons and functional analysis of yeast centromere DNAs." Cell 29(1): 235-44.

Fleig, U., M. Sen-Gupta, et al. (1996). "Fission yeast mal2+ is required for chromosome segregation." Mol Cell Biol 16(11): 6169-77.

Fleming, W. (1882). "Zellsubstanz, Kern und Zelltheilung."

Foltz, D. R., L. E. Jansen, et al. (2006). "The human CENP-A centromeric nucleosome-associated complex." Nat Cell Biol 8(5): 458-69.

Forsburg, S. L. (1994). "Cell cycle. In and out of the cell cycle." Curr Biol 4(9): 828-30.

Fukagawa, T., Y. Mikami, et al. (2001). "CENP-H, a constitutive centromere component, is required for centromere targeting of CENP-C in vertebrate cells." Embo J 20(16): 4603-17.

Fukui, Y., T. Kozasa, et al. (1986). "Role of a ras homolog in the life cycle of Schizosaccharomyces pombe." Cell 44(2): 329-36.

Fukui, Y. and M. Yamamoto (1988). "Isolation and characterization of Schizosaccharomyces pombe mutants phenotypically similar to ras1." Mol Gen Genet 215(1): 26-31.

Funabiki, H., I. Hagan, et al. (1993). "Cell cycle-dependent specific positioning and clustering of centromeres and telomeres in fission yeast." J Cell Biol 121(5): 961-76.

Gachet, Y., S. Tournier, et al. (2001). "A MAP kinase-dependent actin checkpoint ensures proper spindle orientation in fission yeast." Nature 412(6844): 352-5.

Gachet, Y., S. Tournier, et al. (2004). "Mechanism controlling perpendicular alignment of the spindle to the axis of cell division in fission yeast." Embo J 23(6): 1289-300.

Garcia, M. A., N. Koonrugsa, et al. (2002). "Spindle-kinetochore attachment requires the combined action of Kin I-like Klp5/6 and Alp14/Dis1-MAPs in fission yeast." Embo J 21(22): 6015-24.

Garcia, M. A., N. Koonrugsa, et al. (2002). "Two kinesin-like Kin I family proteins in fission yeast regulate the establishment of metaphase and the onset of anaphase A." Curr Biol 12(8): 610-21.

Garcia, M. A., L. Vardy, et al. (2001). "Fission yeast ch-TOG/XMAP215 homologue Alp14 connects mitotic spindles with the kinetochore and is a component of the Mad2-dependent spindle checkpoint." Embo J 20(13): 3389-401.

Gard, D. L. and M. W. Kirschner (1987). "A microtubule-associated protein from Xenopus eggs that specifically promotes assembly at the plus-end." J Cell Biol 105(5): 2203-15.

Gaudet, A. and M. Fitzgerald-Hayes (1989). "Mutations in CEN3 cause aberrant chromosome segregation during meiosis in Saccharomyces cerevisiae." Genetics 121(3): 477-89.

Gillett, E. S., C. W. Espelin, et al. (2004). "Spindle checkpoint proteins and chromosome-microtubule attachment in budding yeast." J Cell Biol 164(4): 535-46.

Goshima, G., T. Kiyomitsu, et al. (2003). "Human centromere chromatin protein hMis12, essential for equal segregation, is independent of CENP-A loading pathway." J Cell Biol 160(1): 25-39.

Goshima, G., S. Saitoh, et al. (1999). "Proper metaphase spindle length is determined by centromere proteins Mis12 and Mis6 required for faithful chromosome segregation." Genes Dev 13(13): 1664-77.

Goshima, G., R. Wollman, et al. (2005). "Length control of the metaphase spindle." Curr Biol 15(22): 1979-88.

Gupta, M. L., Jr., P. Carvalho, et al. (2006). "Plus end-specific depolymerase activity of Kip3, a kinesin-8 protein, explains its role in positioning the yeast mitotic spindle." Nat Cell Biol 8(9): 913-23.

Hagan, I. and M. Yanagida (1990). "Novel potential mitotic motor protein encoded by the fission yeast cut7+ gene." Nature 347(6293): 563-6.

Hagan, I. M. and J. S. Hyams (1988). "The use of cell division cycle mutants to investigate the control of microtubule distribution in the fission yeast Schizosaccharomyces pombe." J Cell Sci 89 (Pt 3): 343-57.

Hardwick, K. G. (2005). "Checkpoint signalling: Mad2 conformers and signal propagation." Curr Biol 15(4): R122-4.

Hardwick, K. G., R. C. Johnston, et al. (2000). "MAD3 encodes a novel component of the spindle checkpoint which interacts with Bub3p, Cdc20p, and Mad2p." J Cell Biol 148(5): 871-82.

Hardwick, K. G., R. Li, et al. (1999). "Lesions in many different spindle components activate the spindle checkpoint in the budding yeast Saccharomyces cerevisiae." Genetics 152(2): 509-18.

Hartwell, L. H. and T. A. Weinert (1989). "Checkpoints: controls that ensure the order of cell cycle events." Science 246(4930): 629-34.

Hayashi, T., Y. Fujita, et al. (2004). "Mis16 and Mis18 are required for CENP-A loading and histone deacetylation at centromeres." Cell 118(6): 715-29.

He, X., S. Asthana, et al. (2000). "Transient sister chromatid separation and elastic deformation of chromosomes during mitosis in budding yeast." Cell 101(7): 763-75.

He, X., T. E. Patterson, et al. (1997). "The Schizosaccharomyces pombe spindle checkpoint protein mad2p blocks anaphase and genetically interacts with the anaphase-promoting complex." Proc Natl Acad Sci U S A 94(15): 7965-70.

He, X., D. R. Rines, et al. (2001). "Molecular analysis of kinetochore-microtubule attachment in budding yeast." Cell 106(2): 195-206.

Helenius, J., G. Brouhard, et al. (2006). "The depolymerizing kinesin MCAK uses lattice diffusion to rapidly target microtubule ends." Nature 441(7089): 115-9.

Higuchi, T. and F. Uhlmann (2005). "Stabilization of microtubule dynamics at anaphase onset promotes chromosome segregation." Nature 433(7022): 171-6.

Hiraoka Y, T. T., Yanagida M (1984). "The NDA3 gene of fission yeast encodes beta-tubulin: a cold-sensitive nda3 mutation reversibly blocks spindle formation and chromosome movement in mitosis." Cell. Dec;39(2 Pt 1):: 349-58.

Hirokawa, N. and R. Takemura (2004). "Kinesin superfamily proteins and their various functions and dynamics." Exp Cell Res 301(1): 50-9.

Hofmann, C., I. M. Cheeseman, et al. (1998). "Saccharomyces cerevisiae Duo1p and Dam1p, novel proteins involved in mitotic spindle function." J Cell Biol 143(4): 1029-40.

Holmfeldt, P., S. Stenmark, et al. (2004). "Differential functional interplay of TOGp/XMAP215 and the Kinl kinesin MCAK during interphase and mitosis." Embo J 23(3): 627-37.

Hori, T., T. Haraguchi, et al. (2003). "Dynamic behavior of Nuf2-Hec1 complex that localizes to the centrosome and centromere and is essential for mitotic progression in vertebrate cells." J Cell Sci 116(Pt 16): 3347-62.

Hornig, N. C., P. P. Knowles, et al. (2002). "The dual mechanism of separase regulation by securin." Curr Biol 12(12): 973-82.

Howell, B. J., B. F. McEwen, et al. (2001). "Cytoplasmic dynein/dynactin drives kinetochore protein transport to the spindle poles and has a role in mitotic spindle checkpoint inactivation." J Cell Biol 155(7): 1159-72.

Howell, B. J., B. Moree, et al. (2004). "Spindle checkpoint protein dynamics at kinetochores in living cells." Curr Biol 14(11): 953-64.

Howman, E. V., K. J. Fowler, et al. (2000). "Early disruption of centromeric chromatin organization in centromere protein A (Cenpa) null mice." Proc Natl Acad Sci U S A 97(3): 1148-53.

Hoyt, M. A., L. Totis, et al. (1991). "S. cerevisiae genes required for cell cycle arrest in response to loss of microtubule function." Cell 66(3): 507-17.

Hyman, A. A., K. Middleton, et al. (1992). "Microtubule-motor activity of a yeast centromere-binding protein complex." Nature 359(6395): 533-6.

Ikeuchi, A., Y. Sasaki, et al. (2003). "Exhaustive identification of interaction domains using a high-throughput method based on two-hybrid screening and PCR-convergence: molecular dissection of a kinetochore subunit Spc34p." Nucleic Acids Res 31(23): 6953-62.

Inclan, Y. F. and E. Nogales (2001). "Structural models for the self-assembly and microtubule interactions of gamma-, delta- and epsilon-tubulin." J Cell Sci 114(Pt 2): 413-22.

Irelan, J. T., G. I. Gutkin, et al. (2001). "Functional redundancies, distinct localizations and interactions among three fission yeast homologs of centromere protein-B." Genetics 157(3): 1191-203.

Janke, C., J. Ortiz, et al. (2002). "Four new subunits of the Dam1-Duo1 complex reveal novel functions in sister kinetochore biorientation." Embo J 21(1-2): 181-93.

Janson, M. E., T. G. Setty, et al. (2005). "Efficient formation of bipolar microtubule bundles requires microtubule-bound gamma-tubulin complexes." J Cell Biol 169(2): 297-308.

Jaspersen, S. L. and M. Winey (2004). "The budding yeast spindle pole body: structure, duplication, and function." Annu Rev Cell Dev Biol 20: 1-28.

Jin, Q. W., A. L. Pidoux, et al. (2002). "The mal2p protein is an essential component of the fission yeast centromere." Mol Cell Biol 22(20): 7168-83.

Jones, M. H., J. B. Bachant, et al. (1999). "Yeast Dam1p is required to maintain spindle integrity during mitosis and interacts with the Mps1p kinase." Mol Biol Cell 10(7): 2377-91.

Jones, M. H., X. He, et al. (2001). "Yeast Dam1p has a role at the kinetochore in assembly of the mitotic spindle." Proc Natl Acad Sci U S A 98(24): 13675-80.

Kang, J., I. M. Cheeseman, et al. (2001). "Functional cooperation of Dam1, Ipl1, and the inner centromere protein (INCENP)-related protein Sli15 during chromosome segregation." J Cell Biol 155(5): 763-74.

Kapoor, T. M., T. U. Mayer, et al. (2000). "Probing spindle assembly mechanisms with monastrol, a small molecule inhibitor of the mitotic kinesin, Eg5." J Cell Biol 150(5): 975-88.

Karess, R. (2005). "Rod-Zw10-Zwilch: a key player in the spindle checkpoint." Trends Cell Biol 15(7): 386-92.

Karess, R. E. and D. M. Glover (1989). "rough deal: a gene required for proper mitotic segregation in Drosophila." J Cell Biol 109(6 Pt 1): 2951-61.

Kawarasaki, Y., Y. Sasaki, et al. (2002). "A method for functional mapping of protein-protein binding domain by preferential amplification of the shortest amplicon using PCR." Anal Biochem 303(1): 34-41.

Kawashima, S. A., T. Tsukahara, et al. (2007). "Shugoshin enables tension-generating attachment of kinetochores by loading Aurora to centromeres." Genes Dev 21(4): 420-35.

Keeney, J. B. and J. D. Boeke (1994). "Efficient targeted integration at leu1-32 and ura4-294 in Schizosaccharomyces pombe." Genetics 136(3): 849-56.

Keith, K. C. and M. Fitzgerald-Hayes (2000). "CSE4 genetically interacts with the Saccharomyces cerevisiae centromere DNA elements CDE I and CDE II but not CDE III. Implications for the path of the centromere dna around a cse4p variant nucleosome." Genetics 156(3): 973-81.

Kerres, A., V. Jakopec, et al. (2006). "Fta2, an essential fission yeast kinetochore component, interacts closely with the conserved Mal2 protein." Mol Biol Cell 17(10): 4167-78.

Kerres, A., V. Jakopec, et al. (2007). "The Conserved Spc7 Protein Is Required for Spindle Integrity and Links Kinetochore Complexes in Fission Yeast." Mol Biol Cell.

Kerres, A., C. Vietmeier-Decker, et al. (2004). "The fission yeast kinetochore component Spc7 associates with the EB1 family member Mal3 and is required for kinetochore-spindle association." Mol Biol Cell 15(12): 5255-67.

Khodjakov, A., R. W. Cole, et al. (2000). "Centrosome-independent mitotic spindle formation in vertebrates." Curr Biol 10(2): 59-67.

Kim, J. H., J. S. Kang, et al. (1999). "Sli15 associates with the ipl1 protein kinase to promote proper chromosome segregation in Saccharomyces cerevisiae." J Cell Biol 145(7): 1381-94.

Kim, S. H., D. P. Lin, et al. (1998). "Fission yeast Slp1: an effector of the Mad2-dependent spindle checkpoint." Science 279(5353): 1045-7.

Kitajima, T. S., S. A. Kawashima, et al. (2004). "The conserved kinetochore protein shugoshin protects centromeric cohesion during meiosis." Nature 427(6974): 510-7.

Klein, F., P. Mahr, et al. (1999). "A central role for cohesins in sister chromatid cohesion, formation of axial elements, and recombination during yeast meiosis." Cell 98(1): 91-103.

Kline, S. L., I. M. Cheeseman, et al. (2006). "The human Mis12 complex is required for kinetochore assembly and proper chromosome segregation." J Cell Biol 173(1): 9-17.

Kline-Smith, S. L., A. Khodjakov, et al. (2004). "Depletion of centromeric MCAK leads to chromosome congression and segregation defects due to improper kinetochore attachments." Mol Biol Cell 15(3): 1146-59.

Knop, M., G. Pereira, et al. (1999). "Microtubule organization by the budding yeast spindle pole body." Biol Cell 91(4-5): 291-304.

Knowlton, A. L., W. Lan, et al. (2006). "Aurora B is enriched at merotelic attachment sites, where it regulates MCAK." Curr Biol 16(17): 1705-10.

Kobayashi, Y., S. Saitoh, et al. (2007). "The fission yeast DASH complex is essential for satisfying the spindle assembly checkpoint induced by defects in the inner-kinetochore proteins." Genes Cells 12(3): 311-28.

Kops, G. J., Y. Kim, et al. (2005). "ZW10 links mitotic checkpoint signaling to the structural kinetochore." J Cell Biol 169(1): 49-60.

Kuhn, R. M., L. Clarke, et al. (1991). "Clustered tRNA genes in Schizosaccharomyces pombe centromeric DNA sequence repeats." Proc Natl Acad Sci U S A 88(4): 1306-10.

Kwon, M. S., T. Hori, et al. (2007). "CENP-C Is Involved in Chromosome Segregation, Mitotic Checkpoint Function, and Kinetochore Assembly." Mol Biol Cell.

Lampson, M. A., K. Renduchitala, et al. (2004). "Correcting improper chromosome-spindle attachments during cell division." Nat Cell Biol 6(3): 232-7.

Lee, J. K., J. A. Huberman, et al. (1997). "Purification and characterization of a CENP-B homologue protein that binds to the centromeric K-type repeat DNA of Schizosaccharomyces pombe." Proc Natl Acad Sci U S A 94(16): 8427-32.

Li, J. M., Y. Li, et al. (2005). "Genetic analysis of the kinetochore DASH complex reveals an antagonistic relationship with the ras/protein kinase A pathway and a novel subunit required for Ask1 association." Mol Cell Biol 25(2): 767-78.

Li, R. and A. W. Murray (1991). "Feedback control of mitosis in budding yeast." Cell 66(3): 519-31.

Li, Y., J. Bachant, et al. (2002). "The mitotic spindle is required for loading of the DASH complex onto the kinetochore." Genes Dev 16(2): 183-97.

Li, Y. and E. C. Chang (2003). "Schizosaccharomyces pombe Ras1 effector, Scd1, interacts with Klp5 and Klp6 kinesins to mediate cytokinesis." Genetics 165(2): 477-88.

Li, Y., S. J. Elledge, et al. (2003). "The DASH complex component Ask1 is a cell cycle-regulated Cdk substrate in Saccharomyces cerevisiae." Cell Cycle 2(2): 143-8.

Li, Y. C., C. R. Chen, et al. (2000). "Fission yeast Ras1 effector Scd1 interacts with the spindle and affects its proper formation." Genetics 156(3): 995-1004.

Liu, X., I. McLeod, et al. (2005). "Molecular analysis of kinetochore architecture in fission yeast." Embo J 24(16): 2919-30.

Mallavarapu, A., K. Sawin, et al. (1999). "A switch in microtubule dynamics at the onset of anaphase B in the mitotic spindle of Schizosaccharomyces pombe." Curr Biol 9(23): 1423-6.

Maney, T., A. W. Hunter, et al. (1998). "Mitotic centromere-associated kinesin is important for anaphase chromosome segregation." J Cell Biol 142(3): 787-801.

Maniatis, T., E. Fritsch, et al. (1982). Molecular cloning: a laboratory manual., Cold Spring Harbour Laboratory Press.

Mao, Y., A. Abrieu, et al. (2003). "Activating and silencing the mitotic checkpoint through CENP-E-dependent activation/inactivation of BubR1." Cell 114(1): 87-98.

Mapelli, M., F. V. Filipp, et al. (2006). "Determinants of conformational dimerization of Mad2 and its inhibition by p31comet." Embo J 25(6): 1273-84.

May, K. M. and K. G. Hardwick (2006). "The spindle checkpoint." J Cell Sci 119(Pt 20): 4139-42.

Mayr, M. I., S. Hummer, et al. (2007). "The human kinesin Kif18A is a motile microtubule depolymerase essential for chromosome congression." Curr Biol 17(6): 488-98.

McAinsh, A. D., J. D. Tytell, et al. (2003). "Structure, function, and regulation of budding yeast kinetochores." Annu Rev Cell Dev Biol 19: 519-39.

McCleland, M. L., R. D. Gardner, et al. (2003). "The highly conserved Ndc80 complex is required for kinetochore assembly, chromosome congression, and spindle checkpoint activity." Genes Dev 17(1): 101-14.

McCleland, M. L., M. J. Kallio, et al. (2004). "The vertebrate Ndc80 complex contains Spc24 and Spc25 homologs, which are required to establish and maintain kinetochore-microtubule attachment." Curr Biol 14(2): 131-7.

McEwen, B. F., G. K. Chan, et al. (2001). "CENP-E is essential for reliable bioriented spindle attachment, but chromosome alignment can be achieved via redundant mechanisms in mammalian cells." Mol Biol Cell 12(9): 2776-89.

McGuinness, B. E., T. Hirota, et al. (2005). "Shugoshin prevents dissociation of cohesin from centromeres during mitosis in vertebrate cells." PLoS Biol 3(3): e86.

Measday, V., D. W. Hailey, et al. (2002). "Ctf3p, the Mis6 budding yeast homolog, interacts with Mcm22p and Mcm16p at the yeast outer kinetochore." Genes Dev 16(1): 101-13.

Megraw, T. L., L. R. Kao, et al. (2001). "Zygotic development without functional mitotic centrosomes." Curr Biol 11(2): 116-20.

Middleton, K. and J. Carbon (1994). "KAR3-encoded kinesin is a minus-end-directed motor that functions with centromere binding proteins (CBF3) on an in vitro yeast kinetochore." Proc Natl Acad Sci U S A 91(15): 7212-6.

Millband, D. N. and K. G. Hardwick (2002). "Fission yeast Mad3p is required for Mad2p to inhibit the anaphase-promoting complex and localizes to kinetochores in a Bub1p-, Bub3p-, and Mph1p-dependent manner." Mol Cell Biol 22(8): 2728-42.

Miranda, J. J., P. De Wulf, et al. (2005). "The yeast DASH complex forms closed rings on microtubules." Nat Struct Mol Biol 12(2): 138-43.

Mitchison, T., L. Evans, et al. (1986). "Sites of microtubule assembly and disassembly in the mitotic spindle." Cell 45(4): 515-27.

Mitchison, T. and M. Kirschner (1984). "Dynamic instability of microtubule growth." Nature 312(5991): 237-42.

Moreno, S., A. Klar, et al. (1991). "Molecular genetic analysis of fission yeast Schizosaccharomyces pombe." Methods Enzymol 194: 795-823.

Murakami, H., D. B. Goto, et al. (2007). "Ribonuclease Activity of Dis3 Is Required for Mitotic Progression and Provides a Possible Link between Heterochromatin and Kinetochore Function." PLoS ONE 2: e317.

Murakami, Y., J. A. Huberman, et al. (1996). "Identification, purification, and molecular cloning of autonomously replicating sequence-binding protein 1 from

fission yeast Schizosaccharomyces pombe." Proc Natl Acad Sci U S A 93(1): 502-7.

Nabeshima, K., H. Kurooka, et al. (1995). "p93dis1, which is required for sister chromatid separation, is a novel microtubule and spindle pole body-associating protein phosphorylated at the Cdc2 target sites." Genes Dev 9(13): 1572-85.

Nabeshima, K., T. Nakagawa, et al. (1998). "Dynamics of centromeres during metaphase-anaphase transition in fission yeast: Dis1 is implicated in force balance in metaphase bipolar spindle." Mol Biol Cell 9(11): 3211-25.

Nabetani, A., T. Koujin, et al. (2001). "A conserved protein, Nuf2, is implicated in connecting the centromere to the spindle during chromosome segregation: a link between the kinetochore function and the spindle checkpoint." Chromosoma 110(5): 322-34.

Nakaseko, Y., G. Goshima, et al. (2001). "M phase-specific kinetochore proteins in fission yeast: microtubule-associating Dis1 and Mtc1 display rapid separation and segregation during anaphase." Curr Biol 11(8): 537-49.

Nakaseko, Y., K. Nabeshima, et al. (1996). "Dissection of fission yeast microtubule associating protein p93Dis1: regions implicated in regulated localization and microtubule interaction." Genes Cells 1(7): 633-44.

Nekrasov, V. S., M. A. Smith, et al. (2003). "Interactions between centromere complexes in Saccharomyces cerevisiae." Mol Biol Cell 14(12): 4931-46.

Nishihashi, A., T. Haraguchi, et al. (2002). "CENP-I is essential for centromere function in vertebrate cells." Dev Cell 2(4): 463-76.

Niwa, O., T. Matsumoto, et al. (1989). "Characterization of Schizosaccharomyces pombe minichromosome deletion derivatives and a functional allocation of their centromere." Embo J 8(10): 3045-52.

Nonaka, N., T. Kitajima, et al. (2002). "Recruitment of cohesin to heterochromatic regions by Swi6/HP1 in fission yeast." Nat Cell Biol 4(1): 89-93.

Obuse, C., O. Iwasaki, et al. (2004). "A conserved Mis12 centromere complex is linked to heterochromatic HP1 and outer kinetochore protein Zwint-1." Nat Cell Biol 6(11): 1135-41.

Ohkura, H., Y. Adachi, et al. (1988). "Cold-sensitive and caffeine-supersensitive mutants of the Schizosaccharomyces pombe dis genes implicated in sister chromatid separation during mitosis." Embo J 7(5): 1465-73.

Ohkura, H., M. A. Garcia, et al. (2001). "Dis1/TOG universal microtubule adaptors - one MAP for all?" J Cell Sci 114(Pt 21): 3805-12.

Ohzeki, J., M. Nakano, et al. (2002). "CENP-B box is required for de novo centromere chromatin assembly on human alphoid DNA." J Cell Biol 159(5): 765-75.

Okada, M., I. M. Cheeseman, et al. (2006). "The CENP-H-I complex is required for the efficient incorporation of newly synthesized CENP-A into centromeres." Nat Cell Biol 8(5): 446-57.

Oliferenko, S. and M. K. Balasubramanian (2002). "Astral microtubules monitor metaphase spindle alignment in fission yeast." Nat Cell Biol 4(10): 816-20.

Osborne, M. A., G. Schlenstedt, et al. (1994). "Nuf2, a spindle pole body-associated protein required for nuclear division in yeast." J Cell Biol 125(4): 853-66.

Pangilinan, F. and F. Spencer (1996). "Abnormal kinetochore structure activates the spindle assembly checkpoint in budding yeast." Mol Biol Cell 7(8): 1195-208.

Peters, J. M. (2002). "The anaphase-promoting complex: proteolysis in mitosis and beyond." Mol Cell 9(5): 931-43.

Petersen, J. and I. M. Hagan (2003). "S. pombe aurora kinase/survivin is required for chromosome condensation and the spindle checkpoint attachment response." Curr Biol 13(7): 590-7.

Pickett-Heaps, J. D. (1969). "Preprophase microtubules and stomatal differentiation; some effects of centrifugation on symmetrical and asymmetrical cell division." J Ultrastruct Res 27(1): 24-44.

Pidoux, A. L. and R. C. Allshire (2004). "Kinetochore and heterochromatin domains of the fission yeast centromere." Chromosome Res 12(6): 521-34.

Pidoux, A. L., W. Richardson, et al. (2003). "Sim4: a novel fission yeast kinetochore protein required for centromeric silencing and chromosome segregation." J Cell Biol 161(2): 295-307.

Pinsky, B. A. and S. Biggins (2005). "The spindle checkpoint: tension versus attachment." Trends Cell Biol 15(9): 486-93.

Pinsky, B. A., C. V. Kotwaliwale, et al. (2006). "Glc7/protein phosphatase 1 regulatory subunits can oppose the Ipl1/aurora protein kinase by redistributing Glc7." Mol Cell Biol 26(7): 2648-60.

Pinsky, B. A., C. Kung, et al. (2006). "The Ipl1-Aurora protein kinase activates the spindle checkpoint by creating unattached kinetochores." Nat Cell Biol 8(1): 78-83.

Pinsky, B. A., S. Y. Tatsutani, et al. (2003). "An Mtw1 complex promotes kinetochore biorientation that is monitored by the Ipl1/Aurora protein kinase." Dev Cell 5(5): 735-45.

Polizzi, C. and L. Clarke (1991). "The chromatin structure of centromeres from fission yeast: differentiation of the central core that correlates with function." J Cell Biol 112(2): 191-201.

Pot, I., V. Measday, et al. (2003). "Chl4p and iml3p are two new members of the budding yeast outer kinetochore." Mol Biol Cell 14(2): 460-76.

Rabitsch, K. P., J. Gregan, et al. (2004). "Two fission yeast homologs of Drosophila Mei-S332 are required for chromosome segregation during meiosis I and II." Curr Biol 14(4): 287-301.

Radcliffe, P., D. Hirata, et al. (1998). "Identification of novel temperature-sensitive lethal alleles in essential beta-tubulin and nonessential alpha 2-tubulin genes as fission yeast polarity mutants." Mol Biol Cell 9(7): 1757-71.

Rajagopalan, S., A. Bimbo, et al. (2004). "A potential tension-sensing mechanism that ensures timely anaphase onset upon metaphase spindle orientation." Curr Biol 14(1): 69-74.

Rea, S., F. Eisenhaber, et al. (2000). "Regulation of chromatin structure by site-specific histone H3 methyltransferases." Nature 406(6796): 593-9.

Reddy, S. K., M. Rape, et al. (2007). "Ubiquitination by the anaphase-promoting complex drives spindle checkpoint inactivation." Nature 446(7138): 921-5.

Riedel, C. G., V. L. Katis, et al. (2006). "Protein phosphatase 2A protects centromeric sister chromatid cohesion during meiosis I." Nature 441(7089): 53-61.

Rieder, C. L., R. W. Cole, et al. (1995). "The checkpoint delaying anaphase in response to chromosome monoorientation is mediated by an inhibitory signal produced by unattached kinetochores." J Cell Biol 130(4): 941-8.

Rieder, C. L., A. Schultz, et al. (1994). "Anaphase onset in vertebrate somatic cells is controlled by a checkpoint that monitors sister kinetochore attachment to the spindle." J Cell Biol 127(5): 1301-10.

Ris, H. and P. L. Witt (1981). "Structure of the mammalian kinetochore." Chromosoma 82(2): 153-70.

Rischitor, P. E., S. Konzack, et al. (2004). "The Kip3-like kinesin KipB moves along microtubules and determines spindle position during synchronized mitoses in Aspergillus nidulans hyphae." Eukaryot Cell 3(3): 632-45.

Rogers, G. C., S. L. Rogers, et al. (2004). "Two mitotic kinesins cooperate to drive sister chromatid separation during anaphase." Nature 427(6972): 364-70.

Sagolla, M. J., S. Uzawa, et al. (2003). "Individual microtubule dynamics contribute to the function of mitotic and cytoplasmic arrays in fission yeast." J Cell Sci 116(Pt 24): 4891-903.

Saitoh, S., K. Ishii, et al. (2005). "Spindle checkpoint signaling requires the mis6 kinetochore subcomplex, which interacts with mad2 and mitotic spindles." Mol Biol Cell 16(8): 3666-77.

Saitoh, S., K. Takahashi, et al. (1997). "Mis6, a fission yeast inner centromere protein, acts during G1/S and forms specialized chromatin required for equal segregation." Cell 90(1): 131-43.

Salah, S. M. and K. Nasmyth (2000). "Destruction of the securin Pds1p occurs at the onset of anaphase during both meiotic divisions in yeast." Chromosoma 109(1-2): 27-34.

Salic, A., J. C. Waters, et al. (2004). "Vertebrate shugoshin links sister centromere cohesion and kinetochore microtubule stability in mitosis." Cell 118(5): 567-78.

Sanchez-Perez, I., S. J. Renwick, et al. (2005). "The DASH complex and Klp5/Klp6 kinesin coordinate bipolar chromosome attachment in fission yeast." Embo J 24(16): 2931-43.

Sandblad, L., K. E. Busch, et al. (2006). "The Schizosaccharomyces pombe EB1 homolog Mal3p binds and stabilizes the microtubule lattice seam." Cell 127(7): 1415-24.

Sato, M., L. Vardy, et al. (2004). "Interdependency of fission yeast Alp14/TOG and coiled coil protein Alp7 in microtubule localization and bipolar spindle formation." Mol Biol Cell 15(4): 1609-22.

Sawin, K. E. and P. T. Tran (2006). "Cytoplasmic microtubule organization in fission yeast." Yeast 23(13): 1001-14.

Scaerou, F., I. Aguilera, et al. (1999). "The rough deal protein is a new kinetochore component required for accurate chromosome segregation in Drosophila." J Cell Sci 112 (Pt 21): 3757-68.

Scaerou, F., D. A. Starr, et al. (2001). "The ZW10 and Rough Deal checkpoint proteins function together in a large, evolutionarily conserved complex targeted to the kinetochore." J Cell Sci 114(Pt 17): 3103-14.

Schaar, B. T., G. K. Chan, et al. (1997). "CENP-E function at kinetochores is essential for chromosome alignment." J Cell Biol 139(6): 1373-82.

Schueler, M. G., A. W. Higgins, et al. (2001). "Genomic and genetic definition of a functional human centromere." Science 294(5540): 109-15.

Severin, F., B. Habermann, et al. (2001). "Stu2 promotes mitotic spindle elongation in anaphase." J Cell Biol 153(2): 435-42.

Shah, J. V., E. Botvinick, et al. (2004). "Dynamics of centromere and kinetochore proteins; implications for checkpoint signaling and silencing." Curr Biol 14(11): 942-52.

Shang, C., T. R. Hazbun, et al. (2003). "Kinetochore protein interactions and their regulation by the Aurora kinase Ipl1p." Mol Biol Cell 14(8): 3342-55.

Shimogawa, M. M., B. Graczyk, et al. (2006). "Mps1 phosphorylation of Dam1 couples kinetochores to microtubule plus ends at metaphase." Curr Biol 16(15): 1489-501.

Shirayama, M., A. Toth, et al. (1999). "APC(Cdc20) promotes exit from mitosis by destroying the anaphase inhibitor Pds1 and cyclin Clb5." Nature 402(6758): 203-7.

Skoufias, D. A., P. R. Andreassen, et al. (2001). "Mammalian mad2 and bub1/bubR1 recognize distinct spindle-attachment and kinetochore-tension checkpoints." Proc Natl Acad Sci U S A 98(8): 4492-7.

Snyder, M. (1994). "The spindle pole body of yeast." Chromosoma 103(6): 369-80.

Starr, D. A., B. C. Williams, et al. (1998). "ZW10 helps recruit dynactin and dynein to the kinetochore." J Cell Biol 142(3): 763-74.

Starr, D. A., B. C. Williams, et al. (1997). "Conservation of the centromere/kinetochore protein ZW10." J Cell Biol 138(6): 1289-301.

Stegmeier, F., M. Rape, et al. (2007). "Anaphase initiation is regulated by antagonistic ubiquitination and deubiquitination activities." Nature 446(7138): 876-81.

Stern, B. M. and A. W. Murray (2001). "Lack of tension at kinetochores activates the spindle checkpoint in budding yeast." Curr Biol 11(18): 1462-7.

Stoyan, T., G. Gloeckner, et al. (2001). "Multifunctional centromere binding factor 1 is essential for chromosome segregation in the human pathogenic yeast Candida glabrata." Mol Cell Biol 21(15): 4875-88.

Sugimoto, K., H. Yata, et al. (1994). "Human centromere protein C (CENP-C) is a DNA-binding protein which possesses a novel DNA-binding motif." J Biochem (Tokyo) 116(4): 877-81.

Sullivan, B. A. and G. H. Karpen (2004). "Centromeric chromatin exhibits a histone modification pattern that is distinct from both euchromatin and heterochromatin." Nat Struct Mol Biol 11(11): 1076-83.

Takahashi, K., E. S. Chen, et al. (2000). "Requirement of Mis6 centromere connector for localizing a CENP-A-like protein in fission yeast." Science 288(5474): 2215-9.

Takahashi, K., S. Murakami, et al. (1992). "A low copy number central sequence with strict symmetry and unusual chromatin structure in fission yeast centromere." Mol Biol Cell 3(7): 819-35.

Takahashi, K., S. Murakami, et al. (1991). "A large number of tRNA genes are symmetrically located in fission yeast centromeres." J Mol Biol 218(1): 13-7.

Takahashi, K., H. Yamada, et al. (1994). "Fission yeast minichromosome loss mutants mis cause lethal aneuploidy and replication abnormality." Mol Biol Cell 5(10): 1145-58.

Takeuchi, M. and M. Yanagida (1993). "A mitotic role for a novel fission yeast protein kinase dsk1 with cell cycle stage dependent phosphorylation and localization." Mol Biol Cell 4(3): 247-60.

Tan, D., A. B. Asenjo, et al. (2006). "Kinesin-13s form rings around microtubules." J Cell Biol 175(1): 25-31.

Tanaka, K., N. Mukae, et al. (2005). "Molecular mechanisms of kinetochore capture by spindle microtubules." Nature 434(7036): 987-94.

Tanaka, K., T. Yonekawa, et al. (2000). "Fission yeast Eso1p is required for establishing sister chromatid cohesion during S phase." Mol Cell Biol 20(10): 3459-69.

Tanaka, T., J. Fuchs, et al. (2000). "Cohesin ensures bipolar attachment of microtubules to sister centromeres and resists their precocious separation." Nat Cell Biol 2(8): 492-9.

Tanaka, T. U. (2002). "Bi-orienting chromosomes on the mitotic spindle." Curr Opin Cell Biol 14(3): 365-71.

Tanaka, T. U., N. Rachidi, et al. (2002). "Evidence that the Ipl1-Sli15 (Aurora kinase-INCENP) complex promotes chromosome bi-orientation by altering kinetochore-spindle pole connections." Cell 108(3): 317-29.

Tang, T. T., S. E. Bickel, et al. (1998). "Maintenance of sister-chromatid cohesion at the centromere by the Drosophila MEI-S332 protein." Genes Dev 12(24): 3843-56.

Tang, Z., H. Shu, et al. (2006). "PP2A is required for centromeric localization of Sgo1 and proper chromosome segregation." Dev Cell 10(5): 575-85.

Toda, T., Y. Adachi, et al. (1984). "Identification of the pleiotropic cell division cycle gene NDA2 as one of two different alpha-tubulin genes in Schizosaccharomyces pombe." Cell 37(1): 233-42.

Tokai-Nishizumi, N., M. Ohsugi, et al. (2005). "The chromokinesin Kid is required for maintenance of proper metaphase spindle size." Mol Biol Cell 16(11): 5455-63.

Tomkiel, J., C. A. Cooke, et al. (1994). "CENP-C is required for maintaining proper kinetochore size and for a timely transition to anaphase." J Cell Biol 125(3): 531-45.

Tournebize, R., A. Popov, et al. (2000). "Control of microtubule dynamics by the antagonistic activities of XMAP215 and XKCM1 in Xenopus egg extracts." Nat Cell Biol 2(1): 13-9.

Tournier, S., Y. Gachet, et al. (2004). "Disruption of astral microtubule contact with the cell cortex activates a Bub1, Bub3, and Mad3-dependent checkpoint in fission yeast." Mol Biol Cell 15(7): 3345-56.

Tran, P. T., L. Marsh, et al. (2001). "A mechanism for nuclear positioning in fission yeast based on microtubule pushing." J Cell Biol 153(2): 397-411.

Trazzi, S., R. Bernardoni, et al. (2002). "In vivo functional dissection of human inner kinetochore protein CENP-C." J Struct Biol 140(1-3): 39-48.

Tytell, J. D. and P. K. Sorger (2006). "Analysis of kinesin motor function at budding yeast kinetochores." J Cell Biol 172(6): 861-74.

Uhlmann, F. (2004). "The mechanism of sister chromatid cohesion." Exp Cell Res 296(1): 80-5.

Uhlmann, F., F. Lottspeich, et al. (1999). "Sister-chromatid separation at anaphase onset is promoted by cleavage of the cohesin subunit Scc1." Nature 400(6739): 37-42.

Uhlmann, F., D. Wernic, et al. (2000). "Cleavage of cohesin by the CD clan protease separin triggers anaphase in yeast." Cell 103(3): 375-86.

Umesono, K., T. Toda, et al. (1983). "Cell division cycle genes nda2 and nda3 of the fission yeast Schizosaccharomyces pombe control microtubular organization and sensitivity to anti-mitotic benzimidazole compounds." J Mol Biol 168(2): 271-84.

Uzawa, S., F. Li, et al. (2004). "Spindle pole body duplication in fission yeast occurs at the G1/S boundary but maturation is blocked until exit from S by an event downstream of cdc10+." Mol Biol Cell 15(12): 5219-30.

van Breugel, M., D. Drechsel, et al. (2003). "Stu2p, the budding yeast member of the conserved Dis1/XMAP215 family of microtubule-associated proteins is a plus end-binding microtubule destabilizer." J Cell Biol 161(2): 359-69.

Varga, V., J. Helenius, et al. (2006). "Yeast kinesin-8 depolymerizes microtubules in a length-dependent manner." Nat Cell Biol 8(9): 957-62.

Vasquez, R. J., D. L. Gard, et al. (1994). "XMAP from Xenopus eggs promotes rapid plus end assembly of microtubules and rapid microtubule polymer turnover." J Cell Biol 127(4): 985-93.

Vaur, S., F. Cubizolles, et al. (2005). "Control of Shugoshin function during fission-yeast meiosis." Curr Biol 15(24): 2263-70.

Vink, M., M. Simonetta, et al. (2006). "In vitro FRAP identifies the minimal requirements for Mad2 kinetochore dynamics." Curr Biol 16(8): 755-66.

Vos, L. J., J. K. Famulski, et al. (2006). "How to build a centromere: from centromeric and pericentromeric chromatin to kinetochore assembly." Biochem Cell Biol 84(4): 619-39.

Walczak, C. E., T. J. Mitchison, et al. (1996). "XKCM1: a Xenopus kinesin-related protein that regulates microtubule dynamics during mitotic spindle assembly." Cell 84(1): 37-47.

Wang, Y. and D. J. Burke (1995). "Checkpoint genes required to delay cell division in response to nocodazole respond to impaired kinetochore function in the yeast Saccharomyces cerevisiae." Mol Cell Biol 15(12): 6838-44.

Watanabe, Y. and P. Nurse (1999). "Cohesin Rec8 is required for reductional chromosome segregation at meiosis." Nature 400(6743): 461-4.

Waters, J. C., R. H. Chen, et al. (1998). "Localization of Mad2 to kinetochores depends on microtubule attachment, not tension." J Cell Biol 141(5): 1181-91.

Weaver, B. A., Z. Q. Bonday, et al. (2003). "Centromere-associated protein-E is essential for the mammalian mitotic checkpoint to prevent aneuploidy due to single chromosome loss." J Cell Biol 162(4): 551-63.

Wei, R. R., J. Al-Bassam, et al. (2007). "The Ndc80/HEC1 complex is a contact point for kinetochore-microtubule attachment." Nat Struct Mol Biol 14(1): 54-9.

Wei, R. R., P. K. Sorger, et al. (2005). "Molecular organization of the Ndc80 complex, an essential kinetochore component." Proc Natl Acad Sci U S A 102(15): 5363-7.

West, R. R., T. Malmstrom, et al. (2002). "Kinesins klp5(+) and klp6(+) are required for normal chromosome movement in mitosis." J Cell Sci 115(Pt 5): 931-40.

West, R. R., T. Malmstrom, et al. (2001). "Two related kinesins, klp5+ and klp6+, foster microtubule disassembly and are required for meiosis in fission yeast." Mol Biol Cell 12(12): 3919-32.

Westermann, S., A. Avila-Sakar, et al. (2005). "Formation of a dynamic kinetochore-microtubule interface through assembly of the Dam1 ring complex." Mol Cell 17(2): 277-90.

Westermann, S., I. M. Cheeseman, et al. (2003). "Architecture of the budding yeast kinetochore reveals a conserved molecular core." J Cell Biol 163(2): 215-22.

Westermann, S., D. G. Drubin, et al. (2007). "Structures and Functions of Yeast Kinetochore Complexes." Annu Rev Biochem.

Westermann, S., H. W. Wang, et al. (2006). "The Dam1 kinetochore ring complex moves processively on depolymerizing microtubule ends." Nature 440(7083): 565-9.

Wigge, P. A., O. N. Jensen, et al. (1998). "Analysis of the Saccharomyces spindle pole by matrix-assisted laser desorption/ionization (MALDI) mass spectrometry." J Cell Biol 141(4): 967-77.

Wigge, P. A. and J. V. Kilmartin (2001). "The Ndc80p complex from Saccharomyces cerevisiae contains conserved centromere components and has a function in chromosome segregation." J Cell Biol 152(2): 349-60.

Williams, B. C., T. L. Karr, et al. (1992). "The Drosophila l(1)zw10 gene product, required for accurate mitotic chromosome segregation, is redistributed at anaphase onset." J Cell Biol 118(4): 759-73.

Winey, M., C. L. Mamay, et al. (1995). "Three-dimensional ultrastructural analysis of the Saccharomyces cerevisiae mitotic spindle." J Cell Biol 129(6): 1601-15.

Wood, K. W., R. Sakowicz, et al. (1997). "CENP-E is a plus end-directed kinetochore motor required for metaphase chromosome alignment." Cell 91(3): 357-66.

Wood, V., R. Gwilliam, et al. (2002). "The genome sequence of Schizosaccharomyces pombe." Nature 415(6874): 871-80.

Xia, G., X. Luo, et al. (2004). "Conformation-specific binding of p31(comet) antagonizes the function of Mad2 in the spindle checkpoint." Embo J 23(15): 3133-43.

Yamashita, Y. M., Y. Nakaseko, et al. (1999). "Fission yeast APC/cyclosome subunits, Cut20/Apc4 and Cut23/Apc8, in regulating metaphase-anaphase progression and cellular stress responses." Genes Cells 4(8): 445-63.

Yanagida, M. (1987). "Yeast tubulin genes." Microbiol Sci 4(4): 115-8.

Yanagida, M. (2000). "Cell cycle mechanisms of sister chromatid separation; roles of Cut1/separin and Cut2/securin." Genes Cells 5(1): 1-8.

Yen, T. J., D. A. Compton, et al. (1991). "CENP-E, a novel human centromere-associated protein required for progression from metaphase to anaphase." Embo J 10(5): 1245-54.

Yoder, T. J., M. A. McElwain, et al. (2005). "Analysis of a spindle pole body mutant reveals a defect in biorientation and illuminates spindle forces." Mol Biol Cell 16(1): 141-52.

Zhang, K., W. Lin, et al. (2005). "The Set1 methyltransferase opposes Ipl1 aurora kinase functions in chromosome segregation." Cell 122(5): 723-34.

Zhou, J., J. Yao, et al. (2002). "Attachment and tension in the spindle assembly checkpoint." J Cell Sci 115(Pt 18): 3547-55.

Zimmerman, S., R. R. Daga, et al. (2004). "Intra-nuclear microtubules and a mitotic spindle orientation checkpoint." Nat Cell Biol 6(12): 1245-6.